PALACKÝ UNIVERSITY
FACULTY OF MEDICINE AND DENTISTRY

Program DSP: Pediatrics

IDENTIFICATION OF TARGETS OF ANTICANCER COMPOUNDS BY PROTEOMIC METHODS

Gabriela Rylová, M.Sc.

Supervising Department:

Institute of Molecular and Translational Medicine, Faculty of Medicine and Dentistry, Palacký University and Faculty Hospital in Olomouc

Supervisor:

Petr Džubák, MD, PhD

Acknowledgments

I would like to thank to my supervisor, Petr Džubák, M.D., Ph.D. for his mentoring, research advices and willing help. My thanks belong also to associate professor Marián Hajdúch, M.D., Ph.D. for mentoring, help with experiments design and mainly for the opportunity to work with many sophisticated instruments in the Institute of Molecular and Translational Medicine.

I would like to thank colleagues from the Department of Medicinal and Organic Chemistry, especially to Ing. Kristýna Burglová, Ph.D., prof. RNDr. Jan Hlaváč, Ph.D. and doc. RNDr. Miroslav Soural, Ph.D., for their help and advices with the chemistry part. I would also like to thank to the colleagues from the Department of Metabolomics, and to Pavla Perlíková, M.Sc., Ph.D. from the Institute of Organic Chemistry and Biochemistry for collaboration on the nucleoside analogs project.

My big thanks belong to my dear colleagues from IMTM, especially to Jana Václavková, M.Sc., Tomáš Oždian, M.Sc., Ph.D., Dušan Holub, M.Sc., Ph.D., Ivo Frydrych, M.Sc., Ph.D., Jirka Řehulka, M.Sc., Ph.D., Petr Konečný, M.Sc., Ph.D., Martina Medvedíková, M.Sc., Bc. Renata Buriánová and many others.

The last big "thank you" belongs to my family and friends for their help, understanding and patience.

Olomouc   …………………

March 2019   Gabriela Rylová, M.Sc.

Bibliografická identifikace

Jméno a příjmení autora	Gabriela Rylová
Název práce	Identifikace cílů protinádorových léčiv proteomickými metodami
Typ práce	Dizertační
Pracoviště	Ústav molekulární a translační medicíny, Lékařská fakulta, Univerzita Palackého v Olomouci
Vedoucí práce	MUDr. Petr Džubák, Ph.D.
Rok obhajoby práce	2019
Klíčová slova	chinolony, identifikace molekulárních cílů, elongační faktor, afinitní purifikace, translace, nukleosidová cytostatika
Jazyk	Anglický

Abstrakt

Tato práce je zaměřena na identifikaci cílů protinádorových léčiv. V teoretické části jsou popsány metody, které se k odhalení cílů a mechanismů účinků léčiv používají. Experimentální část je rozdělena do dvou částí podle dvou projektů. První projekt se zabývá identifikací molekulárního cíle chinolonových derivátů. Využívali jsme zde metody afinitní purifikace spojené s hmotnostní spektrometrií pro identifikaci cílů, dále pro validaci jsme použili enzymatické eseje, analýzu metabolitů a izotermální titrační miktokalorimetrii. Podařilo se nám identifikovat molekulární cíl elongační faktor 1 alfa 1 a objasnit dopady léčby touto látkou na buněčné mechanismy.

Druhým projektem je identifikace molekulárního mechanismu nukleosidového analoga AB61. Cílem bylo zjistit, který proces tato molekula cílí a jaký je mechanismus účinku. Zjistili jsme, že studovaná látka AB61 není účinně fosforylována ve fibroblastech, na rozdíl od nádorových buněk. Dále jsme potvrdili, že templátová RNA s inkorporovaným cytostatikem inhibuje translaci. Při studii jsme použili metody hmotnostní spektrometrie spojené s UPLC a analýzu protoesyntézy.

Bibliographical identification:

Author's name and surname	Gabriela Rylová
Title	Identification of targets of anticancer compounds by proteomic methods
Type of thesis	Dissertation
Department	Institute of Molecular and Translational Medicine, Faculty of Medicine and Dentistry, Palacký University Olomouc
Supervisor	Petr Džubák, MD, PhD
The year of presentation	2019
Key words	quinolones, molecular target identification, elongation factor, affinity purification, translation, nucleoside cytostatics
Language	English

Abstract

The thesis is focused on identification of targets of two selected anticancer compounds. In the theoretical part, methods used for drug target identification are described. Experimental part is divided into two parts corresponding to two projects. The first project is focused on identification of molecular target of quinolone derivatives. We have used affinity purification coupled to mass spectrometry for identification. Further, we have used enzymatic assays, metabolite analysis and isothermal titration microcalorimetry for validation. We have succeeded in identification of the elongation factor 1 alpha 1 as the molecular target of compound 3 and explain how these compound affect cell mechanisms. The second project was focused on identification of molecular mechanism of AB61 nucleoside analogue. The aim was to find the target process that is affected by the compound and describe the mechanism of its action. We have found inefficient phosphorylation of AB61 in fibroblasts compared to cancer cells. Further, we have described that template RNA with incorporated cytostatic inhibits translation. We have used mass spectrometry coupled to UPLC and analysis of proteosynthesis for this purpose.

Table of content

1. Theory

Unknown or off-target mechanisms of drug action are frequent problems in rational drug development[1]. Understanding the mode of drug action may increase treatment efficacy, lead to the improved design of clinical trials, get better selection of appropriate patient cohorts and minimize the side effects of targeted therapies. For this reason, strategies for drug target identification are inevitable part of drug discovery and development processes. One of the most frequently used methods in proteomics is affinity chromatography which has been alone or in connection to mass spectrometry, successfully implemented in drug target identification workflow. Most methods use immobilization of modified compound onto various solid phase matrices with subsequent pull down enrichment and identification. Other ligand-free approaches such as energetics-based methods, cell permeable probes or methods using capturing subproteome of interest enable the use of unmodified compounds[2]. The chapters 1.1, 1.2 and 1.4 were in similar structure published as a part of review[2] (appendix A).

1.1 The importance of knowledge of mechanism of action of anticancer drugs

Drug discovery includes all processes of development and analysis of drug - small molecule that have appropriate features to process and succeed in preclinical and clinical development. The important part of this procedure is to identify the mechanism of action of small molecule and its molecular target. Historically, most therapeutic drugs were used based on their effects without information about their mechanism of action. In fact, Drews in 2000 published that seven percent of FDA (Food and Drug Administration) approved drugs were found to have unknown mechanisms of action[3]. Similarly, Overington *et al*. reported that only 82% of FDA drugs approved between 1989 and 2000 had a delineated target molecule[4]. Approved drugs with unknown mechanism of action include for example Bexarotene and arsenic trioxide for the treatment of cutaneous T-cell lymphoma and acute promyelocytic leukemia, respectively[5]. Another example can be thalidomide that mechanism of action remained unknown for almost 60 years. It was prescribed to pregnant women to treat nausea, but it was discontinued because caused birth defects[6]. Later, was used for leprosy and multiple

myeloma treatment, but the mechanism of action remained elusive[7]. Currently, several publications shed light on the mechanism of action[8]. It targets ubiquitin ligase cereblon, that wrongly marks several proteins for degradation including protein SALL4, transcription factor essential for limb development[9].

Incomplete or missing information of the "molecular targets" that interact with a drug is an obstacle in the development of more efficient drugs. Unravelling the mode of drug action can lead to the design of better structures without serious side effects, increased efficiency of treatment and finally can help us to understand the role of target molecule and identify new therapeutic targets.

The simple theory that one drug aims at only one target is generally incorrect because many drugs such as imatinib and sunitinib maleate[10] originally developed to target only one molecular target, have been found to bind to multiple [11,12]. Targeting more than one cellular structure can be used as an advantage, mainly in anticancer drug development as it is necessary to target more than one dysregulated pathway. On the other hand, such cytotoxic compounds can be a source of harmful side effects. This is a good reason to identify all possible drug targets and increase the specificity of the compound before costly clinical trials[13]. Moreover, drugs with identified off-targets can be in reasonable conditions repurposed. Thalidomide is an illustrative example. Originally prescribed to pregnant women to ease pregnancy-associated nausea and "morning sickness" in 1957, it was discontinued when discovered to cause congenital abnormalities. Five decades later, the drug has found new use in leprosy and cancer treatment[14,15]. Celecoxib is another example. It was designed to treat osteoarthritis but is now prescribed for colorectal cancer prevention[16]. The small-molecule Histone deacetylase 6 inhibitor, tubacin, pharmacological tool for HDAC6 function evaluation, also inhibits Serine Palmitoyl transferase, the rate-limiting enzyme of sphingolipid biosynthesis[17].

With the development of molecular biology, chemical and biochemical approaches, there is a number of methods for studying the effects of pharmaceutical drugs and target interactions of new promising compounds. Methods like affinity chromatography, activity-based proteomic profiling, energetic-based target identification, microarrays and mass spectrometry (MS) are discussed below.

1.2 **Chemical proteomics**

Chemical proteomics is multidisciplinary science that involves a variety of disciplines like structural biology, molecular biology, biochemistry, organic chemistry, mass spectrometry and bioinformatics. This approach enables to elucidate drug´s mechanism of action and cell response to the drug treatment[1,18–20]. Chemical proteomics employs activity or affinity enrichment-based technologies, and gel based expressional profiling methods for these purposes. MS (alternatively MS coupled with quantification labeling) is indispensable part of each chemical proteomics experiment.

1.2.1 **Affinity purification**

Affinity purification (AP) is a powerful method based on interaction between immobilized ligand (probe) and protein. It is widely used for capturing proteins and identification of protein-protein interaction networks[21]. AP was developed in the early 1950s[22] and a number of variants have been developed and successfully applied to identify molecular targets.

Prerequisite for AP is modification or derivatization of the compound of interest, to enable its immobilization on the solid phase (affinity) matrices. Commonly used matrices may be polysaccharide derived (agarose, Affi-Gel®, sepharose), methacrylate derived (Toyopearl®, SG beads) and magnetic beads (Dynabeads® Invitrogen, FG beads)[23]. Polysaccharide derived matrices are hydrophilic and chemically fragile, what can be obstacle for preparation of ligand-immobilized matrices. As majority of pharmaceutical compounds are hydrophobic, there is need to use organic solvents. Therefore, functional polymers derived matrices were developed. Toyopearl® is methacrylate derived alternative stable for organic solvents. Main disadvantage of Toyopearl® is higher level of nonspecific protein interaction. Therefore, hydrophilic polymethacrylate-based matrix (monolithic affinity matrix - AQUAFIRMUS®) was developed by Tanaka, Hosoya and coworkers[24]. The AQUAFIRMUS® is composed of three kinds of methacrylate with ethylene glycol (EG) parts. This kind of matrix reduce nonspecific interactions compared to Toyopearl®.

SG beads (named according the styrene and glycidyl methacrylate) are relatively new latex affinity beads with favorable features. It is copolymer of styrene and glycidyl

methacrylate (GMA). These beads are highly stable, moderate hydrophilic, dispersible in water and exhibits low nonspecific protein binding. On the other hand, time-consuming step - centrifugation - is necessary for the SG beads purification procedure. Therefore, magnetic alternative of SG beads was designed. The ferrite alternative of SG beads is named FG beads (named according ferrite and GMA) and possess comfortable magnetic separation, high dispersibility in water and low nonspecific interaction. Dynabeads® (Invitrogen) are commercially available hydrophilic polymer coated magnetic iron oxide beads. Comfortable magnetic separation, unique polymer surface enabling non-toxic environment and low nonspecific interactions are main advantages for this matrix. Dynabeads® are currently used in many areas as affinity purification (streptavidin coated Dynabeads®), protein-protein interaction, nucleic acid isolation and many others[25]. Affinity matrices are constantly being developed and improved to enhance the binding of the specific target and to minimize nonspecific interactions[23].

A typical AP "pull-down" experiment begins (Fig. 1) with immobilization of studied molecule on the resin and incubation with cell lysate. Post incubation, the resin is washed several times to rid it of nonspecifically bound proteins and other molecules. The captured proteins are eluted by various buffers (high salt buffer, denaturing agent or excess amount of free ligand) which enables disruption of ligand-protein interaction. Eluted proteins can be separated by 1DE or 2DE gel electrophoresis (1D or 2D electrophoresis) and/or identified by MS.
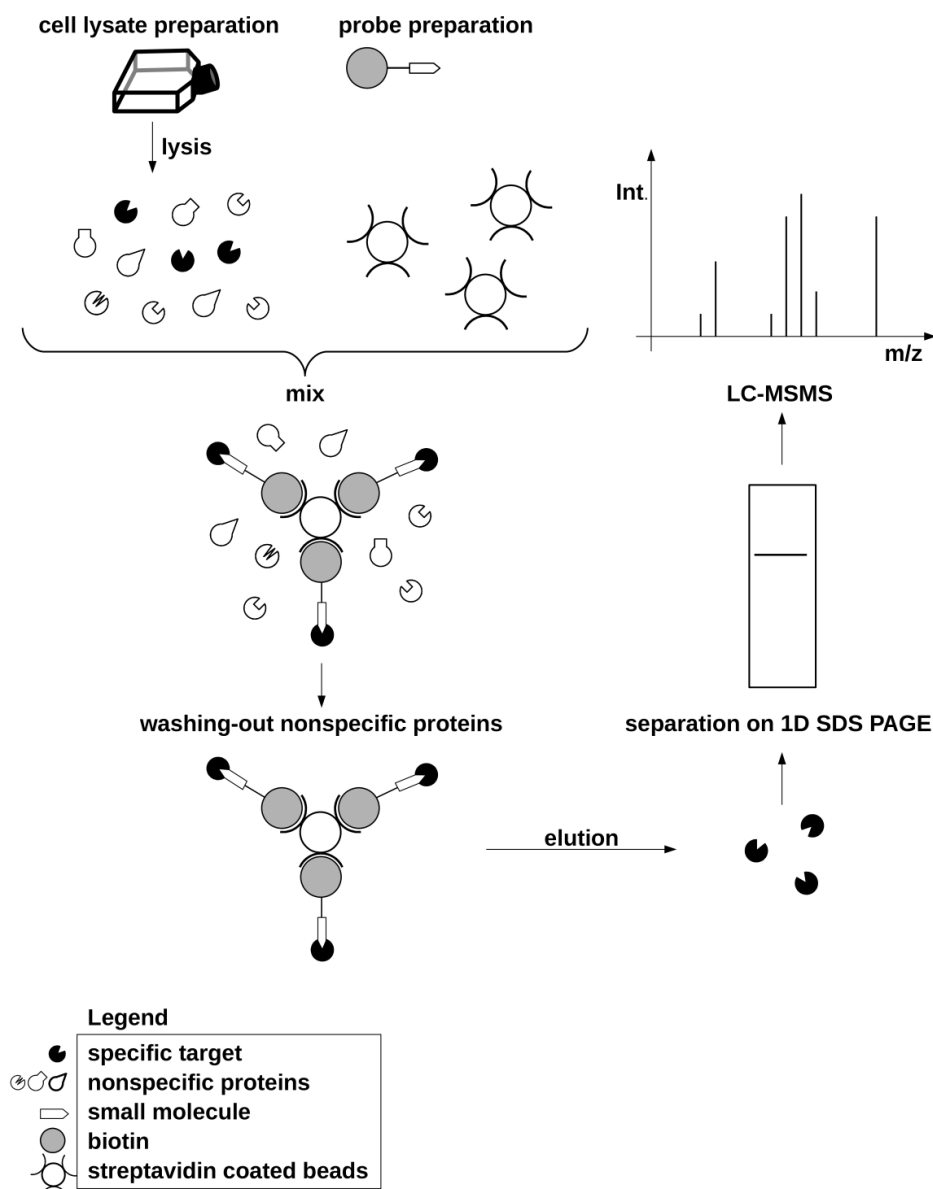
Figure 1. Workflow of affinity purification: Modified (e.g. biotinylated) compound is immobilized onto solid-phase (streptavidin coated beads). Cell lysate is incubated with immobilized compound on the solid-phase. Specific proteins are captured by compound and nonspecific proteins are washed out. Target proteins are then eluted and subjected to 1D SDS PAGE and LC-MS/MS[2].

1.2.1.1 Compound immobilization strategies

There are several ways of immobilizing the active compound to the matrix (Fig. 2). The most common way is to immobilize small molecules by attachment of their sulfhydryl,

hydroxyl, amino or carboxyl functional groups directly onto the matrix. This approach was used to study the selective binding profile of BCR-ABL (break cluster region-ABL kinase) tyrosine kinase inhibitors imatinib, nilotinib and dasatinib. The inhibitors were derivatized to introduce surface amino and acetyl groups. Derivatives were immobilized on N-hydroxysuccinimide activated sepharose and incubated with K562 (chronic myeloid leukemia - CML) cell line and CML primary cell lysates. Following the washing step, proteins were eluted, separated by SDS PAGE, digested and identified by MS. The results showed that dasatinib bound more than thirty Tyr and Ser/Thr kinases, and that nilotinib´s additional target is the tyrosine kinase receptor DDR1 and nilotinib and imatinib mutual target is NQO2 oxidoreductase[12]. In another study on the p38 kinase inhibitor SB 203580 Daub and coworkers immobilized the amine analog of compound SB 203580 to epoxy-activated sepharose. After elution of target protein, they separated biotargets by 2 DE. Spots were excised and identified by MALDI TOF/TOF (matrix assisted laser desorption ionization time of flight). They discovered new targets such as Janus kinase 1 (JAK1) [26]. The same strategy was used for shikonin, a potential anticancer drug that inhibits the pyruvate kinase M2 (PKM2), tumor specific isoform of pyruvate kinase[27].

PROBE	STRUCTURE	IMMOBILISING RESIN	PROPERTIES
Compound modified by NH₂, OH, SH or COOH moieties	COMPOUND — NH₂ / OH / SH / COOH	Agarose, sepharose	Inexpensive, specificity is sometimes an issue
Biotinylated compound	COMPOUND — BIOTIN	Streptavidin coated matrix	Specificity of biotin-straptavidin bond is high and requires stringent elution conditions, spacer design is complicated
Photoaffinity label	COMPOUND — BIOTIN / BENZOPHENONE	Streptavidin coated matrix	Drug binds covalently to target, Photoaffinity probe needs to be carefully selected and derivatized to drug
Compound modified for click chemistry reaction	COMPOUND — ALKYNE ; AZIDE — BIOTIN	Streptavidin coated matrix	The reaction can be performed in a variety of conditions, Long exposures to Cuᴵ catalyst may be cytotoxic
Immuno-chemo-proteomics probe	COMPOUND — LINKER — FLAG	Antiflag beads	Sulfation of FLAG polypeptide can alter antibody specificity
Kinobeads	KINOBEAD — ATP BINDING SITE	Agarose beads	For kinases only, Some kinases do not bind to ATP structural analogs and cannot be enriched by Kinobeads
Activity based probe	WARHEAD — TAG	Streptavidin coated beads, fluorescent or radiolabell scanning	For enzymes only, warheads aren't available for all enzyme types

Figure 2. Examples of compound immobilization strategies[2].

1.2.1.2 Streptavidin-biotin

The strong non-covalent interaction between biotin and streptavidin (or avidin) is the basis for a common type of affinity purification[28]. These interactions are the strongest known non-covalent interactions occurring in nature. The biotin moiety is attached to the active compound which is then immobilized on the streptavidin (or avidin) coated matrix.

Key to the synthesis of the biotin label is the design of the spacer that connects the compound to the biotin moiety[29]. Spacer design and its impact on the affinity purification has been intensively studied and some rules were formulated[30–32]. Spacer design should follow these principles: 1) it must be sufficiently long to prevent steric hindrance between streptavidin and the target biomolecule; 2) it should not interact with the target biomolecule to cause a false-

16

positive result; 3) it must not change the solubility of the biotin probe in water. Aliphatic spacers such as caproic acid derivatives have been used frequently in the past, although the newer EG spacers are now preferred, as they satisfy the above criteria better[33]. The compound of interest is typically attached to the biotin-EG system via a stable amide bond. Derivatization has traditionally been done using solution-phase synthesis and more recently using solid-phase synthesis. The substrate for biotinylation (or conversely the biotin-EG-NH$_2$ system) is pre-immobilized or directly synthesized on an insoluble polymer backbone, and the resulting preloaded resin then used for reaction with an appropriate compound for e.g. the Biotin-PEG-NovaTagTM (Novabiochem)[34–36]. Conversely, the biotin-EG-NH$_2$ system may be immobilized in place of the biotinylated substrate. Preparation of a similar system for immobilization of carboxy-group containing analytes via spacers of different length has also been described[37] (Fig. 3).
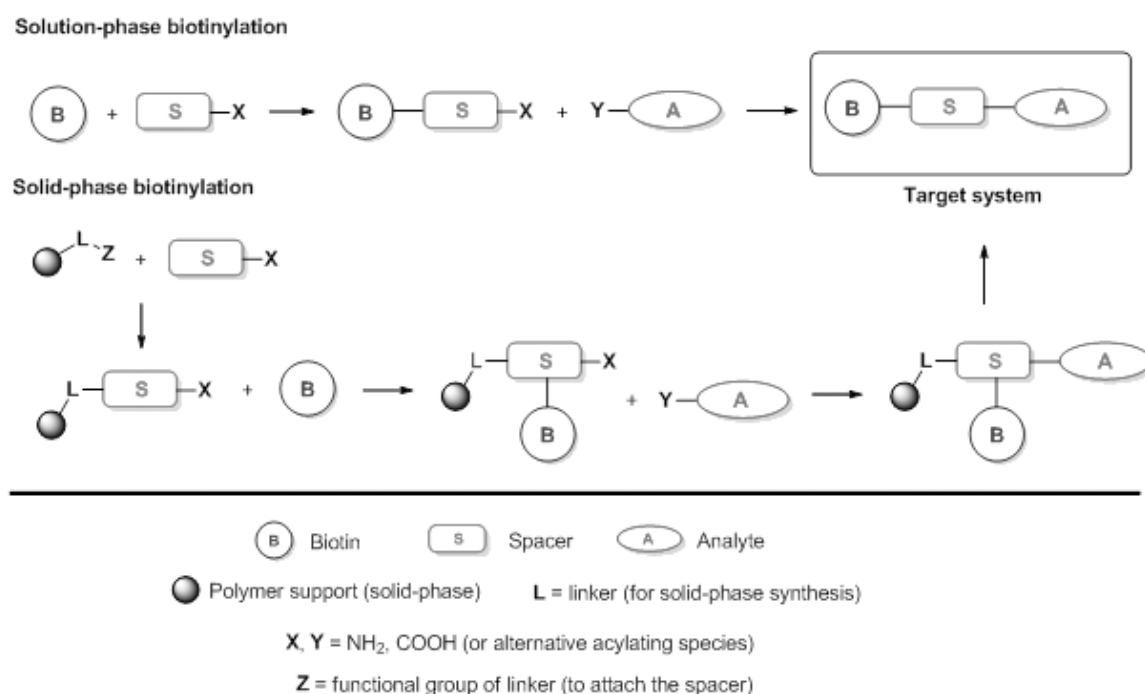
Figure 3. Two alternative approaches to modify compound A: The selection of more suitable method is based on specific requirements such as required quantity of the target system, its stability and availability of analyte (for low quantities the solution-phase method is preferable). A typical polymer support is divinyl-styrene based resin. Except for amides also ester or ether groups are frequently used to attach individual parts of the target system[2].

The example of streptavidin-biotin strategy was used for 2´-Hydroxycinnamaldehyde (HCA), a compound with antiproliferative activity. Biotinylated HCA was studied by an *in vitro* pull-down assay against colon cancer cells SW620 lysate. Proteins eluted from avidin-biotinylated compound complex were separated by 2 DE and analyzed by MALDI-TOF. The proteasome subunits were identified as targets of HCA[38]. A small antimitotic molecule diazonamid A that causes G_2/M phase growth arrest in several human cancer cell lines, was studied by this approach. Biotinylated diazonamid A was immobilized on avidin agarose and incubated it with cervical cancer HeLa nuclear extract. Recovered proteins were separated and visualized by silver-stained SDS PAGE. Ornithine δ-amino transferase, a mitochondrial enzyme was identified as a specific target[39].

Alternatively, the combination of SILAC (stable isotope labeling with amino acid in cell culture) quantitative proteomic labeling (described in detail later) with affinity purification is possible (Fig. 4). Ong and coworkers presented this methodology enabling comparison of the multiple pull-down experiment in one MS analysis. Briefly, Affigel® immobilized small molecule is incubated with heavy labeled and light non-labeled cell lysates separately. Additionally, the light labeled cell lysate is incubated with the immobilized molecule and competed by soluble small molecule. Heavy cell lysate is incubated with the immobilized molecule and DMSO (dimethyl sulfoxide). Subsequently, both beads are washed by lysis buffer, mixed and captured proteins are eluted, separated by SDS PAGE, digested, analyzed by MS and quantified. Since target protein has low heavy to light ratio (H/L) and nonspecific protein has an H/L ratio of approximately one, we can distinguish between specific and nonspecific proteins. The reverse experiment is recommended as well, to confirm specifically bound proteins[40].
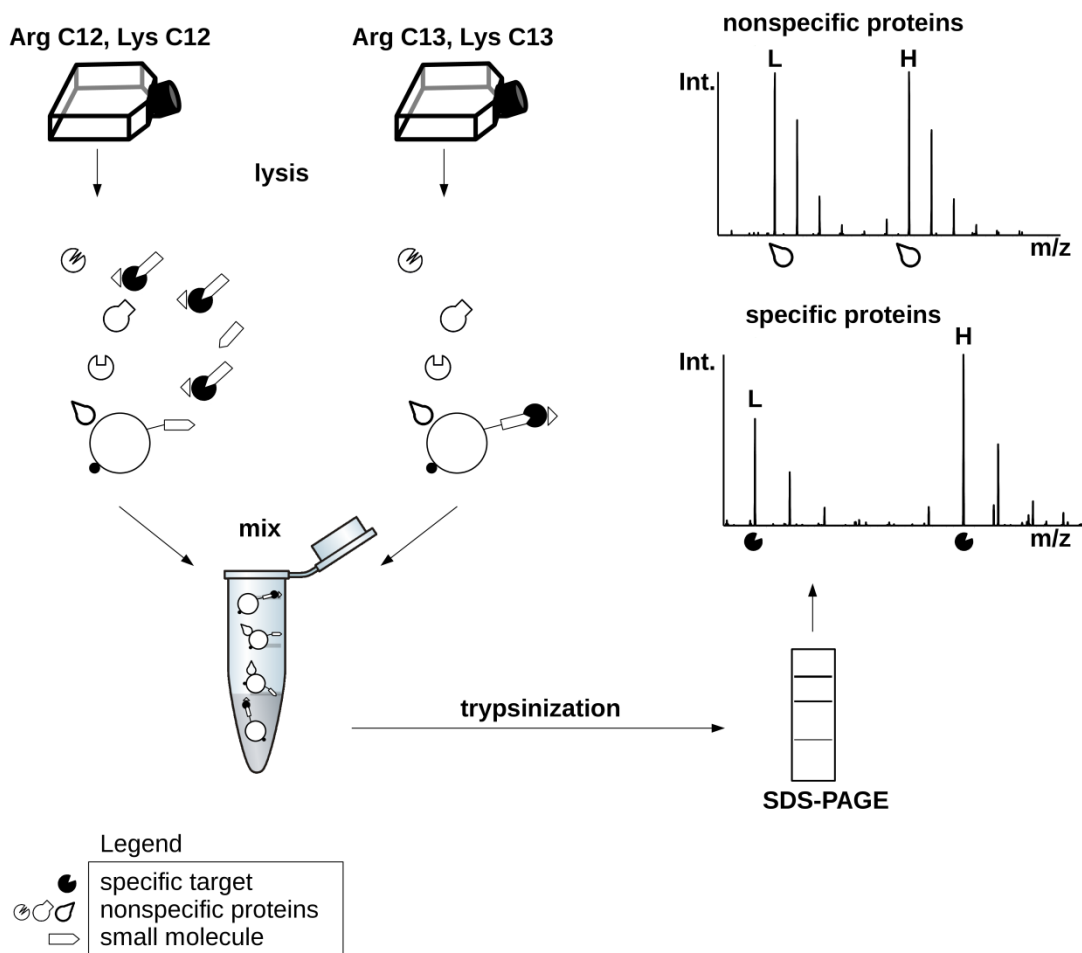
Figure 4. Identification of protein targets by quantitative proteomics: Cells of interest are incubated with labeled (heavy, H) and non-labeled (light, L) aminoacids (SILAC). Non-labeled cell extract is simultaneously incubated with immobilized and free small molecule. Heavy cell lysate is incubated with immobilized small-molecule alone. Afterwards, both bead-types are washed and mixed in equimolar quantities. Captured proteins are eluted, separated by SDS PAGE, analyzed by MS and quantified. Target protein has heavy to light ratio (H/L) above one and nonspecific protein has H/L ratio approximately one[2].

1.2.1.3 Photoaffinity labeling

Another way for affinity-based drug target identification is using photoaffinity labeling. Small active molecule is derivatized by two distinct moieties, a photoreactive group (azide, diazirine, benzophenone *etc.*), which enables creating new covalent bonds between ligand and its biotargets upon irradiation. The second moiety is tag (biotin, radioactive or fluorescent) enabling detection and/or purification of labeled target protein. This bifunctional complex is

called photoaffinity label (PAL)[41,42]. The general workflow starts with incubation of PAL with cell extract to establish non-covalent bonds before irradiation. Covalent crosslinks between PAL and nearby proteins are created upon irradiation by specific wavelength. The protein-label complex can be purified by avidin-biotin affinity chromatography or detected by fluorography[41]. The protein targets of two compounds - fumagillin, an inhibitor of angiogenesis and ovalicin with antitumor, antibacterial and immunosuppressive activity, have been studied. A radioactively labeled photoaffinity derivative of ovalicin was used for identification of its molecular targets. A 67 kDa protein was identified. As the protein was competed with excess ovalicin and fumagilin, both compounds apparently bind the same target. In succeeding experiments, they utilized biotin photoaffinity label for purification of target protein by immobilization onto streptavidin coated resin. After SDS PAGE, they identified by MALDI-TOF type 2 methionine aminopeptidase[43]. PAL methodology was also used for target identification of pladienolide, antitumor compound. ^{3}H–labelled, fluorescence tagged and photoaffinity/ biotin constructed probe was used to identify splicing factor SF3b as a potential antitumor drug target[44].

New type of PAL probe was introduced in photoaffinity labeling. It was composed of affinity tag (biotin) and isotopically labeled photoreactive tag mixed in 1:1 ratio (non/deuterised benzophenone isotope label – marked D_0/D_{11}). Identification of the unique isotopic pattern (containing both M - mass of peptide and M+11- mass of peptide +11 Da) of some peptides helps to confirm identification of protein targets among frequent contaminants (Fig. 5). Authors described use of trifunctional probes on cyclosporin A (cycA), which naturally binds cyclophilin A (cypA). Two isotopically labelled cycA D_0 and D_{11} probes were mixed in a 1:1 ratio with protein mixture containing cypA. Following irradiation, interacting proteins were purified via avidin resin, eluted, trypsinized and identified by LC-MS/MS. Eleven proteins were identified including nonspecific proteins like ubiquitin and keratin. Only two peptides showed the unique isotopic pattern (M, M+11), both belonging to cypA[45].
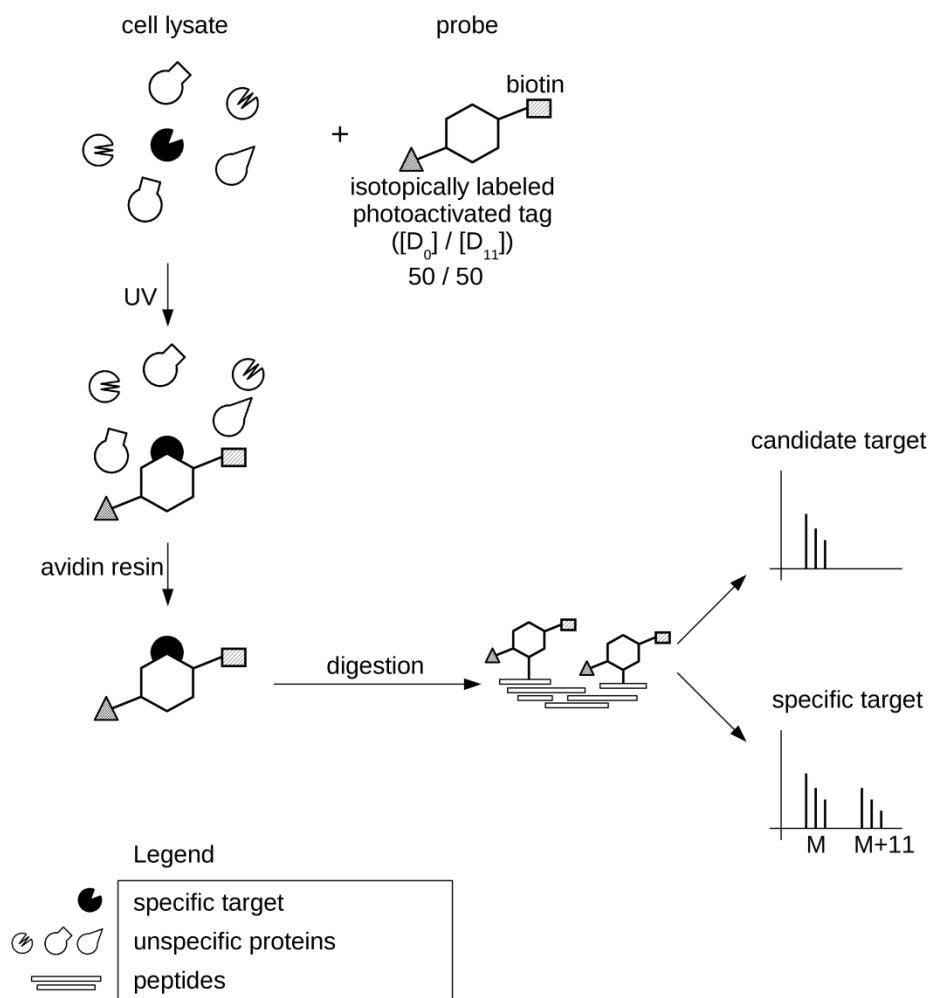
Figure 5. Photoaffinity labeling with two isotopes: PAL probes consisting of an affinity tag (biotin) and an isotopically labeled photoreactive tag (non-deuterized, D_0 and deuterized benzophenone isotope label, D_{11}) are mixed in 1:1 ratio. Probes are incubated with cell lysate and subsequently irradiated by UV-light. Proteins are then purified via avidin resin and identified by MS. Identification of the unique isotopic pattern (M, mass of peptide with non-deuterized tag; M+11, mass of peptide with deuterized tag) of some peptides helps to distinguish valid protein targets from frequent contaminants[2].

1.2.1.4 Cell-permeable probes

Modification of molecules of interest can be the obstacle for identification of the real target, mainly because of compound activity changes, steric hindrance, different cell permeability or demanding and time-consuming synthesis.

Click chemistry[46] is an alternative used in affinity chromatography. An example of click chemistry is Huisgen 1,3-dipolar cycloaddition of azides and alkynes to establish triazoles[47]. Yao and colleagues used this reaction in a study on identification of off-targets of orlistat, an anti-obesity drug with potential antitumor activity. They prepared a cell-permeable probe - orlistat modified by alkyne moiety and added it to cell culture media. Following incubation, the cells were washed to remove the redundant probe and homogenized. After treatment with rhodamine-azid under click chemistry conditions and subsequent separation on SDS PAGE electrophoresis, they detected several fluorescence bands. The authors also used interaction of biotin-azide click chemistry for orlistat target purification. They incubated biotin-azide with cell lysate treated by alkyne orlistat probe. The complex was immobilized onto avidin-agarose beads and eluted proteins were separated by SDS PAGE, trypsinized and identified by MS. Known target - fatty acid synthase and eight new targets were identified[48].

The HIV Trans-activating transcriptional activator (TAT) is a nine-residue peptide (RKKRRQRRR) with majority of positively charged amino acids, and can transport molecular cargo into eukaryotic cells[49,50]. The cargo could be metabolites, peptides, proteins or nucleic acids. The TAT peptide could potentially also transport some of the above mentioned affinity tags into the cell in studies of drug-target interactions. A composite probe consisting of the drug Bisindolylmaleimide III (Bis III), a fluorescent group and the TAT peptide has been used for this purpose. Bis III was coupled to fluorescent-tagged TAT peptide, cells were treated by probes, washed and cell probe uptake was confirmed by fluorescence microscopy. Following cell lysis, proteins interacting with Bis III were isolated by anti-fluorescein magnetic beads. Afterwards, eluted proteins were separated, digested and identified by MS. As before, they identified known target glycogen synthase kinase α/β (GSKα/β) and several new targets[51]. Other cell penetrating peptides are now available and may be similarly used in future for the entire class of affinity-tags[52].

1.2.1.5 Capturing subproteome of interest

The affinity purification procedure may be designed to capture not just one protein but an entire class of proteins. The N-glycoproteome, phosphoproteome or the SUMOylated group of proteins are important druggable post-translational modification (PTM) in cancer and have suitable purification procedures[53–55]. The probe, in this case, binds nonspecifically to all proteins bearing a particular PTM. Antibodies against phosphate group epitopes are commonly used reagents for isolation of phosphorylated proteins[56]. However, because they are specific to an epitope, they allow enrichment of only one kind of phosphorylated peptide at a time. This

problem is circumvented when the purification is based on phosphotyrosine, phosphoserine or phosphothreonine antibodies or a nonspecific electrostatic affinity between the negatively charged phosphate groups and positively charged metal cations (Immobilized Metal Affinity Chromatography IMAC and by Metal Oxide Affinity Chromatography, MOAC)[56–58]. The negative charge on the free carboxyl groups and acidic amino acids must be neutralized for the isolation of peptides with phosphate groups by appropriate affinity resin or by conventional ion-exchange chromatography (hydroxyapatite column enrichment or Hydrophobic Interaction Liquid Chromatography, or HILIC)[59].

An emerging approach for capturing kinase subproteome was developed. As kinases phosphorylates proteins and can regulate different cellular processes, they are interesting subproteome to study. The effective strategy utilizing a special resin called "kinobeads" was described. This approach is utilizing competition between unmodified compound of interest and ATP (adenosine triphosphate)-binding ligands on kinobeads. The kinobeads contain seven ATP-binding site ligands immobilized onto solid matrix. The kinobeads were employed for identification of the mechanism of action of BCR/ABL inhibitors. They incubated cell extracts with three different concentrations of drug, followed by kinobeads precipitation. Proteins eluted from kinobeads were digested and then labelled with iTRAQ (isobaric taq for relative and absolute quantification, described in details later). Mixed samples were analyzed by LC-MS/MS. Decrease in proteins which were eluted from kinobeads were evaluated via iTRAQ quantification[60]. The same kinobeads approach was used for target elucidation of multi-kinase inhibitors. In one described experiment cell lysate from patient isolated leukemic cells was analysed. The cell lysate was mixed with increasing concentrations of tested compounds (staurosporine, BMS-387032, flavopiridol and R-roscovitine). Subsequently, kinobeads were added to this mixture and depletion of target protein bound to kinobeads was measured relative to a vehicle control using iTRAQ labeling and LC-MS/MS. As expected staurosporine bound many kinases. However, BMS-387032 and flavopiridol showed a more selective effect. These inhibited CDK9 (cyclin dependent kinase 9) which is part of the p-TEFb (positive transcription elongation factor) complex and some other kinases. Examples of roscovitine identified targets are p-TEFb or CDK-activating kinase[61]. A similar approach has identified novel targets of the multi-kinase inhibitor E-3810[62].

1.2.1.6 Energetics-based target identification

Protein lysate

small molecule

DMSO

protease

small molecule

DMSO

target protein

SDS PAGE

Legend
- specific target
- nonspecific proteins
- small molecule
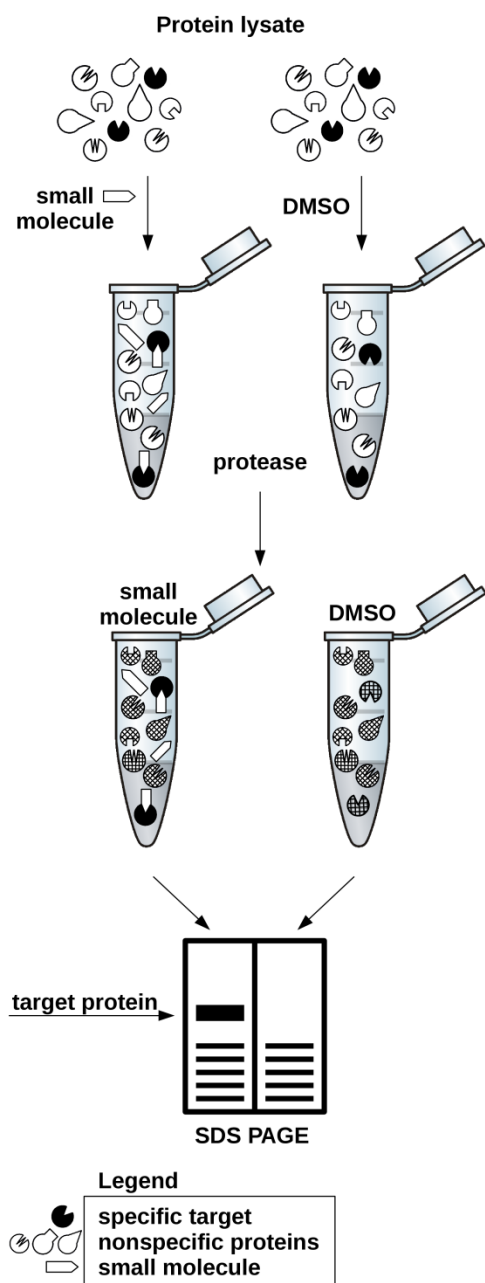
One approach for overcoming compound modification is energetic-based target identification. This enables identification of small-molecule targets in a mixture of proteins. The principle is based on change of conformational stability upon small molecule binding to target proteins[63–66].

The first approach is drug affinity responsive target stability (DARTS) developed by Huang[67]. DARTS use different susceptibility of target protein to protease digestion upon drug binding. Small molecule interaction with protein sterically protects the protease cleavage site. The basic workflow (Fig 6.) starts with protein lysate incubation with small molecule and inactive analogue (or solvent). Subsequently, mixtures are digested by proteases (pronase or thermolysin), separated by 1D SDS PAGE and stained. Bands that differ in abundance are distinguished, cut, digested and analyzed by LC-MS and quantified by spectral counting or other methods to find which protein has been enriched compared to control.

Figure 6. DARTS. Protein lysate is incubated with a small molecule compound and then subjected to protease digestion. Target proteins interacting with the small molecule compound are enriched and protected against protease digestion while nonspecific proteins are digested[2].

DARTS has been validated on well-known interactions as an immunophilin FKBP12 that is target for rapamycin and FK506 or interaction between mammalian target of rapamycin (mTOR) and kinase inhibitor E4. In both cases, the proteolysis of target proteins was

decreased[67]. The same group used DARTS for protein target identification of resveratrol, a compound with various effects, including anticancer potency and lifespan extension. EIF4A (eukaryotic initiation factor-4A) was identified as a potential target[67]. Moreover, there are new modifications of DARTS enabling improved target identification[65,68].

A second similar approach is using differential susceptibility to a denaturation agent followed by proteolysis. Small molecule binding can slow unfolding of protein. Liu et al. studied ATP binding proteins from *E. Coli*. Firstly, they fractionated cell lysate by anion exchange chromatography. Each fraction was then incubated with or without the presence of ATPγS (ATP analogue more resistant to hydrolysis) in different concentrations of urea. Subsequently, fractions were digested by pulse proteolysis, separated by 1D SDS PAGE and differently digested proteins were analyzed by MS. They found 30 tentative ATP binding proteins, 21of which are known for ATP binding and 9 were new potential interacting partners[64].

1.2.1.7 The Recombinant Tag

In a study by Saxena and coworkers[69], a protein kinase C (PKC) inhibitor Bis III was chemically coupled to a FLAG tag (small hydrophilic octopeptide –DYKDDDDK) using a linker. The compound was purified by reverse phase high-performance liquid chromatography (RP-HPLC) and its inhibitory effect determined in a kinase activity inhibition assay. The Bis III was then incubated with HeLa cell lysate and the target protein in complex with FLAG probe was isolated by anti-FLAG affinity resin. Previously known targets were identified protein kinase C (PKC-α), adenosine kinase or cyclin dependent kinase 2-(CDK2) together with a number of new ones as cAMP-dependent protein kinase (PKAC-α), prohibitin or voltage dependent anion channel (VDAC). The FLAG tag was considered generally applicable till a few years ago, when it was shown that a sulfation post-translational modification eliminates the interaction of the FLAG tag and anti-FLAG antibodies[70]. Such a modification lowers the yield of the purification without ever becoming evident.

1.2.1.8 Activity based protein profiling

Activity based protein profiling (ABPP) is a powerful tool for enzyme function characterization. This method is widely used in several fields, from comparison of healthy versus diseased sample enzyme activity, characterization of enzyme active sites to enzyme inhibitor discovery[71]. This approach employs special probes comprised of three parts: a

warhead part which can covalently bind active site of enzyme, tag (fluorophore, biotin or click chemistry handle) for identification and purification of target proteins and linker joining these two parts together[71–73]. The general workflow starts with adding the probe (a small molecule-warhead) to the cells or cell lysate. The probe binds by its warhead target proteins. Subsequently, enzymes are purified by probe tag, separated on SDS PAGE and identified by MS[71].

Yang and coworkers used ABPP in combination with bio-orthogonal click chemistry for identification of novel targets of orlistat[48]. Bachovchin and coworkers[74] used the combination of fluorescence polarization with ABPP to determine the drug target of cancer associated retinoblastoma-binding protein-9 inhibitors.

1.2.1.9   Strengths and limitations of affinity chromatography methods

There are many affinity chromatography approaches, modifications and alternatives. It is difficult to divide them into groups because a number of them utilize a combination of several approaches (quantitative labeling, active compound competition, different probes, etc.) and a number were developed for overcoming drawbacks.

No doubt, affinity chromatography techniques are very powerful tools for drug target identification. This objective approach has many advantages - experiments are done with natural proteins, with preserved post-translational modifications and present binding partners. However, many obstacles such as nonspecific interactions, small molecule modification and immobilization remain as drawbacks of this approach.

Most of the affinity chromatography workflows start with modifications of the small molecule because there is not available moiety for its immobilization onto solid phase. Therefore, it is necessary to have structure activity relationship (SAR) data for selecting appropriate parts of the molecule available for modification. The biological activity of modified compound has to be maintained and confirmed. One approach to increase the probability of proper compound immobilization is to use more routes for immobilizing small molecule to the matrix[75]. Several approaches were developed for overcoming these obstacles like the soluble probes[51], capturing subproteome of interest[60], competitive experiments[40,76] and energetics-based methods[63–66]. In these strategies, we can use unmodified active molecules without the need for immobilization.

Another problem is specificity of target binding. Protein sources contain unequal amounts of protein. Therefore, there are many highly abundant proteins, which can lead to

identification of falsely positive interacting partners. This means that there can be low abundance proteins with high affinity for active molecule together with low or medium affinity proteins with high abundance[18]. There are a number of efficient strategies for overcoming this problem. One of them is using Proteominer[TM] (Biorad), an efficient approach to enrich low abundance protein (LAPs). The strategy is using combinatorial library of hexapeptides attached to the beads support. Each hexapeptide has unique protein binding specificity. Therefore, after protein is mixture loaded on hexapeptide covered beads, high abundance proteins (HAPs) hexapeptides are saturated and excess is washed out. Moreover, low abundance proteins are concentrated by binding on their hexapeptide partners[77,78]. This results in the depletion of HAPs and in the enrichment of LAPs, thereby effectively decreasing the dynamic range of protein concentrations in the sample by a few orders of magnitude.

Other, more conventional strategies for reducing the dynamic range of protein concentrations in serum utilize antibodies that target the most abundant proteins[79–81]. The relative rate of trypsin digestion of high- and low-abundance proteins is also a basis for improving the dynamic range of detection of proteins[82]. This technique, named DigDeAPr, has been used with cell lysates but can be utilized for complex mixtures with wide range of protein concentrations[82].

Another strategy is using non-active analogue of immobilized compound as a negative control. Comparison of proteins eluted from the active and non-active immobilized compound can lead to elucidation of nonspecific protein targets[76,83]. Tanaka and colleagues developed a simple method called serial affinity chromatography to identify specific binding proteins. They incubated cell lysate with affinity resin with immobilized compound, in the second step the resin was removed, and the same lysate was incubated with fresh resin. Most of the specific biotargets were captured by the first resin but in the second, the resin captured mostly unspecific targets[84]. Alternatively, competitive experiments can be used[40,76], where the free active compound competes for targets with immobilized compound. However, insolubility of active compound is a frequent obstacle.

An intelligent choice of the affinity matrix can go some distance in alleviating the problem of nonspecific interactions, as the matrix and probe linkers can be a source of such interactions[29,85]. Matrices that are incompletely derivatized may also bind contaminants with high affinity. The proteins that bind nonspecifically to the common matrix types have been identified and listed for reference[86–88].

1.2.2 Microarrays

Microarrays are robust high-throughput screening tools that have been significantly developed and upgraded[89,90]. Their application for drug target identification can proceed in several ways. The first strategy, protein microarrays, utilizes immobilization of different purified proteins onto glass or silicon surface. The protein microarray is incubated with the labeled small molecule in solution and after several washing steps, target protein is recognized according to array position. Schreiber and colleagues utilized this approach for target identification of small molecular inhibitor of rapamycin (SMIR), which suppresses the rapamycin effect. The authors used biotinylated variants of SMIR and fluorescently labeled streptavidin to probe the yeast proteome chip. They found two proteins with previously unknown function. Both proteins are associated with phosphatidylinositol (3,4)-bisphosphate, suggesting connection with the mTOR pathway involving phosphatidylinositides[91].

The second strategy, small-molecule microarray (SMM) was developed by MacBeath and Schreiber in 1999[92]. SMMs enable to evaluate thousands of chemical structures against a large number of protein targets. A small-molecule library is immobilized on microarray, screened against potential cell lysate or purified proteins and the small molecule bound to target is identified by immunoassays[89].

Another interesting approach, transfected cell microarray, was developed by Ziauddin and Sabatini. This unique method called reverse transfection cell microarray, couples genomic and proteomic approaches. Plasmid cDNA in gelatin solution is spotted on defined area of glass slide. Dried spots are briefly exposed to transfection reagent and covered by mammalian cells in medium. Cells are transfected by different cDNA and each cell cluster overexpresses specific protein. Radiolabeled chemical compound is added and its target is detected by autoradiography. Experimental workflow was verified on FK506-FKBP12 interaction and affinity of dopamine antagonist for the dopamine D1 receptor[93].

The last method named desorption/ionization on silicon (DIOS) - modification of MALDI is a matrix-free method utilizing laser desorption and ionization on porous silicon surface[94]. This enables on probe direct-binding assay to identify molecular target. Purified proteins are immobilized on porous silicon probe surface. Immobilized proteins are incubated with active compounds, and nonspecific small molecules are washed out. Following direct on probe TOF-MS analysis can directly identify the binding partners of specific protein[95]. Zou and colleagues tested DIOS on Bovine Serum Albumin (BSA) binding partners. They immobilized

BSA on silicon surface and incubated BSA-covered probe with a mixture of two molecules - ketoprofen, a compound which binds BSA and sulpride which does not. Ketoprofen signal (and no sulpride signal) was observed after TOF-MS analysis[95].

A large number of microarray variations and extension have been developed. Each has its advantages and disadvantages, but some features have microarrays in common. Microarrays are high-throughput screening methods that enable study of the interaction of large numbers of small molecules with their cellular target (and the reverse) in one experiment. They expose all biotargets uniformly; low abundant proteins are not diminished. The necessity for molecule immobilization is a limiting factor. Most experiments are conducted under non-physiological conditions (except in the case of reverse transfection cell microarray). Another restricting factor is limited availability of purified proteins for protein microarrays as well as the necessity for trackable chemical compounds that can alter their binding potency[19,96,97].

1.2.3 Proteomics in drug target identification

Proteomics is studying protein identification, protein-protein interaction, post-translational modification, quantification, domain structure or protein activity. The main comprehensive and versatile tool of proteomics is mass spectrometry. It is based on measuring exact mass (exactly mass to charge – *m/z* ratio) of whole proteins or their fragments (peptides) to get list of masses. Subsequently, masses are searched by protein databases to get list of identified proteins. The main parts of mass spectrometer are ion source, mass analyzer and detecting system[98]. Ion source produces ionized peptides/proteins in gas phase. There are two main soft ionization techniques used in proteomic – MALDI and ESI (electrospray ionization)[99,100]. MALDI is based on mixing protein/peptide mixture with matrix that absorbs laser energy and transfers it into the analyte. It generates mainly singly charged ions $[M+H]^+$. ESI ionization generates ions from solutions, therefore is usually coupled to liquid based chromatographic tools as a HPLC (high-performance liquid chromatography). The ions generated by ESI are multiply charged and are produced by high voltage applied in the interface between the end of separation pipeline and inlet of mass spectrometer[98,101].

Mass analyzer is the key part of mass spectrometer where ions are separated to get their exact mass. There are four main types of analyzers: time-of-flight (TOF), ion trap (IT, linear ion trap LIT, LTQ Thermo Scientific version of LIT Orbitrap, quadrupole (Q, triple quadrupole -TQ) and Fourier-transform ion cyclotron resonance (FTICR). The simplest analyzer TOF is based on measurement time of flight in the vacuum of flight tube. Ions are accelerated and their

time of flight by is measured – heavier ions reach detector slower than lighter ones. IT, Orbitrap and FTICR separate ions according their resonance frequency. Orbitrap is powerful tool from Thermo Scientific based on ion separation in an oscillating electric field. In FTICR instrumentation ions are retained in magnetic field and their m/z ratio is measured according their frequency. Q separation is based on m/z ion stability in electrical fields between four parallel rods[98,102–104]. Table 1 shows comparison of main features and applications of the most used mass spectrometers.

There are two main proteomic approaches: top-down and bottom-up proteomics[105]. Briefly, bottom up proteomics is the most popular and based on proteotolytic digestion (usually trypsinization) of proteins prior MS analysis of peptide fragments. This method is used mainly for analysis of high complex samples. On the other hand, top-down approach measure masses of intact proteins. This approach has higher sequence coverage, enables to characterize post-translational modifications, and full characterization of proteoforms. Recent developments in instrumentations or bioinformatics tools allowed top down proteomic to be more and more popular[106]. This approach is currently use for PTM identification[107], quantitation[108], protein identification from complex sample[109] or single proteins[110].

MS Instrument	Ion source	Mass resolution	Mass accuracy	Sensitivity	Dynamic range	Applications
LIT (LTQ)	ESI	2000	100 ppm	femtomole	1e4	Bottom-up protein identification of complex samples, high-throughput analysis, LC-MS^n
TOF-TOF	MALDI	10000-20000	<5 ppm*	femtomole	1e4	Protein identification by peptide mass fingerprinting, sequence tagging by collision induced dissociation MS/MS
TQ	ESI	2000	100 ppm	attomole	1e6	Peptide and protein quantification (SRM, PTM detection, precursor ion and neutral loss scanning)
LTQ-Orbitrap	ESI, MALDI	100000	2 ppm	femtomole	1e4	Protein identification from high complexity mixtures, PTM characterization, top-down proteomics, quantification
Q-TOF	MALDI ,ESI	10000	2-5 ppm	attomole	1e6	Protein identification from high complexity mixtures, PTM identification, bottom up, top-down proteomics
FTICR	ESI, MALDI	50000-750000	<2 ppm	femtomole	1e3	High mass accuracy protein identification, PTM characterization, top-down, bottom-up proteomics

*with internal calibration

Table 1. Comparison of MS instruments and their main characteristics (adapted from[101,102]. Mass resolution is ability to separate two peaks with similar m/z ratio. Mass accuracy defines uncertainty in measurement in ppm units. Dynamic range is range between the largest and smallest detectable signal.

Mass spectrometry is an indispensable part of protein target identification. It can be used as a stand-alone method or with combination with gel-based or liquid chromatography separation. 2DE and alternatives like a DIGE (Difference Gel Electrophoresis)[111] enable identification and quantification of protein target under drug treatment. In these experiments

protein profiles of treated and untreated samples are compared and evaluated by 2DE (alternatively DIGE) and/or by different quantitative labeling. Excision of spot of interest, digestion and MS analysis enable identification and quantification of up- and down-regulated proteins[112,113]. Differential expression experiments using gel-based methods enabled the finding of potential targets of drugs such as staurosporine[114], vinblastine and rapamycin[115]. The quantitative approach utilizing peptide labeling was used for imatinib[116] and vorinostat target elucidation[117].

Drug-target identification frequently requires the relative or absolute quantification of one or more proteins in multiple samples. Protein identification and quantification is performed downstream of an affinity purification. The sample preparation protocol, the mass-spectrometer and the quantitation procedure (Fig. **7**) is chosen according the experiment.

1.2.3.1 Quantification using isotopic labels

Quantification has traditionally been done using isotope tags. Common tagging protocols include the Stable Isotope Labeling with Amino acids in Cell culture (SILAC), Isotope Coded Affinity Tags (ICAT), Tandem Mass Tags (TMT) and the Isobaric Tag for Relative and Absolute quantification (iTRAQ)[118–121]. SILAC and ICAT are isotopic labeling protocols that use isotopes of hydrogen, carbon and nitrogen (^{2}H, ^{13}C, ^{15}N). They are based on a mass-difference between the light and the heavy isotope labels. The mass difference causes a shift in the peaks of the labeled peptides relative to the unlabeled peptide. The intensities of the two peaks indicate the relative quantities of the two peptides. SILAC involves the labeling of cells in culture in minimal media. Cells are grown in media containing normal or labeled amino acids. Labeled amino acids are incorporated into cellular proteins via natural biosynthetic pathways. Five-ten cell doublings later, the two cell samples are harvested, mixed, processed and trypsinized and subsequently analyzed by mass spectrometry. Because samples are labeled during cell culture, the method is suitable only for samples derived from culture and not for samples from other sources. Samples that cannot be labeled in culture may be labeled after collection using the ICAT, TMT or iTRAQ labeling procedures.

ICAT resolves some of the issues of SILAC[119]. The ICAT tag consists of three groups- a thiol-reactive group, an isotope coded tag and a biotin moiety. A cleavable linker is sometimes included between the isotope tag and the biotin to facilitate purification[122]. The two collected samples are reduced and trypsinized and incubated with ICAT labels to allow thiol reactive groups to react with the reduced thiols on cysteine residues. Differentially labeled

samples are then mixed and subject to mass-spectrometry. The property of thiol specificity is at once useful and problematic - useful because tagged peptides can be purified, and problematic because peptides lacking cysteines are lost[123].

1.2.3.2   Quantification Using Isobaric Labels

Labeled quantification evolved further with the introduction of isobaric tags called Tandem Mass Tags (TMTs) and isobaric tags for relative and absolute quantification (iTRAQ)[120,121]. Isobaric tagging allows analysis of more than two samples and does not require the isolation of tagged peptides. TMTs consist of at least three groups, a reporter group, a mass normalization group and a protein reactive group. These tags are amine reactive and are therefore more likely to have a higher efficiency of labeling than ICAT tags. TMTs are available in sets of two, six or ten labeling reagents (2-plex, 6-plex and 10-plex respectively)[120,124]. Tags of a particular set have identical mass. For this reason, two identical peptides tagged with different TMTs will co-elute from a reverse-phase column and have the same MS1 spectral peaks. Depending on the labeling reagent, two, six or ten samples can be simultaneously analyzed by MS. The control and treated sample sets are trypsinized, labeled, pooled and analyzed. Upon peptide fragmentation of selected MS1 precursor-ions by collision-induced dissociation in the mass spectrometer, the MS2 spectrum exhibits the reporter group peaks in addition to the characteristic peptide fragmentation peaks. The intensities of the different reporter group ions indicate the relative quantities of the peptide in the different sample sets. Untagged peptides will not have reporter-group peaks in the MS2 and will therefore be disregarded in the quantification process. This makes isobaric tagging more accurate than the ICAT labeling. TMT has been used in the determination of targets of antidepressant drugs[125]. The above description of tandem mass tags is also true of the iTRAQ tags, except that iTRAQ is also meant for absolute quantification. iTRAQ tags come in 4-plex and 8-plex reagent kits and enable the use of up to 8 samples[121,126].
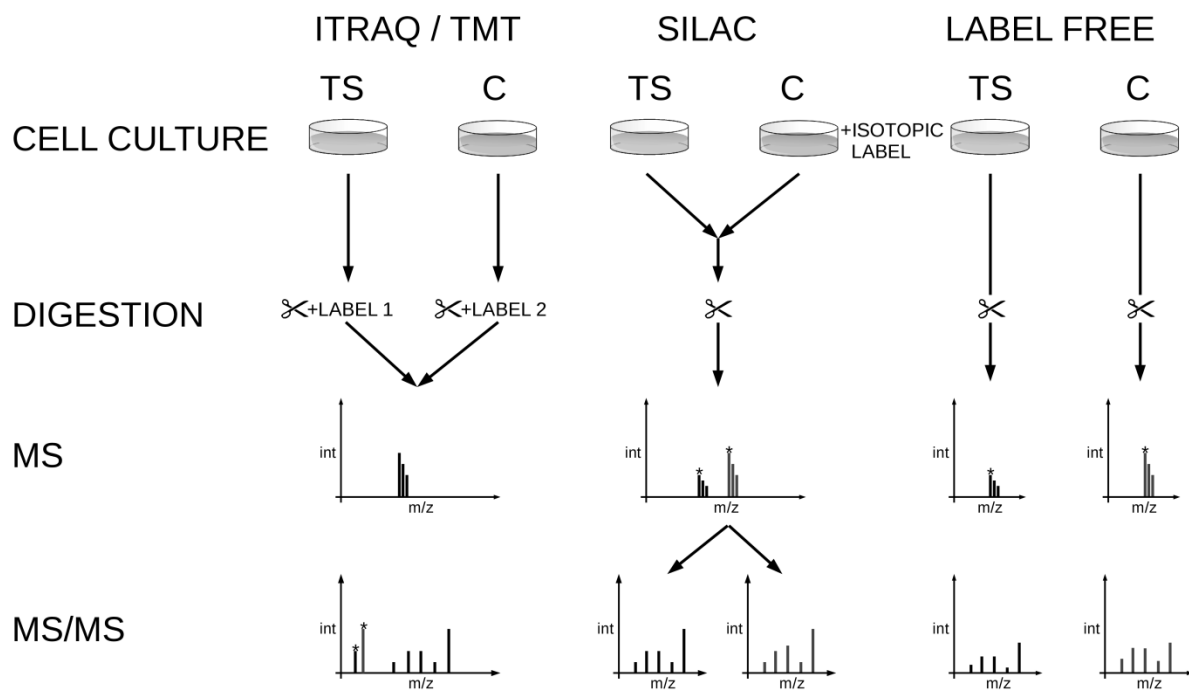
Figure 7. A principle of mass-spectrometry peptide-labeling techniques: iTRAQ/TMT labeling is based on isobaric tag and quantification is done at the MS/MS level. SILAC labeling is based on metabolic incorporation of isotopic label into cell culture and quantification is done at the MS level. This is ideal for high resolution mass spectrometry where MS has usually higher accuracy than MS/MS. However, SILAC is more or less limited to cell cultures. Label free techniques rely on peak-intensity, spectral-count, peptide count and/or fragment –ion intensity for quantification of protein. TS – tested sample, C – control[2].

1.2.3.3   Quantification by selected reaction monitoring (SRM)

SRM is the detection and quantification of specific proteins in a sample. It is based on the prior knowledge of one or more proteotypic peptides from the protein of interest. A proteotypic peptide is one which is always formed upon protein digestion and has complete or near complete ionization. The mass-to-charge ratio of a peptide's precursor- and fragment-ions and its chromatographic retention time are characteristic of the peptide and together constitute a "transition". There may be more than one transition per peptide. The mass spectrometer is directed to follow pre-specified transitions for a specified duration and to measure their intensities. The quantity of the peptide may be calculated from a standard curve of an identical labeled peptide (intensity versus concentration). SRM transitions for most of the human, yeast

and bacterial proteins are now publicly available online in the SRMAtlas[127]. SRM can precisely measure multiple proteins in a mixture of proteins based on transition information.

1.2.3.4 Label free quantification

Label free techniques are relatively new convenient methods that can be applied to multiple datasets and to datasets retrospectively without laborious and costly labeling steps. Two basic approaches were introduced in label free mass spectrometry techniques. The first is a relative quantification of peak intensity of LC/MS [128]. This method is assigned to electrospray ionisation because it was found that signal intensity correlates with ion concentration[129]. Another label free approach is named spectral counting[130]. This method is based on the fact that the number of identified peptides or sum of spectra (spectral count) is dependent on the protein abundance[128]. The main advantage of spectral counting against peak intensity is that this method is computationally simple without need to use LC separation.

1.3 Validation techniques

Following drug target identification, it is necessary to validate the results. There is a number of possibilities for validating potential small molecule-target interactions. The choice of method depends on the compound-target interaction, target protein properties and availability of equipment.

One of the most sensitive and accurate methods for ligand-protein interaction is X-ray crystallography. There are several possibilities for obtaining protein-ligand crystal complexes: cocrystallization of protein and ligand, soaking ligand into crystallized proteins, co-expression of protein and ligand and protein purification in the presence of ligand[131]. Crystallography allows us to determine the structure of protein ligand complexes. The method is expensive owing to the necessity for large amounts of high purity target protein and the crystallization process is time-consuming[132].

Another approach to drug target validation is Nuclear Magnetic Resonance (NMR) which involves small molecule binding through changes in the resonant frequencies of NMR-active nuclei[133]. There are two approaches to confirming small molecule-ligand interaction. The first is based on the resonance of target protein. This allows study of any kind of small molecules with no upper limit to affinity and allows identify small molecule binding sites. On

the other hand, there is need for isotopically labeled target protein. Moreover, the protein has to be highly soluble and the size of the protein is limited. The second approach is based on ligand resonance. The main disadvantage here is the restriction on analyzing ligands with high affinity. There is no requirement for isotopically labeled protein and the size of protein is unlimited[134].

Isothermal titration microcalorimetry (ITC) is another way of small molecule-target protein validation. ITC is versatile and frequently used method. It enables to detect the change in heat or enthalpy in any chemical reaction and therefore to characterize drug target interactions. During ITC experiments, ligand is titrated into the sample cell with target protein in appropriate buffer. The heat change is measured: either energy (heat) received from surroundings (endothermic reaction) or heat release in the case of exothermic reaction. The main advantage is that the experiment runs in a physiological buffer and there is no need for immobilization or tagging of ligand[135]. On the other hand, ITC does not provide us with structural information on the binding site. The protein and ligand also need to be dissolved in the same buffer and the compound has to be highly soluble.

New bioinformatics tool molecular docking is widely used last two decades in drug discovery and validation. Molecular docking is based on *in silico* prediction the most favorable conformations of protein-ligand (or other biological molecules) interaction. It can also predict potential and activity of newly designed drug or help to predict optimization of its structure. It is based on computational simulation of protein-ligand interaction with the minimum of free energy in the specific conformation. Affinity scoring function ΔG (kcal/mol) is value used for ranking the candidate. It is function of sum of electrostatic and van der Waals interactions. There are many programs and algorithms used in this field that are under continuous improvement and optimization[136].

1.4 Relating identified targets to pathways

All these methods can provide us with big amount of data. Understanding to all the consequences is not often easy. Acquired results as a list of target proteins, mRNA, metabolites and their cell levels are necessary to connect with all the cell processes and networks.

The observed effect of a drug is the result of interaction of multiple cellular and physiological systems. Systems biology has contributed to this realization. This is a relatively new discipline but has become indispensable part of drug-development in recent years. It deals

with the relationships between the different components of a system to determine how they interact and how they function as a whole[137,138]. It enables the integration of genomic and proteomic data with environmental data to better describe the organism's phenotype and to predict its response to a stimulus. Systems biology has developed computational tools for viewing a potential target in the larger cellular or physiological context and to increase the confidence of target identification. They include MetaCoreTM (Thomson Reuters), Pathway Studio (Elsevier), IPA (Ingenuity Systems), the Software Tool for Researching Annotations of Proteins (STRAP), Gene Map Annotator and Pathway Profiler (GeneMAPP), Pathway Tools and the Database for Annotation, Visualization and Integrated Discovery (DAVID)[139–142].

1.5 Quinolones and their derivatives

1.5.1 Quinolones

Quinolones are well known synthetic antibacterial compounds which have been discovered in early 1960s. They have been used for treatment of urinary tract infection, respiratory tract infections and later as broad-spectrum antibiotics. Till today, plenty of quinolone analogs have been developed to enhance their activity. These compounds are appreciated mainly for their high potential, bioavailability, relatively low toxicity and favorable pharmacokinetics. It has been shown that they have antibacterial, antiviral, antimalarial and also anticancer activities[143]. The mechanism of action is binding DNA topology enzymes, namely gyrase and topoisomerase IV (Fig. 8). These enzymes are essential for processes as replication, recombination transcription and chromosome separation including changes in DNA topology[144].
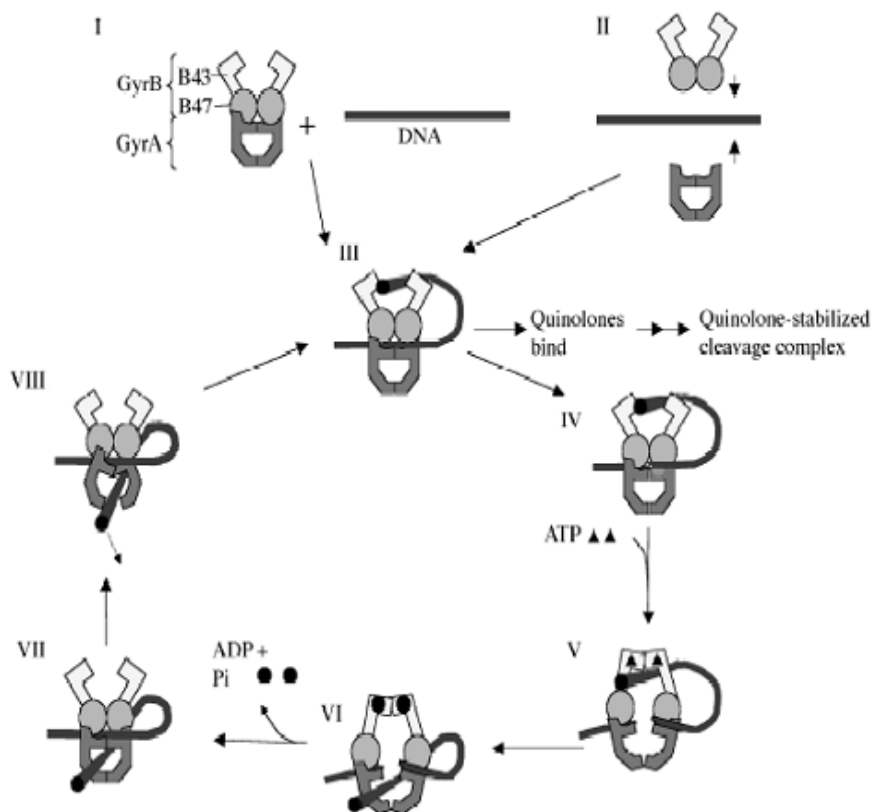
Figure 8. Schematic picture of the quinolone binding effect on gyrase supercoiling cycle. Quinolones binds gyrase and stabilize cleavage complex (stage III) what is leading to double strand breaks and inhibition of topology dependent processes[145].

Quinolone binding to the enzyme creates stabilized enzyme-DNA complex. This "toxic" cleavable complex (Fig. 9) is able to produce double strand brakes and is responsible for inhibition of replication fork movement and inhibition of transcription. Till today, there was patented or published more than 10000 quinolone derivatives what shows their potential[146,147].
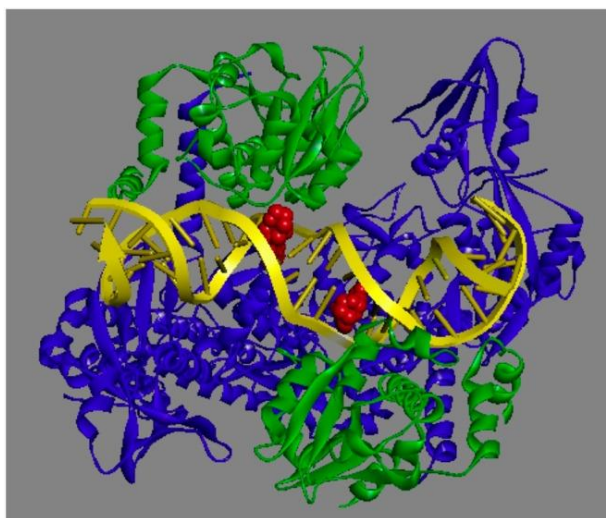
Figure 9. Crystal structure of a quinolone moxifloxacin-topoisomerase IV−DNA cleavage complex. The catalytic core of the enzyme is depicted. Moxifloxacin is colored red, the topoisomerase IV subunit A in blue and B subunit is green, DNA is colored yellow. (adapted from[147])

1.5.2 Quinolinone derivatives

Quinolinone derivatives have been studied intensively, especially in the context of their various biological activities. Plenty of derivatives were developed and studied to optimize structure to enhance their advantageous activities.

2-phenyl-3-hydroxy -4(1*H*)-quinolinones (Fig. 10) are ones of the very promising group of these derivatives that are currently studied for their favorable biological activities.

1.5.2.1   2-phenyl-3-hydroxy -4(1*H*)-quinolinones

2-phenyl-3-hydroxy -4(1*H*)-quinolinones (3-HQs) are considered as aza-analogues of flavones, compounds with variety of biological and spectral properties. Many synthetic routes of their preparation have been developed since 1971[148]. The key reaction – cyclization of phenacyl ester of anthranilic acid were developed by Jirman and Hradil in 1995[149]. Further, introducing carboxy moiety to the position 7 was important step for derivatization 3-HQs by phenacylesters, amids, salts and other carboxy moieties. This optimization enabled possibility to enhance biological activity, solubility and bioavailability[150]. Solid phase organic synthesis

(SPOS), efficient method with high purity and high yield has been employed for synthesis of hydroxyquinolinones in 2007[151]. The advantages of SPOS are immobilizing compounds on a resin and further use convenient washing steps that facilitate all synthetic procedures. SPOS is currently one of the most powerful methods for drug discovery and their optimization. It enables fast synthesis of highly diverse chemical libraries for SAR information.
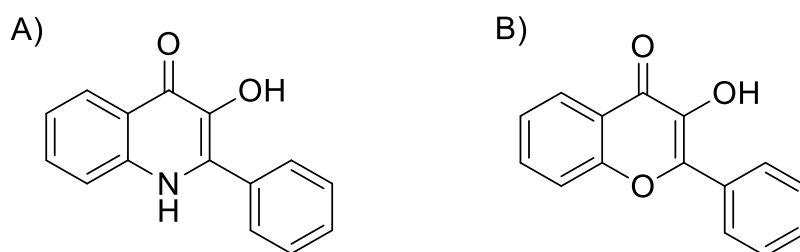
Figure 10. A) Basic structure of 3-HQs and B) flavone

Various biological effects of these compounds have been found in the last decades. For these substances were similarly to the parent derivative 4*(1H)*-quinolinones, well known antibiotics, demonstrated antibacterial activities. Sui with co-workers made SAR study of specific group of 3-HQs. They proved inhibition of bacterial gyrase and mammalian topoisomerase II. The compounds showed different SAR to each of the enzyme. This shows different 3-HQs binding sites for both enzymes[152].

3-HQs have been also demonstrated as immunosuppressive agents. Lymphocytes are mostly in quiescent state upon stimulation by antigen or polyclonal mitogen. Inhibition of concavaline A activated lymphocytes was tested by MTT [3-(4,5-dimethylthiazol-2-yl)-2,5-diphenyltetrazolium bromide salt] assay. Some compounds showed preferential inhibition activity to stimulated versus quiescent lymphocytes[153]. 3-HQs structures displayed inhibition activity of inosine monophosphate dehydrogenase (IMPDH). IMPDH enzyme that is responsible for guanosin *de novo* synthesis. The enzyme is crucial for differentiation and proliferation of cells. Therefore, proliferating lymphocytes and cancer cell lines are interesting targets for these structures. Specific 3-HQs derivates were tested by IMPDH assay measuring spectrophotometric NADH (nicotine amide adenine dinucleotide) increase and many potent inhibitors were discovered[154].

Only few studies[37,148,150,155–159] have described an anticancer activity of these compounds until today. Several normal tissues and cancer cell lines were tested for *in vitro* anticancer activity by using the MTT assay or NCI (National Cancer Institute) *in vitro* drug

evaluation system. NCI system involves testing against three cancer cell lines. Compounds significantly reducing the cell growth (to approximately 32 %) of at least one of them are further tested on extended panels of 60 cell lines. Chloro derivates 3-HQs were tested for cytotoxic activity by this method in 2004. Some compounds were active for example against breast cancer (MCF7), melanoma (M147), ovarian cancer (IGROV1) and some others[158].

Later, series of 2-phenyl-3-hydroxy-4(1*H*)-quinolinones-7-carboxylic acid (Fig. 11) were tested for their cytotoxic activity by MTT assay. MTT assay is based on metabolizing of MTT 3-(4,5-dimethylthiazol-2-yl)-2,5-diphenyltetrazolium bromide salt to formazan by viable cells. The purple color of dissolved formazan is measured spectrofotometrically. They tested this group of 3-HQs by MTT assay on cancer cell lines CCRF-CEM (T-lymphoblastic leukemia), CEM-DNR (T-lymphoblastic leukemia resistant to doxorubicine, expressing multidrug resistant phenotype depending on multidrug resistance gene 1-mdr1 and lacking topoisomerase IIα gene), A549 (lung adenocarcinoma), K-562 (human myeloid leukemia), and K562-TAX (human myeloid leukemia resistant to paclitaxel, expressing multidrug resistant phenotype depending on P-glycoprotein - pgp gene). When the carboxy moiety remained unmodified, the cytotoxic activity is weak. The reason can be low permeability through plasmatic membrane. By introducing the phenacylester group instead of the carboxylic group, the cytotoxicity increased sharply to micromolar and submicromolar concentrations[150].
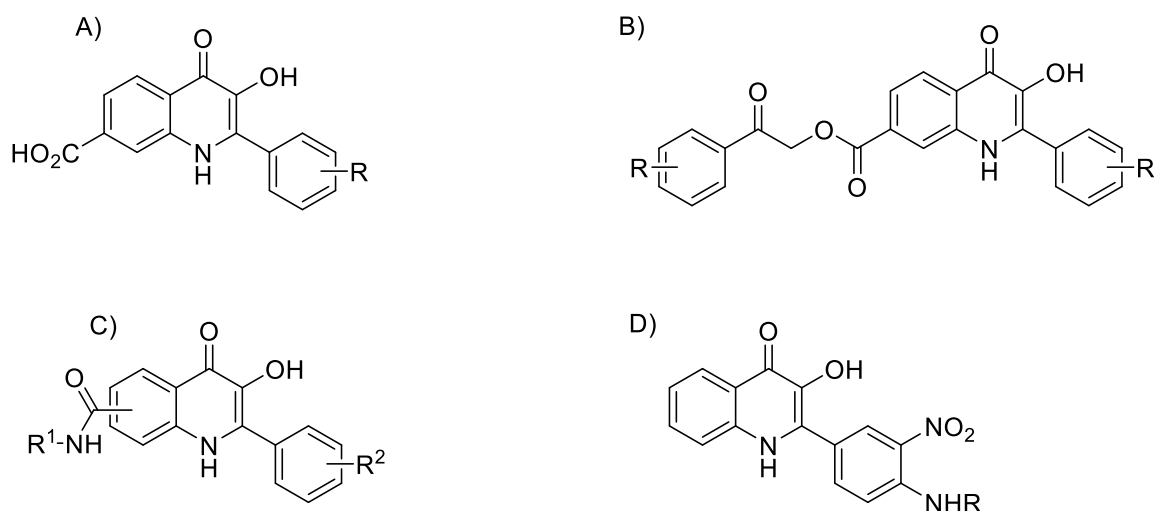
Figure 11. Structures of A) 2-phenyl-3-hydroxy-4(1*H*)-quinolinones-7-carboxylic acid B) 2-phenyl-3-hydroxy-4(1*H*)-quinolinones-7-phenacylester   C)   2-phenyl-3-hydroxy-4(1*H*)-quinolinones-7-carboxamide D) 3-nitro 4-amino 3-HQs

Another group 3-nitro 4-amino 3-HQs was tested again by MTT assay on CCRF-CEM, CEM-DNR, K562, K562-TAX and A549 cell lines. All derivatives were active in micromolar concentrations on CEM cell line. Moreover, these compounds also exhibit high cytotoxic activity against multidrug resistance cell lines overexpressing PGP1 and/or MRP1 proteins from family of ABC (ATP binding cassette) transporters (K562-TAX and CEM-DNR, respectively)[148].

Further, vast SAR study of 2-substituted-3-hydroxyquinolin-4(1H)-one-carboxamides was done in 2011. The effect of carboxamide position in 6-8 and substitution was described and new potent compounds were found. Optimization of carboxamide substitution leads to the increased cytotoxic activity in submicromolar concentration (about 250 nM)[155]. Follow-up study from 2015 is focused on in solution synthesis of 2-substituted-3-hydroxyquinolin-4(1H)-one-5-carboxamides. 2-Aryl-3-hydroxyquinolin-4(1H)-ones generally exhibit dual fluorescent properties with two separated emission bands. These features show their potential application as molecular probes and in fluorescence labeling[156,160–162]. It was proved that different positioning of carboxamide group in 3-HQs affect fluorescence properties of 3-HQs[160]. Study of 2-substituted-3-hydroxyquinolin-4(1H)-one-5-carboxamides displayed similar features as 7 isomers. These structures can be therefore used as molecular probes or pH indicators. Furthermore, fluorescence microscopy study displayed capability of 5-carboxamides entering live cells with specific cytoplasmic staining (Fig.12). The cytotoxic activity was comparable with phenacylester derivatives mentioned above (micromolar and submicromolar cytotoxic activity)[156].
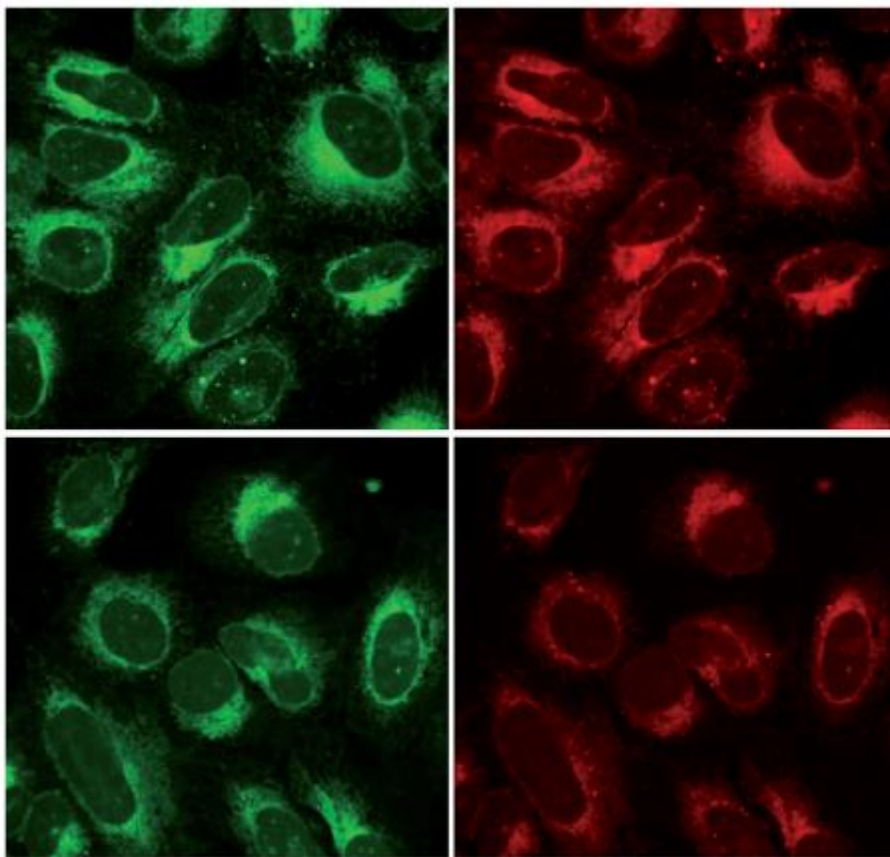
Figure 12. U2OS osteosarcoma cancer cells treated with 2-substituted-3-hydroxyquinolin-4(1*H*)-one-5-carboxamide. The cytoplasmic staining is displayed in green and red color[156].

The mechanism of action of 2-phenyl-3-hydroxy -4(1*H*)-quinolinones hasn´t been still elucidated. Gyrase and topoisomerase inhibition has been proven in discussed derivatives[152]. In view of the fact that some mentioned derivatives are also active on cell lines with topoisomerase deletion, there are probably additional targets.

1.6 Eukaryotic Elongation factor 1 alpha (eEF1A)

1.6.1 The eEF1A and its complexing proteins

eEF1A is one of the most abundant proteins in the cell, containing 1-3% of the total protein content. It is a member of G protein family and catalyzes GTP-dependent positioning of aminoacyl tRNA (aa-tRNA) into the A site of ribosome during elongation step of protein

synthesis[163,164]. In higher vertebrates, it exists in two forms (eEF1A1 and eEF1A2) encoded by two distinct genes[165]. While eEF1A1 is highly expressed in all tissues, eEF1A2 is expressed only in adult muscle, heart, brain, and neuron cells in non-proliferation state[166,167]. In spite of the fact that these two isoforms share 96 % of amino-acid sequence identity and 75% nucleotide identity[168], they exhibit distinct functions. The only exception is their similar canonical translational function, but they exhibit distinct binding affinity for GDP and GTP. eEF1A2 has lower affinity for GTP than eEF1A1. Moreover, they show various pro-apoptic and anti-apoptic activity, different phosphorylation pattern and involvement in cell signaling pathways[163,164] . In addition, eEF1A requires guanosine exchange factor eEF1B promoting GDP/GTP exchange. In *saccharomyces cerevisiae* eEF1B comprises of two subunits eEF1Bα and eEF1Bγ, in plants there is one more subunit eEF1Bβ, and in metazoan eEF1Bδ, respectively. eEF1Bα, eEF1Bβ, eEF1Bδ have nucleotide exchange function and eEF1Bγ has anchoring function to localize eEF1B to the endoplasmic reticulum (ER)[169].

eEF1A crystal structure include three domains. Domain I (1) binds GTP/GDP and is made of Rossmann fold topology, domain II (2) is involved in aa-tRNA binding and domain I and II interact with EF1Bα, domain III (3) interacts with actin. Domain II and III is formed from two beta sheets creating beta barrels (Fig. 13)[170–172].
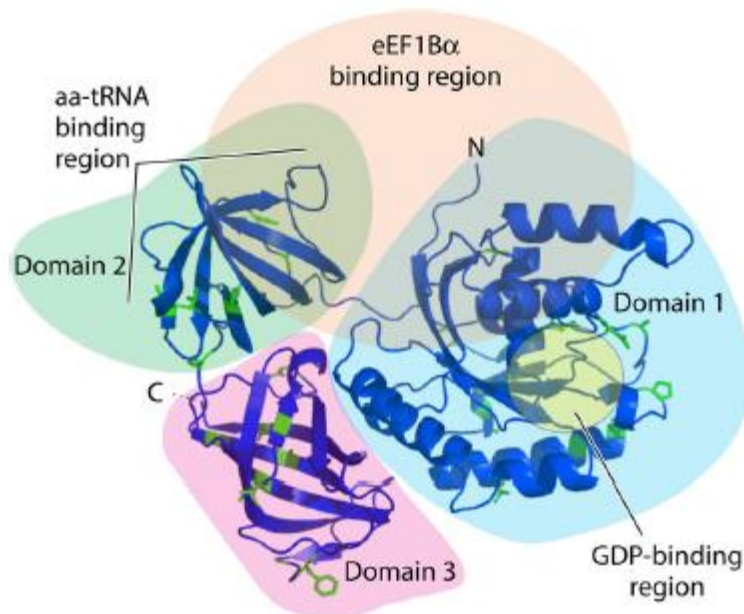
Figure 13. Three-dimensional (3-D) model of yeast homolog of eEF1A1. Domain 1 (blue), domain 2 (green), domain 3 (pink), EF1Bα binding region (peach) and aa-tRNA binding region, GDP-binding region (yellow) are depicted. In green are different eEF1A2 aminoacid sequences displayed[171].

1.6.2 Role of eEF1A in translation

Eukaryotic protein synthesis is one of the most complicated biochemical process in the cell. During translation, collaboration of many molecules (mRNA, tRNA, soluble initiation, elongation or release factors, ribosomes, etc.) is needed. The process of translation is divided into three steps: initiation, elongation and termination. After initiation step during which Met-tRNA^{Met} is paired with codon AUG, the nascent peptide is produced cyclically in elongation step. Elongation factor alpha 1 (eEF1A, former named eEF1α) delivers aa-tRNA into the A site of the ribosome in the first step of elongation. The ribosome contains (except the A site) P site with the growing nascent peptide chain. EF1A is G protein, therefore it is active in GTP-bounded state. As the intrinsic GTPase activity of eEF1A is slow, the GTP/GDP switch enables nucleotide exchange factor elongation factor 1 beta (eEF1B, former eEF1β). This factor enables cyclic regeneration of eEF1A for delivery aa-tRNA into the A site of the ribosome. After creating a new peptide bond by ribosomal peptidyl transferase, the peptidyl-tRNA: mRNA is translocated from the A site into the P site by elongation factor 2 (EF-2) in the third elongation step. This step enables positioning the next codon into the A site. This process is cyclically repeated (Fig. 14)[173].
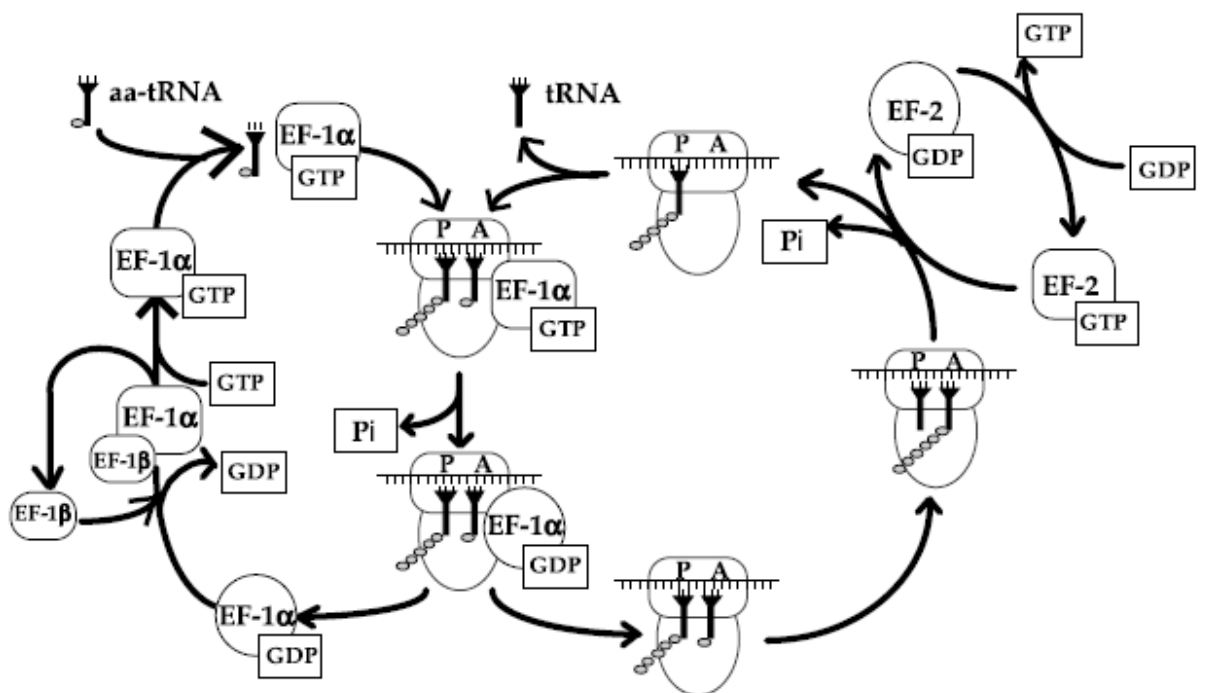
Figure 14. The role of eEF1A (eEF-1α), eEF1B (eEF1-β) and EF-2 in translation elongation[173]

1.6.3 Non-canonical function of EF1A

eEF1A is called moonlighting (multifunction) protein. It´s primary function is participation in protein biosynthesis, but it also has many non-canonical functions that this protein has gained during evolution.

1.6.3.1 Nuclear export

One of the non-canonical function of eEF1A is the nuclear transport. The participation of eEF1A on tRNA nuclear export has been studied on *S. cerevisiae* mutant in aa-tRNA binding domain II of eEF1A. This mutant showed defects in the nuclear export of aa-tRNA and accumulation of tRNA in the nucleus. Although it is a question if aa-tRNA transport can be considered as a non-canonical function[170,174], as the binding aa tRNA is connected with the translation function. However, eEF1A was found to be involved in transcription-dependent nuclear protein export in mammals. This role of eEF1A was found to be executed from the cytoplasmic side of the nuclear envelope[175]. In previous studies of nuclear transport eEF1A was localized in the cytoplasm[175–177]. On the other hand, eEF1A was shown to be able to access the nucleus, as it was detected in nuclear export mutant (msn5Δ, yeast analogue of exportin-5), where eEF1A was found to be essential for tRNA nuclear transport[178]. Moreover, Mingot and coworkers described nuclear function of eEF1A in 2013. Here, eEF1A participate on the nuclear transport of SNAG-containing proteins (Snail transcription factors) in aa-tRNA:exportin5:EF1A complex from the nucleus[179].

In 2014, Nudler *et al.* published the involvement of the isoform eEF1A1 (but not isoform eEF1A2) in the heat shock response. During stress reaction eEF1A1 was found to recruit HSF-1 (heat shock factor 1) regulator to HSP70 (heat shock protein 70) promoter to activate its transcription. eEF1A1 then associates with RNA polymerase II and stabilizes HSP70 mRNA. Elongation factor further facilitates HSP70 mRNA nuclear transport through nuclear pore complex (NPC) to the ribosomes (Fig. 15)[180].
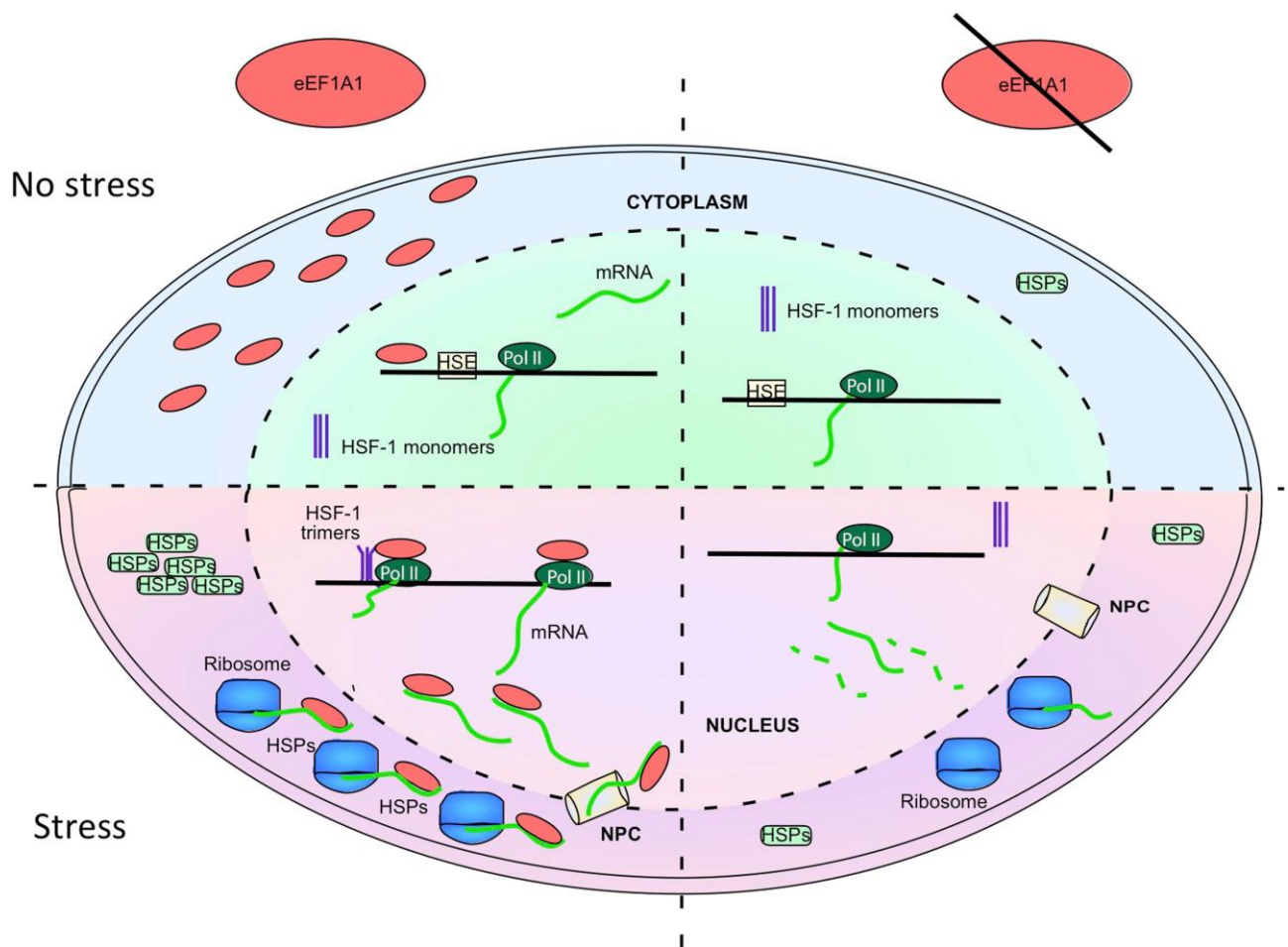
Figure 15. eEF1A1 connecting HSP70 transcription to translation. In top left quadrant is normal state depicted, eEF1A1 resides mainly in cytoplasm as a part of translational machinery, upon stress (heat shock) eEF1A1 associates with RNA polymerase II and brings activator HSF-1 to the HSP70 promoter HSE (heat shock elements). Further stabilizes its mRNA and transport it to the ribosome (bottom left quadrant). In eEF1A1 knockdown the level of HSP70 remains low (right quadrants)[180].

1.6.3.2 eEF1A1 in protein degradation

Couple of studies support the idea that eEF1A has also an antagonistic function as a part of the degradation process. The first study displayed eEF1A as a factor essential for ubiquitin dependent degradation of N^α-acetylated proteins by 26S proteasome complex[181]. Moreover, eEF1A was found to interact with nascent polypeptide chains of different length and sequence and can bind misfolded proteins acting as a chaperone[182]. This is in agreement with

the fact that EF-Tu (elongation factor thermo-unstable, prokaryotic analogue of eEF1A) demonstrates chaperon like activities[183]. Later, Chuang *et al*. published the ability of eEF1A to bind ubiquitinated proteins and the proteasome subunit Rpt1. They created model consistent with their results and other studies – eEF1A can recognize and mediate the degradation of damage nascent proteins (Fig. 16)[184].
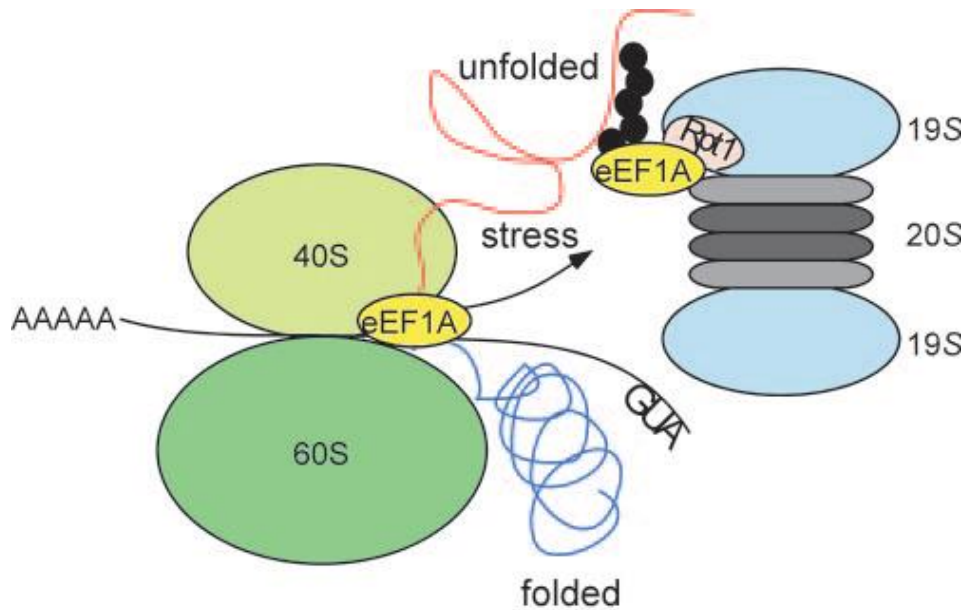
Figure 16. Model of potential role of eEF1A in protein degradation. eEF1A can binds ubiquitinated proteins and the proteasome subunit Rpt1and further mediate the degradation of misfolded nascent proteins[184].

1.6.3.3 eEF1A and the cytoskeleton

In the last decades many studies support the connection between the cytoskeletal organization and protein synthesis. The main cytoskeletal role in this interaction is played by actin. Data support the hypothesis that cytoskeleton participates in the regulation of protein biosynthesis and its spatial organization. Many parts of translation have been found to associate with the cytoskeleton. For example, eukaryotic initiation factors, eukaryotic elongation factors, aminoacyl-tRNA synthetase or Cap binding proteins[185].

The first study supporting this hypothesis comes from 1990. The eEF1A was isolated as an actin-binding protein in *Dictyostelium discoideum*[186]. Later, this interaction was confirmed in several species[187,188] and it was found that eEF1A is able to cross-link F-actin and generate actin bundles *in vitro*[189]. F-actin inhibits aa-tRNA binding to eEF1A and this two interactions are mutually exclusive[190]. It seems that there are two forms of eEF1A, one GTP bound – translationally active, and second F-actin binding – translationally inactive. Another study shows an important relationship between eEF1A, eEF1Bα and F-actin. This study demonstrates that eEF1Bα and F-actin binding eEF1A are mutually exclusive. eEF1A in complex with eEF1Bα is unable to bind and cross-link actin[191]. These results demonstrate complex relationships between eEF1A, eEF1Bα and F-actin resulting in translational control and cytoskeleton organization. A hypothetical model of connection between translation a cytoskeletal organization was depicted by Kim and Coulombe (Fig. 17)[185].
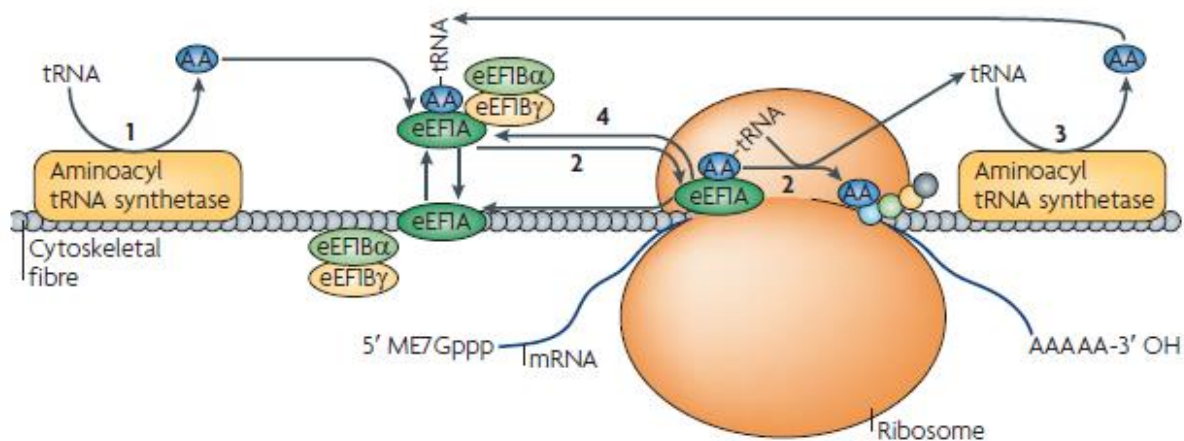
Figure 17. Hypothetical model of connection between cytoskeleton and translation. Here is depicted how can be components involved in translation (aa-tRNA, eEF1A, eEF1Bα) found in cytoskeletal fibre (actin) bound form and free form. In the step 1 free tRNA is aminoacylated and further used as a building block for protein biosynthesis (step 2) and recycled (step 3). eEF1A is recycled (step 4) as well by GDP/GDP exchange facilitated by eEF1Bα and eEF1Bγ[185].

Mutation analysis of *S. cerevisiae* eEF1A found that specific eEF1A mutations show reduction in actin cross-linking and bundling activity. Intriguingly, these mutations don´t affect translational function, pointing out the fact that these two functions of *S. cerevisiae* eEF1A are

separate[192]. Oppositely, genetic perturbation of F-actin by mutations in actin remodeling proteins (tropomyosin I and mitochondrial disruption and morphological protein 20) demonstrate reduced actin bundling properties and moreover, shows large reduction in protein biosynthesis. In the same study Kinzy and Gross found that translation initiation more than translation elongation is disrupted in these mutants[193]. All this data support the hypothesis that translation and cytoskeleton undergo reciprocal regulation. Cytoskeleton probably act as a scaffold for macromolecules involved in translation[185].

1.6.3.4   eEF1A in viral propagation

Viruses depend on host cells proteins to be able to replicate. Therefore, it is quite logical that they evolutionary found to hijack eEF1A, one of the most abundant proteins, for their effective replication and propagation. The function of eEF1A in these processes seems to be various among many viruses[171].

eEF1A is involved in binding tRNA - like sequence (TLS) in 3´ UTR RNA of some plant viruses. This sequence was found in turnip yellow mosaic virus (TYMV), tobacco mosaic virus (TMV), and brome mosaic virus (BMV), for example[171,194]. TLS´s have important roles in virus protein synthesis, inhibition of minus-strand RNA synthesis and virus packaging[195,196]. Moreover, TMV translation was decreased after mutation in EF1A1 binding site of TLS[195]. eEF1A was found to interact with other RNA structures, for example replication silencer element in 3´UTR of *Tombusvirus* or stem loop at the 3´ UTR region of West Nile virus (WNV), both interactions stimulate the minus-strand synthesis[197,198].

Other studies demonstrate that eEF1A interacts with viral polymerase proteins to enable assembling the virus replication complex. Interaction of RNA-dependent RNA polymerase (RdRp) was identified in TMV[199]. Downregulation of eEF1A reduced TMV infection propagation in plants[200]. eEF1A1 and its complexing proteins (eEF1B, eEF1G) are necessary for function of RdRp (named L protein) in *Vesiculovirus*[201]. It was described that eEF1A1 interaction is important for virus mRNA transcription[202]. Further, HIV-1 reverse transcriptase has been found to interact with eEF1A and eEF1G proteins. Downregulation of these two proteins exhibits inhibition of reverse transcriptase complex[203].

eEF1A has obviously a role in pathogenicity of several diseases. It can bind oncoproteins E6 and E7 from human papilloma virus 38. It was found that eEF1A interaction with E7 enables cell immortalization and transformation in primary human keratinocytes. This interaction is crucial for impairment of actin stress fibers leading to cell transformation[204].

Other interactions of eEF1A in diseases include X protein from hepatitis B virus, Nef protein, integrase or Gag protein from HIV-1 virus and many others. All these data show diversities in eEF1A1 viral interaction. Obviously, eEF1A and its complexing proteins are crucial for viral life cycle[171].

1.6.3.5 eEF1A in apoptosis, cell signaling and cancer

Several studies have been made to elucidate the eEF1A role in apoptosis. First study from 1998 demonstrated that eEF1A has pro-apoptotic function in 3T3 mouse fibroblasts[205] . Later, it was shown that eEF1A levels significantly increases upon H_2O_2 treatment in rat heart myoblast cells. H_2O_2 causes dose-dependent apoptosis. Lethal dose of H_2O_2 together with treatment by transcriptional inhibitor significantly upregulates eEF1A protein levels. Therefore, eEF1A expression is regulated apparently on post-transcriptional level[206].

 The role of this protein in apoptosis is controversial and can have both pro-apoptotic and anti-apoptotic activity. This was explained by the existence of two isoforms eEF1A1 and eEF1A2. The levels of eEF1A1 and eEF1A2 were monitored during serum-deprivation induced apoptosis. They found eEF1A2 to be completely replaced by eEF1A1 during this process on myotubes. Other experiments showed that continual expression of eEF1A2 has pro-survival effect in skeletal muscle. On the other hand, myotube apoptosis was accelerated by introduction of eEF1A1 homolog, whereas transfection by antisense eEF1A1 have pro-survival effect[207].

The role of eEF1A1 in cell death seems to be important. eEF1A1 was demonstrated as a mediator of lipotoxic cell death. It was found to participate in lipotoxic mediated cell death in hamster ovary cells and H9c2 cardiomyoblasts. This process is caused by fatty acid overload that leads to endoplasmic reticulum (ER) stress and reactive oxygen species (ROS) lipotoxic stress. The regulation of cytoskeletal remodeling during progression of these cell death/apoptosis is mediated by eEF1A1[208].

Phosphorylation of serine (Ser), threonine (Thr) and tyrosine (Tyr) is crucial post-translation modification that has regulatory role in majority of cell processes (survival, signaling pathways, proliferation, cell death, etc.). eEF1A as a one of the most abundant proteins is subjected to phosphorylation on several residues by different kinases (Fig. 18)[164]. Different isoforms eEF1A1 and eEF1A2 exert various features as Tyr substrates. eEF1A1 has ability to interact with adaptor proteins containing SH2 domains. On the other hand, eEF1A2 can interact with adaptor proteins containing SH2 (Src homology 2) and SH3 (Src homology

3) domains and therefore has bigger opportunity to participate in phosphotyrosine-mediated signaling pathways[209]. The phosphorylation status of eEF1A can possibly explain the moonlighting function of this protein and possible switch among its involvement in different processes[164].

One of the proteins promoting eEF1A phosphorylation is brain-derived neutrophic factor (BDNF). BDNF can regulate neural activity and postsynaptic development and plasticity in brain[210]. BDNF can promote eEF1A phosphorylation that cause enhancing of translation rate and dephosporylation of EF-2 enabling translocation from ribosomal A site to P site through mTOR signaling pathway. Similar effect on eEF1A and eEF-2 was observed in insulin treated cells[211–213].

PAS kinase (PASKIN) is nutrient-sensing protein kinase involved in metabolic regulation and glucose homeostasis[214,215]. eEF1A1 is phosphorylated at Thr 432 by PASKIN what results in enhancing protein synthesis *in vitro*[216] .

Protein kinase C is Ser/Thr kinase involved in cell growth regulation, apoptosis, differentiation and motility. Isoenzyme PKC δ can phosphorylate eEF1A at Thr 431[217]. Higher nucleotide exchange rate and translation elongation was demonstrated after eEF1 phosphorylation by PKC in rabbit reticulocytes[218,219]. Moreover, PKCβI can phosphorylate eEF1A2 at Ser 53 in mouse myoblasts. This interaction depends on eEF1A2 phosphorylation status[220].

Rho-associated kinases (Ras homologous) is a group of kinases involved in adhesion, cell motility, microvillus formation, and as well in organizing actin structures (stress fibers). Rho-GTP was found to be able to phosphorylate eEF1A and cause decrease in F-actin bundling. Further, eEF1A can interact with myosin-binding subunit (MBS) of myosin phosphatase and regulates by that the phosphorylation state of eEF1A[221].

Interferon α (INFα) induces apoptosis in cancer cells mostly through c-Jun N-terminal kinase 1 (JNK-1) and/or by p38 MAPK (mitogen activated protein kinase) signaling. The interaction between EF1A and C-Raf was described in a study focused on INFα mediated survival response through by epidermal growth factor (EGF) signaling in lung cancer. This interaction and following Raf phosphorylation of eEF1A can protect eEF1A from proteasome-mediated degradation and leads to cell survival[222].

Further studies focused on phosphorylation sites found Ser21 and Thr88 as eEF1A1 phosphorylation sites of B-Raf (but not C-Raf). On the other hand, Ser 21 EF1A2 was phosphorylated by both B-Raf and C-Raf. In the same study they found that eEF1A1 and

eEF1A2 hetorodimerize to enhance Ser21 phosphorylation. This phosphorylation event is probably crucial in switch between translation and other non-canonical function of eEF1A[223].

TGF-β receptor (TβR-I) is important part of transforming growth factor β (TGF-β) signaling involved in cell proliferation. TβR-I was found to phosphorylate eEF1A1 at Ser300 *in vitro* and *in vivo* leading to inhibition of translation and regulation of cell proliferation[224].

The phosphatide-3-kinase (PI3K)/AKT signaling is important in many cellular processes as a cell growth, survival, motility, and proliferation. Moreover, activation in this pathway is crucial in hepatocellular carcinoma (HCC)[225–227]. In the study interested in higher rate of mouse double minute homolog 4 (MDM4) in hepatocellular carcinoma, the important role of eEF1A2 was found. MDM4, the negative regulator of p53[228], is upregulated in HCC. eEF1A2 was found to activate PI3K/AKT/ mTOR cascade resulting in MDM4 stabilization by post-transcription mechanism[229]. Moreover, silenced eEF1A2 resulted in inhibition of PI3K/AKT/mTOR/NF-κB pathway, and the cell motility, invasion, and proliferation were reduced, and apoptosis inhibited. Oppositely, eEF1A2 overexpression increased cell proliferation, motility and invasion. Therefore, eEF1A2 plays role as a potential oncogene[230]. The putative oncogenic role and high overexpression was described in many cancers (ovarian cancer, breast cancer, lung cancer, HCC)[163].

Recently, eEF1A1 was found to have an important role in many cancers. P21 activated kinase 4 (PAK4), involved in cytoskeletal organization, has been found to interact with eEF1A1 in gastric cancer. This interaction promoted metastasis and invasion in gastric cancer[231].

Human HLA-F adjacent factor 10 (FAT10) is ubiquitin-like protein capable of direct targeting the substrate to proteasome degradation, and has significant role in cell proliferation and cancer development[232,233]. FAT10 can promote cancer proliferation by protecting eEF1A1 from degradation. Overexpression of FAT10 results in decrease in ubiquitin-eEF1A1 complexes and increase in FAT10-eEF1A1 complexes. Therefore, FAT10 competes with ubiquitin in eEF1A1 binding, and FAT10-eEF1A1 complexes are not degraded by the proteasome[233].

Another study shows that eEF1A1 is a binding partner of p53 and p73 proteins, key proteins regulating cell proliferation and cell death. By the silencing experiments they downregulated eEF1A1 and found enhancement of chemotherapy sensitivity in p53 and p73 wild type cells. Therefore, eEF1A1 is probably the negative regulator of p53- and p73-mediated apoptosis[234].

Recently, eEF1A1 was found to be the new potential promising biomarker in HCC, as the expression and mRNA levels correlate with poor prognosis and disease-free survival in patients[235].

Certainly, EF1A is an important multifunctional protein with many roles and binding partners. Synthesis and development of compounds targeting this protein can bring new pharmacological possibilities and new information of this biotarget.
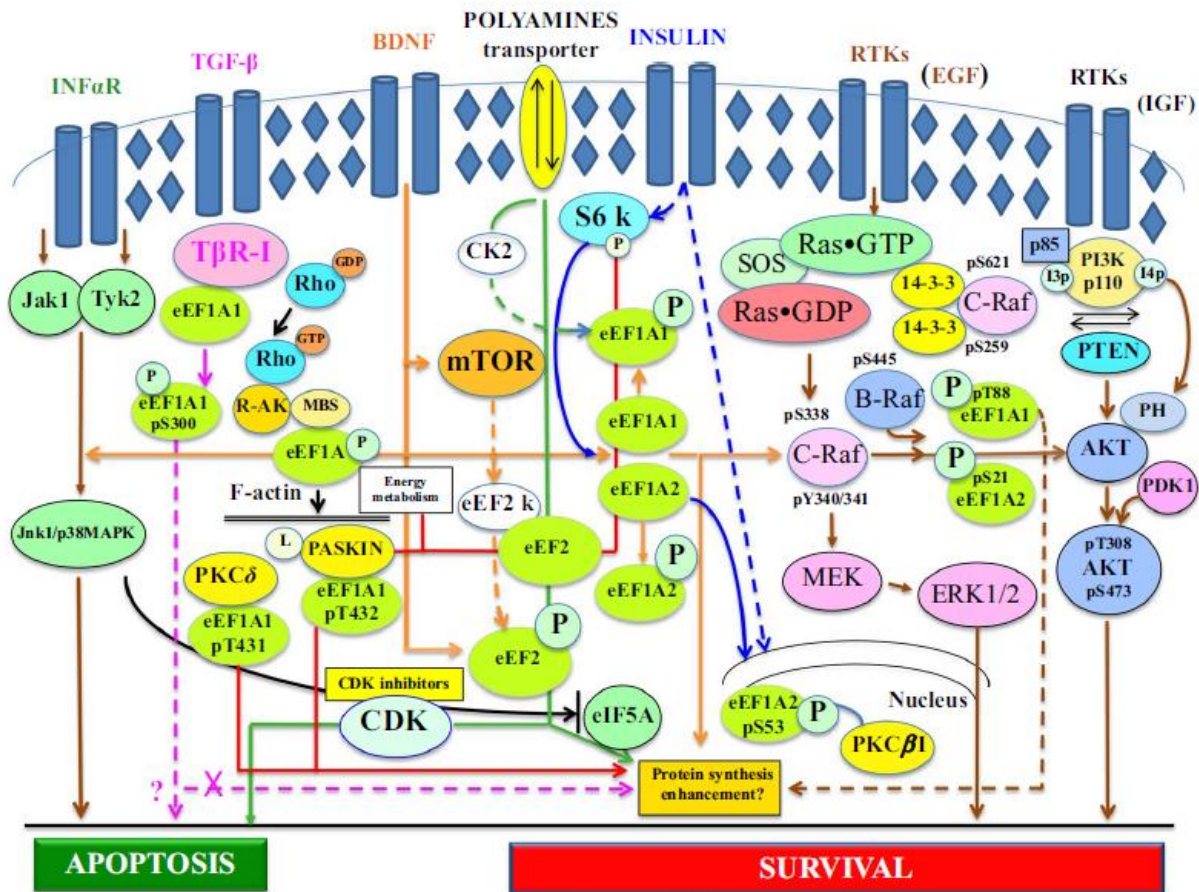
Figure 18. eEF1A1 and eEF1A2 involvements in signaling pathways and their potential effect on apoptosis, survival and translation. Polyamines are multifunctional cations important for protein kinase CK-2 (CK-2) and cyclin dependent kinase (CDK). For other abbreviations see text[164].

1.7 **Pyruvate kinase M2**

Pyruvate kinase is the key glycolytic enzyme catalyzing the final-rate limiting step of glycolysis. It catalyzes dephosphorylation of phosphoenolpyruvate (PEP) to pyruvate and generates ATP (Fig. 19). There are four isoforms of pyruvate kinase: PKL, PKR, PKM1 and PKM2. Pyruvate kinase type L (PKL) is expressed in kidney and liver, pyruvate kinase type R is expressed in erythrocytes, and both are encoded by PKL gene[236]. Pyruvate kinase M1 (PKM1) is expressed in brain and muscle, and pyruvate kinase M2 (PKM2) is expressed in almost all tissues except brain, muscle and liver, and in all proliferating tissues, embryonic cells and mainly in tumour cells. Both PKM1 and PKM2 are product of PKM2 gene and are expressed by alternative splicing[237].

PKL, PKR, and PKM1 exist in tetramer quaternary structure; PKM2 can exist in tetramer or dimer[238,239]. Tetramer form of PKM2 is the active form with higher affinity to PEP and it regenerates energy. On the other hand, dimeric form of PKM2 has lower affinity to PEP and is less active, therefore it mediates an accumulation of glycolytic intermediates for biosynthetic process. In tumour cells, PKM2 is found predominantly in dimeric inactive form that enables accumulation of glycolytic intermediates for biosynthesis processes. Glycolytic intermediates such as glucose 6-phosphate, fructose 6-phosphate, glyceraldehyde 3-phospate, dihydroxyacetone phosphate (DHAP) and glycerate-3-phosphate are necessary for nucleotide, phospholipid, sphingolipid and amino acid biosynthesis (Fig. 19)[238].
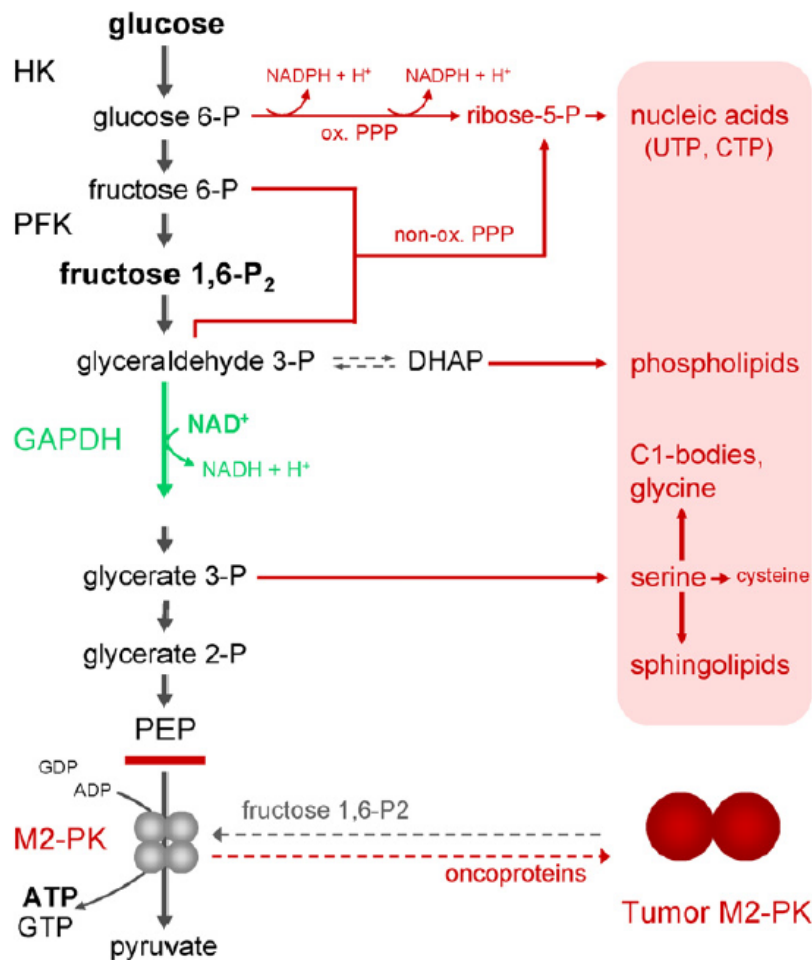
Figure 19. Pyruvate kinase M2 (in the picture named M2-PK) and its role in glycolysis to generate glycolytic intermediates for biosynthetic processes. HX: hexokinase, PFK: 6-phosphofructo 1-kinase, GAPDH: glyceraldehyde 3-phosphate dehydrogenase, LDHA: lactate dehydrogenase, PPP: pentose phosphate pathway[238].

PKM2 tetramer-dimer ratio can be regulated in several manners. Fructose 1,6-bis phosphate (FBP) can tetramerize PKM2; it induces association of PKM2 dimers into active PKM2 tetramers[238]. Other activators of PKM2 is serine[240], metabolite of *de novo* purine synthesis of succinyl-5- aminoimidazole-4-carboxamide-1-ribose-5-phosphate (SAICAR)[241]. On the other hand, interaction with some oncoproteins (e.g. HPV 16-human papillomavirus 16 E7 protein, PML-promyelocytic leukemia tumour suppressor), or PKM2 post-translational modification by phosphorylation (e.g. FGFR1-fibroblast growth factor 1, JAK2, BCR-ABL)[242], PKM2 acetylation[243] or oxidation[244] cause PKM2 dimerization and thereby decrease of its activity.

Further investigation revealed that PKM2 can be translocated into the nucleus and transactivate genes important for tumour growth. Through direct interaction with HIF1α (hypoxia inducible factor 1 α) it activates HIF1α target genes LDHA, GLUT1 and PKM2 itself[245]. Upon EGF stimulation PKM2 binds phosphotyrosine peptides of β-catenin and the complex is translocated into the nucleus. In the nucleus PKM2 transactivate c-Myc and cyclin D1 gene through HDAC3 (histone deacetylase 3) dissociation from promoters[246]. Another study reveals that PMK2 dimer can act as a tyrosine kinase utilizing PEP as a phosphate donor. Results show that the inactive dimer acts as a tyrosine kinase, and the active tetramer acts as a pyruvate kinase. It can phosphorylate STAT-3 (signal transducer and activator of transcription 3) and thereby transcactivate STAT-3 target genes[247]. The STAT-3 is not only target of PKM2 tyrosine kinase; it was described recently that PKM2 can phosphorylate spindle checkpoint protein Bub3 controlling the accurate chromosome segregation during mitosis[248]. Another phosphorylation targets of PKM2 are for example MLC2 (myosin light chain 2) and ERK1/2 (extracellular signal regulated kinase 1/2). Phosphorylation of MLC2 leads to cytokinesis initiation[249], and phosphorylation of ERK1/2 leads to transactivation genes of proliferation[241]. Moreover, it was found that PKM2 can bind Oct-4, transcription factor maintaining stem cells pluripotency, and enhance Oct-4 mediated transcription [250]. Recently, it was described that by binding HIF1-α and NF-kB, PKM2 can stimulate VEGF (vascular endothelial growth factor) secretion and angiogenesis (Fig. 20)[251].
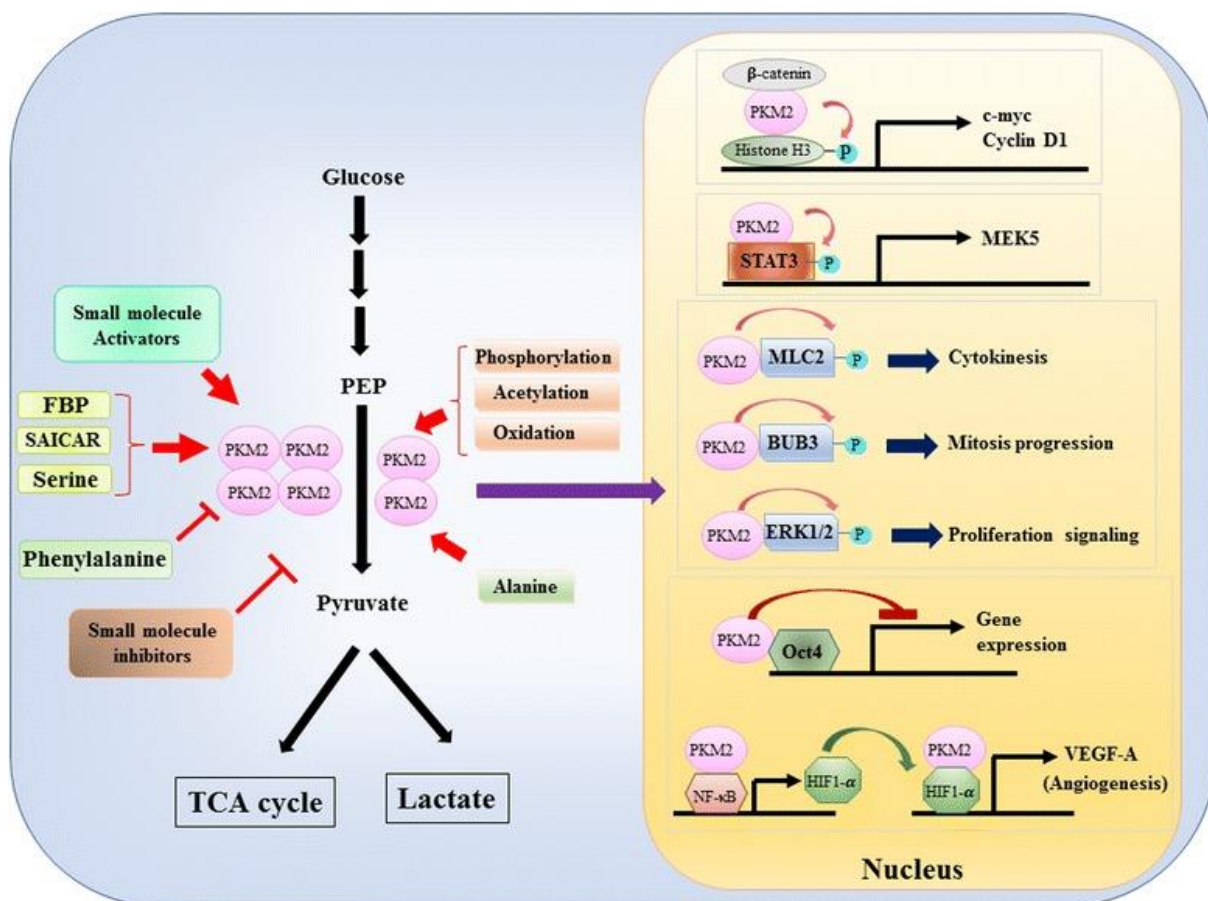
Figure 20. Modulation of PKM2 activity and PKM2 role in cell signaling[252].

Increased expression of PKM2 has been detected in many cancers and is connected with poor prognosis. The PKM2 overexpression was described in gastric cancer, esophageal cancer, hepatocellular carcinoma, cervical cancer, breast cancer, colorectal cancer and many others[252].

No doubt, pyruvate kinase is the crucial enzyme for tumorigenesis. Originally, it was known as a key glycolytic enzyme, but in the past two decades many new roles of this protein were described. Certainly, there will be attempts for developing of new compounds targeting PKM2 in cancer treatment[252].

1.8 **Nucleoside analogs**

Purines and pyrimidines are naturally occurring heteroaromatic compounds with wide spectrum of biological activities. They have various roles in the cell, they act as enzyme cofactors (coenzyme A), second messengers (cAMP, cGMP - cyclic guanosine monophosphate), coenzymes (NADH), storage of energy (ATP), and most importantly they are part of nucleosides, building blocks of nucleic acids DNA and RNA (purine nucleosides adenine and guanine, pyrimidine nucleosides thymine, uracil and cytosine). Nucleoside analogs are important group of compounds with pharmacologically diverse effects. They exhibit antimicrobial, antiviral, anticancer or immunosuppressive effects[253] and their potency inspires to synthetize and optimize many compounds for diverse pharmacology applications.

1.8.1 **Purine analogs**

Purine is the most common natural N-heterocyclic compound. Its name "purine" was attributed to imidazole [4,5-*d*] pyrimidine compound by Emil Fisher in 1884[254]. Plenty of naturally occurring purines have been described, for example caffeine from coffee beans and tea leaves, several purine derivatives isolated from marine organisms (3,7-dimethylisoguanine with antibacterial activity, 1-methylherbipoline- inhibitor of collagenase) or cytokine zeatin from *Zea mays* and many others (reviewed in[255]).

Many synthetic routes of purines analogs have been developed and described including solid phase synthesis[256]. Purine libraries were synthesized and the compounds screened for their biological activities and some of them were further approved for disease treatment. The potency of purine analogs is clear from their wide biological activities. They exhibit antimicrobial (for mycobacterium tuberculosis treatment)[257], antiviral (acyclovir for herpes simplex virus[258], carbovir for HIV[259], anticancer (fludarabine or cladribine for hematological malignancies treatment (Fig. 21) and immunosupresive effects (azathioprine)[260].
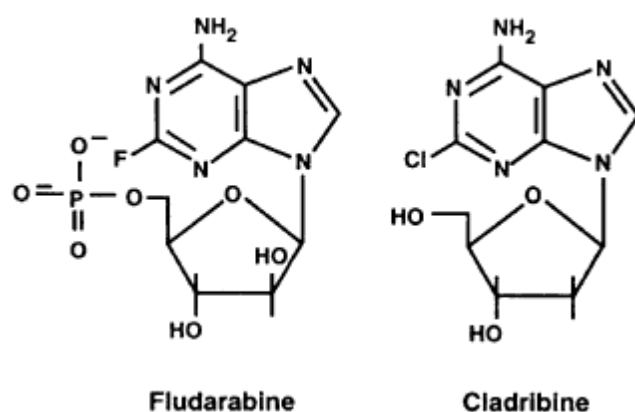
Figure 21. Structure of clinically used purine analogs fludarabine and cladribine for hematologic malignancies (modified from[261]).

They act by various mechanism of action. Most of nucleoside analogs act as antimetabolites. They enter the cell (mediated by specific membrane proteins) and are subsequently phosphorylated by various enzymes (deoxdycitidine kinase, deoxyguanosine kinase). Further, they compete with natural nucleotides what leads to many processes. They act as antimetabolites, so they incorporate into DNA or RNA, leading to nucleic acid synthesis inhibition. Moreover, they are substrates for many enzymes during DNA repair, which leads to enzyme inhibition, DNA damage and apoptosis (Fig. 22)[253,261,262].
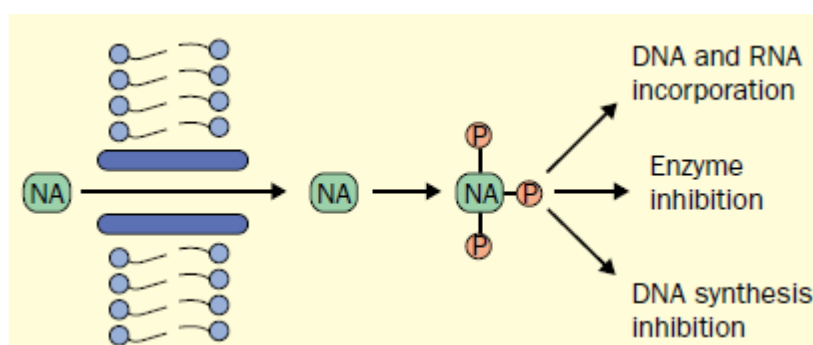
Figure 22. Mechanism of action of nucleoside analogues (NA). When NA enters the cell, it is activated - phosphorylated by specific enzyme and subsequently exerts its function (incorporation into DNA or RNA, interfere with enzyme function), resulting in DNA synthesis inhibition and cell death[253].

Some of purine-based small molecules exhibit various effects, some of them act as interferon inducers[263], kinase inhibitors[264], inhibitors of HSP90 (heat shock protein 90)[265], phosphodiesterase inhibitors[266], microtubule assembly inhibitors[267] or act by other mechanism of action[256].

1.8.1.1 Pyrrolo [2,3-*d*] pyrimidine (7-deazapurine)

7-Deazapurines (IUPAC name: Pyrrolo [2,3-d] pyrimidine) are compounds similar to purine nucleosides and have been intensively studied for their powerful biological (antimicrobial, anti-inflammatory, anticancer, antifungal) activities[268]. The replacement of nitrogen N7 by carbon possess new possibility of compound modification, and makes five membered ring more electron-rich and therefore probably more prone to cation interactions. As the 7-deazapurines resemble purine nucleosides (Fig. 23), they can act as antimetabolites, incorporating into DNA and RNA. However, many other mechanism of action have been discovered for these compounds[269].
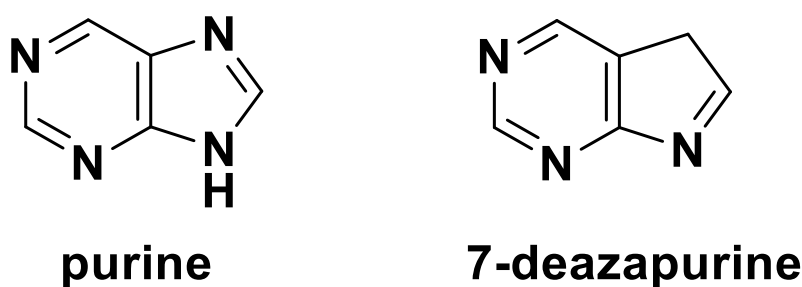
Figure 23. Structure of purine and 7-deazapurine.

Several 7-deazapurines have been described to occur naturally: hypermodified guanosine nucleoside analogue queuosine (**1a**) isolated from bacterial tRNA[270] or archaeosine (**2**), isolated from archeal tRNA[271] or 2´-deoxyqueuosine (**1b**) recently found in bacterial DNA[272] (Fig. 24).
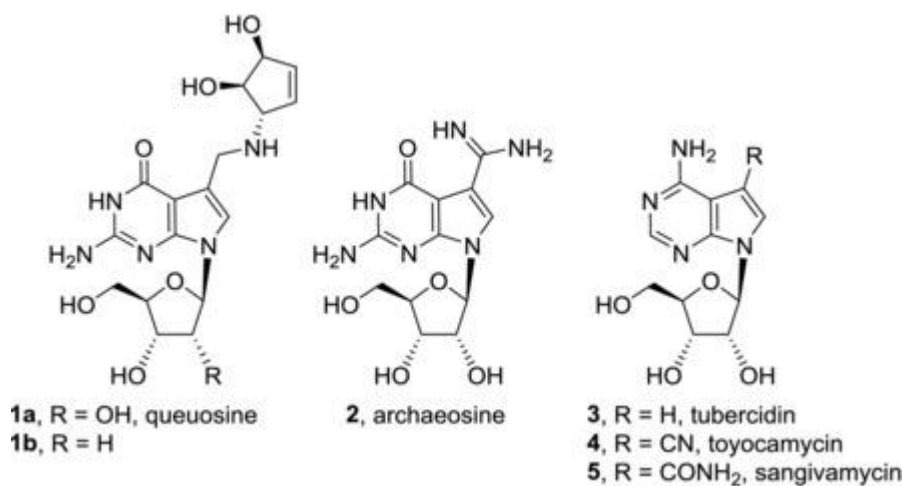
Figure 24. Deazapurines occurring in the nature (modified from[269]).

Several natural 7-deazapurines with cytotoxic effect have been described including tubercidin (**3**), toyocamycin (**4**) and sangivamycin (**5**) isolated from *Streptomyces* (Fig. 24). These compounds are very similar, but their mode of action is distinct. All compounds are upon cell penetration phosphorylated by various kinases to mono-, di- and triphosphates (MP, DP, TP) and subsequently incorporated into DNA and RNA[273–275]. Tubercidin impairs many cellular processes as nucleic acid synthesis, protein translation, mitochondrial respiration, rRNA processing, purine synthesis[275] and it inhibits S-adenosylhomocysteine hydrolase[276]. Toyocamycin (**4**) inhibits phosphatidylinositol kinase[277], rRNA transcription[278] and recently was found to be inhibitor of XBP1 (X-box binding protein 1) mRNA splicing. XBP1 is a key regulator of ER stress response and it is important for multiple myeloma survival[279]. Sangivamycin (**5**) is known to inhibit PKC and recently was found to induce apoptosis via Erk and Akt signaling[280] and binds molecular chaperone HSP70[281].

Many compounds based on 7-deazapurine scaffold have been synthetized and tested for their biologic and pharmacology activities. In this group are compounds with anticancer activities, inhibitors of adenosine kinase with anticonvulsant, analgesics and anti-inflammatory effect, inhibitors of antimycobacterial adenosine kinase and many antiviral compounds targeting hepatitis C virus, dengue virus, hepatitis B virus, HIV virus and some others (reviewed in[269]).

A group of 7- and 8-substituted 7-deazapurines is are biologically active compounds with potency of application in medicinal chemistry. The studied derivatives have been found to act by different mechanism of action and often hit several cellular pathways. Therefore, it is difficult to distinguish the main cellular target. We can mention halogenated derivatives of

tubercidin that were synthetized and studied for their cytotoxicity. While 7-Iodo, -bromo and -chlorotubercidin have lower cytotoxic activity than tubercidin[282], 7-fluorotubercidin has higher cytotoxicity with selectivity to lymphoblast cells (Table 2.)[283]. Other molecules were derived from sangivamycin, for example ARC or Xylocydine. Both 8-hydrazinosangivamycin (ARC)[284,285] and xylocydine (sugar modified 8-bromosangivamycin)[286] performed cytotoxic activity against several cancer cell lines[269]. One of the most interesting group of 7- and 8-substituted 7-deazapurines are 7-deazaadenosines with heterocycle in C7 position. It was found that heterocycles in C7 position (i.e. thiophene or furan) perform nanomolar cytotoxic activity against several cancer cell lines[287].

Compound	IC$_{50}$ [μM] (cell line)
Tubercidin	0.001 (A549)
Toyocamycin	0.012 (HTB-81)
Sangivamycin	0.006 (A549)
7-Iodotubercidin	2.6 (HeLa)
7-Bromotubercidin	2.9 (HeLa)
7-Chlorotubercidin	13.3 (HeLa)
7-Fluorotubercidin	1 (L-1210)
ARC	0.97 (SW620)

Table 2. Cytotoxic activities of some 7-deazapurine derivatives (modified from[269]). A549 (human lung carcinoma), HeLa (human cervix adenocarcinoma), HTB-81 (human prostate carcinoma), L-1210 (mouse lymphocytic leukemia), SW620 (human colorectal adenocarcinoma).

In general, 7- and 8-substituted 7-deazapurines act by many complex mechanisms of action including DNA and RNA synthesis inhibition, inhibition of adenosine kinase (7-iodotubercidin), DNA damage, DOT1 (disruptor of telomeric silencing 1) methyltransferase inhibitors, affecting of Akt pathway causing p53 independent apoptosis (ARC) or inhibiting CDK (Xylocydine)[269]. Many 7-deazapurines have been synthetized and show favorable biological and pharmacological activities. The mechanism of action of some of them is under investigation for better understanding their molecular actions and their potential use in medicine.

2. Experimental part

2.1 **Aims**

The first aim of this thesis was identification of molecular target of specific group of 2-phenyl-3-hydroxy -4(1*H*)-quinolinones.

The second aim was identifying mechanism of action of nucleoside analogue AB61.

2.2 Identification of molecular target of 2-phenyl-3-hydroxy-4(1*H*)-quinolinones

This project is focused on identification of molecular target of flavonoid aza-analogues 2-phenyl-3-hydroxy-4(1*H*)-quinolones (3-HQ). The identification of molecular target is crucial for information about mechanism of action, potential side effects and further compound synthesis and optimization.

These derivatives were in past studied for their *in vitro* anticancer properties, and showed high cytotoxicity (micromolar and submicromolar) against several cancer cell lines[148,150,156,159].

Our aim was to elucidate specific drug target of 3-HQ and analyze biological impact on cancer cells. We have analyzed cytotoxic activity of 3-HQ derivates and chosed one(based on previous molecular docking studies[157]) for pull down affinity purification. Two variants of the original compound were synthetized, one biotinylated out of the active site and second biotinylated directly in the active site (previously identified pharmacophore). We have identified three potential targets by the affinity purification coupled with mass spectrometry. One of them was validated by western blot as a primary target - elongation factor 1 alpha 1 (eEF1A1), other two proteins were identified as eEF1A1 interacting partners.

eEF1A1 protein is indispensable component of translation elongation but many others functions were revealed, including changes in the apoptosis rate, actin remodeling, viral functions and others[170]. In spite of interesting activities of this protein, just few compounds were identified to bind this protein. The male contraceptive agent Gamendazole (Fig. 25) was found to bind directly to eEF1A1 and probably disrupt eEF1A1 F-actin bundling activity[288]. Other compound, phosphodiesterase inhibitor Cilostazol (Fig. 25) influences neurite outgrowth by binding to eEF1A1[289]. Moreover, eEF1A1 was found to be target of two natural flavonoid derivatives (Fig. 25) exhibiting high cytotoxicity against breast cancer cells through their interaction with eEF1A1[290].

Following identification of 3-HQ targets, we validated results by western blot and affinity purification with recombinant target proteins. The interaction of the compound and eEF1A1 was validated by isothermal titration microcalorimetry. Further, several enzymatic assays, analysis of proteosynthesis, monitoring of actin fragmentation or metabolite profiling was performed to analyze biological impact on treated cancer cells. Some data from this project were published in Journal of Medicinal Chemistry (appendix B)[157].

This work is first study focused on identification of molecular target of 2-phenyl-3-hydroxy-4(1H)-quinolones and its mechanism of action.
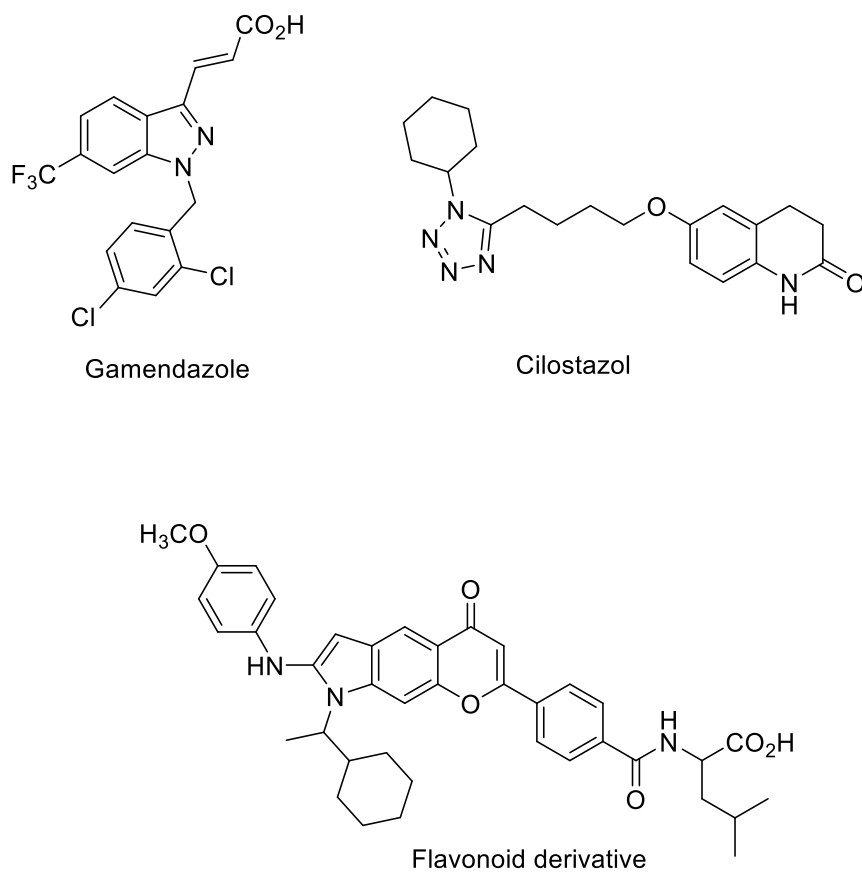
Figure 25. Structures targeting eEF1A1 (modified from[157]).

2.2.1 Material and methods

Captures 2.2.1.1, 2.2.1.2, 2.2.1.4 and 2.1.1.10 were previously published in similar version in[157] (appendix B).

2.2.1.1 Cell lines

All used cell lines were purchased from the American Tissue Culture Collection (ATCC), unless otherwise indicated. CCRF-CEM line are highly chemosensitive T-lymphoblastic leukemia cells, K562 cells were derived from a patient with acute myeloid leukemia with *BCR-ABL* translocation, A549 cell line is derived from lung carcinoma, NCI-H520 - squamous lung carcinoma, colorectal carcinoma HCT116, prostate adenocarcinoma PC-3, breast adenocarcinoma MCF-7, uterine sarcoma MES-SA, cervix adenocarcinoma HeLa, osteosarcoma U2OS and mouse lymphoid tumor P388D1. Further, colorectal carcinoma HCT116 with mutated or deleted p53 or K-Ras gene [HCT116p53-/-, HCT116p53(R248W/-), HCT116K-Ras(G13D/-), HCT116K-Ras(+/-) from Horizon Discovery, UK]. The daunorubicin-resistant CCRF-CEM (CEM-DNR) and paclitaxel-resistant K562-TAX sublines were selected in our laboratory by cultivation of maternal cell lines in increasing concentrations of daunorubicin and paclitaxel, respectively[291,292]. The CEM-DNR cells overexpress multidrug resistance associated protein 1(MRP-1), while K562-TAX cells overexpress P-glycoprotein (PGP1), both of which belong to the family of ABC transporters and are involved in primary and/or acquired multidrug resistance phenomenon. MRC-5 and BJ are non-tumor human fibroblasts. All cell lines were regularly tested for mycoplasma contamination and genetically authenticated.

2.2.1.2 Cytotoxic MTT Assay

The cells were maintained in Nunc/Corning 80 cm^2 plastic tissue culture flasks and cultured in cell culture medium (DMEM/ RPMI 1640 with 5 g·L^{-1} glucose, 2 mM L-glutamine, 100 U·mL^{-1} penicillin, 100 μg·mL^{-1} streptomycin, 10% fetal calf serum, and NaHCO$_3$). Cell suspensions were prepared and diluted according to the particular cell type and expected target cell density (25,000–30,000 cells·well^{-1} based on cell growth characteristics). Cells were added by a pipette (80 μL) into 96-well microtiter plates. Inoculates were preincubated for 24 h at 37 °C and 5% CO$_2$ to stabilize. Four-fold dilutions of 20 μL aliquots, of the intended test

concentrations were added to the microtiter plate walls at time zero. All test compound concentrations were examined in duplicates. Incubation of the cells with the compounds lasted for 72 h at 37 °C in 5% CO_2 atmosphere and 100% humidity. At the end of the incubation period, the cells were assayed using MTT. Aliquots (10 µL) of a MTT stock solution were pipetted into each well and incubated for further 1 - 4 h. After this incubation period the produced formazan was dissolved in 100 µL·well^{-1} of 10% aq. SDS (pH 5.5), followed by further incubation at 37 °C overnight. The optical density (OD) was measured at 540 nm with a Labsystem iEMS Reader MF. Tumor cell survival (IC50) was calculated using the following equation: IC = (ODdrug-exposed well/mean ODcontrol wells) × 100%. The IC50 value, corresponding to the drug concentration lethal for 50% of the tumor cells, was calculated from appropriate dose-response curves.

2.2.1.3   Cell Cycle and apoptosis Analysis

This part was in similar version published as a part of publication[287]

Subconfluent CCRF-CEM cells (ATCC), seeded at the density of 5 x 10^5 cells/mL in 6-well panels, were cultivated with the 1x IC50 of tested compounds in a humidified CO_2 incubator at 37 °C in RMPI 1640 cell culture medium containing 10% fetal calf serum, 10 mM glutamine, 100 U/mL penicillin, and 100 µg/mL streptomycin. Controls containing vehicle dimethylsulfoxid (DMSO) were harvested at the same time point (12 h). Cells were washed with cold phosphate buffer saline (PBS) and fixed in 70% ethanol overnight at -20 °C. The next day the cells were washed in hypotonic citrate buffer, treated with RNase (50 µg/mL), stained with propidium iodide, and analyzed by flow cytometry using a 488 nm single beam laser (Becton Dickinson). Cell cycle was analyzed in the program ModFitLT (Verity), and apoptosis was measured in logarithmic mode as percentage of the particles with propidium content lower than cells in G0/G1 phase (sub-G1) of the cell cycle. Half of the sample was used for phospho-histon H3^{Ser10} antibody (Sigma) labeling and subsequent flow cytometry analysis of mitotic cells.

5-bromo-20-deoxyuridine (BrdU) Incorporation Analysis

Cells were cultured as for cell cycle analysis. Before harvesting, they were pulse-labeled with10 µM BrdU for 30 min. The cells were trypsinized, fixed with ice-cold 70%

ethanol, incubated on ice for 30 min, washed with PBS, and resuspended in 2 M HCl for 30 min at room temperature to denature their DNA. Following neutralization with 0.1 M $Na_2B_4O_7$, the cells were washed with PBS containing 0.5% Tween-20 and 1% bovine serum albumin (BSA). They were then stained with primary anti-BrdU antibody (Exbio) for 30 min at room temperature in the dark. Cells were then washed with PBS and stained with secondary antimouse-FITC antibody (Sigma). The cells were then washed with PBS, incubated with propidium iodide (0.1 mg/mL) and RNase A (0.5 mg/mL) for 1 h at room temperature in the dark, and finally analyzed by flow cytometry using a 488 nm single beam laser (FACSCalibur, Becton Dickinson).

5-bromo-20-uridine (BrU) Incorporation Analysis

Cells were cultured as for cell cycle analysis. Before harvesting, they were pulse-labeled with 1mM BrU for 30 min. The cells were fixed in 1% buffered paraformaldehyde with 0.05% of NP-40, incubated in room temperature for 15 min and then in the fridge overnight. They were then washed in 1% glycin in PBS, washed in PBS, and stained with primary anti-BrdU antibody crossreacting to BrU (Exbio) for 30 min at room temperature in the dark. Cells were then washed with PBS and stained with secondary antimouse-FITC antibody (Sigma). Following the staining, the cells are washed with PBS and fixed with 1% PBS buffered paraformaldehyde with 0.05% of NP-40. The cells were then washed with PBS, incubated with propidium iodide (0.1 mg/mL) and RNase A (0.5 mg/mL) for 1 h at room temperature in the dark, and finally analyzed by flow cytometry using a 488 nm single beam laser (FACSCalibur, Becton Dickinson).

2.2.1.4   Protein target identification

Cell lysis and lysate depletion

CEM cell pellets (100 x10^6 cells) were repeatedly washed in PBS with inhibitors (protease inhibitor cocktail-Sigma, 5 mM $Na_4P_2O_7$, 1 mM Na_3VO_4, 5 mM NaF, 1 mM $C_7H_7FO_2S$), resuspended in 1 ml of lysate buffer IP (20 mM Tris, 150 mM NaCl, 1 mM EGTA, 1 mM EDTA, 0.5% Triton X-100, 0.5% NP-40, 2.5 mM $Na_4P_2O_7$, 1 mM Na_3VO_4, 5 mM NaF, 830 µM benzamidine, 1 mM B-glycerolphosphate, 1 µg/ml leupeptine, 1 µg/ml aprotinin, 1 mM $C_7H_7FO_2S$), briefly sonicated and incubated for 30 min at 4 °C. Streptavidin coated

magnetic beads (Dynabeads MyOne Streptavidin C1, Invitrogen) were 30 min preincubated with biotin by adding 100 µl of 100 µM biotin in beads buffer (BB) (1.9 mM NaH_2PO_4 x H_2O, 8.1 mM Na_2HPO_4 x 2 H_2O, 150 mM NaCl, pH 7.4) to 50 µl magnetic beads. Afterwards, 100 µl of whole cell lysate was repeatedly incubated with streptavidin-biotin coupled beads (30 min, 4 °C) in three steps (each step with fresh beads) for lysate depletion.

Affinity purification

100 µl of beads were three times washed in 100 µl BB and incubated with 100 µl 100 µM biotinylated compound (**derivative A** or **derivative B**) at room temperature (rt) for 30 min. Negative control was incubated with 100 µl 100 µM biotin. Beads with complex streptavidin-biotinylated compound were then repeatedly washed in BB and 100 µl 100 µM biotin/BB were added. After washing in BB/ 100 µM biotin / 0.1% BSA, beads were incubated with 150 µg of depleted cell lysate and incubated at 4 °C for 90 min. Beads were then three times washed in BB and two times in 0.25% SDS.

SDS PAGE

Afterwards, beads with complex streptavidin-biotinylated compound-proteins were resuspended in 15 µl 3x SDS loading buffer with 10% β-mercaptoethanol 5 min at rt, beads were separated from proteins and protein denaturation was accomplished by warmth at 95 °C 5 min and cooled down in ice. Samples were separated in 12% gel in 160 V, 60 min. Separated proteins were silverstained[293].

Protein digestion

Bands were excised from gel and cut into small pieces, destained[294], reduced, alkylated and trypsinized to peptides. Peptides were extracted from gel and purified by MacroTrap (Michrom). A MacroTrap colon was equilibrated by 500 µl 0.1% trifluoracetic acid (TFA), sample was loaded and then desalted in 500 µl 0.1% TFA, peptides were eluted by 200 µl 0.1% TFA /80% acetonitrile (ACN). The eluate was evaporated and dissolved in 1 µl 0.1% TFA /80% ACN and then diluted in 19 µl 0.1 % TFA.

Capillary liquid chromatography and mass spectrometry

Sample peptides were separated by high performance liquid chromatography (CapLC 1200 Series Agilent Technologies) with reverse phase column (Magic C18AQ 5 µM, 200Å, 0.2 x 150 mm, MICHROM). Solutions A (0.2% formic acid in 5% ACN/ H_2O) and B (0.2% formic acid in 95% ACN/ H_2O) were used for gradient elution with increasing of solution B (from 5% to 35%) in 55 minutes. Eluted peptides were continuously measured by mass spectrometer APEX^{TM} Ultra 9.4 T (Bruker Daltonics – BDAL) connected with Apollo II ESI ion source (BDAL). One full scan and three MS/MS scans were measured in each cycle. Spectra were analyzed in program DataAnalysis 4.0., further analysis and databasing were mediated by program ProteinScape 2.l. (BDAL). SwissProt and NCBI databases and algorithms MASCOT and PHENYX were used for protein identification.

2.2.1.5 Validation

Affinity purification with recombinant proteins

Affinity purification was done as was described. The beads were incubated with 1 µg of recombinant proteins separately (Tumour Type M2 Pyruvate Kinase, Origene; EF1A1 and ACTB, Genway Biotech Inc.) in 50 µl of IP buffer and incubated for 90 min at 4 °C. Beads were then three times washed in BB and two times in 1 % SDS and SDS PAGE separated as was described before.

Western blot analysis

Antibodies were obtained from commercial sources: anti-eEF1A1 (Sigma), anti - PKM2 XP™ (Cell Signaling), anti-β-Actin (Sigma). Separated proteins from one-dimension electrophoresis gel were transferred to nitrocellulose membrane (GE Healthcare). Membrane was blocked in 5% low fat milk in Tris-buffered saline/ 0.1 % Tween 20, incubated overnight with antibodies in 5% BSA at 4 °C and analyzed by enhanced chemiluminescence (Amersham).

Immunoprecipitation

Protein G agarose (Sigma Aldrich) was incubated with antibody PKM2 XP™ (Cell Signaling) or eEF1A1 (Cell Signaling) overnight at 4°C. CCRF-CEM were cultivated as described previously. Cells were treated by 1x IC50 compound **3** for 12 hours and control cells were treated by vehicle (DMSO). Cells were lysed by IP buffer. The concentration of proteins was measured by pierce 660 nm protein assay (Thermo) according manufacturer instructions. 500 µg of proteins were incubated with protein G coupled agarose (2 h, 4°C) in roller. After spinning down, pellets containing immune complexes were washed with IP buffer and denatured by 3x SDS buffer, separated by SDS PAGE and western blotted.

2.2.1.6 Proteosynthesis analysis

This methodics was previously published in similar version[269] (appendix C).

In vitro transcription of EGFP-luciferase DNA

In vitro transcription was performed by MEGAscript T7 kit (Ambion). As a template we used PCR amplified DNA coding EGFP-luciferase under T7 promoter. *In vitro* transcription reactions were performed according to manufacturer's instructions. Each transcription reaction (20 µL) contained of EGFP-luciferase 200 ng DNA template, ribonucleotide mix (ATP, GTP, CTP and UTP, 7.5 mM each), enzyme mix, and buffer. All reagents were mixed, centrifuged and incubated at 37 °C for 2 h. Afterwards, DNase I (2 U/µL, 1 µL) was added and the mixtures were incubated at 37 °C for 15 min. RNA transcripts were purified by NucAway Spin Columns (Ambion). The quantity and purity of RNA transcripts was tested by Agilent 2100 Bioanalyzer (RNA 600 Nano Total RNA kit, Agilent) and by NanoDrop 1000 Spectrophotometer.

In vitro translation of EGFP-luciferase RNA in presence of compound 3

For *in vitro* translation of EGFP-luciferase RNA transcripts we used reticulocyte lysate system (Retic Lysate IVT Kit, Ambion) according to manufacturer's instructions. The *in vitro* translation mixture (25 µl) contained 500 ng EGFP-luciferase RNA transcript, Low Salt Mix (1 µL), High Salt Mix (0.25 µL), methionine (0.83 mM, 1.5 µL), compound **3** in final concentration 1 µM or 10 µM and the reticulocyte lysate (17 µL). In the control experiment vehicle (DMSO) was used instead compound **3**. In the positive control reaction was used

inhibitor of translation fucidic acid (600 µM). Negative control experiment mixture was incubated without EGFP-luciferase RNA transcript. All reagents were mixed and incubated in water bath at 30 °C for 1.5 h. Efficacy of *in vitro* translation was evaluated by measurement of luciferase enzymatic activity on EnVision Multilabel Reader (PerkinElmer).

2.2.1.7 *In vitro* actin formation changes

U2OS cells were seeded at the density of 5 x 10^5 cells/ml in 12-well panels and cultivated as described before. Subconfluent cells were transfected by 1 µg pmKate2-actin vector (Evrogen). PmKate2-actin is mammalian expression vector encoding actin DNA sequence fused with red fluorescence protein pmKate2 under strong CMV promoter. The transient transfection was performed by JetPrime transfection reagent (Polypus transfection) according manufacturer instructions. Transfected cells were treated with the 1x IC50 of tested compound **3** and scanned in specific intervals by fluorescence microscope (excitation 588 nm/emission 633nm).

2.2.1.8 Pyruvate kinase assay

The pyruvate kinase assay was done similarly as in[295]. Briefly, the assay was based on generation ATP from ADP and PEP by pyruvate kinase M2. The amount of ATP was measured via luminiscence produced by enzyme firefly luciferase. Thirty µl of substrate mix – final concentration - 0.1 mM ADP, 0.5 mM PEP in assay buffer (50 mM imidazole pH 7.2, 50 mM KCl, 7mM $MgCl_2$, 0.01% Tween 20, 0.05% BSA), 10 µl of compound **3** (final concentration 10 µM) and 10 µl of enzyme mix were added. In the case of *in vitro* pyruvate kinase assay in enzyme mix was added 0.1 nm commercial pyruvate kinase (Tumour Type M2 Pyruvate Kinase: Human, Recombinant, E Coli recombinant protein, Genway Biotech). In the case of immunoprecipitated PKM2, CCRF-CEM cells were treated by 1x IC50 compound **3** in time intervals 1, 3 and 6 hours, control was treated by DMSO for 12 hours. Further, immunoprecipitation of PKM2 via anti-PKM2 or anti-EF1A1 was done as described before. Afterwards, 4 µl of agarose beads with immunoprecipitated PKM2 via anti-PKM2 or 6 µl anti eEF1A1-antibody, 50 mM imidazole pH 7.2, 0.05% BSA, 4 °C) in white 96 well plate. The mixture was incubated for 15 minutes and 50 µl of cooled luciferase detection mix protected from the light (Kinase-Glo, Promega) was added. Immediately luminiscence was measured by

Envision (Perkin Elmer). In both experiments shikonin, known inhibitor of PKM2, was used as a positive control in 0.5 µM concentration.

2.2.1.9 GTPase assay

For the eEF1A1 GTPase activity evaluation the colorimetric assay kit (Innova Biosciences) was chosen. We followed manufacturer protocol. Briefly, we have prepared reaction mixture in 96 well plate by mixing 20µl of immunoprecipitated eEF1A1 (from CCRF-CEM cells treated by 1x IC50 of compound **3,** 12 hours) and 100µl of substrate/buffer mix (0.5mM GTP, 2.5mM $MgCl_2$, 50mM Tris pH 7.4). The total volume of the reaction has been brought to 200µl by adding 80µl of Tris, pH 7.4. The reaction was immediately stopped by adding 50µl of Gold mix followed by addition of 20µl of stabilizer after 2 min incubation. After 60 min the absorbance at 625 nM was read on EnSpire plate reader (PerkinElmer).

2.2.1.10 Isothermal Titration Calorimetry

ITC experiments were performed at 25 °C with a Nano ITC Low Volume (TA Instruments, New Castle, DE, USA). During all measurements, injections of 2.5 µl of ligand (16µM) was titrated into 250 µl eEF1A1 (2µM) with time intervals 300 s, a stirring speed of 250 rpm. All ITC experiments were conducted with degassed buffered solutions 100 mM phosphate buffer, pH 7.4, in the presence of 1% DMSO. Recombinant eEF1A1 was purchased from Origene (Rockville, MD, USA).

The resulting thermograms were analyzed using Independent model of the NanoAnalyze Software. ITC is a straightforward method for measuring the binding affinity constant (K) and binding stoichiometry (n), enthalpy of binding (ΔH) that occur over the course of a reaction in solution, and the entropy changes (ΔS), is calculated from the equation $\Delta G = -RT \ln Ka = \Delta H - T\Delta S$.

2.2.1.11 Metabolic profiling

CCRF-CEM cells were seeded in concentration 1×10^6 cells/ml, treated by 1x IC50 compound **3**, 12 hours, cells were quenched by 60% methanol with NH_4HCO_3 (8.5 g/l) cooled to -50 °C. Cells were spined down (400 x g / 5 min). Supernatant was discarded and metabolites from pellet were extracted by 80% methanol cooled to -50 °C and frozen by liquid nitrogen. Samples were thawed, resuspended and spined down (1700 x g / 5 min). Supernatant was

stored, the pellet was extracted again and supernatants were pooled, stored and lyophilized. Before lyophilization, 20 µl of each sample was mixed for quality control sample. Lyophilized supernatants were dissolved in LC-MS/MS pure water (100 µl), vortexed, spined down (15800 g, 15 min) and transferred to glass vials.

LC-MS/MS analysis

All samples were analyzed by HPLC (UHPLC Dionex Ultimate 3000 RS, Thermo Fisher Scientific, MA, USA) using modified method previously published[296]. As detector triple quadrupole mass spectrometer 5500 QTrap (AB Sciex, CA, USA) was used. Normal phase LC system with conditions of HILIC separation was used with column Luna 3 µm NH2 100 Å, 150 x 2 mm (Phenomenex, Torrance, USA). The solvent A was aqueous buffer: 20 mM ammonium acetate (pH 9.45), solvent B: acetonitrile. The gradient with flow rate of 0.3 mL/min for HPLC was: t=0.0, 95% B; t=15.0, 30% B; t=17.0, 5% B; t=23.0, 5% B; t=23.1, 95% B; t=28.0 min 95% B. MS method settings was as follows: acquiring samples were done in both ionization modes (positive, negative) with ionspray voltage of +/- 4500 V, capillary temperature 400 °C, Curtain Gas - 30arb, Ion Source Gas (GS1) - 40arb and Ion Source Gas (GS2) - 40arb. Metabolomics data were processed by software MultiQuant 2.1.1. (AB Sciex, CA, USA).

Statistical analysis

The obtained dataset was interpolated and statistically evaluated in R software (R Core Team, 2013). First step in the data processing was reduction of systematic error by data interpolation by means of quality control samples. Metabolomics data was considered as compositional data and clr (centered log ratio) transformation and centering was applied on the dataset. For statistical evaluation several approaches were chosen - unsupervised PCA method (principal component analysis), cluster analysis and supervised DFA method (discriminant function analysis). Metabolite levels were incorporated into metabolic pathways by „pathway projector"(http://ws.g-language.org/g4/). Size of dots in map represents p-value and color of dots represents relative difference between two tested groups of samples.

2.2.2 Results

2.2.2.1 Compound 3 shows different cytotoxicity against cancer cells and fibroblasts

Several 3-nitro 4-amino 3-HQs derivatives (Fig. 26 A) was tested for their cytotoxic activity against cancer and normal cell lines. They exhibited micromolar and submicromolar activities against several cancer cell lines and significantly lower cytotoxicity to BJ fibroblasts (Fig. 26 B). We have chosen derivative **3** as a candidate for molecular target identification based on favorable biological properties. The compound **3** was tested by MTT assay for *in vitro* cytotoxic activity. Expanded panel of human and mouse malignant cell lines or human fibroblasts were tested (T-lymphoblastic leukemia CCRF-CEM, chronic myeloid leukemia K562, lung carcinoma A549, squamous lung carcinoma NCI-H520, colorectal carcinoma HCT116, prostate adenocarcinoma PC-3, breast adenocarcinoma MCF-7, uterine sarcoma MES-SA, cervix adenocarcinoma HeLa, osteosarcoma U2OS and mouse lymphoid tumor P388D1). Moreover, compound **3** was highly active against deleted or mutated cell lines [(HCT116p53-/-, HCT116p53(R248W/-), HCT116K-Ras(G13D/-), HCT116K-Ras(+/-)]. For most of cancer cell lines was compound **3** cytotoxic in submicromolar and micromolar concentrations. Cytotoxicity of compounds against lung fibroblasts (BJ) and foreskin fibroblasts (MRC-5) were significantly lower (9.39 µM for BJ and 63.38 µM for MRC-5). Moreover, derivative was highly cytotoxic as well against cell lines CEM-DNR, K562-TAX - resistant cancer cells expressing the multidrug resistance proteins from the family of the ABC membrane transporters MRP1 or PGP1, respectively (Fig. 26 C).

A

B

Comp. Nº	R	CCRF-CEM	CEM-DNR	U2OS	K562	K562-TAX	A549	BJ
1	(piperidine)	1.55	3.00	7.51	0.75	2.02	1.62	9.83
2	(diethylamino)	1.72	6.75	8.57	0.75	2.71	1.89	9.73
3	(ethylamino)	1.42	3.01	9.98	0.66	1.96	0.94	9.39

C
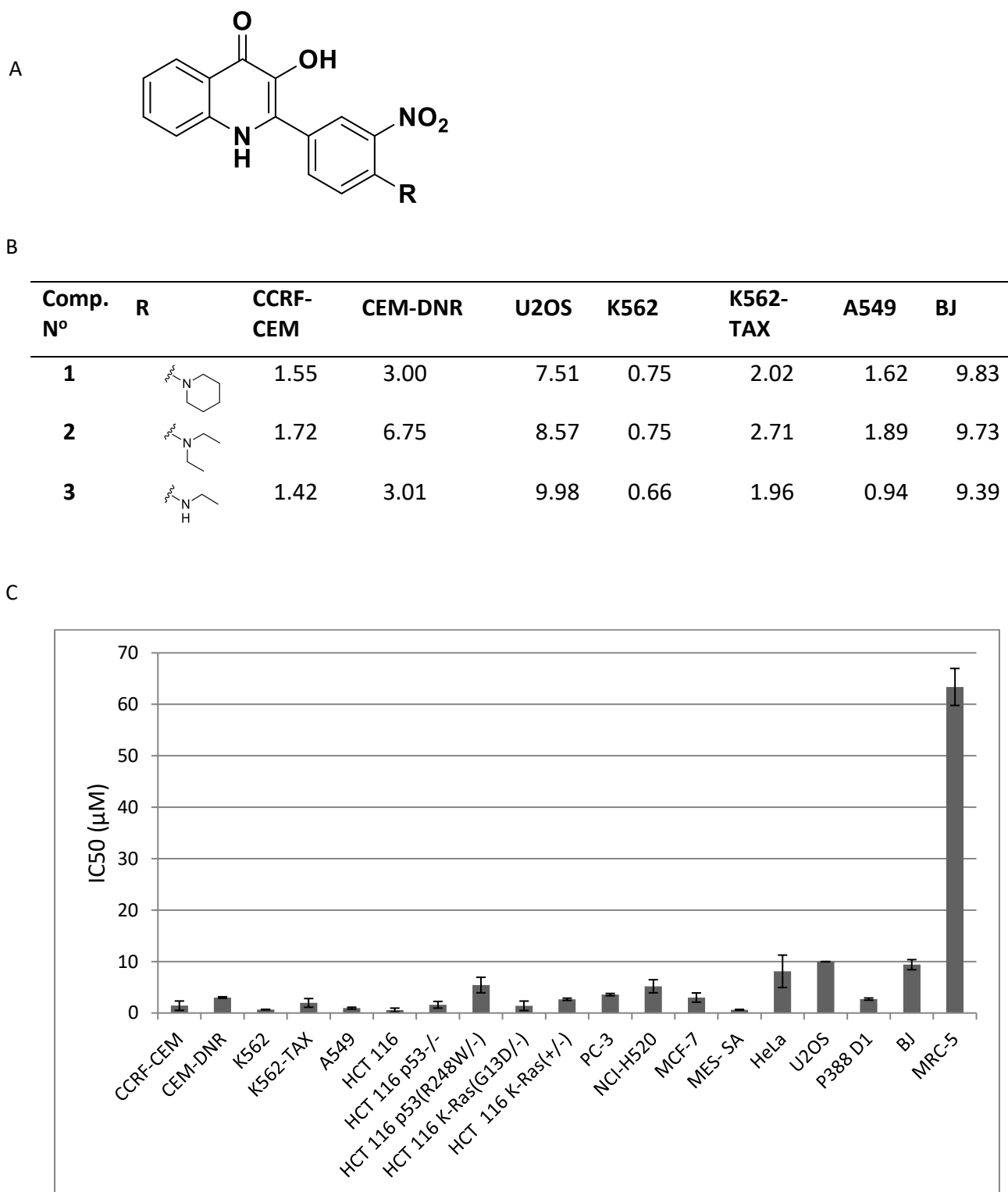
Figure 26. A) general structure of 3-nitro 4-amino 3-HQ B) IC50 values (in µM) of selected 3-HQ structures C) IC50 values for compound **3** against several cancer cell lines and fibroblasts. The A and B part of the picture were published before as a part of publication[157] (appendix B).

2.2.2.2 Compound 3 accumulates cells in G1 phase and inhibits DNA and RNA synthesis

Cell cycle analysis of CCRF-CEM cell line treated by compound **3** was performed. Cells were treated by 1x IC50 (1.42 µM, 12 hours) and showed apoptosis induction (increase of subG1) and accumulation cells in G1 phase. Significantly decreased marker of mitosis phospho-histone pH3Ser10 and cell decrease in G2/M points to mitosis inhibition. Moreover, DNA synthesis was almost completely inhibited and RNA synthesis was strongly inhibited what correlates with decrease cells in S phase (Fig. 27).
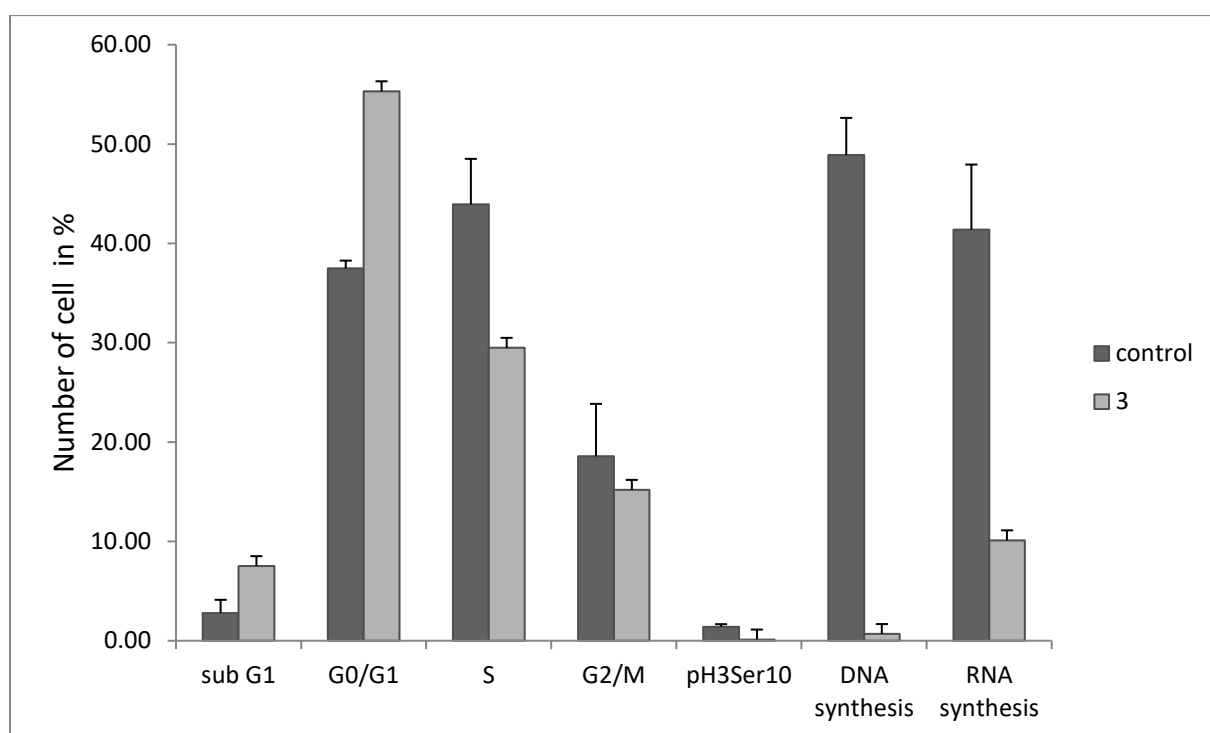
Figure 27. Flow cytometry analysis of CCRF-CEM cells treated by compound **3** and control (DMSO treated). The cell cycle analysis shows cell increase in G1 phase together with decrease in S phase, significant decrease of mitosis marker pH3Ser10 and DNA/RNA synthesis.

2.2.2.3 Biotinylated derivative of compound 3 binds proteins PKM2, eEF1A1 and β-actin

This data were published before as a part of publication[157] (appendix B).

We used affinity purification on magnetic beads for molecular target identification. For compound immobilization, we modified original compound **3** by biotinylation. Two variants of the original compound **3** were synthetized - one biotinylated out of the active site (actively biotinylated compound, **derivative A**) and second biotinylated directly in the active site of the compound (inactively biotinylated compound, **derivative B**) (Fig. 28).
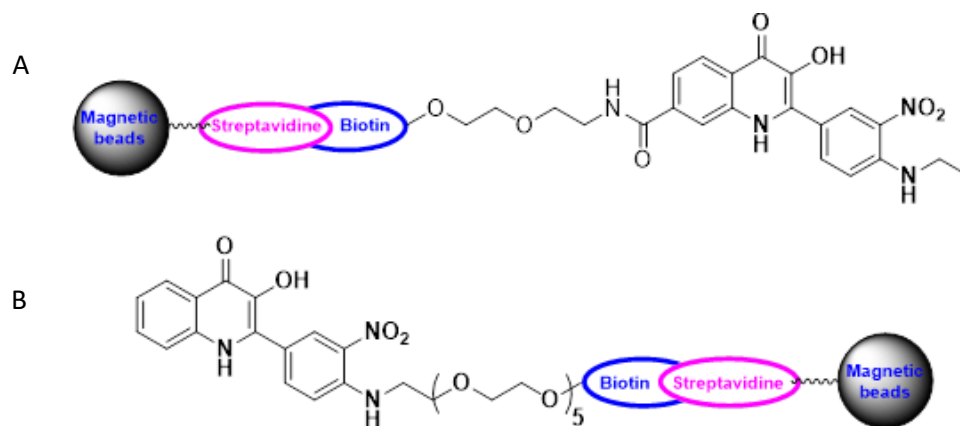
Figure 28. Immobilization of tested compound **3**. **Derivative A** biotinylated out of the active site and **derivative B** biotinylated directly in the active site. Interaction with streptavidin coated magnetic beads is depicted. The picture was published before as a part of publication[157] (appendix B).

CCRF-CEM or U2OS protein lysate was incubated with biotinylated molecules immobilized to streptavidin coated magnetic beads. Proteins were catch, eluted and SDS PAGE separated followed by silver staining. By comparing proteins from actively biotinylated **derivative A** with nonspecifically bound proteins catch by inactively biotinylated **derivative B** and negative control (magnetic beads incubated with no compound), we repeatedly found specific bands (Fig. 29). These bands were identified by mass spectrometry analysis as pyruvate kinase M2 (PKM2), elongation factor 1α1 (eEF1A1) and β-actin.
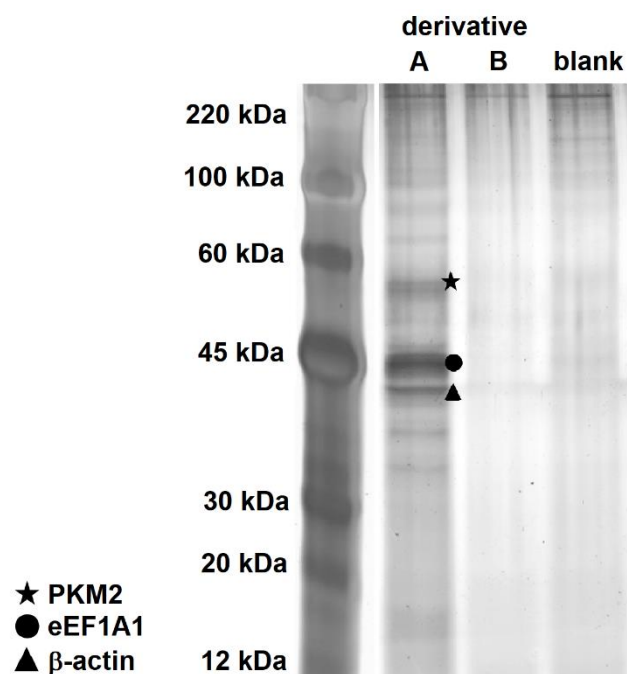
Sample	Protein code	Scores	Peptides	Sequence coverage
★	PKM2	325.7	8	23.4
●	eEF1A1	478.5	9	22.1
▲	β-actin	182.4	4	18.9

Figure 29. Specific bands eluted by pull down experiment with actively biotinylated **derivative A** and inactively biotinylated **derivative B** after incubation with CCRF-CEM cell lysate. Repeatedly identified proteins are marked by asterisk (PKM2), circle (eEF1A1) and triangle (β-actin). The picture of the gel was published before as a part of publication[157] (appendix B).

2.2.2.4 Validation of identified targets by western blot

For validation of identified targets, we used western blot of previously described pull down experiment. We identified specific bands for PKM2, eEF1A1 and β-actin only in the line for proteins captured by actively biotinylated compound, **derivative A** (Fig. 30 A). In the line of **derivative B** and negative control were no bands detected.

Further, we wanted to evaluate if these three proteins are in complex or binds separately to the compound **3**. We used affinity purification with pure recombinant proteins for this purpose. Magnetic beads with immobilized **derivative A** or **derivative B** were incubated with pure recombinant proteins PKM2, eEF1A1 or β-actin. Afterwards, captured proteins were eluted, separated and visualized by western blot. We found specific band just in the case of eEF1A1 for derivative **A** (Fig. 30 B), PKM2 and β-actin was not detected. Therefore, eEF1A1 is primary target and PKM2 and β-actin are just in complex with eEF1A1.

A
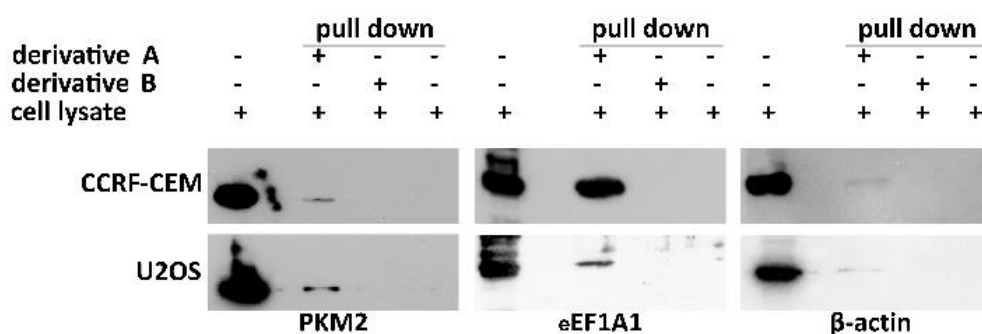
B
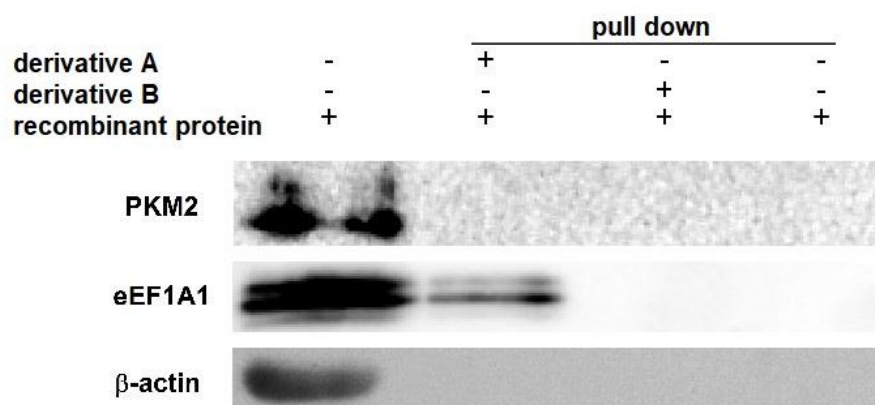
Figure 30. A) Identified proteins were validated by pull down experiments of total cell lysate from CCRF-CEM and U2OS cell lines and by B) pull down of purified recombinant proteins PKM2, eEF1A1 and β-actin. The picture A was published before as a part of publication[157] (appendix B).

2.2.2.5 Identification of new complex of PKM2 and eEF1A1

To gain the information about interaction between identified proteins, we used immunoprecipitation of PKM2 and eEF1A1 interacting proteins. We have found new interaction between PKM2 and eEF1A1 in compound **3** treated CCRF-CEM cell line. This interaction was clearly visible either by immunoprecipitation via anti-PKM2 and anti-eEF1A1 antibody (Fig. 31).
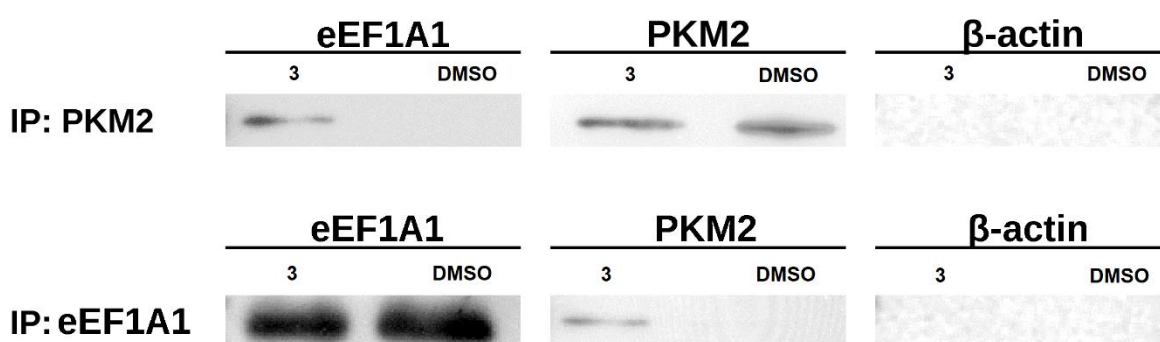
Figure 31. Immunoprecipitation of binding partners of PKM2 and eEF1A1. PKM2 interacts with eEF1A1 after treatment of CCRF-CEM cells by compound **3** (1x IC50, 12 hours). PKM2 from vehicle (DMSO) treated cells hasn´t showed this interaction. Interaction of β-actin with PKM2 or eEF1A1 was not proved.

2.2.2.6 Treatment by compound 3 doesn´t affect translation efficiency

Efficiency of proteosynthesis was tested to elucidate effect of compound **3** binding to eEF1A1. We have used *in vitro* transcription of gene for GFP-luciferase to be able detect GFP (green fluorescent protein) or luciferase as an evidence of *in vitro* protein translation. After *in vitro* transcription of EGFP-luciferase DNA into RNA, we used *in vitro* translation reaction to evaluate effect of compound **3** on protein synthesis. To detect translated protein EGFP-luciferase, we measured luminescence intensity. We have found no significant effect of compound **3** treatment on translation (Fig. 32).
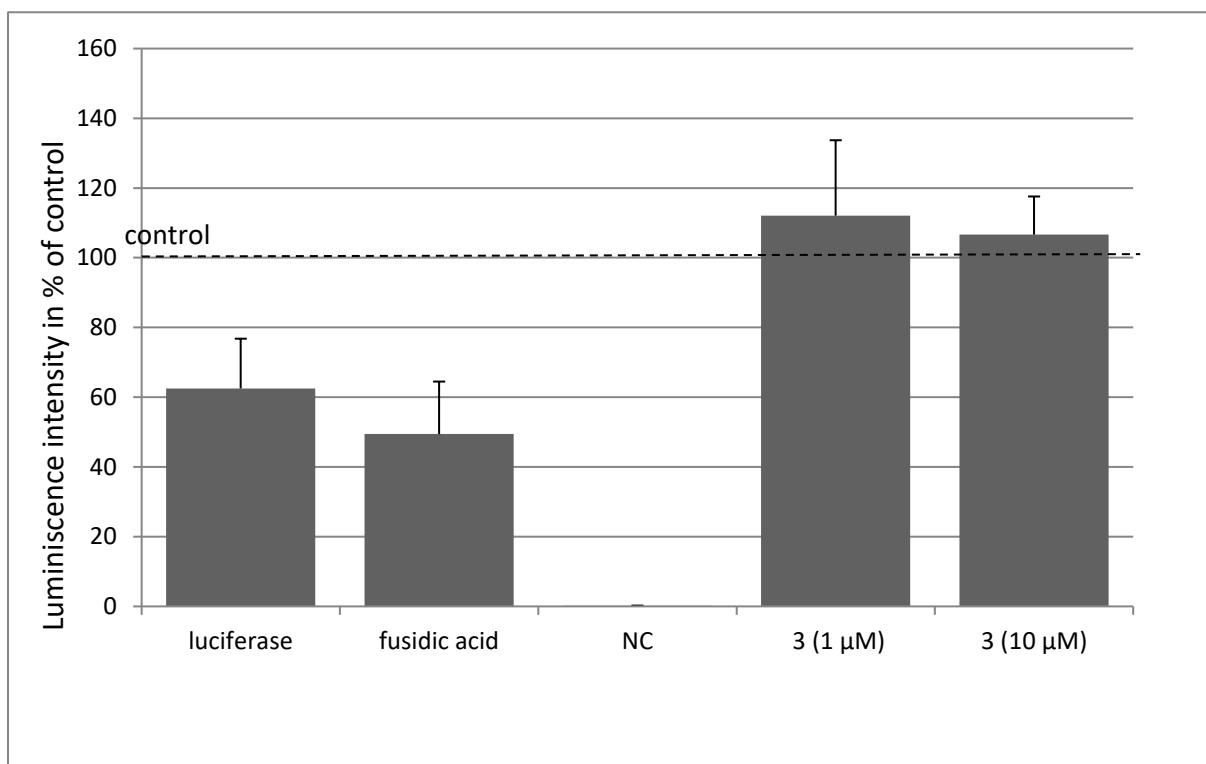
Figure 32. Analysis of translation efficiency by *in vitro* translation, 1ng luciferase is used for luminiscence comparison, fusidic acid is used as a known inhibitor of translation, negative control (NC) is reaction without RNA EGFP-luciferase, positive control (control) is translation reaction with RNA EGFP-luciferase treated by vehicle (DMSO) and is set to 100 % of luminescence intensity. Compound **3** was tested in two concentrations 1 µM and 10 µM. The difference between control and treated translation reactions is not significant (p value for control and 1 µM treatment is p=0.404 and for control and 10 µM treatment is p=0.461).

2.2.2.7 Treatment by compound 3 leads to massive actin fragmentation

As one of the identified target was β-actin, we have monitored actin changes in U2OS cells transfected by pmKate2-actin, far-red fluorescent protein. Transfected cells were treated by compound **3** and scanned in specific intervals (Fig. 33).
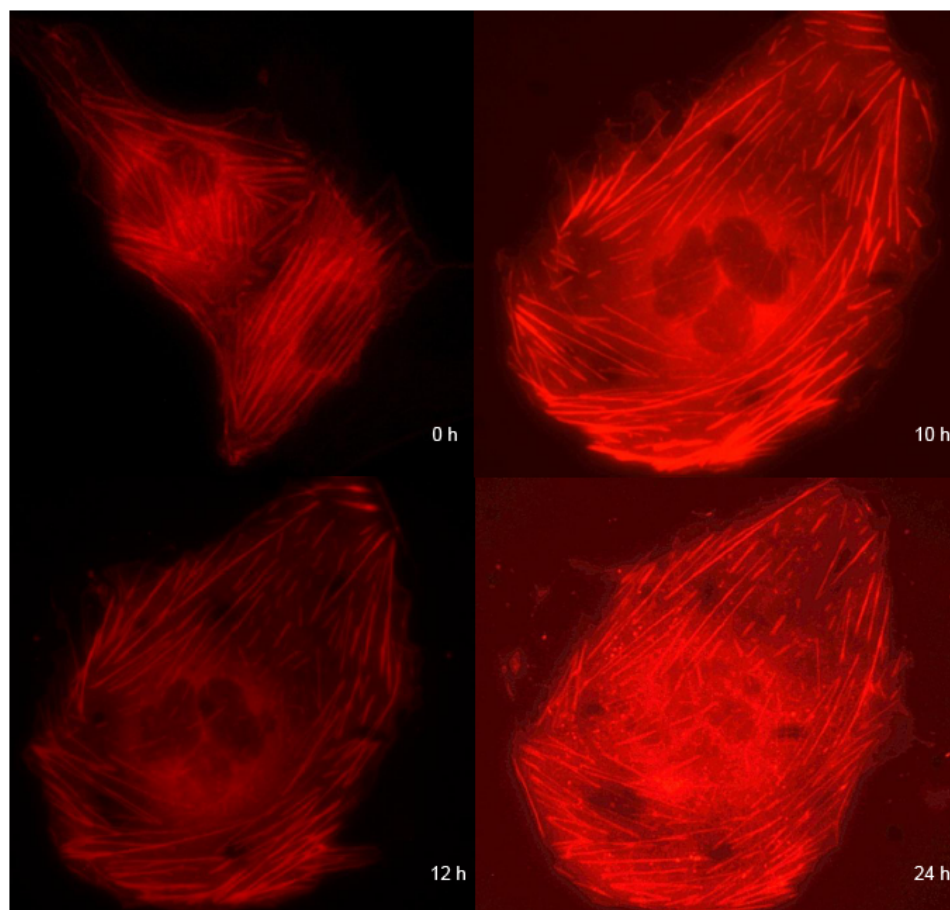
Figure 33. Monitoring of actin changes on U2OS transfected by pmKate2-actin vector after treatment by 1x IC50 of compound **3**. In the 10, 12 and 24 hour intervals actin fibres becomes fragmented. Excitation 588 nm/emission 633 nm, magnification 600x.

2.2.2.8 Pyruvate kinase assay and GTPase assay

As one of the captured targets was identified PKM2 and the interaction between eEF1A1 with PKM2 was observed after compound **3** treatment, we have decided to analyze PKM2 functional changes. Activity of PKM2 was studied by pyruvate kinase assay. Firstly, we analyzed PKM2 activity of commercial recombinant PKM2. Shikonin, known inhibitor of pyruvate kinase M2 was used as a positive control. There was no significant effect of compound **3** on PKM2 activity (Fig. 34).

Secondly, we analyzed activity of immunoprecipitated PKM2 by the same pyruvate kinase assay as before. We used PKM2 immunoprecipitated by anti-PKM2 and anti-eEF1A1 antibody from CCRF-CEM treated by compound **3** (1x IC50; 1, 3 and 6 hours interval). As we know that compound **3** may stabilize PKM2-eEF1A1 interaction, we added 10 µM compound

3 directly to the reaction to stabilize this interaction. There is evident inhibition of phosphorylation of ADP comparable with shikonin. PKM2 activity was inhibited to 70 % in the case of anti-PKM2 immunoprecipitated PKM2 and to 53% in case of anti-EF1A1 immunoprecipitated PKM2, both with compound **3** stabilization (Fig. 35A, B).

Further, we were interested in changes of GTPase activity of eEF1A1. We used immunoprecipitated eEF1A1 from CCRF-CEM treated by 1x IC50 compound **3** (12 hours) to analyze GTPase activity by GTPase assay. GTPase activity of eEF1A1 complex was upregulated to 161 % compare to immunoprecipitated eEF1A1 from vehicle (DMSO) treated CCRF-CEM cells (Fig. 36).
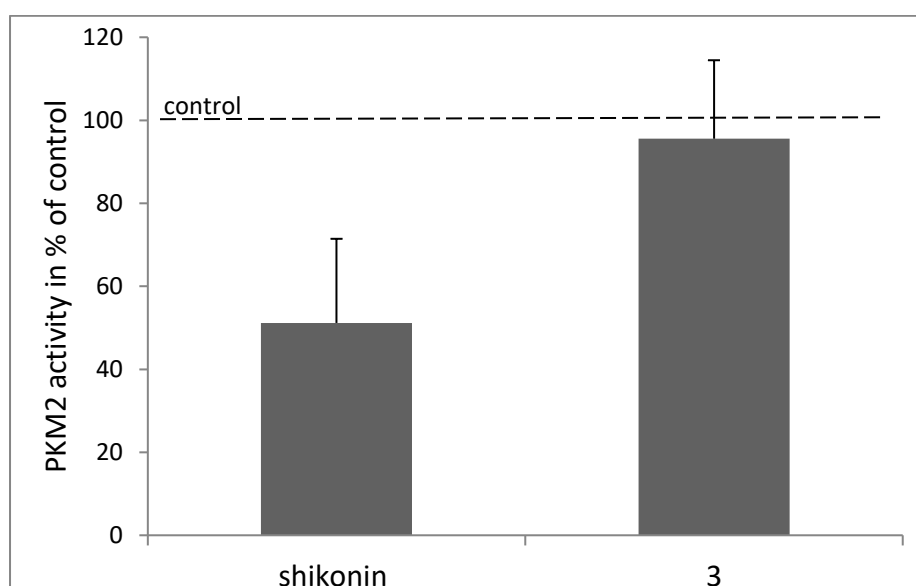
Figure 34. *In vitro* pyruvate kinase assay of commercial recombinant PKM2. Control is PKM2 activity of recombinant PKM2 treated by vehicle (DMSO) and is set to 100 %. The difference is not significant, compound **3** (10 µM) has no effect to the activity of the recombinant PKM2 (p=0.39).
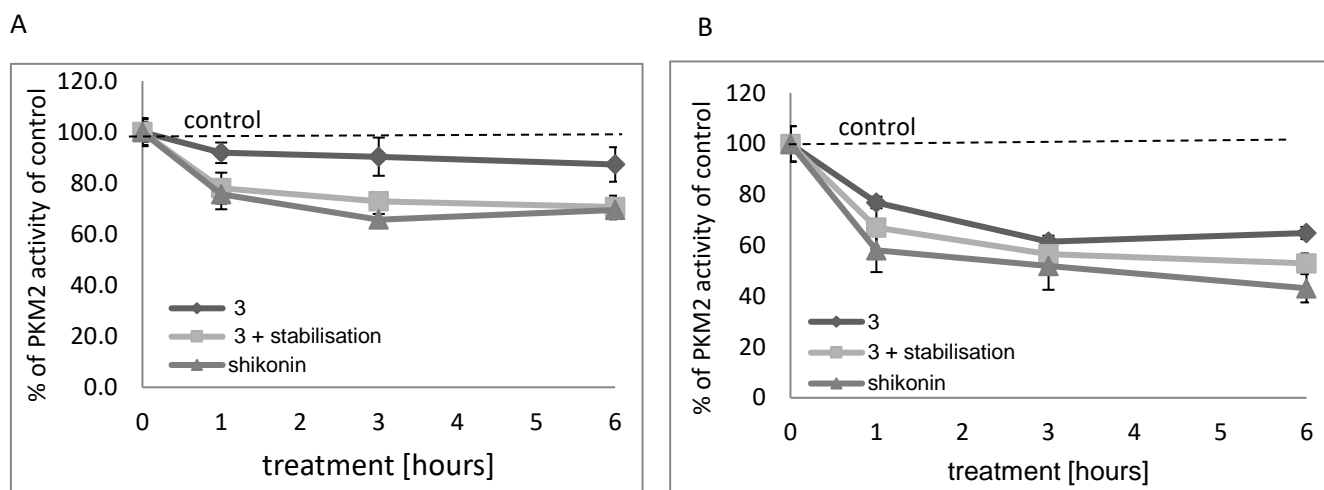
Figure 35. A) Pyruvate kinase assay with immunoprecipitated PKM2 from compound **3** treated CCRF-CEM via anti-PKM2 and B) anti-EF1A1 antibody in 1, 3 and 6 hour intervals. Treatment by shikonin (0.5 µM), well known inhibitor of PKM2, was used as a positive control. Controls for A, B are PKM2 immunoprecipitated (via anti-PKM2 or anti-eEF1A1, respectively) from CCRF-CEM cells treated by DMSO for 12 hours.
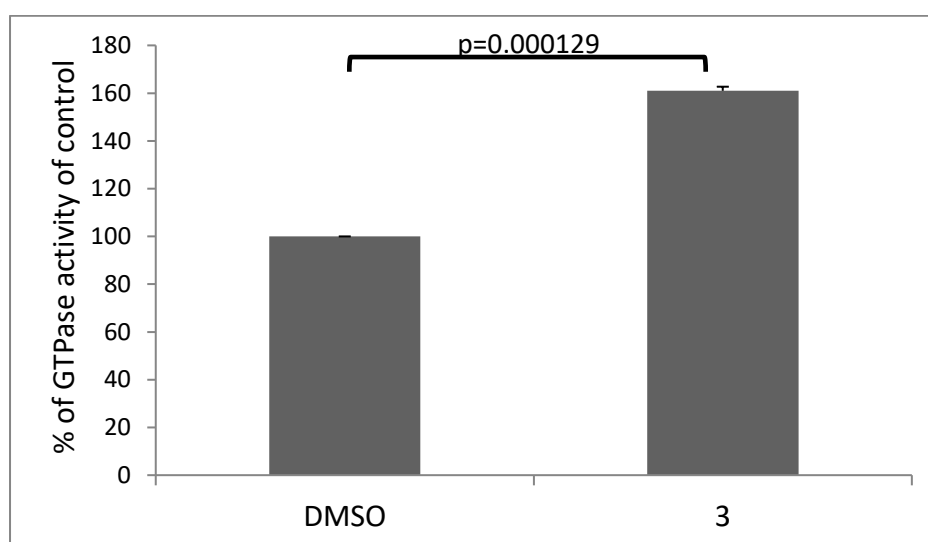
Figure 36. GTPase assay of immunoprecipitated eEF1A1 treated by vehicle (DMSO) and by compound **3** (1x IC50, 12 hours). The difference is significant (p=0.000129).

2.2.2.9 Isothermal titration calorimetry

Isothermal titration calorimetry of compound **3** and eEF1A1 was performed to validate their interaction. A representative calorimetric titration profile of compound **3** with eEF1A1 is shown in figure 37. Each peak in the binding isotherm represents a single injection of ligand to protein. This profile demonstrates biphasic behavior - both endothermic and exothermic processes. At the beginning of the titrations, negative peaks indicated endothermic binding interaction, which were followed by positive peaks of exothermic interaction (Fig. 37). The endothermic binding indicate the dominance of hydrophobic interactions in complex and the exothermic binding would imply dominant role of polar interaction (ionic, hydrogen bond). The biphasic behavior of interaction may occur due to an entropy gain, in the form of release of water molecules, followed by strong ionic interactions between ligand and protein.

ITC data were fitted to independent binding sites model and the data analysis revealed an association constant (Ka = 8.401 x10^6 M^{-1}), dissociation constant (Kd = 1.190 x 10^{-7} M). The enthalpy of binding (ΔH) is 504.3 kJ/mol, entrophy change is ΔS = 1823 J·K^{-1}·mol^{-1}, Gibbs free energy change is ΔG = -39227,4 J·mol^{-1} and stoichiometry is 1.740. Data were evaluated after subtraction of the ligand compound **3** into buffer control data.
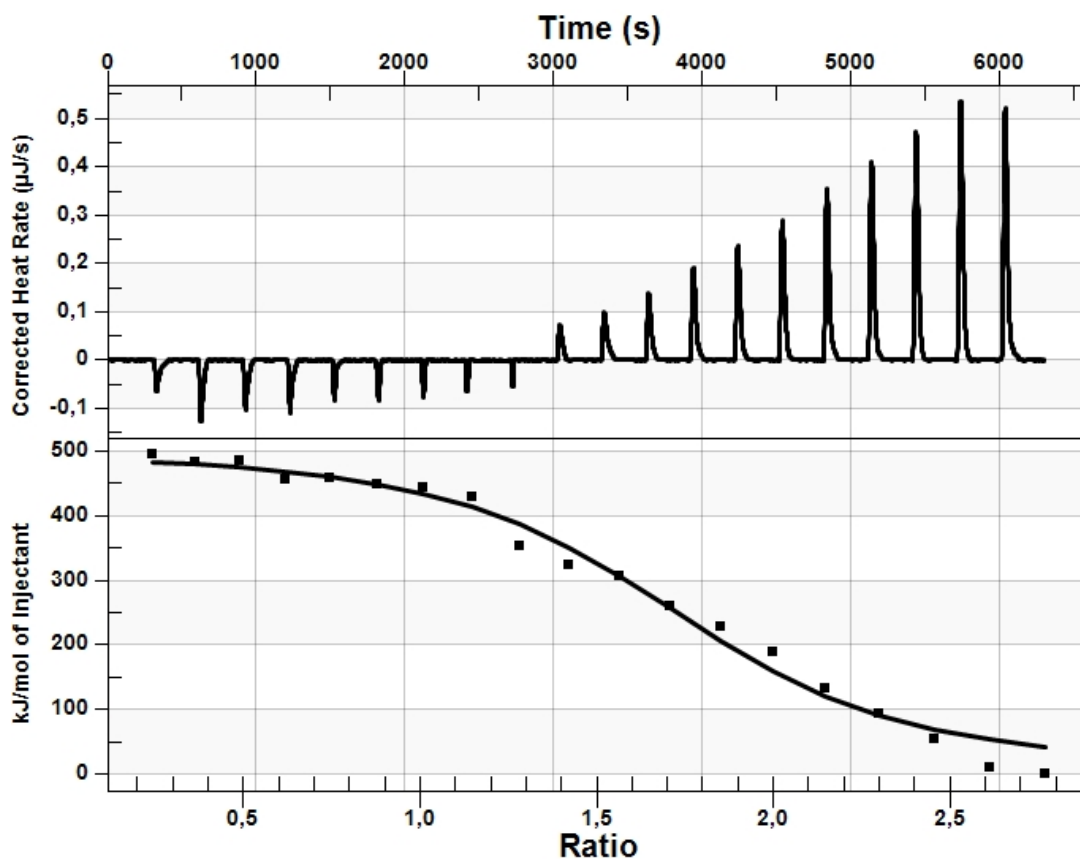
Figure 37. The calorimetric titration profile of interaction between compound **3** and eEF1A1.

2.2.2.10 Metabolic profiling

In order to analyze changes of PKM2 metabolism connected with new interaction between eEF1A1 and PKM2, we have performed metabolic profiling of CCRF-CEM cells treated by compound **3** (1x IC50, 12 hours). This part of work was done in collaboration with Department of Metabolomics and some results are described in diploma thesis of Barbora Halířová, M.Sc.[297]. Significant changes in close pathway proximity of PKM2 were found. The metabolites upstream PKM2 are in higher concentration: 3-phosphoglycerate (fold change - FCH 1.53), DHAP (FCH 4.15), glucose-1-phosphate (FCH 1.45), erythrose-4-phosphate (FCH 2.71) (Fig. 38). Additionally, some metabolites of citrate cycle were detected in high concentration: citrate/isocitrate (FCH 8.93), aconitate (FCH 2.81) and acetyl-CoA (FCH 4.19) (Fig. 38). Other changes are visible in oxidative stress routes – depletion of taurine (FCH 0.19) and changes of ratio of oxidised glutathione GSSG (FCH 0.27) and reduced glutathione GSH (FCH 2.27). Other routes affected was nucleotide basis synthesis - depletion of orotic acid

(FCH 0.19), 5-Amino-4-imidazolecarboxamide Riboside (AICAR) depletion (FCH 0.29), hypoxantine abundance (FCH 8.78), decreased UTP (FCH 0.48) and 2-deoxyadenosine (FCH 0.31). On the other hand, some metabolites of nucleotide synthesis are in higher concentration after compound **3** treatment (adenine FCH 2.25; uracil FCH 2.19; dGDP FCH 4.10). Some amino acids were depleted (N-acetylmethionine FCH 0.25; glutamate FCH 0.52) (Fig. 39), p-value for all mentioned metabolites fold changes $p \leq 0.05$.
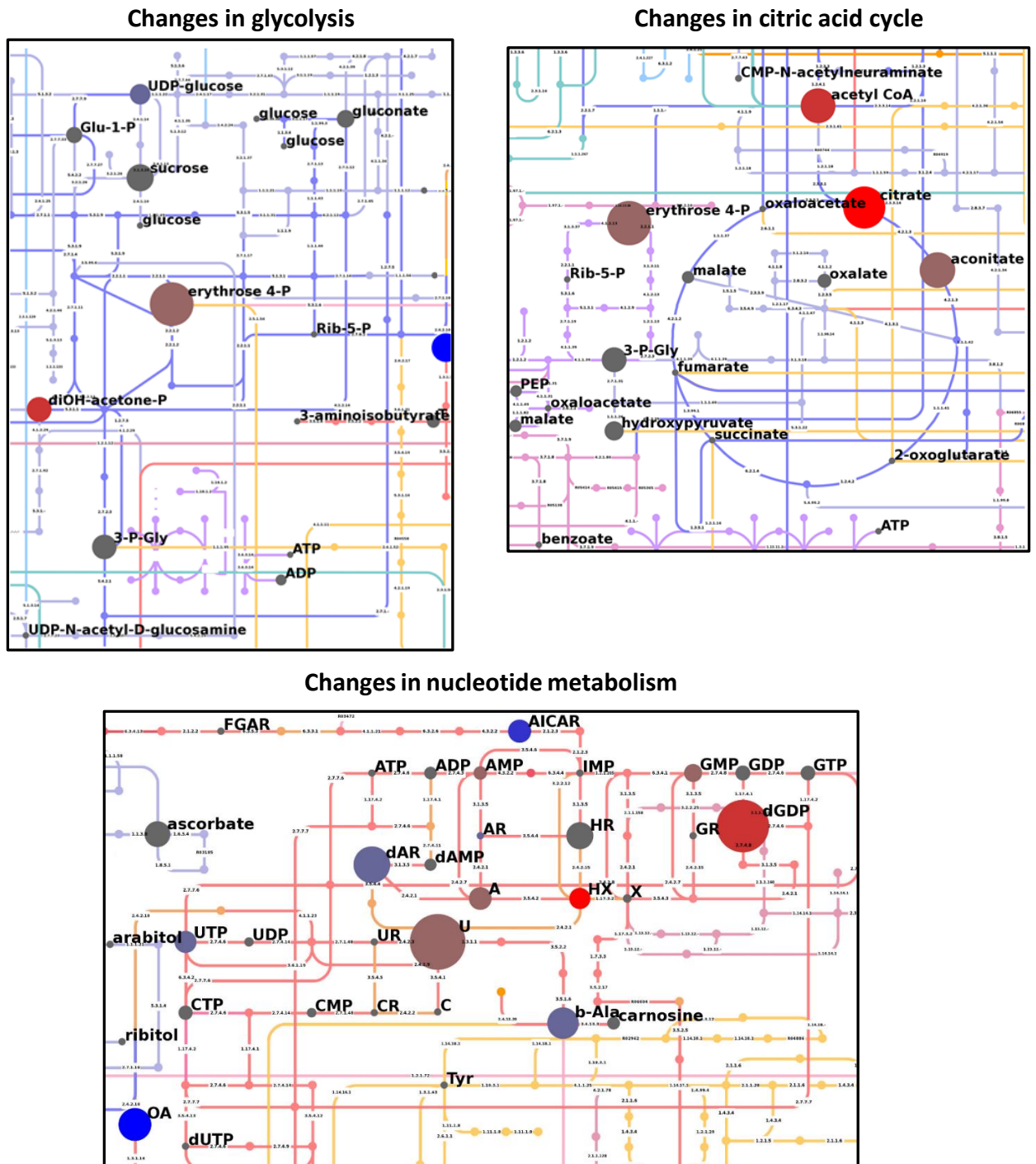
Figure 38. Metabolic profiling. Metabolic pathways with depicted increased (red) and decreased (blue) metabolites after 1x IC50 compound **3** treatment CCRF-CEM, 12 hours. Size of dots in map represents p-value and color of dots represents relative difference between two tested groups of samples (metabolites from treated and control cells). Changes of metabolites in glycolysis, citric acid cycle and nucleotide metabolism. Legend of significantly changed metabolites Glu-1-P (glucose 1 phosphate), 3-P-Gly (3 phospho glycerate), OA (orotic acid), HX (hypoxantin), A (adenine), U (uracil), dGDP (deoxyguanosine diphosphate)

The part of the picture was published before as a part of[297].
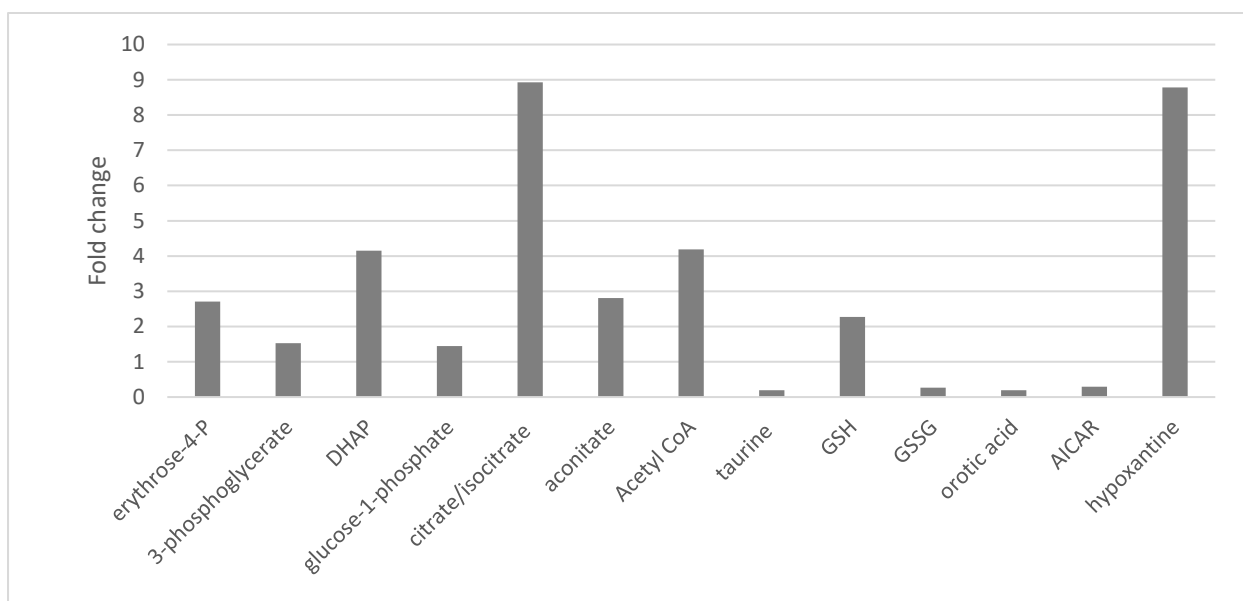
Figure 39. Fold change after treatment (1x IC50 of compound **3**, 12 hours, CCRF-CEM) of several metabolites, p-value ≤ 0.05.

2.2.2.11 Following structure design of new 3-HQ and their biological evaluation

This data were published before as a part of publication[157] (appendix B).

Based on the favorable biological features of compound **1-3**, set of potentially improved 3-HQ was synthetized. According previous experience three positions R^1, R^2 and R^3 were chosen for derivatization and new derivates were tested first by molecular docking[157]. Those with most favorable docking energy (lower than -35589.5 $J.mol^{-1}$) were selected and based on ease of synthesis, seven derivatives were synthetized (Fig. 40, Tab. 3).
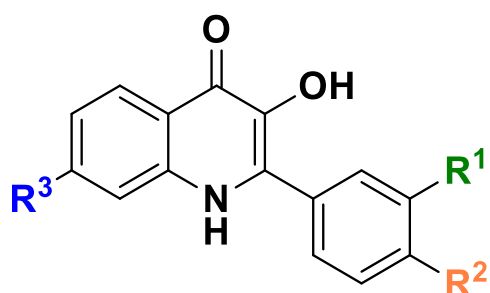
Comp. Nº	R^1	R^2	R^3
4	-CO₂H	—N(piperidine)	-H
5	-CO₂H	—N(morpholine)	-H
6	-CONH₂	—N(piperidine)	-H
7	-CONH₂	—N(morpholine)	-H
8	-CONH₂	—N(pyrrolidine)	-CONH-Pent
9	-CONH₂	—N(pyrrolidine)	-CONH-Bn
10	-H	-H	-H

Figure 40. 3-HQ derivatives selected for synthesis. Pent-pentyl, Bn-benzyl. The picture and table were published before as a part of publication[157] (appendix B).

Further, all the derivatives were tested by ITC to detect potential interaction between eEF1A1 and derivatives. Gamendazole was tested as a positive control and unsubstituted derivative **10** as a negative control. The measured enthalpies of all compounds and K_a suggest high affinities (Tab. 3) except compound **10** that exhibits no interaction. Stoichiometric number (n) is approximately one for all compounds. The negative values of free energy and enthalpy confirm spontaneous and exothermic binding ligands to eEF1A1.

Compound Nº	$\Delta_r H_m^\circ$ (kJ mol⁻¹)	K_a° (M⁻¹)	n	$\Delta_r S_m^\circ$ (J mol⁻¹ K⁻¹)	$\Delta_r G_m^\circ$ (J mol⁻¹)
4	-11272	2.536×10^6	0.798	-37686	-35919
5	-1872	1.029×10^7	1.640	-6147	-39272
6	-15999	2.899×10^6	0.932	-53539	-36347
7	-7932	6.796×10^6	0.746	-26474	-38777
8	-9416	5.297×10^6	1.129	-31454	-37990
9	-9213	1.809×10^7	1.694	-30764	-40713
10			*no interaction*		
Gamendazole	-1209	1.268×10^7	1.777	-3919	-40550

Table 3. Thermodynamic and binding parameters for the interaction of the 3-HQ compounds with eEF1A1 ($\Delta_r H_m^\circ$ = enthalpy change of binding; K_a = association constant; n = stoichiometry; $\Delta_r S_m^\circ$ = entropy change, $\Delta_r G_m^\circ$ = Gibbs energy change). The table was published before as a part of publication[157] (appendix B).

Finally, all compounds were tested by MTT assay for *in vitro* cytotoxic activity against human cancer and normal cell lines. The replacement of nitro group caused loss of activity (derivative **4** and **5**) compared to the compound **1**. This can be caused by carboxy moiety that can diminish penetration of compound through cell membrane. Transformation carboxy moiety to carboxamide improved activity of compound **6** and reach similar activity as compound **1** except for CEM-DNR and U2OS. The cytotoxicity against normal fibroblasts BJ was lower by one order. When the piperidine ring was exchanged by morpholine, the activity was lost (derivative **6** and **7**). Pentylamide moiety in position 7 increased significantly activity (derivative **8**), but the cytotoxicity to BJ fibroblasts was similar as with compound **1**. Transformation pentylamide with benzylamide (derivative **9**) leads to activity in micomolar concentrations but it was not active against multidrug resistance cell lines CEM-DNR and

K562-TAX. Moreover, the cytotoxicity against fibroblasts was significantly lower than compound **1-3** (Tab. 4).

3-HQ	R^1	R^2	R^3	A549	U2OS	CCRF-CEM	CEM-DNR	HCT-116	K562	K562-TAX	BJ
4	-CO$_2$H	1-piperidinyl	H-	50	50	49.56	50	50	50	50	50
5	-CO$_2$H	4-morpholinyl	H-	50	50	49.56	50	50	50	50	50
6	-CONH$_2$	1-piperidinyl	H-	9.96	26.02	3.34	21.43	4.46	7.1	6.41	48.92
7	-CONH$_2$	4-morpholinyl	H-	44.37	50	16.24	50	30.6	50	50	50
8	-CONH$_2$	1-piperidinyl	C$_5$H$_{11}$CONH-	1.89	0.56	1.73	8.03	0.64	2.39	32.71	10.24
9	-CONH$_2$	1-piperidinyl	PhCH$_2$CONH-	3.77	0.58	1.73	>50	1.01	8.30	>50	>50
10	-H	-H	H-	>50	46.96	26.74	22.49	44.20	47.96	27.44	>50

Table 4. Cytotoxic activities of new synthetized 3-HQ. The table was published before as a part of publication[157] (appendix B).

2.2.3 Discussion

A group of 3-nitro 4-amino 3-HQs compounds were tested by MTT assay to define their biologic activity. They exhibited high cytotoxic activity against several cancer cell lines in submicromolar and micromolar concentrations. Moreover, they show biologic activity against cell lines CEM-DNR and K562-TAX, multidrug resistance cell lines expressing ABC family transporters MRP and PGP1, respectively. Compound **3** was chosen for further analysis and tested against extended panel of cancer cell lines and fibroblasts. This compound exhibits high cytotoxicity against various cancer cell lines (leukemia cell lines CCRF-CEM, CEM-DNR, K562, K562-TAX, lung carcinomas - A549 and NciH-520, colorectal carcinoma HCT 116, prostate adenocarcinoma PC-3, breast adenocarcinoma MCF-7, uterine sarcoma MES-SA, cervix adenocarcinoma HeLa, osteosarcoma U2OS and mouse lymphoid tumor P388D1). Moreover, compound **3** was highly active against deleted or mutated cell lines [(HCT 116 p53-/-, HCT 116 p53(R248W/-), HCT 116 K-Ras(G13D/-), HCT 116 K-Ras(+/-)]. Cytotoxicity of compound **3** against normal fibroblasts (foreskin fibroblasts BJ, lung fibroblasts MRC-5) was significantly lower, 9.39 for BJ and 63.38 for MRC-5.

The analysis of cell cycle performed on CCRF-CEM cells treated by compound **3** showed increased number of cells in G1 phase, together with S phase decrease and reduction of G2/M cells. This result is consistent with decrease of mitotic marker phospho-histone H3^{Ser10} and strong inhibition of DNA and RNA synthesis. Enhanced number of cells in subG1 indicates cells going to the apoptosis. Apparently, treatment by compound **3** leads to synthetic processes decrease, DNA and RNA synthesis inhibition and cell death.

The favorable features of the compound **3** suggest us to study its molecular target. For molecular target identification, we choose affinity purification pull down experiment. Two biotinylated variants of compound **3** were synthetized. One was biotinylated out of the active site (**derivative A**) to capture real target and second was biotinylated directly in the active site (**derivative B**) as a control to capture unspecific proteins. By the affinity purification coupled to mass spectrometry, we have identified repeatedly three proteins binding **derivative A**: pyruvate kinase M2, elongation factor 1 alpha 1 and β-actin. We have validated all three proteins by western blot. In order to know if all three proteins bind **derivative A** or are just in complex we have performed pull down of pure recombinant proteins PKM2, eEF1A1 or β-actin. By the validation of affinity purification result via western blot, we have identified eEF1A1 to be direct target of **derivative A** and PKM2 and β-actin are just eEF1A1 complexing

proteins. As was mentioned before, the interaction of eEF1A1 and β-actin is known from the literature[186,189–191], but interaction with PKM2 and eEF1A1 was not previously described. Recently, increased number of PKM2 interacting proteins was identified and eEF1A1 can be one of the new interacting partners of this key protein of tumorigenesis[252,298].

To characterize the interaction of eEF1A1 and PKM2 we have performed immunoprecipitation experiment of compound **3** treated or vehicle treated CCRF-CEM cells. We have found that interaction between eEF1A1 is dependent on compound **3** treatment. The interaction between eEF1A1 and PKM2 was not proved on vehicle treated CCRF-CEM cells. Therefore, compound **3** treatment leads to the eEF1A1 PKM2 interaction and may influence key regulation functions of the binding partners. eEF1A1 has been studied as important tumorigenesis protein[231,234,235]. Therefore, its binding by compound **3** can negatively influence its key tumorigenesis functions. Moreover, by the eEF1A1 PKM2 binding, the key tumorigenesis features of PKM2 can be broke up. As PKM2 can in dimer state enter the nucleus and influence expression of key tumorigenesis proteins (HIF1-α, VEGF-A, c-myc etc.)[246,251], binding PKM2 by eEF1A1 may abolish some of these processes.

Further, we have tested main functions of identified proteins. We have performed *in vitro* translation experiment to validate effect of compound **3** on translation. There was no significant effect on translation. Therefore, compound **3** has no effect on translational function of eEF1A1.

In the case of actin, we have studied cytoskeletal changes by actin pmKate2 transfected U2OS osteosarcoma cells. We have observed significant actin fragmentation in clearly visible 10, 12 and 24 hour intervals after compound **3** treatment. The fragmentation can be caused be late apoptosis changes.

To study PKM2 activity, we performed pyruvate kinase assay by monitoring ATP production and subsequent luminescence activity. We have found no effect of compound **3** on recombinant PKM2 activity. As we know, that PKM2 is in treated cells in the complex with other proteins, mainly with eEF1A1, we have decided to study effect on immunoprecipitated PKM2 from compound **3** treated CCRF-CEM cells. PKM2 was immunoprecipitated via anti-PKM2 antibody or anti-eEF1A1 antibody. Subsequently, we have performed pyruvate kinase assay directly with immunoprecipitated PKM2. To stabilize eEF1A1 PKM2 interaction the compound **3** was added in to the reaction. Pyruvate kinase M2 was inhibited to 70 % for anti-PKM2 immunoprecipitated PKM2 and to 53 % for anti-eEF1A1 imunoprecipitated PKM2. Both reactions were stabilized by compound **3**. This results suggest that compound **3** can support eEF1A1 binding PKM2 and decrease its activity. Decrease of its activity can be

triggered by PKM2 tetramer break up to dimer or by other conformation changes. The necessity of eEF1A1 participation in PKM2 inhibition is evident from pyruvate kinase assay with commercial recombinant PKM2, where no effect of compound **3** on its activity was observed.

Two kinds of small molecules that inhibits cancer growth via PKM2 are described in the literature. The first are PKM2 inhibitors, compounds that inhibits transfer of phosphate from PEP to ADP and following ATP generation. Several PKM2 inhibiting compounds was described by Vander Heiden and the most potent small molecule demonstrated more than 60 % inhibition and induced cell death of cancer cells [299]. Later, highly potent inhibitors shikonin and its enantiomer isomer alkanin were found to inhibit enzymatic function of PKM2 in submicromolar concentrations and also can overcome cancer drug resistance[27]. The second group of small molecules are PKM2 activators, compounds that induces tetramerization of PKM2. By the tetramerization the glycolytic metabolic advantage of PKM2 dimer formation is broke up and therefore cancer proliferation and viability is affected. The inhibition of lung cancer cells proliferation was observed after treatment by compounds that can tetramerize PKM2[300]. Our results suggest that compound **3** belongs to the inhibitors of PKM2.

Another function assay analyzed GTPase function of eEF1A1. The GTPase assay was studied by commercial GTPase assay based on malachite green colorimetric measurement. Immunoprecipitated eEF1A1 from compound **3** treated CCRF-CEM cells was measured compare to untreated control immunoprecipitated eEF1A1. The increase of GTPase activity to 161% was detected in treated sample. This enhanced GTPase activity is not connected with higher rate of translation as is obvious from the translation analysis studied before.

The metabolic profiling of CCRF-CEM cells treated by compound **3** was performed to analyze the effect of PKM2 on binding to eEF1A1. We have observed several changes in the cell metabolism. There is evident effect on nucleotide synthesis - almost depleted ortotic acid – intermediate of pyrimidine synthesis, almost depleted AICAR, intermediate in purine *de novo* synthesis, high abundant hypoxantine, product of purine degradation, decreased UTP and 2-deoxy adenosine. On the other hand, some metabolites were detected in higher concentration (adenosine, uracil and dGDP).

The changes of glucose metabolism support decrease of PKM2 activity. The metabolites upstream PKM2 are upregulated: 3-phosphoglycerate, DHAP, glucose-1-phosphate and erythrose-4-phosphate. Additionaly, some metabolites of citric acid cycle are highly upregulated (Acetyl-CoA, citrate/isocitrate, aconitate). The citrate cycle (TCA) is crucial for cancer cell, as the pyruvate from glycolysis is converted to lactate, cell replenishes TCA intermediates by alternative pathways. One of the crucial metabolic pathways is

glutaminolysis that replenishes intermediates of TCA for ATP production[301]. We have found interesting connection with our proteomic and metabolomics data. The glutamate, intermediate of glutaminolysis, is decreased in the compound **3** treated cells. Glutaminolysis is cancer cells is positively regulated by MYC protein[302]. Additionally, c-Myc gene transcription have been recently found to be positively regulated by PKM2[246]. As PKM2 function is affected by binding compound **3** and eEF1A1, MYC production can be deregulated and glutaminolysis affected. Unfortunately, we haven´t detected all metabolites of TCA citrate and glutaminolysis to explain more consequences.

The evidence of eEF1A1 interaction with compound **3** was measured by ITC. The titration profile and measured K_a proved compound **3** and eEF1A1 interaction.

Based on the favorable biological features of compounds **1-3**, seven new 3-HQ compounds was synthetized. All compounds were tested by ITC for interaction with eEF1A1 and for all the interaction was confirmed, only exception was compound **10**, non-active derivative used as a negative control. The activity of new compounds was evaluated by MTT cytotoxic assay. Some derivatives were active in micromolar and submicromolar concentration against cancer cell lines (derivative **6**, **8** and **9**). Importantly, derivatives **6** and **9** has significantly lower activity against BJ fibroblasts. Derivative **9** has toxicity against fibroblasts comparable with original compounds **1-3**. On the other hand, derivative **9** has no effect to the resistant cancer cell lines CEM-DNR and K562-TAX.

2.2.4 Conclusion

In this work, the new biologically active compounds 3-HQ are described. Their primary target eEF1A1 was elucidated and its interacting partner PKM2 was described. We have found that compound **3** can trigger eEF1A1 PKM2 interaction. The treatment by compound **3** has PKM2 inhibitory effect, probably connected also by the interaction with eEF1A1. Recently, a lot of moonlighting functions of PKM2 and eEF1A1 key for tumorigenesis process has been observed[172,252,298]. Therefore, 3-HQ are very promising compounds that aims at least two key tumorigenesis proteins: directly eEF1A1 and indirectly PKM2. Apparently, there is probably more inhibitory effects of 3-HQ that leads to apoptosis of cancer cells.

2.2.5 Author´s contribution

The data from this work were partly published in the Journal of Medicinal Chemistry with title Identification of Eukaryotic Translation Elongation Factor 1-α 1 Gamendazole-Binding Site for Binding of 3-Hydroxy-4(1 H)-quinolinones as Novel Ligands with Anticancer Activity[157] (appendix B). The author contributed to the design of experiments, performing and optimization of identification of protein target experiments (affinity purification, sample preparation for mass spectrometry analysis and MS identification), validation of results (affinity purification with recombinant proteins, enzymatic assays, analysis of *in vitro* translation and actin fragmentation monitoring), sample preparation and analysis of metabolic profiling results and cell cycle analysis. Author contributed to the data analysis of all experiments and wrote the biological part of the publication[157] (appendix B).

2.3 Identification of mechanism of action of new nucleoside cytostatic AB61

In our collaborating laboratory in the Instutute of Organic Chemistry and Biochemistry, was synthetized and studied cytotoxic activity of group of hetaaryl-7-deazapurine ribonucleosides. They have exhibited nanomolar cytotoxic activities against panel of cancer cell lines. 6-hetaryl-7-deazapurine ribonucleosides are highly cytotoxic comparable to conventional nucleoside cytostatics as clofarabine[303]. Later, 7-hetaaryl-7-deazaadenosines were studied for their strong antiproliferative effect against several solid tumor and hematological malignancies[287]. SAR study revealed that modification of the ribose leads to the decrease of cytotoxicity or complete inefficiency of these compounds[304,305]. On the other hand, base-modified compound with substitution of 7- deazapurine in positions 2 or 6 exhibited submicromolar cytotoxicities[306].

The most promising compound is 7-(2-thienyl)-7-deazaadenosine named AB61 (Fig. 41). It exhibits subnanomolar cytotoxicity against several leukemic and solid cancer cell lines and more importantly, its cytotoxicity is lower against normal fibroblasts (2-3 orders of magnitude). The cell cycle analysis of AB61 on CCRF-CEM cells discovered G2/M inhibition, fast apoptosis onset, strong RNA synthesis inhibition and in higher concentration as well DNA synthesis inhibition. Further, AB61 was found to be efficiently phosphorylated in the Du-145 human prostate cancer cells. AB61-TP (triphosphate) was discovered to be very mild inhibitor of RNA polymerase II and weak inhibitor of adenosine kinase. To study in vivo AB61 activity, the P388D1 leukemia survival model was performed and demonstrated prolonged mice survival[287].
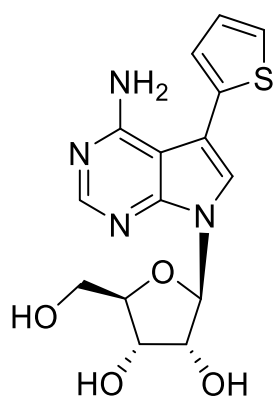
AB61

Figure 41. The structure of AB61 (modified from[307]).

Further, the ability of AB61-TP to incorporate into DNA and RNA was tested. It was found that AB61-TP is substrate for viral T7 RNA polymerase and that ATP can be substituted by AB61-TP within the transcription. Moreover, AB61-TP is substrate for Klenow fragment of DNA polymerase and DNA polymerase γ during primer extension experiment. In addition, AB61 incorporation into DNA and RNA were confirmed in living CCRF-CEM cell line using ₃H-labeled AB61 and measured by liquid scintillation counting or HPLC/MS with UV/VIS detection. By the gene expression analysis coupled with pathway analysis DNA damage network was identified to be highly affected by AB61 treatment. Further analysis of U2OS-53BP1-GFP cells (enabling detection of DNA damage lesions by accumulation of 53BP1 protein in DNA double strain breaks) treated by AB61 confirmed accumulation of 53BP1 foci in the nuclei of treated cells. Therefore, AB61 induces DNA damage[307].

The aim of the project was analysis of the AB61 different cytotoxicity in cancer cells and fibroblasts and analysis how the protein synthesis is affected by AB61. The data from this project were published in Molecular Cancer Therapeutics[307] (appendix C).

2.3.1 Material and methods

The methods were previously published in similar version in[307] (appendix C).

Cell lines

The CCRF-CEM, HCT116, A549, K-562, BJ and MRC-5 cell lines were purchased from the American Tissue Culture Collection (ATCC). HCT116p53-/- cell line was purchased from Horizon Discovery, UK. The daunorubicin resistant subline of CCRF-CEM cells (CEM-DNR) and paclitaxel resistant subline K562-TAX were selected in our laboratory[291,292].

Cytotoxic MTT assay

The cells were maintained in Nunc/Corning 80 cm^2 plastic tissue culture flasks and cultured in cell culture medium (DMEM/ RPMI 1640 with 5 $g \cdot L^{-1}$ glucose, 2 mM L-glutamine, 100 $U \cdot mL^{-1}$ penicillin, 100 $\mu g \cdot mL^{-1}$ streptomycin, 10% fetal calf serum, and $NaHCO_3$). Cell suspensions were prepared and diluted according to the particular cell type and expected target cell density (25,000–30,000 $cells \cdot well^{-1}$ based on cell growth characteristics). Cells were added by a pipette (80 μL) into 96-well microtiter plates. Inoculates were preincubated for 24 h at 37 °C and 5% CO_2 to stabilize. Four-fold dilutions of 20-μL aliquots, of the intended test concentrations were added to the microtiter plate walls at time zero. All test compound concentrations were examined in duplicates. Incubation of the cells with the compounds lasted for 72 h at 37 °C in 5% CO_2 atmosphere and 100% humidity. At the end of the incubation period, the cells were assayed using MTT. Aliquots (10 μL) of a MTT stock solution were pipetted into each well and incubated for further 1 - 4 h. After this incubation period the produced formazan was dissolved in 100 $\mu L \cdot well^{-1}$ of 10% aq. SDS (pH 5.5), followed by further incubation at 37 °C overnight. The optical density (OD) was measured at 540 nm with a Labsystem iEMS Reader MF. Tumor cell survival (IC50) was calculated using the following equation: IC = (ODdrug-exposed well/mean ODcontrol wells) × 100%. The IC50 value, corresponding to the drug concentration lethal for 50% of the tumor cells, was calculated from appropriate dose-response curves.

Intracellular phosphorylation

HCT116 and BJ cells were seeded into 6-well plates at 60% confluence in the cultivation medium (McCoy's 5A and DMEM medium, respectively, supplemented with 5 g/L glucose, 2 mM glutamine, 100 U/mL penicillin, 100 μg/mL streptomycin, 10% fetal calf serum, and NaHCO$_3$). Next day, cells were treated by 1 μM or 10 μM AB61. After 3 h incubation, cells were washed 2 times with phosphate buffered saline containing 0.5% FBS and 3 times with phosphate buffered saline. The cell pellets were extracted with 70% cold MeOH (1 mL). Supernatants were collected, dried under vacuum, and samples were resuspended in DMSO-water (1:1100 μL) for analysis. The samples were analyzed using ultra-performance reversed phase chromatography coupled to triple tandem mass spectrometry UPLC-MS/MS. The UPLC chromatograph used in this study was Accela Thermo Scientific system consisting of gradient quaternary pump, thermostated autosampler, degasser, column oven and triple quadrupole mass spectrometer TSQ Quantum Access (Thermo Scientific). Xcalibur™ data system software was used for an instrument control and data analysis. The C18 column (XBridge™ BEH C18, 2.5 μm, 2.1 x 50 mm) and ammonium acetate (pH 5.04)/acetonitrile gradient elution were applied for chromatographic separation. The electrospray ionization and negative selected reaction mode MS/MS were used for analyte quantification. Standard curves and quality control samples were generated for all analytes using extracts from untreated cells.

In vitro **transcription of EGFP-luciferase DNA template**

To evaluate functionality of RNA with incorporated AB61-TP or Tub-TP, we first PCR-amplified template DNA coding EGFP-luciferase under T7 promoter. MEGAscript T7 kit (Ambion) was used for *in vitro* transcription of EGFP-luciferase template in the presence of hetaryl-7-deazapurine ribonucleoside triphosphates. *In vitro* transcription reactions were performed according to manufacturer's protocol. Each transcription reaction (20 mL) contained of EGFP-luciferase DNA template (2751 bp, 100 ng), ATP, GTP, CTP, and UTP (7.5 mM each), enzyme mix (2 mL), and AB61-TP or Tub-TP (final concentration: 1 mM). In the control experiment, water was used instead of the solution of the tested compound. The transcription reactions were performed at 37 °C for 2 hours. Then, DNase I (2 U/mL, 1 mL) was added and

the mixtures were incubated at 37 °C for 15 minutes. RNA transcripts were purified on NucAway Spin Columns (Ambion). The quantity and purity of RNA transcripts was determined on Agilent 2100 Bioanalyzer (RNA 600 Nano Total RNA kit, Agilent) and by NanoDrop 1000 Spectrophotometer.

In vitro translation efficacy of EGFP-luciferase RNA transcripts with incorporated AB61-TP or Tub-TP

The EGFP-luciferase RNA transcripts with or without incorporated AB61-TP or Tub-TP were used as templates for *in vitro* translation using reticulocyte lysate system (Retic Lysate IVT Kit, Ambion) according to the manufacturer's protocol. The *in vitro* translation mixture (25 mL) contained EGFP-luciferase RNA transcript (500 ng), low salt mix-met (1 mL), high salt mix-met (0.25 mL), methionine (0.83 mM, 1.5 mL), and the reticulocyte lysate (17 mL). In the positive control experiment, unmodified EGFP-luciferase RNA transcript was used, in the negative control experiment no RNA template was added. The translation reactions were incubated in water bath at 30 °C for 1.5 hours. Efficacy of *in vitro* translation was evaluated via measurement of luciferase enzymatic activity (Luciferase Assay System, Promega) on EnVision Multilabel Reader (PerkinElmer) and by western blot analysis using primary anti-Luciferase antibody (Promega) and secondary peroxidase-conjugated antibody (Sigma-Aldrich) analyzed by enhanced chemiluminescence (Amersham).

2.3.2 Results

This data was previously pulished as a part of publication[307] (appendix C).

AB61 shows differential *in vitro* cytotoxic activity against cancer cell lines and normal fibroblasts

We have retested AB61 and its monophosphate against several cancer a normal cell lines. AB61 is strongly cytotoxic against cancer cell lines A549, CCRF-CEM, HCT116 and K562. AB61 cytotoxicity is in subnanomolar concentrations. Moreover, it is highly active against multidrug resistance cell lines CEM-DNR and K562-TAX expressing multidrug resistance transporters. Further, it is highly active against HCT116 p53-/- colorectal cancer cell line with inactivated p53 gene. Significantly, the cytotoxicity against normal cells (fibroblasts BJ, MRC-5) has been lower 2-5 orders of magnitude. Oppositely, AB61-MP has significantly lower activity (approximately 2 orders of magnitude) and difference between cancer cell lines and fibroblast was not so straight (Tab. 5).

Cell line	MTT, IC50 (µM)	
	AB61	**AB61-MP**
A549	0.010	1.06
CCRF-CEM	0.00036	0.16
CEM-DNR	0.043	0.45
HCT116	0.0019	0.18
HCT116p53-/-	0.067	0.83
K562	0.0095	0.21
K562-TAX	0.0083	0.99
BJ	8.00	0.24
MRC-5	11.4	7.84

Table 5. The cytotoxicity of AB61 and A61-MP against several cancer and normal cell lines. The table was published before as a part of publication[307] (appendix C).

Intracellular phosphorylation of AB61 is limited in normal fibroblasts

The efficiency of phosphorylation of AB61 was studied in colon cancer cell line HCT116 and BJ fibroblasts. Cells were treated by AB61 in two concentrations (1 and 10 µM) and extracted by methanol in two time intervals (1 and 3 hours). The amount of AB61 monophosphate (AB-MP), AB61 diphosphate (AB-DP) and AB61 triphosphate (AB61-TP) was analyzed by U

PLC analysis. In HCT116 1-hour treatment no or only a minor amount of AB61-MP was detected after treatment with both concentration (1 or 10 µM) of AB61 but high concentrations of AB61-MP were observed in HCT116 cells after 3-hour treatment.

BJ fibroblasts exhibited good uptake of AB61 but no AB61-MP was detected (Fig. 42). Therefore, cellular phosphorylation of AB61 is ineffective in BJ fibroblasts. AB61-DP and AB61-TP were not detected in any cell line, probably due to short treatment time, fast incorporation into macromolecules and/or concentrations under the detection limit.

A

Cell line	Dosing (1 µM; 1 hour; pmol/5x10^5 cells)		Dosing (10 µM; 1 hour; pmol/5x10^5 cells)	
	AB61	AB61-MP	AB61	AB61-MP
HCT116	81.6 ± 3.48	0	88.1 ± 13.0	0.56 ± 0.44
BJ	76.7 ± 7.30	0	82.7 ± 7.33	0

B

Cell line	Dosing (1 µM; 3 hours; pmol/5x10^5 cells)		Dosing (10 µM; 3 hours; pmol/5x10^5 cells)	
	AB61	AB61-MP	AB61	AB61-MP
HCT116	117 ± 21.6	32.0 ± 5.65	120 ± 22.8	15.6 ± 3.62
BJ	68.0 ± 1.33	0	67.6 ± 3.07	0

Figure 42. Intracellular phosphorylation of AB61 at various concentrations. A) 1 hour AB61 treatment interval B) 3 hours AB61 treatment interval. The tables were published before as a part of publication[307] (appendix C).

Incorporation of AB61-TP into mRNA blocks its translation *in vitro*

This part of work was done in collaboration with the Institute of Organic Chemistry and Biochemistry of and was partly described in dissertation thesis of Pavla Perlíková, M.Sc., Ph.D.[308] The ability of AB61-TP incorporation into the RNA by T7 RNA polymerase have been studied previously[307]. Further, we wanted to evaluate functional properties of RNA containing nucleoside analogue and the efficiency of protein translation of such RNA. We have performed commercial *in vitro* transcription of EFGP-luciferase fusion gene under T7 promoter into RNA in the presence of all natural nucleotides (ATP, GTP, CTP, UTP) with/without AB61-TP or tubercidin triphosphate (Tub-TP) so that AB61-TP or Tub-TP could be incorporated into RNA template. The purified transcripts were used as templates for *in vitro* translation reaction using commercial *in vitro* translation kit from reticulocyte lysate. The efficiency of translation was measured by luminescence intensity and western blot detecting luciferase protein (Fig. 43). Comparable luminescence intensity and the presence of luciferase protein was detected in the case of translation from unmodified RNA and Tub-TP modified RNA. Interestingly, there was no measurable protein (luminescence or western blot) translated from AB61-TP modified mRNA. This result shows that AB61-TP can be incorporated into RNA by T7 RNA polymerase in the presence of ATP. Moreover, the presence of AB61 in the RNA block its function as a template for protein translation.
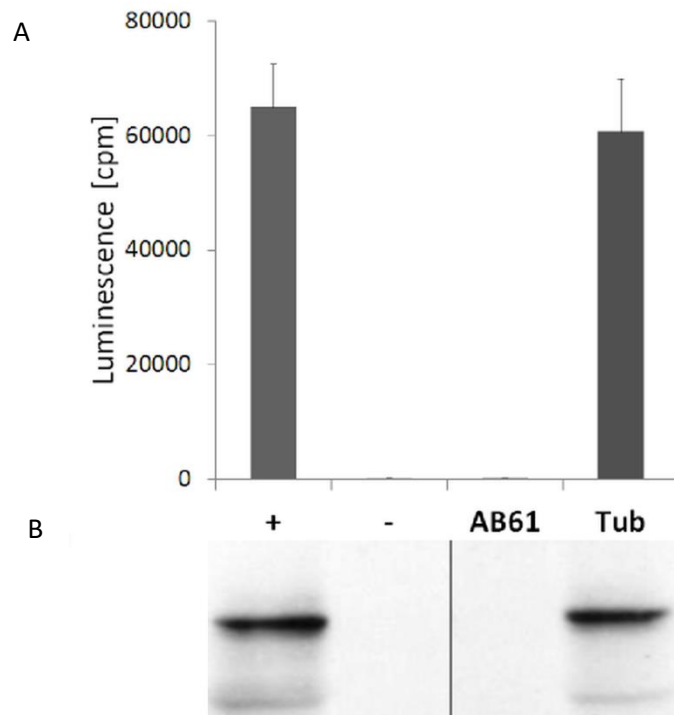
Figure 43. *In vitro* translation reactions with different RNA templates for EGFP-luciferase. A) luminiscence intensity, data represent averages of two independent experiments; B) western blot analysis with anti-luciferase antibody. Key: +: unmodified RNA template; -: no template; AB61: RNA template produced in the presence of AB61-TP; Tub: RNA template produced in the presence of Tub-TP. The picture was published before as a part of publication[307] (appendix C).

2.3.3 Discussion

In this study, we have focused on analysis of differential cytotoxicity of AB61 on cancer cell lines and fibroblasts. In addition, specific mechanism of action of this compound is described.

The cytotoxicity of AB61 was measured by MTT assay in subnanomolar concentrations against several cancer cell lines (A549, CCRF-CEM, CEM-DNR, HCT116, HCT116p53 -/-, K562, K562-TAX) and more importantly the activity against normal fibroblasts (BJ, MRC-5) was significantly lower (2-5 orders of magnitude). On the other hand, AB61-MP cytotoxicity against cancer cell lines was lower (typically by 2 orders of magnitude) and the specificity compared to the fibroblasts was poor.

We were interested in mechanism of difference of toxicity of cancer cells and fibroblasts. We have demonstrated that AB61 is effectively phosphorylated in the colon cancer HCT116 cell line (IC50 1.9 nM) but phosphorylation is inefficient in normal BJ fibroblasts. These data are supported by the fact that adenosine kinase, enzyme overexpressed in colorectal tumors[309] may be involved in AB61 phosphorylation and contribute to AB61 efficiency and selectivity.

Previous data proved that AB61 is incorporated into RNA and RNA polymerase II is not inhibited[307]. Therefore, we were interested how the AB61-TP modified RNA can be translated into the protein. The commercial *in vitro* transcription assay with all nucleotides plus AB61-TP coupled to *in vitro* translation revealed that AB61-TP modified template could not be translated into the protein. On the other hand, Tub-TP modified mRNA was translated into the fully active protein. This unique mechanism of action to our knowledge it is the first description of such an effect in the class of cytostatic nucleosides. Therefore, AB61 is very potent and promising compound. Further studies of the compound are currently under way.

2.3.4 Conclusion

In this work, the cytotoxicity and mechanism of action of very promising nucleoside analogue AB61 have been described. The different phosphorylation of the compound AB61 in colon cancer cells HCT116 and fibroblasts BJ have been dicovered. The translation block of proteosynthesis of template RNA containing nucleoside analogue AB61-TP was proved and new mechanism of action for the nucleotide analogues compounds have been described.

2.3.5 Author´s contribution

The data from this work were published in the Molecular Cancer Therapeutics with title 7-(2-Thienyl)-7-Deazaadenosine (AB61), a New Potent Nucleoside Cytostatic with a Complex Mode of Action[308] (appendix C). The author performed intracellular phosphorylation of AB61 experiment, developed and optimized the methodology for *in vitro* translation experiment. The author contributed to the writing of the manuscript.

3. **Summary**

This thesis is divided into three parts. In the first theoretical part the methods for drug target identification and two groups of anticancer compounds (quinolone derivatives and nucleoside analogs) are described. The necessity of identification the direct target of drugs and describing exact mechanism of action is obvious. It is crucial to describe the most actions triggered by the small molecule (drug) to describe exact mechanism of action. This information can be used for explaining drug side effects, small molecule optimization, potential use for another disease (drug repurposing) and give us new information about targeted processes, biomolecules or signaling pathways.

In the last decades many new methods and instruments were developed, optimized and used for describing drug mode of action and drug target identification. Chemical proteomics is scientific branch connecting molecular biology, structural biology, bioinformatics, biochemistry, organic chemistry and many proteomic and analytical methods such as mass spectrometry that are used for drug target deconvolution.

Affinity purification is key method for drug target identification. It is based on immobilizing modified small molecule on the resin. Afterwards, the immobilized small molecule probe is incubated with complex mixture of proteins of interest. Captured proteins are washed, eluted, separated and identified mainly by mass spectrometry. It was used with variety of modifications for target deconvolution of many compounds. We can modify a lot of aspect of the AP experiment - the choose of immobilizing matrix, optimization of linkers connecting the compound, the experimental procedure (washing steps, purification procedure) or identification process and/or quantification. When the immobilization of the compound is problem, we can use cell permeable probes (TAT, FLAG), energetic-based target identification (DARTS), click chemistry probes or serial affinity chromatography. The experiment design is always chosen according experimental requirements.

The mass spectrometry is mostly inseparable part of the affinity purification experiment. The precision of contemporary mass spectrometers enables us exact identification of target protein(s) from the protein mixture. The possibility of protein quantification allows to compare more samples or states (disease/healthy; treated/untreated) in the experiment. Some methods enable to quantify 8-10 samples in one experiment (iTRAQ, TMTs). The help of bioinformatics tools analyzing big amount of data (for example from mRNA profiling, protein

profiling or metabolic profiling etc.) is currently indispensable part for analysis of such big dataset enabling connect more molecular processes.

With the development of instrumentation, bioinformatics tools, databases and growing information about biomolecules, signaling routes and protein function, we can describe and understand many pharmacological processes in detail.

Second part of the thesis is focused on quinolone derivative project. The aim was to identify protein target of specific group of 3-HQ. This compounds exhibits favorable biological activities (high cytotoxicity for cancer cells versus low cytotoxicity for fibroblasts), accumulation of cells in G1 phase, together with strong inhibition of RNA and DNA synthesis and decrease of mitotic marker pH3Ser10. The identification of protein target of compound **3** was performed by affinity purification coupled to mass spectrometry and three proteins were repeatedly identified. eEF1A1 as a direct target, PKM2 and β-actin as interacting partners of eEF1A1. We have found many consequences and effects of the compound **3** by the functional analysis of this proteins. Compound **3** treatment (in CCRF-CEM cell line) induces interaction between eEF1A1 and PKM2 and subsequently inhibition of PKM2 activity (phosphorylation of ADP by phosphate from PEP). Furthermore, translation efficiency is not affected, but GTPase activity of eEF1A1 is upregulated to 161%. Actin fibers are highly fragmented after treatment in several hours. Metabolic profiling revealed many changes. Some of them are in agreement with the pyruvate kinase inhibition effect of the compound (upregulation of glycolytic metabolites upstream PKM2) and some of them are consistent with cell cycle analysis (downregulation of some nucleotides and their precursors, high abundance of hypoxanthine, product of purine degradation). All these data show how the compound **3** influence the CCRF-CEM cells. The compound **3** induces eEF1A1 PKM2 interaction that leads to the PKM2 activity decrease. This probably affect glucose cancer cell metabolism and further may influence key tumorigenesis functions of PKM2 and eEF1A1. The third protein β-actin is affected as well by the massive fragmentation of actin fibres. All the processes together with DNA, RNA synthesis inhibition leads to the apoptosis.

The eEF1A1 interaction with compound **3** was proved by ITC and based on this results several new 3-HQ was synthetized, tested for the eEF1A1 binding by ITC and tested for the cytotoxicity by MTT assay. The interaction was proved for all 6 compounds and the cytotoxicity showed some new optimized candidates with favorable activities. Further optimization of 3-HQs are currently in process.

The third part of the thesis is focused on nucleoside analogs, especially on the compound 7-(2-thienyl)-7-deazaadenosine named AB61. Previously, favorable biological

activities of the compound were studied (cancer specific cytotoxicity, G2/M inhibition, fast apoptosis onset, strong RNA synthesis inhibition, ability to incorporate into DNA and RNA). The task was explaining differential cytotoxicity in cancer cells and fibroblasts (2-5 orders of magnitude) by UPLC-MS/MS analysis of AB61 treated colorectal cancer cells HCT116 and fibroblasts BJ. Further, to analyze translation efficiency of RNA with incorporated AB61. The results show that AB61 is inefficiently phosphorylated in the fibroblasts and therefore the cytotoxicity is significantly lower. The *in vitro* translation analysis of RNA with incorporated AB61 was found to block translation. These data describe completely new mechanism of action of nucleoside cytostatic.

This work brings summary of methods used for drug target identification and identification of target/mechanism of action of two promising group of anticancer compounds, quinolone derivatives (compound **3**) and nucleoside analogs (compound AB61).

4. Souhrn

Tato práce je rozdělena do tří částí. V první části jsou popsány metody používané k identifikaci cílů léčiv a dvě skupiny léčiv (chinolonové deriváty a nuklesidová cytostatika). Potřeba přesně popsat cíle léčiv a jejich mechanismus účinku je zjevná. Je nezbytné popsat co nejvíce procesů, které látky v buňce spustí a přesně popsat jejich mechanismus účinku. Tyto informace jsou použity pro vysvětlení vedlejších účinků, optimalizaci látek, jejich potenciálním použití pro léčbu jiných nemocí a v neposlední řadě nám dávají cenné informace o cíleném procesu, biomolekulách a signálních drahách.

V posledních desetiletích bylo vyvinuto, optimalizováno a testováno mnoho nových metod a přístrojů pro identifikaci cílů léčiv. Chemická proteomika je vědecké odvětví spojující molekulární biologii, strukturální biologii, bioinformatiku, biochemii, organickou chemii a mnoho proteomických a analytických metod jako je hmotnostní spektrometrie, které jsou použity pro odhalení cílů léčiv.

Afinitní purifikace je klíčová metoda pro identifikaci cílů malých molekul. Je založena na imobilizaci malé molekuly na matrici, která je následně inkubována se směsí proteinů. Proteiny, jež jsou molekulou zachyceny, jsou dále promyty, separovány a následně identifikovány hmotnostní spektrometrií. Afinitní purifikace byla použita v mnoha obměnách pro identifikaci cílů léčiv. Můžeme pozměnit mnoho aspektů v experimentu afinitní purifikace od výběru matrice, linkerů, průběhu purifikace (odmývání, purifikační metoda), identifikačního procesu a/nebo kvantifikace. Pokud je imobilizace látky problematická, můžeme přistoupit k některé metodě, která modifikaci látky nevyžaduje – sondy, jež jsou schopny proniknout do buňky (FLAG, TAT), metoda DARTS, sondy využívající chemické reakce uvnitř buňky tzv. "click chemistry" nebo metodu sériové afinitní chromatografie. Experimentální design je vždy vybírán podle požadavků experimentu.

Hmotnostní spektrometrie je nedílnou součástí afinitní purifikace. Precizní měření dnešních hmotnostních spektrometrů nám umožňuje přesnou identifikaci cílového proteinu ve směsi proteinů. Kvantifikace proteinů umožňuje porovnat více vzorků nebo stavů (zdravý/nemocný; léčený/neléčený) v experimentu. Některé metody kvantifikace umožňují kvantifikaci 8-10 vzorků v jednom experimentu (iTRAQ, TMTs).

Při analýze velkých souborů dat (mRNA profilování, proteomické profilování nebo metabolické profilování atd.) se dnes používají bioinformatické nástroje, které jsou pro

zpracování velkého množství dat vyvinuty a jsou nepostradatelnou pomocí v propojení a porozumění více molekulárních procesů najednou.

S rozvojem nových přístrojů, bioinformatických nástrojů, databází a rostoucí informací o biomolekulách, signálních drahách a proteinových funkcí, můžeme podrobněji popsat a porozumět mnoha farmakologickým dějům.

Druhá část dizertační práce je zaměřená na projekt chinolonových derivátů. Cílem bylo identifikovat biologický cíl specifické skupiny chinolonových derivátů, zejména látky **3**. Tyhle látky vykazují výhodné biologické vlastnosti (vysoká cytotoxicita pro nádorové buňky, nízká pro fibroblasty), akumulace buněk v G1 fázi buněčného cyklu spolu s inhibicí DNA, výraznou inhibicí RNA syntézy a pokles mitotického markeru pH3Ser10.

Pomocí afinitní purifikace spojené s hmotnostní spektrometrií se podařily opakovaně identifikovat 3 proteiny: eEF1A1 přímý cíl a dva jeho vazební partneři PKM2 a β-aktin. Funkční analýzou těchto proteinů jsme objevili mnoho dějů spuštěných přeléčením látkou **3** a několik dalších souvislostí. Bylo zjištěno, že látka **3** indukuje interakci mezi eEF1A1 a PKM2, tato vazba nadále vede ke snížení aktivity PKM2 (fosforylace ADP na ATP pomocí fosfátu z PEP). Na druhou stranu, efektivita translace, jako primární funkce eEF1A1, nebyla nijak látkou ovlivněna, ale jeho GTPázová aktivita se zvýšila na 161 %. Vlákna aktinu jsou po inkubaci s látkou **3** výrazně fragmentována. Metabolické profilování odhalilo mnoho změn. Některé z nich jsou v souladu s inhibicí PKM2 (zvýšení množství glykolytických metabolitů "nad" PKM2) a některé z nich jsou v souladu s analýzou buněčného cyklu (snížení množství některých nukleotidů a jejich prekurzorů, nadbytek hypoxantinu, produktu purinové degradace). Všechny tyto změny ukazují, jak látka **3** ovlivňuje nádorové buňky CCRF-CEM. Látka **3** indukuje interakci eEF1A1 a PKM2, což vede k poklesu aktivity PKM2. To zřejmě ovlivňuje glukózový metabolismus nádorové buňky a dále pronádorové vlastnosti eEF1A1 a PKM2. Třetí protein, β-aktin je ovlivněn rozsáhlou fragmentací aktinových vláken. Všechny tyto děje spolu s inhibicí DNA a RNA syntézy vedou k apoptóze.

Interakce eEF1A1 a látky **3** byla prokázána metodou ITC. Na základě těchto dat bylo syntetizováno několik nových chinolonových derivátů, které byly testovány pomocí ITC na vazbu k eEF1A1 a pomocí MTT testu byla testována jejich cytotoxicita vůči nádorovým buňkám a fibroblastům. Interakce s eEF1A1 byla prokázána pro všech 6 optimalizovaných derivátů. Některé deriváty mají výhodnou cytotoxicitu a výhodný poměr cytoxicity nádorové buňky versus nenádorové fibroblasty. Další optimalizace těchto látek je v procesu.

Třetí část dizertační práce se zaměřuje na nukleosidová analoga, zejména na látku 7-(2-thienyl)-7-deazaadenosine nazvanou AB61. V předchozích studiích byly studovány

výhodné vlastnosti této látky (specifická cytotoxicita vůči nádorovým buňkám, G2/M inhibice, časný nástup apoptózy, inhibice RNA syntézy, schopnost inkorporovat se do DNA a RNA). Úkolem bylo vysvětlit rozdílnou cytotoxicitu nádorových buněk a fibroblastů (o 2-5 řádů) pomocí UPLC-MS/MS analýzy AB61 léčených buněk HCT116 (kolorektální karcinom) a BJ fibroblastů. Dále otestovat účinnost translace RNA s inkorporovanou látkou AB61.

Výsledky dokazují, že látka AB61 není účinně fosforylována ve fibrolastech a proto je cytotoxicita výrazně nižší. Test *in vitro* translace RNA s inkorporovanou látkou AB61 ukazuje, že takto modifikovaná RNA není schopna translace do proteinu, AB61 tedy blokuje translaci. Tyhle data popisují úplně nový mechanismus účinku u nukleosidových cytostatik.

Tato práce přináší souhrn metod používaných k identifikaci cílů a identifikuje cíle/popisuje mechanismus účinku dvou skupin protinádorových látek, chinolonových derivátů (látky **3**) a nukleosidových analog (látky AB61).

5. References:

1. Sakamoto, S., Hatakeyama, M., Ito, T. & Handa, H. Tools and methodologies capable of isolating and identifying a target molecule for a bioactive compound. *Bioorg. Med. Chem.* **20**, 1990–2001 (2012).

2. Rylova, G. *et al.* Affinity-based methods in drug-target discovery. *Curr. Drug Targets* **16**, 60–76 (2015).

3. Drews, J. Drug discovery: a historical perspective. *Science* **287**, 1960–1964 (2000).

4. Overington, J. P., Al-Lazikani, B. & Hopkins, A. L. How many drug targets are there? *Nat. Rev. Drug Discov.* **5**, 993–996 (2006).

5. Imming, P., Sinning, C. & Meyer, A. Drugs, their targets and the nature and number of drug targets. *Nat. Rev. Drug Discov.* **5**, 821–834 (2006).

6. Miller, M. T. & Strömland, K. Teratogen update: thalidomide: a review, with a focus on ocular findings and new potential uses. *Teratology* **60**, 306–321 (1999).

7. Singhal, S. *et al.* Antitumor activity of thalidomide in refractory multiple myeloma. *N. Engl. J. Med.* **341**, 1565–1571 (1999).

8. Ito, T. *et al.* Identification of a primary target of thalidomide teratogenicity. *Science* **327**, 1345–1350 (2010).

9. Donovan, K. A. *et al.* Thalidomide promotes degradation of SALL4, a transcription factor implicated in Duane Radial Ray syndrome. *eLife* **7**, (2018).

10. Broxterman, H. J. & Georgopapadakou, N. H. Anticancer therapeutics: 'Addictive' targets, multi-targeted drugs, new drug combinations. *Drug Resist. Updat. Rev. Comment. Antimicrob. Anticancer Chemother.* **8**, 183–197 (2005).

11. Morphy, R., Kay, C. & Rankovic, Z. From magic bullets to designed multiple ligands. *Drug Discov. Today* **9**, 641–651 (2004).

12.   Rix, U. *et al.* Chemical proteomic profiles of the BCR-ABL inhibitors imatinib, nilotinib, and dasatinib reveal novel kinase and nonkinase targets. *Blood* **110**, 4055–4063 (2007).

13.   Barros, S. A. & Martin, R. B. Predictive toxicogenomics in preclinical discovery. *Methods Mol. Biol. Clifton NJ* **460**, 89–112 (2008).

14.   Sheskin, J. THALIDOMIDE IN THE TREATMENT OF LEPRA REACTIONS. *Clin. Pharmacol. Ther.* **6**, 303–306 (1965).

15.   Pan, B. & Lentzsch, S. The application and biology of immunomodulatory drugs (IMiDs) in cancer. *Pharmacol. Ther.* **136**, 56–68 (2012).

16.   Kawamori, T., Rao, C. V., Seibert, K. & Reddy, B. S. Chemopreventive activity of celecoxib, a specific cyclooxygenase-2 inhibitor, against colon carcinogenesis. *Cancer Res.* **58**, 409–412 (1998).

17.   Siow, D. & Wattenberg, B. The histone deacetylase-6 inhibitor tubacin directly inhibits de novo sphingolipid biosynthesis as an off-target effect. *Biochem. Biophys. Res. Commun.* **449**, 268–271 (2014).

18.   Rix, U. & Superti-Furga, G. Target profiling of small molecules by chemical proteomics. *Nat. Chem. Biol.* **5**, 616–624 (2009).

19.   Saxena, C., Higgs, R. E., Zhen, E. & Hale, J. E. Small-molecule affinity chromatography coupled mass spectrometry for drug target deconvolution. *Expert Opin. Drug Discov.* **4**, 701–714 (2009).

20.   Bantscheff, M., Scholten, A. & Heck, A. J. R. Revealing promiscuous drug-target interactions by chemical proteomics. *Drug Discov. Today* **14**, 1021–1029 (2009).

21.   Azarkan, M., Huet, J., Baeyens-Volant, D., Looze, Y. & Vandenbussche, G. Affinity chromatography: a useful tool in proteomics studies. *J. Chromatogr. B Analyt. Technol. Biomed. Life. Sci.* **849**, 81–90 (2007).

22.   Campbell, D. H., Luescher, E. & Lerman, L. S. Immunologic Adsorbents: I. Isolation of Antibody by Means of a Cellulose-Protein Antigen. *Proc. Natl. Acad. Sci. U. S. A.* **37**, 575–578 (1951).

23.   Sakamoto, S., Kabe, Y., Hatakeyama, M., Yamaguchi, Y. & Handa, H. Development and application of high-performance affinity beads: toward chemical biology and drug discovery. *Chem. Rec. N. Y. N* **9**, 66–85 (2009).

24.   Mori, T. *et al.* An easy preparation of 'monolithic type' hydrophilic solid phase: capability for affinity resin to isolate target proteins. *Bioorg. Med. Chem.* **14**, 5549–5554 (2006).

25.   https://www.thermofisher.com/hk/en/home/brands/product-brand/dynal.html.

26.   Godl, K. *et al.* An efficient proteomics method to identify the cellular targets of protein kinase inhibitors. *Proc. Natl. Acad. Sci. U. S. A.* **100**, 15434–15439 (2003).

27.   Chen, J. *et al.* Shikonin and its analogs inhibit cancer cell glycolysis by targeting tumor pyruvate kinase-M2. *Oncogene* **30**, 4297–4306 (2011).

28.   Stayton, P. S. *et al.* Streptavidin-biotin binding energetics. *Biomol. Eng.* **16**, 39–44 (1999).

29.   Shiyama, T., Furuya, M., Yamazaki, A., Terada, T. & Tanaka, A. Design and synthesis of novel hydrophilic spacers for the reduction of nonspecific binding proteins on affinity resins. *Bioorg. Med. Chem.* **12**, 2831–2841 (2004).

30.   Fasoli, E. *et al.* Para-aminobenzamidine linked regenerated cellulose membranes for plasminogen activator purification: effect of spacer arm length and ligand density. *J. Chromatogr. B Analyt. Technol. Biomed. Life. Sci.* **930**, 13–21 (2013).

31.   Zamolo, L. *et al.* Experimental and theoretical investigation of effect of spacer arm and support matrix of synthetic affinity chromatographic materials for the purification of monoclonal antibodies. *J. Phys. Chem. B* **114**, 9367–9380 (2010).

32.   Busini, V., Moiani, D., Moscatelli, D., Zamolo, L. & Cavallotti, C. Investigation of the influence of spacer arm on the structural evolution of affinity ligands supported on agarose. *J. Phys. Chem. B* **110**, 23564–23577 (2006).

33.   Diamandis, E. P. & Christopoulos, T. K. The biotin-(strept)avidin system: principles and applications in biotechnology. *Clin. Chem.* **37**, 625–636 (1991).

34.   Gilmore, B. F. *et al.* Expedited solid-phase synthesis of fluorescently labeled and biotinylated aminoalkane diphenyl phosphonate affinity probes for chymotrypsin- and elastase-like serine proteases. *Bioconjug. Chem.* **20**, 2098–2105 (2009).

35.   Dang, T. H. T. *et al.* Chemical probes of surface layer biogenesis in Clostridium difficile. *ACS Chem. Biol.* **5**, 279–285 (2010).

36.   Berry, A. F. H. *et al.* Rapid multilabel detection of geranylgeranylated proteins by using bioorthogonal ligation chemistry. *Chembiochem Eur. J. Chem. Biol.* **11**, 771–773 (2010).

37.   Cankarova, N., Funk, P., Hlavac, J. & Soural, M. Novel preloaded resins for solid-phase biotinylation of carboxylic acids. *Tetrahedron Lett.* **52**, 5782–5788 (2011).

38.   Hong, S. H. *et al.* Apoptosis induction of 2'-hydroxycinnamaldehyde as a proteasome inhibitor is associated with ER stress and mitochondrial perturbation in cancer cells. *Biochem. Pharmacol.* **74**, 557–565 (2007).

39.   Wang, G., Shang, L., Burgett, A. W. G., Harran, P. G. & Wang, X. Diazonamide toxins reveal an unexpected function for ornithine -amino transferase in mitotic cell division. *Proc. Natl. Acad. Sci.* **104**, 2068–2073 (2007).

40.   Ong, S.-E. *et al.* Identifying the proteins to which small-molecule probes and drugs bind in cells. *Proc. Natl. Acad. Sci. U. S. A.* **106**, 4617–4622 (2009).

41.   Dormán, G. & Prestwich, G. D. Using photolabile ligands in drug discovery and development. *Trends Biotechnol.* **18**, 64–77 (2000).

42.   Han, S.-Y. & Hwan Kim, S. Introduction to Chemical Proteomics for Drug Discovery and Development. *Arch. Pharm. (Weinheim)* **340**, 169–177 (2007).

43.   Griffith, E. C. *et al.* Methionine aminopeptidase (type 2) is the common target for angiogenesis inhibitors AGM-1470 and ovalicin. *Chem. Biol.* **4**, 461–471 (1997).

44.   Kotake, Y. *et al.* Splicing factor SF3b as a target of the antitumor natural product pladienolide. *Nat. Chem. Biol.* **3**, 570–575 (2007).

45. Lamos, S. M. *et al.* Mixed Isotope Photoaffinity Reagents for Identification of Small-Molecule Targets by Mass Spectrometry. *Angew. Chem. Int. Ed.* **45**, 4329–4333 (2006).

46. Kolb, H. C., Finn, M. G. & Sharpless, K. B. Click Chemistry: Diverse Chemical Function from a Few Good Reactions. *Angew. Chem. Int. Ed Engl.* **40**, 2004–2021 (2001).

47. Kolb, H. C. & Sharpless, K. B. The growing impact of click chemistry on drug discovery. *Drug Discov. Today* **8**, 1128–1137 (2003).

48. Yang, P.-Y. *et al.* Activity-based proteome profiling of potential cellular targets of Orlistat--an FDA-approved drug with anti-tumor activities. *J. Am. Chem. Soc.* **132**, 656–666 (2010).

49. Brooks, H., Lebleu, B. & Vivès, E. Tat peptide-mediated cellular delivery: back to basics. *Adv. Drug Deliv. Rev.* **57**, 559–577 (2005).

50. Fawell, S. *et al.* Tat-mediated delivery of heterologous proteins into cells. *Proc. Natl. Acad. Sci. U. S. A.* **91**, 664–668 (1994).

51. Saxena, C. *et al.* Capture of drug targets from live cells using a multipurpose immuno-chemo-proteomics tool. *J. Proteome Res.* **8**, 3951–3957 (2009).

52. Foerg, C. & Merkle, H. P. On the biomedical promise of cell penetrating peptides: limits versus prospects. *J. Pharm. Sci.* **97**, 144–162 (2008).

53. Huang, W. *et al.* Triptolide inhibits the proliferation of prostate cancer cells and down-regulates SUMO-specific protease 1 expression. *PloS One* **7**, e37693 (2012).

54. Driscoll, J. J. & Dechowdhury, R. Therapeutically targeting the SUMOylation, Ubiquitination and Proteasome pathways as a novel anticancer strategy. *Target. Oncol.* **5**, 281–289 (2010).

55. Fíla, J. & Honys, D. Enrichment techniques employed in phosphoproteomics. *Amino Acids* **43**, 1025–1047 (2012).

56. Andersson, L. & Porath, J. Isolation of phosphoproteins by immobilized metal (Fe^{3+}) affinity chromatography. *Anal. Biochem.* **154**, 250–254 (1986).

57. Matsuda, H., Nakamura, H. & Nakajima, T. New ceramic titania: Selective adsorbent for organic phosphates. *Anal. Sci.* **6**, 911–912 (1990).

58. Pan, X. *et al.* Global protein phosphorylation dynamics during deoxynivalenol-induced ribotoxic stress response in the macrophage. *Toxicol. Appl. Pharmacol.* **268**, 201–211 (2013).

59. Alpert, A. J. Hydrophilic-interaction chromatography for the separation of peptides, nucleic acids and other polar compounds. *J. Chromatogr.* **499**, 177–196 (1990).

60. Bantscheff, M. *et al.* Quantitative chemical proteomics reveals mechanisms of action of clinical ABL kinase inhibitors. *Nat. Biotechnol.* **25**, 1035–1044 (2007).

61. Kruse, U. *et al.* Chemoproteomics-based kinome profiling and target deconvolution of clinical multi-kinase inhibitors in primary chronic lymphocytic leukemia cells. *Leukemia* **25**, 89–100 (2011).

62. Colzani, M. *et al.* Quantitative Chemical Proteomics Identifies Novel Targets of the Anti-cancer Multi-kinase Inhibitor E-3810. *Mol. Cell. Proteomics* **13**, 1495–1509 (2014).

63. West, G. M. *et al.* Quantitative proteomics approach for identifying protein-drug interactions in complex mixtures using protein stability measurements. *Proc. Natl. Acad. Sci. U. S. A.* **107**, 9078–9082 (2010).

64. Liu, P.-F., Kihara, D. & Park, C. Energetics-based discovery of protein-ligand interactions on a proteomic scale. *J. Mol. Biol.* **408**, 147–162 (2011).

65. Lomenick, B., Olsen, R. W. & Huang, J. Identification of direct protein targets of small molecules. *ACS Chem. Biol.* **6**, 34–46 (2011).

66. Chang, Y., Schlebach, J. P., VerHeul, R. A. & Park, C. Simplified proteomics approach to discover protein-ligand interactions. *Protein Sci. Publ. Protein Soc.* **21**, 1280–1287 (2012).

67. Lomenick, B. *et al.* Target identification using drug affinity responsive target stability (DARTS). *Proc. Natl. Acad. Sci. U. S. A.* **106**, 21984–21989 (2009).

68. Pai, M. Y. *et al.* Drug affinity responsive target stability (DARTS) for small-molecule target identification. *Methods Mol. Biol. Clifton NJ* **1263**, 287–298 (2015).

69. Saxena, C., Zhen, E., Higgs, R. E. & Hale, J. E. An immuno-chemo-proteomics method for drug target deconvolution. *J. Proteome Res.* **7**, 3490–3497 (2008).

70.   Schmidt, P. M. *et al.* Taking down the FLAG! How insect cell expression challenges an established tag-system. *PloS One* **7**, e37779 (2012).

71.   Cravatt, B. F., Wright, A. T. & Kozarich, J. W. Activity-based protein profiling: from enzyme chemistry to proteomic chemistry. *Annu. Rev. Biochem.* **77**, 383–414 (2008).

72.   Verhelst, S. H. L. & Bogyo, M. Chemical proteomics applied to target identification and drug discovery. *BioTechniques* **38**, 175–177 (2005).

73.   Sadaghiani, A. M. *et al.* Design, synthesis, and evaluation of in vivo potency and selectivity of epoxysuccinyl-based inhibitors of papain-family cysteine proteases. *Chem. Biol.* **14**, 499–511 (2007).

74.   Bachovchin, D. A., Brown, S. J., Rosen, H. & Cravatt, B. F. Identification of selective inhibitors of uncharacterized enzymes by high-throughput screening with fluorescent activity-based probes. *Nat. Biotechnol.* **27**, 387–394 (2009).

75.   Missner, E. *et al.* Off-Target Decoding of a Multitarget Kinase Inhibitor by Chemical Proteomics. *ChemBioChem* **10**, 1163–1174 (2009).

76.   Zhang, S. & Gerhard, G. S. Heme mediates cytotoxicity from artemisinin and serves as a general anti-proliferation target. *PloS One* **4**, e7472 (2009).

77.   Boschetti, E. & Righetti, P. G. The ProteoMiner in the proteomic arena: a non-depleting tool for discovering low-abundance species. *J. Proteomics* **71**, 255–264 (2008).

78.   Thulasiraman, V. *et al.* Reduction of the concentration difference of proteins in biological liquids using a library of combinatorial ligands. *Electrophoresis* **26**, 3561–3571 (2005).

79.   Yadav, A. K. *et al.* A systematic analysis of eluted fraction of plasma post immunoaffinity depletion: implications in biomarker discovery. *PloS One* **6**, e24442 (2011).

80.   Chromy, B. A. *et al.* Proteomic analysis of human serum by two-dimensional differential gel electrophoresis after depletion of high-abundant proteins. *J. Proteome Res.* **3**, 1120–1127 (2004).

81.   Björhall, K., Miliotis, T. & Davidsson, P. Comparison of different depletion strategies for improved resolution in proteomic analysis of human serum samples. *Proteomics* **5**, 307–317 (2005).

82.   Fonslow, B. R. *et al.* Digestion and depletion of abundant proteins improves proteomic coverage. *Nat. Methods* **10**, 54–56 (2013).

83.   Oda, Y. *et al.* Quantitative chemical proteomics for identifying candidate drug targets. *Anal. Chem.* **75**, 2159–2165 (2003).

84.   Yamamoto, K., Yamazaki, A., Takeuchi, M. & Tanaka, A. A versatile method of identifying specific binding proteins on affinity resins. *Anal. Biochem.* **352**, 15–23 (2006).

85.   von Rechenberg, M. *et al.* Ampicillin/penicillin-binding protein interactions as a model drug-target system to optimize affinity pull-down and mass spectrometric strategies for target and pathway identification. *Proteomics* **5**, 1764–1773 (2005).

86.   Trinkle-Mulcahy, L. *et al.* Identifying specific protein interaction partners using quantitative mass spectrometry and bead proteomes. *J. Cell Biol.* **183**, 223–239 (2008).

87.   Chen, G. I. & Gingras, A.-C. Affinity-purification mass spectrometry (AP-MS) of serine/threonine phosphatases. *Methods San Diego Calif* **42**, 298–305 (2007).

88.   Gingras, A.-C. *et al.* A novel, evolutionarily conserved protein phosphatase complex involved in cisplatin sensitivity. *Mol. Cell. Proteomics MCP* **4**, 1725–1740 (2005).

89.   Ma, H. & Horiuchi, K. Y. Chemical microarray: a new tool for drug screening and discovery. *Drug Discov. Today* **11**, 661–668 (2006).

90.   Uttamchandani, M., Wang, J. & Yao, S. Q. Protein and small molecule microarrays: powerful tools for high-throughput proteomics. *Mol. Biosyst.* **2**, 58–68 (2006).

91.   Huang, J. *et al.* Finding new components of the target of rapamycin (TOR) signaling network through chemical genetics and proteome chips. *Proc. Natl. Acad. Sci. U. S. A.* **101**, 16594–16599 (2004).

92.   MacBeath, G. & Schreiber, S. L. Printing proteins as microarrays for high-throughput function determination. *Science* **289**, 1760–1763 (2000).

93.   Ziauddin, J. & Sabatini, D. M. Microarrays of cells expressing defined cDNAs. *Nature* **411**, 107–110 (2001).

94. Shen, Z. *et al.* Porous silicon as a versatile platform for laser desorption/ionization mass spectrometry. *Anal. Chem.* **73**, 612–619 (2001).

95. Zou, H. *et al.* A Mass Spectrometry Based Direct-Binding Assay for Screening Binding Partners of Proteins. *Angew. Chem.* **114**, 668–670 (2002).

96. Terstappen, G. C., Schlüpen, C., Raggiaschi, R. & Gaviraghi, G. Target deconvolution strategies in drug discovery. *Nat. Rev. Drug Discov.* **6**, 891–903 (2007).

97. Sleno, L. & Emili, A. Proteomic methods for drug target discovery. *Curr. Opin. Chem. Biol.* **12**, 46–54 (2008).

98. Aebersold, R. & Mann, M. Mass spectrometry-based proteomics. *Nature* **422**, 198–207 (2003).

99. Karas, M. & Hillenkamp, F. Laser desorption ionization of proteins with molecular masses exceeding 10,000 daltons. *Anal. Chem.* **60**, 2299–2301 (1988).

100. Fenn, J. B., Mann, M., Meng, C. K., Wong, S. F. & Whitehouse, C. M. Electrospray ionization for mass spectrometry of large biomolecules. *Science* **246**, 64–71 (1989).

101. Yates, J. R., Ruse, C. I. & Nakorchevsky, A. Proteomics by mass spectrometry: approaches, advances, and applications. *Annu. Rev. Biomed. Eng.* **11**, 49–79 (2009).

102. Han, X., Aslanian, A. & Yates, J. R. Mass spectrometry for proteomics. *Curr. Opin. Chem. Biol.* **12**, 483–490 (2008).

103. Domon, B. & Aebersold, R. Mass spectrometry and protein analysis. *Science* **312**, 212–217 (2006).

104. Cañas, B., López-Ferrer, D., Ramos-Fernández, A., Camafeita, E. & Calvo, E. Mass spectrometry technologies for proteomics. *Brief. Funct. Genomic. Proteomic.* **4**, 295–320 (2006).

105. Messana, I. *et al.* Unraveling the different proteomic platforms. *J. Sep. Sci.* **36**, 128–139 (2013).

106. Catherman, A. D., Skinner, O. S. & Kelleher, N. L. Top Down proteomics: facts and perspectives. *Biochem. Biophys. Res. Commun.* **445**, 683–693 (2014).

107. Peng, Y., Ayaz-Guner, S., Yu, D. & Ge, Y. Top-down mass spectrometry of cardiac myofilament proteins in health and disease. *Proteomics Clin. Appl.* **8**, 554–568 (2014).

108.   Mao, P. & Wang, D. Top-down proteomics of a drop of blood for diabetes monitoring. *J. Proteome Res.* **13**, 1560–1569 (2014).

109.   Catherman, A. D. *et al.* Large-scale top-down proteomics of the human proteome: membrane proteins, mitochondria, and senescence. *Mol. Cell. Proteomics MCP* **12**, 3465–3473 (2013).

110.   Siuti, N., Roth, M. J., Mizzen, C. A., Kelleher, N. L. & Pesavento, J. J. Gene-specific characterization of human histone H2B by electron capture dissociation. *J. Proteome Res.* **5**, 233–239 (2006).

111.   Unlü, M., Morgan, M. E. & Minden, J. S. Difference gel electrophoresis: a single gel method for detecting changes in protein extracts. *Electrophoresis* **18**, 2071–2077 (1997).

112.   Koncarevic, S. *et al.* Differential genomic and proteomic profiling of glioblastoma cells exposed to terpyridineplatinum(II) complexes. *Free Radic. Biol. Med.* **46**, 1096–1108 (2009).

113.   Tyleckova, J. *et al.* Cancer cell response to anthracyclines effects: mysteries of the hidden proteins associated with these drugs. *Int. J. Mol. Sci.* **13**, 15536–15564 (2012).

114.   Short, D. M. *et al.* Apoptosis induced by staurosporine alters chaperone and endoplasmic reticulum proteins: Identification by quantitative proteomics. *PROTEOMICS* **7**, 3085–3096 (2007).

115.   Campostrini, N. *et al.* Proteomic analysis of anti-angiogenic effects by a combined treatment with vinblastine and rapamycin in an endothelial cell line. *PROTEOMICS* **6**, 4420–4431 (2006).

116.   Liang, X. *et al.* Quantification of change in phosphorylation of BCR-ABL kinase and its substrates in response to Imatinib treatment in human chronic myelogenous leukemia cells. *PROTEOMICS* **6**, 4554–4564 (2006).

117.   Zhou, F., Xing, D., Wu, S. & Chen, W. R. Intravital Imaging of Tumor Apoptosis with FRET Probes During Tumor Therapy. *Mol. Imaging Biol.* **12**, 63–70 (2010).

118.   Ong, S.-E. & Mann, M. A practical recipe for stable isotope labeling by amino acids in cell culture (SILAC). *Nat. Protoc.* **1**, 2650–2660 (2006).

119.   Gygi, S. P. *et al.* Quantitative analysis of complex protein mixtures using isotope-coded affinity tags. *Nat. Biotechnol.* **17**, 994–999 (1999).

120.   Thompson, A. *et al.* Tandem mass tags: a novel quantification strategy for comparative analysis of complex protein mixtures by MS/MS. *Anal. Chem.* **75**, 1895–1904 (2003).

121.   Ross, P. L. *et al.* Multiplexed protein quantitation in Saccharomyces cerevisiae using amine-reactive isobaric tagging reagents. *Mol. Cell. Proteomics MCP* **3**, 1154–1169 (2004).

122.   Vaughn, C. P., Crockett, D. K., Lim, M. S. & Elenitoba-Johnson, K. S. J. Analytical characteristics of cleavable isotope-coded affinity tag-LC-tandem mass spectrometry for quantitative proteomic studies. *J. Mol. Diagn. JMD* **8**, 513–520 (2006).

123.   Shiio, Y. & Aebersold, R. Quantitative proteome analysis using isotope-coded affinity tags and mass spectrometry. *Nat. Protoc.* **1**, 139–145 (2006).

124.   Werner, T. *et al.* Ion coalescence of neutron encoded TMT 10-plex reporter ions. *Anal. Chem.* **86**, 3594–3601 (2014).

125.   Malki, K. *et al.* Pharmacoproteomic investigation into antidepressant response in two mouse inbred strains. *Proteomics* **12**, 2355–2365 (2012).

126.   Christoforou, A., Arias, A. M. & Lilley, K. S. Determining protein subcellular localization in mammalian cell culture with biochemical fractionation and iTRAQ 8-plex quantification. *Methods Mol. Biol. Clifton NJ* **1156**, 157–174 (2014).

127.   Hüttenhain, R. *et al.* N-glycoprotein SRMAtlas: a resource of mass spectrometric assays for N-glycosites enabling consistent and multiplexed protein quantification for clinical applications. *Mol. Cell. Proteomics MCP* **12**, 1005–1016 (2013).

128.   Zhu, W., Smith, J. W. & Huang, C.-M. Mass spectrometry-based label-free quantitative proteomics. *J. Biomed. Biotechnol.* **2010**, 840518 (2010).

129.   Voyksner, R. D. & Lee, H. Investigating the use of an octupole ion guide for ion storage and high-pass mass filtering to improve the quantitative performance of electrospray ion trap mass spectrometry. *Rapid Commun. Mass Spectrom. RCM* **13**, 1427–1437 (1999).

130.   Arike, L. & Peil, L. Spectral counting label-free proteomics. *Methods Mol. Biol. Clifton NJ* **1156**, 213–222 (2014).

131.   Hassell, A. M. *et al.* Crystallization of protein–ligand complexes. *Acta Crystallogr. D Biol. Crystallogr.* **63**, 72–79 (2007).

132.   Palmer, R. A. & Niwa, H. X-ray crystallographic studies of protein-ligand interactions. *Biochem. Soc. Trans.* **31**, 973–979 (2003).

133.   *Protein-ligand interactions: methods and applications*. (Humana Press ; Springer, 2013).

134.   Fernández, C. & Jahnke, W. New approaches for NMR screening in drug discovery. *Drug Discov. Today Technol.* **1**, 277–283 (2004).

135.   Freyer, M. W. & Lewis, E. A. Isothermal Titration Calorimetry: Experimental Design, Data Analysis, and Probing Macromolecule/Ligand Binding and Kinetic Interactions. in *Methods in Cell Biology* **84**, 79–113 (Elsevier, 2008).

136.   Pagadala, N. S., Syed, K. & Tuszynski, J. Software for molecular docking: a review. *Biophys. Rev.* **9**, 91–102 (2017).

137.   Hood, L. & Friend, S. H. Predictive, personalized, preventive, participatory (P4) cancer medicine. *Nat. Rev. Clin. Oncol.* **8**, 184–187 (2011).

138.   Hood, L. & Perlmutter, R. M. The impact of systems approaches on biological problems in drug discovery. *Nat. Biotechnol.* **22**, 1215–1217 (2004).

139.   Bhatia, V. N., Perlman, D. H., Costello, C. E. & McComb, M. E. Software tool for researching annotations of proteins: open-source protein annotation software with data visualization. *Anal. Chem.* **81**, 9819–9823 (2009).

140.   Dahlquist, K. D., Salomonis, N., Vranizan, K., Lawlor, S. C. & Conklin, B. R. GenMAPP, a new tool for viewing and analyzing microarray data on biological pathways. *Nat. Genet.* **31**, 19–20 (2002).

141.   Karp, P. D., Paley, S. & Romero, P. The Pathway Tools software. *Bioinforma. Oxf. Engl.* **18 Suppl 1**, S225-232 (2002).

142.   Huang, D. W., Sherman, B. T. & Lempicki, R. A. Systematic and integrative analysis of large gene lists using DAVID bioinformatics resources. *Nat. Protoc.* **4**, 44–57 (2009).

143. Naeem, A., Badshah, S., Muska, M., Ahmad, N. & Khan, K. The Current Case of Quinolones: Synthetic Approaches and Antibacterial Activity. *Molecules* **21**, 268 (2016).

144. Wang, J. C. DNA topoisomerases. *Annu. Rev. Biochem.* **54**, 665–697 (1985).

145. Hawkey, P. M. Mechanisms of quinolone action and microbial response. *J. Antimicrob. Chemother.* **51 Suppl 1**, 29–35 (2003).

146. Ahmed, A. & Daneshtalab, M. Nonclassical biological activities of quinolone derivatives. *J. Pharm. Pharm. Sci. Publ. Can. Soc. Pharm. Sci. Soc. Can. Sci. Pharm.* **15**, 52–72 (2012).

147. Aldred, K. J., Kerns, R. J. & Osheroff, N. Mechanism of quinolone action and resistance. *Biochemistry* **53**, 1565–1574 (2014).

148. Hradil, P. *et al.* 3-Hydroxy-2-phenyl-4(1H)-quinolinones as promising biologically active compounds. *Mini Rev. Med. Chem.* **9**, 696–702 (2009).

149. Hradil, P. & Jirman, J. Synthesis of 2-Aryl-3-hydroxyquinolin-4(1H)-ones. *Collect. Czechoslov. Chem. Commun.* **60**, 1357–1366 (1995).

150. Soural, M. *et al.* Synthesis and cytotoxic activity of substituted 2-phenyl-3-hydroxy-4(1H)-quinolinones-7-carboxylic acids and their phenacyl esters. *Eur. J. Med. Chem.* **41**, 467–474 (2006).

151. Soural, M. & Krchňák, V. Efficient Solid-Phase Synthesis of 2-Substituted-3-Hydroxy-4(1 *H*)-Quinolinone-7-Carboxamides with Two Diversity Positions. *J. Comb. Chem.* **9**, 793–796 (2007).

152. Sui, Z. *et al.* Synthesis and topoisomerase inhibitory activities of novel aza-analogues of flavones11Part of the work was presented at the XIVth International Symposium on Medicinal Chemistry, Maastricht, NL, 1996 (Abst. P–10.17). *Eur. J. Med. Chem.* **34**, 381–387 (1999).

153. Petr Krejčí, Pavel Hradil Jan Hlaváč, Marián Hajdúch. Derivatives of 2-phenyl-3-hydroxyquinoline-4(1H)-one and methods of their preparation and utilization.

154. Edvin J Iwanowitz, Scott H Watterson T.G. Murali Dhar, William J Pitts. HETEROCYCLES THAT ARE INHIBITORS OF IMPDH ENZYME. (2000).

155. Soural, M., Hlaváč, J., Funk, P., Džubák, P. & Hajdúch, M. 2-Phenylsubstituted-3-Hydroxyquinolin-4(1 *H*)-one-Carboxamides: Structure-Cytotoxic Activity Relationship Study. *ACS Comb. Sci.* **13**, 39–44 (2011).

156. Funk, P. *et al.* Preparation of 2-phenyl-3-hydroxyquinoline-4(1H)-one-5-carboxamides as potential anticancer and fluorescence agents. *RSC Adv.* **5**, 48861–48867 (2015).

157. Burglová, K. *et al.* Identification of Eukaryotic Translation Elongation Factor 1-α 1 Gamendazole-Binding Site for Binding of 3-Hydroxy-4(1 H)-quinolinones as Novel Ligands with Anticancer Activity. *J. Med. Chem.* **61**, 3027–3036 (2018).

158. Hradil, P. *et al.* Synthesis, NMR spectra and X-ray data of chloro and dichloro derivatives of 3-hydroxy-2-phenylquinolin-4(1 *H*)-ones and their cytostatic activity. *J. Heterocycl. Chem.* **41**, 375–379 (2004).

159. Soural, M., Hlaváč, J., Hradil, P. & Hajdúch, M. Efficient Synthesis and Cytotoxic Activity of Some Symmetrical Disulfides Derived from the Quinolin-4(1 *H*)-one Skeleton. *Eur. J. Org. Chem.* **2009**, 3867–3870 (2009).

160. Motyka, K., Hlaváč, J., Soural, M. & Funk, P. Fluorescence properties of 2-aryl-3-hydroxyquinolin-4(1H)-one-carboxamides. *Tetrahedron Lett.* **51**, 5060–5063 (2010).

161. Yushchenko, D. A. *et al.* 2-Aryl-3-hydroxyquinolones, a new class of dyes with solvent dependent dual emission due to excited state intramolecular proton transfer. *New J Chem* **30**, 774–781 (2006).

162. Yushchenko, D. A. *et al.* Synthesis and fluorescence properties of 2-aryl-3-hydroxyquinolones, a new class of dyes displaying dual fluorescence. *Tetrahedron Lett.* **47**, 905–908 (2006).

163. Lee, M.-H. & Surh, Y.-J. eEF1A2 as a Putative Oncogene. *Ann. N. Y. Acad. Sci.* **1171**, 87–93 (2009).

164. Migliaccio, N. *et al.* Ser/Thr kinases and polyamines in the regulation of non-canonical functions of elongation factor 1A. *Amino Acids* **48**, 2339–2352 (2016).

165. Lund, A., Knudsen, S. M., Vissing, H., Clark, B. & Tommerup, N. Assignment of human elongation factor 1alpha genes: EEF1A maps to chromosome 6q14 and EEF1A2 to 20q13.3. *Genomics* **36**, 359–361 (1996).

166. Chambers, D. M., Peters, J. & Abbott, C. M. The lethal mutation of the mouse wasted (wst) is a deletion that abolishes expression of a tissue-specific isoform of translation elongation factor 1alpha, encoded by the Eef1a2 gene. *Proc. Natl. Acad. Sci. U. S. A.* **95**, 4463–4468 (1998).

167. Lee, S., Francoeur, A. M., Liu, S. & Wang, E. Tissue-specific expression in mammalian brain, heart, and muscle of S1, a member of the elongation factor-1 alpha gene family. *J. Biol. Chem.* **267**, 24064–24068 (1992).

168. Knudsen, S. M., Frydenberg, J., Clark, B. F. & Leffers, H. Tissue-dependent variation in the expression of elongation factor-1 alpha isoforms: isolation and characterisation of a cDNA encoding a novel variant of human elongation-factor 1 alpha. *Eur. J. Biochem.* **215**, 549–554 (1993).

169. Sasikumar, A. N., Perez, W. B. & Kinzy, T. G. The many roles of the eukaryotic elongation factor 1 complex: The many roles of the eukaryotic elongation factor 1 complex. *Wiley Interdiscip. Rev. RNA* **3**, 543–555 (2012).

170. Mateyak, M. K. & Kinzy, T. G. eEF1A: Thinking Outside the Ribosome. *J. Biol. Chem.* **285**, 21209–21213 (2010).

171. Li, D., Wei, T., Abbott, C. M. & Harrich, D. The Unexpected Roles of Eukaryotic Translation Elongation Factors in RNA Virus Replication and Pathogenesis. *Microbiol. Mol. Biol. Rev.* **77**, 253–266 (2013).

172. Abbas, W., Kumar, A. & Herbein, G. The eEF1A Proteins: At the Crossroads of Oncogenesis, Apoptosis, and Viral Infections. *Front. Oncol.* **5**, (2015).

173. Lamberti, A. *et al.* The translation elongation factor 1A in tumorigenesis, signal transduction and apoptosis: review article. *Amino Acids* **26**, 443–448 (2004).

174. Grosshans, H., Simos, G. & Hurt, E. Review: transport of tRNA out of the nucleus-direct channeling to the ribosome? *J. Struct. Biol.* **129**, 288–294 (2000).

175. Khacho, M. *et al.* eEF1A is a novel component of the mammalian nuclear protein export machinery. *Mol. Biol. Cell* **19**, 5296–5308 (2008).

176. Calado, A., Treichel, N., Müller, E.-C., Otto, A. & Kutay, U. Exportin-5-mediated nuclear export of eukaryotic elongation factor 1A and tRNA. *EMBO J.* **21**, 6216–6224 (2002).

177. Bohnsack, M. T. *et al.* Exp5 exports eEF1A via tRNA from nuclei and synergizes with other transport pathways to confine translation to the cytoplasm. *EMBO J.* **21**, 6205–6215 (2002).

178. Murthi, A. *et al.* Regulation of tRNA Bidirectional Nuclear-Cytoplasmic Trafficking in **Saccharomyces cerevisiae**. *Mol. Biol. Cell* **21**, 639–649 (2010).

179. Mingot, J. M., Vega, S., Cano, A., Portillo, F. & Nieto, M. A. eEF1A Mediates the Nuclear Export of SNAG-Containing Proteins via the Exportin5-Aminoacyl-tRNA Complex. *Cell Rep.* **5**, 727–737 (2013).

180. Vera, M. *et al.* The translation elongation factor eEF1A1 couples transcription to translation during heat shock response. *eLife* **3**, (2014).

181. Gonen, H. *et al.* Protein synthesis elongation factor EF-1 alpha is essential for ubiquitin-dependent degradation of certain N alpha-acetylated proteins and may be substituted for by the bacterial elongation factor EF-Tu. *Proc. Natl. Acad. Sci. U. S. A.* **91**, 7648–7652 (1994).

182. Hotokezaka, Y. *et al.* Interaction of the eukaryotic elongation factor 1A with newly synthesized polypeptides. *J. Biol. Chem.* **277**, 18545–18551 (2002).

183. Caldas, T. D., El Yaagoubi, A. & Richarme, G. Chaperone properties of bacterial elongation factor EF-Tu. *J. Biol. Chem.* **273**, 11478–11482 (1998).

184. Chuang, S.-M. *et al.* Proteasome-Mediated Degradation of Cotranslationally Damaged Proteins Involves Translation Elongation Factor 1A. *Mol. Cell. Biol.* **25**, 403–413 (2005).

185. Kim, S. & Coulombe, P. A. Emerging role for the cytoskeleton as an organizer and regulator of translation. *Nat. Rev. Mol. Cell Biol.* **11**, 75–81 (2010).

186. Yang, F., Demma, M., Warren, V., Dharmawardhane, S. & Condeelis, J. Identification of an actin-binding protein from Dictyostelium as elongation factor 1a. *Nature* **347**, 494–496 (1990).

187. Edmonds, B. T. *et al.* Elongation factor-1 alpha is an overexpressed actin binding protein in metastatic rat mammary adenocarcinoma. *J. Cell Sci.* **109 (Pt 11)**, 2705–2714 (1996).

188. Suda, M. *et al.* Overproduction of elongation factor 1alpha, an essential translational component, causes aberrant cell morphology by affecting the control of growth polarity in fission yeast. *Genes Cells Devoted Mol. Cell. Mech.* **4**, 517–527 (1999).

189. Owen, C. H., DeRosier, D. J. & Condeelis, J. Actin crosslinking protein EF-1a of Dictyostelium discoideum has a unique bonding rule that allows square-packed bundles. *J. Struct. Biol.* **109**, 248–254 (1992).

190. Liu, G. *et al.* F-actin sequesters elongation factor 1alpha from interaction with aminoacyl-tRNA in a pH-dependent reaction. *J. Cell Biol.* **135**, 953–963 (1996).

191. Pittman, Y. R., Kandl, K., Lewis, M., Valente, L. & Kinzy, T. G. Coordination of eukaryotic translation elongation factor 1A (eEF1A) function in actin organization and translation elongation by the guanine nucleotide exchange factor eEF1Balpha. *J. Biol. Chem.* **284**, 4739–4747 (2009).

192. Gross, S. R. & Kinzy, T. G. Translation elongation factor 1A is essential for regulation of the actin cytoskeleton and cell morphology. *Nat. Struct. Mol. Biol.* **12**, 772–778 (2005).

193. Gross, S. R. & Kinzy, T. G. Improper organization of the actin cytoskeleton affects protein synthesis at initiation. *Mol. Cell. Biol.* **27**, 1974–1989 (2007).

194. Dreher, T. W. Role of tRNA-like structures in controlling plant virus replication. *Virus Res.* **139**, 217–229 (2009).

195. Matsuda, D. & Dreher, T. W. The tRNA-like structure of Turnip yellow mosaic virus RNA is a 3'-translational enhancer. *Virology* **321**, 36–46 (2004).

196. Matsuda, D., Yoshinari, S. & Dreher, T. W. eEF1A binding to aminoacylated viral RNA represses minus strand synthesis by TYMV RNA-dependent RNA polymerase. *Virology* **321**, 47–56 (2004).

197. Davis, W. G., Blackwell, J. L., Shi, P.-Y. & Brinton, M. A. Interaction between the cellular protein eEF1A and the 3'-terminal stem-loop of West Nile virus genomic RNA facilitates viral minus-strand RNA synthesis. *J. Virol.* **81**, 10172–10187 (2007).

198. Li, Z. *et al.* Translation elongation factor 1A facilitates the assembly of the tombusvirus replicase and stimulates minus-strand synthesis. *PLoS Pathog.* **6**, e1001175 (2010).

199. Yamaji, Y. *et al.* In vivo interaction between Tobacco mosaic virus RNA-dependent RNA polymerase and host translation elongation factor 1A. *Virology* **347**, 100–108 (2006).

200. Yamaji, Y. *et al.* Significance of eukaryotic translation elongation factor 1A in tobacco mosaic virus infection. *Arch. Virol.* **155**, 263–268 (2010).

201. Das, T., Mathur, M., Gupta, A. K., Janssen, G. M. & Banerjee, A. K. RNA polymerase of vesicular stomatitis virus specifically associates with translation elongation factor-1 alphabetagamma for its activity. *Proc. Natl. Acad. Sci. U. S. A.* **95**, 1449–1454 (1998).

202. Qanungo, K. R., Shaji, D., Mathur, M. & Banerjee, A. K. Two RNA polymerase complexes from vesicular stomatitis virus-infected cells that carry out transcription and replication of genome RNA. *Proc. Natl. Acad. Sci. U. S. A.* **101**, 5952–5957 (2004).

203. Warren, K. *et al.* Eukaryotic elongation factor 1 complex subunits are critical HIV-1 reverse transcription cofactors. *Proc. Natl. Acad. Sci. U. S. A.* **109**, 9587–9592 (2012).

204. Yue, J. *et al.* Cutaneous human papillomavirus type 38 E7 regulates actin cytoskeleton structure for increasing cell proliferation through CK2 and the eukaryotic elongation factor 1A. *J. Virol.* **85**, 8477–8494 (2011).

205. Duttaroy, A., Bourbeau, D., Wang, X. L. & Wang, E. Apoptosis rate can be accelerated or decelerated by overexpression or reduction of the level of elongation factor-1 alpha. *Exp. Cell Res.* **238**, 168–176 (1998).

206. Chen, E., Proestou, G., Bourbeau, D. & Wang, E. Rapid up-regulation of peptide elongation factor EF-1alpha protein levels is an immediate early event during oxidative stress-induced apoptosis. *Exp. Cell Res.* **259**, 140–148 (2000).

207. Ruest, L.-B., Marcotte, R. & Wang, E. Peptide elongation factor eEF1A-2/S1 expression in cultured differentiated myotubes and its protective effect against caspase-3-mediated apoptosis. *J. Biol. Chem.* **277**, 5418–5425 (2002).

208.   Borradaile, N. M. *et al.* A critical role for eukaryotic elongation factor 1A-1 in lipotoxic cell death. *Mol. Biol. Cell* **17**, 770–778 (2006).

209.   Panasyuk, G., Nemazanyy, I., Filonenko, V., Negrutskii, B. & El'skaya, A. V. A2 isoform of mammalian translation factor eEF1A displays increased tyrosine phosphorylation and ability to interact with different signalling molecules. *Int. J. Biochem. Cell Biol.* **40**, 63–71 (2008).

210.   Nawa, H. & Takei, N. BDNF as an anterophin; a novel neurotrophic relationship between brain neurons. *Trends Neurosci.* **24**, 683–684; discussion 684-685 (2001).

211.   Inamura, N., Nawa, H. & Takei, N. Enhancement of translation elongation in neurons by brain-derived neurotrophic factor: implications for mammalian target of rapamycin signaling. *J. Neurochem.* **95**, 1438–1445 (2005).

212.   Chang, Y. W. & Traugh, J. A. Insulin stimulation of phosphorylation of elongation factor 1 (eEF-1) enhances elongation activity. *Eur. J. Biochem.* **251**, 201–207 (1998).

213.   Redpath, N. T., Foulstone, E. J. & Proud, C. G. Regulation of translation elongation factor-2 by insulin via a rapamycin-sensitive signalling pathway. *EMBO J.* **15**, 2291–2297 (1996).

214.   Hao, H.-X. & Rutter, J. The role of PAS kinase in regulating energy metabolism. *IUBMB Life* **60**, 204–209 (2008).

215.   DeMille, D. & Grose, J. H. PAS kinase: a nutrient sensing regulator of glucose homeostasis. *IUBMB Life* **65**, 921–929 (2013).

216.   Eckhardt, K. *et al.* Male germ cell expression of the PAS domain kinase PASKIN and its novel target eukaryotic translation elongation factor eEF1A1. *Cell. Physiol. Biochem. Int. J. Exp. Cell. Physiol. Biochem. Pharmacol.* **20**, 227–240 (2007).

217.   Kielbassa, K., Müller, H. J., Meyer, H. E., Marks, F. & Gschwendt, M. Protein kinase C delta-specific phosphorylation of the elongation factor eEF-alpha and an eEF-1 alpha peptide at threonine 431. *J. Biol. Chem.* **270**, 6156–6162 (1995).

218.   Peters, H. I., Chang, Y. W. & Traugh, J. A. Phosphorylation of elongation factor 1 (EF-1) by protein kinase C stimulates GDP/GTP-exchange activity. *Eur. J. Biochem.* **234**, 550–556 (1995).

219.	Venema, R. C., Peters, H. I. & Traugh, J. A. Phosphorylation of elongation factor 1 (EF-1) and valyl-tRNA synthetase by protein kinase C and stimulation of EF-1 activity. *J. Biol. Chem.* **266**, 12574–12580 (1991).

220.	Piazzi, M. *et al.* eEF1A phosphorylation in the nucleus of insulin-stimulated C2C12 myoblasts: Ser[53] is a novel substrate for protein kinase C βI. *Mol. Cell. Proteomics MCP* **9**, 2719–2728 (2010).

221.	Izawa, T. *et al.* Elongation factor-1 alpha is a novel substrate of rho-associated kinase. *Biochem. Biophys. Res. Commun.* **278**, 72–78 (2000).

222.	Lamberti, A. *et al.* C-Raf antagonizes apoptosis induced by IFN-alpha in human lung cancer cells by phosphorylation and increase of the intracellular content of elongation factor 1A. *Cell Death Differ.* **14**, 952–962 (2007).

223.	Sanges, C. *et al.* Raf kinases mediate the phosphorylation of eukaryotic translation elongation factor 1A and regulate its stability in eukaryotic cells. *Cell Death Dis.* **3**, e276 (2012).

224.	Lin, K. W., Yakymovych, I., Jia, M., Yakymovych, M. & Souchelnytskyi, S. Phosphorylation of eEF1A1 at Ser300 by TβR-I results in inhibition of mRNA translation. *Curr. Biol. CB* **20**, 1615–1625 (2010).

225.	Calvisi, D. F. *et al.* Increased lipogenesis, induced by AKT-mTORC1-RPS6 signaling, promotes development of human hepatocellular carcinoma. *Gastroenterology* **140**, 1071–1083 (2011).

226.	Wang, C. *et al.* Inactivation of Spry2 accelerates AKT-driven hepatocarcinogenesis via activation of MAPK and PKM2 pathways. *J. Hepatol.* **57**, 577–583 (2012).

227.	Ho, C. *et al.* AKT (v-akt murine thymoma viral oncogene homolog 1) and N-Ras (neuroblastoma ras viral oncogene homolog) coactivation in the mouse liver promotes rapid carcinogenesis by way of mTOR (mammalian target of rapamycin complex 1), FOXM1 (forkhead box M1)/SKP2, and c-Myc pathways. *Hepatol. Baltim. Md* **55**, 833–845 (2012).

228.	Marine, J.-C. & Jochemsen, A. G. MDMX (MDM4), a Promising Target for p53 Reactivation Therapy and Beyond. *Cold Spring Harb. Perspect. Med.* **6**, (2016).

229. Pellegrino, R. *et al.* EEF1A2 inactivates p53 by way of PI3K/AKT/mTOR-dependent stabilization of MDM4 in hepatocellular carcinoma. *Hepatol. Baltim. Md* **59**, 1886–1899 (2014).

230. Qiu, F.-N. *et al.* Eukaryotic elongation factor-1α 2 knockdown inhibits hepatocarcinogenesis by suppressing PI3K/Akt/NF-κB signaling. *World J. Gastroenterol.* **22**, 4226–4237 (2016).

231. Li, X., Li, J. & Li, F. P21 activated kinase 4 binds translation elongation factor eEF1A1 to promote gastric cancer cell migration and invasion. *Oncol. Rep.* **37**, 2857–2864 (2017).

232. Liu, L. *et al.* As an independent prognostic factor, FAT10 promotes hepatitis B virus-related hepatocellular carcinoma progression via Akt/GSK3β pathway. *Oncogene* **33**, 909–920 (2014).

233. Hipp, M. S., Kalveram, B., Raasi, S., Groettrup, M. & Schmidtke, G. FAT10, a ubiquitin-independent signal for proteasomal degradation. *Mol. Cell. Biol.* **25**, 3483–3491 (2005).

234. Blanch, A., Robinson, F., Watson, I. R., Cheng, L. S. & Irwin, M. S. Eukaryotic translation elongation factor 1-alpha 1 inhibits p53 and p73 dependent apoptosis and chemotherapy sensitivity. *PloS One* **8**, e66436 (2013).

235. Chen, S.-L. *et al.* eEF1A1 Overexpression Enhances Tumor Progression and Indicates Poor Prognosis in Hepatocellular Carcinoma. *Transl. Oncol.* **11**, 125–131 (2018).

236. Noguchi, T., Yamada, K., Inoue, H., Matsuda, T. & Tanaka, T. The L- and R-type isozymes of rat pyruvate kinase are produced from a single gene by use of different promoters. *J. Biol. Chem.* **262**, 14366–14371 (1987).

237. Noguchi, T., Inoue, H. & Tanaka, T. The M1- and M2-type isozymes of rat pyruvate kinase are produced from the same gene by alternative RNA splicing. *J. Biol. Chem.* **261**, 13807–13812 (1986).

238. Mazurek, S. Pyruvate kinase type M2: a key regulator of the metabolic budget system in tumor cells. *Int. J. Biochem. Cell Biol.* **43**, 969–980 (2011).

239. Mazurek, S., Boschek, C. B., Hugo, F. & Eigenbrodt, E. Pyruvate kinase type M2 and its role in tumor growth and spreading. *Semin. Cancer Biol.* **15**, 300–308 (2005).

240. Chaneton, B. *et al.* Serine is a natural ligand and allosteric activator of pyruvate kinase M2. *Nature* **491**, 458–462 (2012).

241.   Keller, K. E., Tan, I. S. & Lee, Y.-S. SAICAR Stimulates Pyruvate Kinase Isoform M2 and Promotes Cancer Cell Survival in Glucose-Limited Conditions. *Science* **338**, 1069–1072 (2012).

242.   Mazurek, S. Pyruvate kinase type M2: a key regulator of the metabolic budget system in tumor cells. *Int. J. Biochem. Cell Biol.* **43**, 969–980 (2011).

243.   Lv, L. *et al.* Acetylation targets the M2 isoform of pyruvate kinase for degradation through chaperone-mediated autophagy and promotes tumor growth. *Mol. Cell* **42**, 719–730 (2011).

244.   Anastasiou, D. *et al.* Inhibition of pyruvate kinase M2 by reactive oxygen species contributes to cellular antioxidant responses. *Science* **334**, 1278–1283 (2011).

245.   Luo, W. *et al.* Pyruvate kinase M2 is a PHD3-stimulated coactivator for hypoxia-inducible factor 1. *Cell* **145**, 732–744 (2011).

246.   Yang, W. *et al.* Nuclear PKM2 regulates β-catenin transactivation upon EGFR activation. *Nature* **480**, 118–122 (2011).

247.   Gao, X., Wang, H., Yang, J. J., Liu, X. & Liu, Z.-R. Pyruvate kinase M2 regulates gene transcription by acting as a protein kinase. *Mol. Cell* **45**, 598–609 (2012).

248.   Jiang, Y. *et al.* PKM2 regulates chromosome segregation and mitosis progression of tumor cells. *Mol. Cell* **53**, 75–87 (2014).

249.   Jiang, Y. *et al.* PKM2 phosphorylates MLC2 and regulates cytokinesis of tumour cells. *Nat. Commun.* **5**, (2014).

250.   Lee, J., Kim, H. K., Han, Y.-M. & Kim, J. Pyruvate kinase isozyme type M2 (PKM2) interacts and cooperates with Oct-4 in regulating transcription. *Int. J. Biochem. Cell Biol.* **40**, 1043–1054 (2008).

251.   Azoitei, N. *et al.* PKM2 promotes tumor angiogenesis by regulating HIF-1α through NF-κB activation. *Mol. Cancer* **15**, (2016).

252.   Hsu, M.-C. & Hung, W.-C. Pyruvate kinase M2 fuels multiple aspects of cancer cells: from cellular metabolism, transcriptional regulation to extracellular signaling. *Mol. Cancer* **17**, (2018).

253.   Galmarini, C. M., Mackey, J. R. & Dumontet, C. Nucleoside analogues and nucleobases in cancer treatment. *Lancet Oncol.* **3**, 415–424 (2002).

254.   Fischer, E. & Ach, L. Neue Synthese der Harnsäure und ihrer Methylderivate. *Berichte Dtsch. Chem. Ges.* **28**, 2473–2480 (1895).

255.   Rosemeyer, H. The chemodiversity of purine as a constituent of natural products. *Chem. Biodivers.* **1**, 361–401 (2004).

256.   Legraverend, M. & Grierson, D. S. The purines: potent and versatile small molecule inhibitors and modulators of key biological targets. *Bioorg. Med. Chem.* **14**, 3987–4006 (2006).

257.   Ferrari, V. & Serpi, M. Nucleoside analogs and tuberculosis: new weapons against an old enemy. *Future Med. Chem.* **7**, 291–314 (2015).

258.   Vere Hodge, R. A. & Field, H. J. Antiviral agents for herpes simplex virus. *Adv. Pharmacol. San Diego Calif* **67**, 1–38 (2013).

259.   Balzarini, J. *et al.* Improved antiviral activity of the aryloxymethoxyalaninyl phosphoramidate (APA) prodrug of abacavir (ABC) is due to the formation of markedly increased carbovir 5'-triphosphate metabolite levels. *FEBS Lett.* **573**, 38–44 (2004).

260.   Liu, H. N. & Wong, C. K. In vitro immunosuppressive effects of methotrexate and azathioprine on Langerhans cells. *Arch. Dermatol. Res.* **289**, 94–97 (1997).

261.   Juliusson, G. & Liliemark, J. Purine Analogues: Rationale for Development, Mechanisms of Action, and Pharmacokinetics in Hairy Cell Leukemia. *Hematol. Oncol. Clin. North Am.* **20**, 1087–1097 (2006).

262.   Robak, P. & Robak, T. Older and new purine nucleoside analogs for patients with acute leukemias. *Cancer Treat. Rev.* **39**, 851–861 (2013).

263.   Kurimoto, A. *et al.* Synthesis and evaluation of 2-substituted 8-hydroxyadenines as potent interferon inducers with improved oral bioavailabilities. *Bioorg. Med. Chem.* **12**, 1091–1099 (2004).

264.   Sharma, S. *et al.* Purine Analogues as Kinase Inhibitors: A Review. *Recent Patents Anticancer Drug Discov.* **10**, 308–341 (2015).

265.   Llauger, L. *et al.* Evaluation of 8-arylsulfanyl, 8-arylsulfoxyl, and 8-arylsulfonyl adenine derivatives as inhibitors of the heat shock protein 90. *J. Med. Chem.* **48**, 2892–2905 (2005).

266. Ahn, H. S. *et al.* Potent tetracyclic guanine inhibitors of PDE1 and PDE5 cyclic guanosine monophosphate phosphodiesterases with oral antihypertensive activity. *J. Med. Chem.* **40**, 2196–2210 (1997).

267. Chang, Y. T. *et al.* Synthesis and biological evaluation of myoseverin derivatives: microtubule assembly inhibitors. *J. Med. Chem.* **44**, 4497–4500 (2001).

268. De Coen, L. M., Heugebaert, T. S. A., García, D. & Stevens, C. V. Synthetic Entries to and Biological Activity of Pyrrolopyrimidines. *Chem. Rev.* **116**, 80–139 (2016).

269. Perlíková, P. & Hocek, M. Pyrrolo[2,3-d]pyrimidine (7-deazapurine) as a privileged scaffold in design of antitumor and antiviral nucleosides. *Med. Res. Rev.* **37**, 1429–1460 (2017).

270. Morris, R. C. & Elliott, M. S. Queuosine modification of tRNA: a case for convergent evolution. *Mol. Genet. Metab.* **74**, 147–159 (2001).

271. Gregson, J. M. *et al.* Structure of the archaeal transfer RNA nucleoside G*-15 (2-amino-4,7-dihydro- 4-oxo-7-beta-D-ribofuranosyl-1H-pyrrolo[2,3-d]pyrimidine-5-carboximi dam ide (archaeosine)). *J. Biol. Chem.* **268**, 10076–10086 (1993).

272. Thiaville, J. J. *et al.* Novel genomic island modifies DNA with 7-deazaguanine derivatives. *Proc. Natl. Acad. Sci. U. S. A.* **113**, E1452-1459 (2016).

273. Hardesty, C. T., Chaney, N. A., Waravdekar, V. S. & Mead, J. A. The disposition of the antitumor agent, sangivamycin, in mice. *Cancer Res.* **34**, 1005–1009 (1974).

274. Suhadolnik, R. J., Uematsu, T. & Uematsu, H. Toyocamycin: phosphorylation and incorporation into RNA and DNA and the biochemical properties of the triphosphate. *Biochim. Biophys. Acta* **149**, 41–49 (1967).

275. Acs, G., Reich, E. & Mori, M. BIOLOGICAL AND BIOCHEMICAL PROPERTIES OF THE ANALOGUE ANTIBIOTIC TUBERCIDIN. *Proc. Natl. Acad. Sci. U. S. A.* **52**, 493–501 (1964).

276. Fabianowska-Majewska, K., Duley, J. A. & Simmonds, H. A. Effects of novel anti-viral adenosine analogues on the activity of S-adenosylhomocysteine hydrolase from human liver. *Biochem. Pharmacol.* **48**, 897–903 (1994).

277.   Nishioka, H. *et al.* Inhibition of phosphatidylinositol kinase by toyocamycin. *J. Antibiot. (Tokyo)* **43**, 1586–1589 (1990).

278.   Iapalucci-Espinoza, S., Cereghini, S. & Franze-Fernández, M. T. Regulation of ribosomal RNA synthesis in mammalian cells: effect of toyocamycin. *Biochemistry* **16**, 2885–2889 (1977).

279.   Ri, M. *et al.* Identification of Toyocamycin, an agent cytotoxic for multiple myeloma cells, as a potent inhibitor of ER stress-induced XBP1 mRNA splicing. *Blood Cancer J.* **2**, e79 (2012).

280.   Wakao, K. *et al.* Sangivamycin induces apoptosis by suppressing Erk signaling in primary effusion lymphoma cells. *Biochem. Biophys. Res. Commun.* **444**, 135–140 (2014).

281.   Cheeseman, M. D. *et al.* Exploiting Protein Conformational Change to Optimize Adenosine-Derived Inhibitors of HSP70. *J. Med. Chem.* **59**, 4625–4636 (2016).

282.   Bergstrom, D. E. *et al.* Antiviral activity of C-5 substituted tubercidin analogues. *J. Med. Chem.* **27**, 285–292 (1984).

283.   Wang, X., Seth, P. P., Ranken, R., Swayze, E. E. & Migawa, M. T. Synthesis and biological activity of 5-fluorotubercidin. *Nucleosides Nucleotides Nucleic Acids* **23**, 161–170 (2004).

284.   Bhat, U. G. & Gartel, A. L. Differential sensitivity of human colon cancer cell lines to the nucleoside analogs ARC and DRB: Differential Sensitivity of Colon Cancer Cells to ARC and DRB. *Int. J. Cancer* **122**, 1426–1429 (2008).

285.   Bhat, U. G., Zipfel, P. A., Tyler, D. S. & Gartel, A. L. Novel anticancer compounds induce apoptosis in melanoma cells. *Cell Cycle Georget. Tex* **7**, 1851–1855 (2008).

286.   Sun, C. *et al.* Apoptosis is induced in cancer cells via the mitochondrial pathway by the novel xylocydine-derived compound JRS-15. *Int. J. Mol. Sci.* **14**, 850–870 (2013).

287.   Bourderioux, A. *et al.* Synthesis and significant cytostatic activity of 7-hetaryl-7-deazaadenosines. *J. Med. Chem.* **54**, 5498–5507 (2011).

288.   Tash, J. S. *et al.* Gamendazole, an orally active indazole carboxylic acid male contraceptive agent, targets HSP90AB1 (HSP90BETA) and EEF1A1 (eEF1A), and stimulates Il1a transcription in rat Sertoli cells. *Biol. Reprod.* **78**, 1139–1152 (2008).

289.   Hashimoto, K. & Ishima, T. Neurite outgrowth mediated by translation elongation factor eEF1A1: a target for antiplatelet agent cilostazol. *PloS One* **6**, e17431 (2011).

290.   Yao, N. *et al.* Novel flavonoids with antiproliferative activities against breast cancer cells. *J. Med. Chem.* **54**, 4339–4349 (2011).

291.   Gottesman, M. M., Fojo, T. & Bates, S. E. Multidrug resistance in cancer: role of ATP-dependent transporters. *Nat. Rev. Cancer* **2**, 48–58 (2002).

292.   Noskova, V. *et al.* In vitro chemoresistance profile and expression/function of MDR associated proteins in resistant cell lines derived from CCRF-CEM, K562, A549 and MDA MB 231 parental cells. *Neoplasma* **49**, 418–425 (2002).

293.   Hardy, E. & Castellanos-Serra, L. R. 'Reverse-staining' of biomolecules in electrophoresis gels: analytical and micropreparative applications. *Anal. Biochem.* **328**, 1–13 (2004).

294.   Gharahdaghi, F., Weinberg, C. R., Meagher, D. A., Imai, B. S. & Mische, S. M. Mass spectrometric identification of proteins from silver-stained polyacrylamide gel: a method for the removal of silver ions to enhance sensitivity. *Electrophoresis* **20**, 601–605 (1999).

295.   Boxer, M. B. *et al.* Evaluation of Substituted N,N'-Diarylsulfonamides as Activators of the Tumor Cell Specific M2 Isoform of Pyruvate Kinase. *J. Med. Chem.* **53**, 1048–1055 (2010).

296.   Bajad, S. U. *et al.* Separation and quantitation of water soluble cellular metabolites by hydrophilic interaction chromatography-tandem mass spectrometry. *J. Chromatogr. A* **1125**, 76–88 (2006).

297.   Halířová, B. Vliv kancerostatik na intracelulární metabolom. (2013).

298.   Yang, W. & Lu, Z. Pyruvate kinase M2 at a glance. *J. Cell Sci.* **128**, 1655–1660 (2015).

299.   Vander Heiden, M. G. *et al.* Identification of small molecule inhibitors of pyruvate kinase M2. *Biochem. Pharmacol.* **79**, 1118–1124 (2010).

300.   Anastasiou, D. *et al.* Pyruvate kinase M2 activators promote tetramer formation and suppress tumorigenesis. *Nat. Chem. Biol.* **8**, 839–847 (2012).

301. Anderson, N. M., Mucka, P., Kern, J. G. & Feng, H. The emerging role and targetability of the TCA cycle in cancer metabolism. *Protein Cell* **9**, 216–237 (2018).

302. Wise, D. R. *et al.* Myc regulates a transcriptional program that stimulates mitochondrial glutaminolysis and leads to glutamine addiction. *Proc. Natl. Acad. Sci. U. S. A.* **105**, 18782–18787 (2008).

303. Nauš, P. *et al.* 6-(Het)aryl-7-Deazapurine Ribonucleosides as Novel Potent Cytostatic Agents. *J. Med. Chem.* **53**, 460–470 (2010).

304. Nauš, P. *et al.* Sugar-modified derivatives of cytostatic 7-(het)aryl-7-deazaadenosines: 2'-C-methylribonucleosides, 2'-deoxy-2'-fluoroarabinonucleosides, arabinonucleosides and 2'-deoxyribonucleosides. *Bioorg. Med. Chem.* **20**, 5202–5214 (2012).

305. Perlíková, P. *et al.* Synthesis and cytostatic and antiviral activities of 2'-deoxy-2',2'-difluororibo- and 2'-deoxy-2'-fluororibonucleosides derived from 7-(Het)aryl-7-deazaadenines. *ChemMedChem* **8**, 832–846 (2013).

306. Nauš, P. *et al.* Synthesis, cytostatic, antimicrobial, and anti-HCV activity of 6-substituted 7-(het)aryl-7-deazapurine ribonucleosides. *J. Med. Chem.* **57**, 1097–1110 (2014).

307. Perlíková, P. *et al.* 7-(2-Thienyl)-7-Deazaadenosine (AB61), a New Potent Nucleoside Cytostatic with a Complex Mode of Action. *Mol. Cancer Ther.* **15**, 922–937 (2016).

308. Perlíková, P. Synthesis of novel cytostatic deazapurine nucleosides and pronucleotides. (2012).

309. Giglioni, S. *et al.* Adenosine kinase gene expression in human colorectal cancer. *Nucleosides Nucleotides Nucleic Acids* **27**, 750–754 (2008).

6. Abbreviations

1DE	1-dimension gel electrophoresis
2DE	2-dimension gel electrophoresis
3-HQs	2-phenyl-3-hydroxy -4(1H)-quinolinones
ABC	ATP binding cassette
ABPP	activity based protein profiling
Acetyl-CoA	acetyl coenzyme A
ADP	adenosine diphosphate
AICAR	5-Amino-4-imidazolecarboxamide Riboside
AMP	adenosine monophosphate
AP	affinity purification
ARC	8-hydrazinosangivamycin
ATP	adenosine triphosphate
BCR-ABL	break point cluster region ABL kinase
BDNF	brain-derived neutrophic factor
BisIII	bisindolylmaleimide III
BMV	brome mosaic virus
BSA	bovine serum albumin
cAMP	cyclic adenosine monophosphate
CDK	cyclin dependent kinase
CDK9	cyclin dependent kinase 9
cGMP	cyclic guanosine monophosphate
CK-2	protein kinase 2
CML	chronic myeloid leukemia
CTP	cytidine triphosphate
cycA	cyclosporin A
cypA	cyclophilin A
DARTS	drug affinity responsive target stability
dGDP	2'-deoxyguanosine-5'-diphosphate
DIGE	difference gel electrophoresis
DIOS	desorption/ionization on silicon
DMSO	dimethyl sulfoxide
DOT 1	disruptor of telomeric silencing 1
DP	diphosphate
eEF1A	eukaryotic elongation factor 1A
ER	endoplasmic reticulum
EF-2	elongation factor 2
EF-Tu	elongation factor thermo unstable
EG	ethylene glycol
EGF	epidermal growth factor
ERK ½	extracellular signal regulated kinase ½
ESI	electrospray ionization
FAT10	HLA-F adjacent factor 10
FBP	fructose 1,6-bis phosphate
FDA	food and drug administration
FGFR1	fibroblast growth factor receptor 1
FTICR	fourier-transform ion cyclotron resonance

GAPDH	glyceraldehyde 3-phosphate dehydrogenase
GDP	guanosine diphosphate
GFP	green fluorescent bprotein
GLUT1	glucose transporter 1
GMA	glycidyl methacrylate
GSH	reduced glutathione
GSKα/β	glycogen synthase kinase α/β
GSSG	oxidized glutathione
GTP	guanosine triphosphate
HAPs	high abundance proteins
HCA	2´-hydroxycinnamaldehyde
HCC	hepatocellular carcinoma
HDAC3	histone deacetylase 3
HIF1α	hypoxia inducible factor 1 α
HILIC	hydrophobic interaction liquid chromatography
HIV-1	human immunodeficiency virus
HLA	human leukocyte antigen
HPLC	high-performance liquid chromatography
HPV 16	human papillomavirus 16
HSE	heat shock elements
HSF-1	heat shock factor 1
HSP70	heat shock protein 70
HSP90	heat shock protein 90
HX	hexokinase
ICAT	isotope coded affinity tags
IMAC	immobilized metal affinity chromatography
IMPDH	inosine monophosphate dehydrogenase
INFα	interferon α
IT	ion trap
ITC	isothermal titration microcalorimetry
iTRAQ	isobaric taq for relative and absolute quantification
JAK1	Janus kinase 1
JNK-1	c-Jun N-terminal kinase 1
LAPs	low abundance proteins
LC	liquid chromatography
LDHA	lactate dehydrogenase
LIT	linear ion trap
LQT	Thermo scientific version of linear ion trap (Orbitrap)
MALDI	matrix assisted laser desorption ionization
MAPK	mitogen activated protein kinase
MBS	myosin binding subunit
MDM4	mouse double minute homolog 4
MLC2	myosin light chain 2
MOAC	metal oxide affinity chromatography
MP	monophosphate
mrp1	multidrug resistance associated protein 1
MS	mass spectrometry
mTOR	mammalian target of rapamycin
MTT	3-(4,5-dimethylthiazol-2-yl)-2,5-diphenyltetrazolium bromide salt
NA	nucleoside analogs

NADH	nicotine amide adenine dinucleotide
NCI	National Cancer Institute
NF-κB	nuclear factor κB
NMR	nuclear magnetic resonance
NPC	nuclear pore complex
PAK4	P21 activated kinase 4
PAL	photoaffinity label
PASKIN	PAS (Per-Arnt-Sim) kinase
PEP	phosphoenolpyruvate
PFK	6-phosphofructo 1-kinase
pgp 1	P-glycoprotein 1
PI3K	phosphatide-3-kinase
PKAC-α	cAMP-dependent protein kinase
PKC	protein kinase C
PKL	pyruvate kinase L
PKM1	pyruvate kinase M1
PKM2	pyruvate kinase M2
PKR	pyruvate kinase R
PML	promyelocytic leukemia tumor suppressor
PPP	pentose phosphate pathway
pTEFb	positive transcription elongation factor
PTL	post-translational modification
Q	quadrupole
RAS	Rho-associated kinases
RdRp	RNA dependent RNA polymerase
ROS	reactive oxygen species
RP-HPLC	reverse phase high-performance liquid chromatography
SAICAR	succinyl-5- aminoimidazole-4-carboxamide-1-ribose-5-phosphate
SAR	structure activity relationship
SDS PAGE	sodium dodecyl sulfate polyacrylamide gel electrophoresis
Ser	serine
SH2	Src homology 2
SH3	Src homology 3
SILAC	stable isotope labeling with amino acid in cell culture
SMIR	small molecular inhibitor of rapamycin
SMM	small-molecule microarray
SPOS	solid phase organic synthesis
SRM	Selected Reaction Monitoring
STAT-3	signal transducer and activator of transcription 3
TAT	HIV Trans-activating transcriptional activator
TCA	tricarboxylic acid cycle
TGF-β	transforming growth factor β
Thr	threonine
TLS	tRNA – like sequence
TMT	tandem mass tags
TMV	tobacco mosaic virus
TOF	time of flight
TP	triphosphate
TQ	triple quadrupole
TYMV	turnip yellow mosaic virus

Tyr	tyrosine
UTP	uridine triphosphate
VDAC	voltage dependent anion channel
VEGF	vascular endothelial growth factor
WNV	West Nile virus
XBP1	X-box binding protein 1
XICPA	extracted ion chromatogram peak area

7. Bibliography

Original articles and reviews

The publications related to the thesis are marked by +

+ **RYLOVÁ G***, OŽDIAN T*, VARANASI L*, SOURAL M, HLAVÁČ J, HOLUB D, DŽUBÁK P, HAJDÚCH M. Affinity-Based Methods in Drug-Target Discovery. Curr Drug Targets. 2015,16(1), 60-76. PMID: 25410410 (*authors contributed equally)

OŽDIAN, T., HOLUB, D., **RYLOVÁ**, G., VÁCLAVKOVÁ, J., HAJDÚCH, M., DŽUBÁK, P. Porovnání hmotnostně spektrometrických přístupů v proteomickém profilování léčiv. Chemagazín. 2016, XXVI(5), 8-11. ISSN 1210-7409.

+ PERLÍKOVÁ P, **RYLOVÁ G**, NAUŠ P, ELBERT T, TLOUŠŤOVÁ E, BOURDERIOUX A, SLAVĚTÍNSKÁ LP, MOTYKA K, DOLEŽAL D, ZNOJEK P, NOVÁ A, HARVANOVÁ M, DŽUBÁK P, ŠILLER M, HLAVÁČ J, HAJDÚCH M, HOCEK M. 7-(2-Thienyl) 7-Deazaadenosine (AB61), a New Potent Nucleoside Cytostatic with a Complex Mode of Action. *Mol. Cancer Ther.* **15**, 922–937 (2016). PMID: 26819331

OŽDIAN T, HOLUB D, MACEČKOVÁ Z, VARANASI l, **RYLOVÁ G**, ŘEHULKA J, VACLAVKOVÁ J, SLAVÍK H, MOUDRÝ P, ZNOJEK P, STAŇKOVÁ J, DE SANSTICS JB, HALJDÚCH M, DŽUBÁK P. Proteomic profiling reveals DNA damage, nucleolar and ribosomal stress are the main responses to oxaliplatin treatment in cancer cells. J Proteomics. 2017 Jun 6;162:73-85. PMID: 28478306

+ BURGLOVÁ K*, **RYLOVÁ G***, MARKOS A, PŘICHYSTALOVÁ H, SOURAL M, PETRÁČEK M, MEDVEDÍKOVÁ M, TEJRAL G, SOPKO B, HRADIL P, DŽUBÁK P, HAJDÚCH M, HLAVÁČ J. Identification of Eukaryotic Translation Elongation Factor 1-α 1 Gamendazole-Binding Site for Binding of 3-Hydroxy-4(1 H)-quinolinones as Novel Ligands with Anticancer Activity. *J. Med. Chem.* **61**, 3027–3036 (2018). PMID: 29498519 (*authors contributed equally)

8. Appendix-full text publications related to the thesis

2.4 Appendix A

RYLOVÁ G*, OŽDIAN T*, VARANASI L*, SOURAL M, HLAVÁČ J, HOLUB D, DŽUBÁK P, HAJDÚCH M. Affinity-Based Methods in Drug-Target Discovery. Curr Drug Targets. 2015,16(1), 60-76. PMID: 25410410 (*authors contributed equally)

Affinity-Based Methods in Drug-Target Discovery

Gabriela Rylova[1,#], Tomas Ozdian[1,#], Lakshman Varanasi[1,#], Miroslav Soural[1,2], Jan Hlavac[1,2], Dusan Holub[1], Petr Dzubak[1] and Marian Hajduch[1,*]

[1]*Laboratory of Experimental Medicine, Institute of Molecular and Translational Medicine, Faculty of Medicine and Dentistry, Palacky University and University Hospital in Olomouc, Hnevotinska 5, 77515 Olomouc, The Czech Republic;* [2]*Department of Medicinal Chemistry, Institute of Molecular and Translational Medicine, Faculty of Science, Palacky University, 17. Listopadu 12, 771 46 Olomouc, The Czech Republic*

Abstract: Target discovery using the molecular approach, as opposed to the more traditional systems approach requires the study of the cellular or biological process underlying a condition or disease. The approaches that are employed by the "bench" scientist may be genetic, genomic or proteomic and each has its rightful place in the drug-target discovery process. Affinity-based proteomic techniques currently used in drug-discovery draw upon several disciplines, synthetic chemistry, cell-biology, biochemistry and mass spectrometry. An important component of such techniques is the probe that is specifically designed to pick out a protein or set of proteins from amongst the varied thousands in a cell lysate. A second component, that is just as important, is liquid-chromatography tandem mass-spectrometry (LC-MS/MS). LC-MS/MS and the supporting theoretical framework has come of age and is the tool of choice for protein identification and quantification. These proteomic tools are critical to maintaining the drug-candidate supply, in the larger context of drug discovery.

Keywords: Affinity purification, drug-target discovery, immobilization, mass-spectrometry, probe, quantification.

1. INTRODUCTION

The identification of one or more "druggable" components of a biological pathway or network is often the starting point for the de-novo development of a drug although it has not always been so. The use of many therapeutic agents has traditionally been on the basis of their observed effects (phenotypic screening) and not on the basis of their cellular mechanism of action (rational drug design) [1-3]. Overington *et al.* have reported that only 82% of Food and Drug Administration (FDA) drugs approved between 1989 and 2000 had one or more defined cellular target [4, 5]. Approved drugs with unknown mechanisms of action include Bexarotene and arsenic trioxide, for the treatment of cutaneous T-cell lymphoma and acute promyelocytic leukemia (PML) respectively [6]. Such drugs may have off-target effects that are the result of drug-binding to targets that are not known or not intended, and may be detrimental or beneficial to the patient [6-8]. Drugs having poly-pharmacological effects that are beneficial, especially in diseases like cancer, are at a premium [9]. Conversely, drugs with adverse off-target effects can sometimes be repurposed. Thalidomide is an illustrative example. Originally prescribed to expectant women to ease pregnancy-associated nausea and "morning sickness"

in 1957, it was discontinued when discovered to cause horrific congenital abnormalities. Five decades later, the drug has found new use in leprosy and cancer treatment [10]. Celecoxib is another example. It was designed to treat osteoarthritis but is now prescribed for colorectal cancer prevention [11]. The small-molecule Histone deacetylase 6 (HDAC6) inhibitor, tubacin also inhibits Serine Palmitoyl transferase (SPT), the rate-limiting enzyme of sphingolipid biosynthesis [12].

A clearer understanding of the in-vivo interaction behavior of the drug-candidate will facilitate the design of a drug that has a more defined target or targets. Such a drug-candidate is likely to have more predictable effects and can better inform clinical trials. In any case, the rationale for more complete knowledge of drug-targets is considerable and must be heeded.

Our knowledge of cellular and physiological processes of the human body has gone hand-in-hand with the development of analytical tools and procedures in the chemical and biomedical sciences. Conventional techniques such as electrophoresis and chromatography still form the mainstay of protein analyses, but now work alongside newer instruments such as microarrays and mass spectrometers [13].

The following is a discussion of some proteomic analytical techniques frequently used in drug-target isolation and identification. They are affinity-based and occur at the confluence of synthetic organic chemistry, cell biology, biochemistry and mass spectrometry. A unifying feature in the techniques is the use of a probe molecule to isolate a target-

*Address correspondence to this author at the Institute of Molecular and Translational Medicine Faculty of Medicine and Dentistry Palacky University in Olomouc, Hněvotínská 5, 779 00 Olomouc, Czech Republic;
Tel: +420 585 632 082; Fax:+420 585 632 180;
E-mail: marian.hajduch@upol.cz

[#]*These authors contributed equally to the paper.*

protein(s). Another such feature is the mass-spectrometric identification and quantification of isolated targets. Some of the techniques discussed here have been previously grouped under the descriptor Chemical Proteomics (a technique in which the probe bonds covalently with the target) [14, 15]. The common issues that accompany each technique are presented, as are the efforts made to get around them.

2. AFFINITY PURIFICATION

Affinity purification is a generic technique based on interaction between a ligand (probe) and protein of interest (target or target molecule). The technique was first developed in the early 1950s and has evolved since then to include a number of variants that have been successfully applied to molecular target identification [16].

A typical affinity purification experiment (Fig. **1**) begins with the modification of the probe (a drug, drug-candidate or an inhibitor) and its immobilization on a solid phase matrix. To ensure that the probe's target specificity is retained after derivatization, the structure and activity of the modified probe is compared with that of the unmodified parent compound. The immobilized probe is then incubated with the sample of interest, usually cell-lysate. Biomolecules in the sample that interact with the probe are captured during incubation. The resin is then washed free of non-specifically bound proteins and other "contaminant" molecules. Captured target proteins are eluted by a buffer that disrupts the ligand-protein interaction. These proteins are analyzed and identified by different techniques such as 1D or 2D gel electrophoresis, Western blotting and mass spectrometry. This approach is frequently used for studying protein interaction networks and in identification of drug targets [17]. The type of tag used for the purification varies with the purpose, with the scale of the purification and on the ease of preparation of the affinity matrix.

2.1. The Issue of the Non-Specific Interaction

An affinity purification or a protein-protein interaction is characterized by at least two parameters, sensitivity and specificity. These parameters indicate the "goodness" of the affinity purification technique and are necessary for the purpose of comparison of two or more techniques.

Sensitivity is a feature by virtue of which a true interaction is detected. It is denoted as a ratio of the number of true
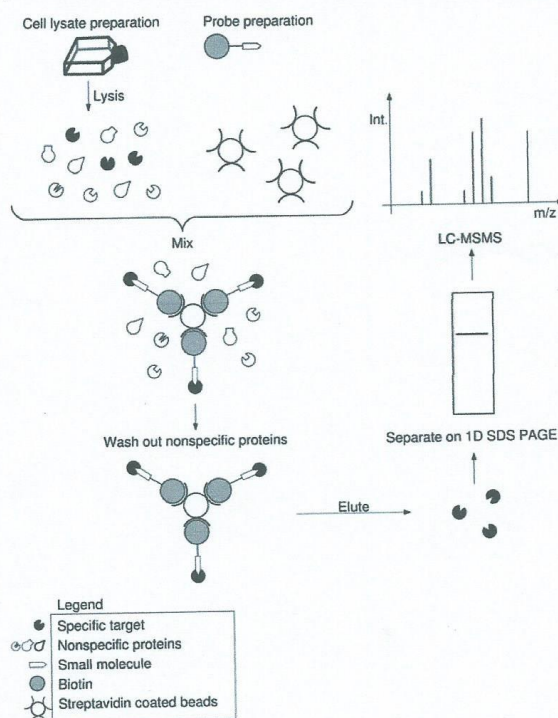

Fig. (1). Typical workflow of affinity purification: Modified (e.g. biotinylated) compound is immobilized onto solid-phase (streptavidin coated beads). Cell lysate is incubated with immobilized compound on the solid-phase. Specific proteins are captured by compound and non-specific ones are washed out. Target proteins are then eluted and subjected to 1D SDS PAGE and LC-MS/MS.

interactions that are *detected* to the *total* number of true interactions. Thus,

$$Sensitivity = TP/(TP + FN) \qquad \dots (1)$$

Where,

TP - True-positives are true interactions that are detected by the technique

FN - False-negatives are true interactions that are *not* detected by the technique

Specificity is a feature by virtue of which a false interaction does not happen and is not detected. It is expressed as a ratio of the truly non-interacting proteins to the total number of non-interacting proteins. Thus,

$$Specificity = TN/(TN + FP) \qquad \dots (2)$$

Where,

TN = True-negatives are interactions that are not supposed to happen and are not detected

FP = False-positives are interactions that are not supposed to happen, but are detected

Equation 2 suggests that the specificity of a technique is an inverse function of the number of false-positives. The specificity of a protein interaction may also be indicated by a dissociation constant, K_D. The higher the K_D, the higher is the probability that the binding-site of the protein will be populated by its true binding-partner or ligand.

The primary challenge in affinity purification lies in isolating "real" target proteins while excluding non-specifically bound "contaminants", the false-positives. Interactions which escape detection because of the experimental conditions or because of a limitation of the technique are false-negatives. For example, probes that target post-translational modifications will be rendered ineffective if the modification is absent or is lost in sample preparation. Steric hindrance of the probe or target protein by another molecular entity will also preclude a fruitful interaction. From equation 1 above, it is evident that as the number of false negatives decreases, there is a proportional increase in the sensitivity i.e. sensitivity is inversely proportional to the number of false negatives.

An intelligent choice of the affinity matrix can go some distance in alleviating the problem of non-specific interactions, as the matrix and probe linkers can be a source of such interactions [18, 19]. Matrices that are incompletely derivatized may also bind contaminants with high affinity. The proteins that bind non-specifically to the common matrix types (agarose, Sepharose etc) have been identified and listed for reference [20-22].

There are different ways of separating valid targets (true-positives) from non-specifically bound proteins (false-positives) and improving the confidence of discovery. Pre-incubating the sample with non-derivatized and inactive matrix before the actual experiment improves the purity of the isolated product. Serial incubation of cell-lysate with the affinity resin is yet another option (serial affinity-chromatography) [23]. Cell-lysate is incubated with two successive batches of affinity-resin. The first batch captures most of the true targets and the second, most of the non-specifically bound contaminants.

There are several ways of immobilizing a compound to a matrix (Fig. 3). The probe may be chemically bonded to the matrix via its functional group, for eg. a sulfhydryl, a hydroxyl, amino or carboxyl. This approach has been used for
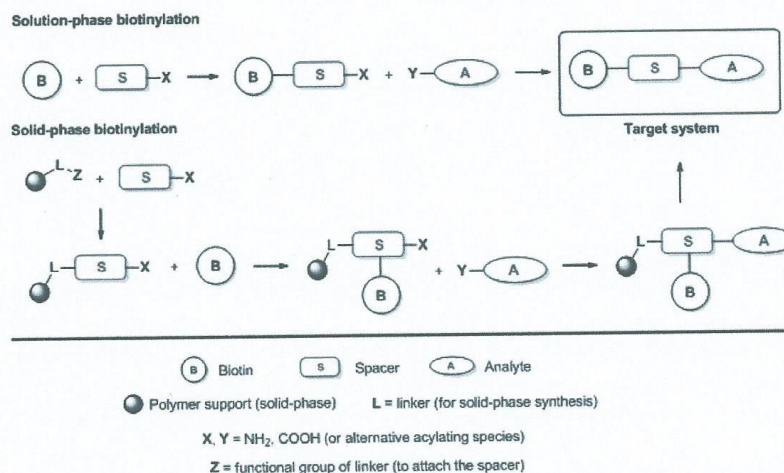
Fig. (2). Two alternative approaches to modify compound A: The selection of more suitable method is based on specific requirements such as required quantity of the target system, its stability and availability of analyte (for low quantities the solution-phase method is preferable). A typical polymer support is divinyl-styrene based resin. Except for amides also ester or ether groups are frequently used to attach individual parts of the target system.
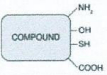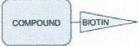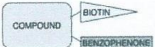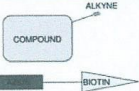
PROBE	STRUCTURE	IMMOBILISING RESIN	PROPERTIES
Compound modified by NH_2, OH, SH or COOH moieties	COMPOUND (NH₂, OH, SH, COOH)	Agarose, sepharose	Inexpensive, specificity is sometimes an issue
Biotinylated compound	COMPOUND – BIOTIN	Streptavidin coated matrix	Specificity of biotin-straptavidin bond is high and requires stringent elution conditions, spacer design is complicated
Photoaffinity label	COMPOUND – BIOTIN / BENZOPHENONE	Streptavidin coated matrix	Drug binds covalently to target, Photoaffinity probe needs to be carefully selected and derivatized to drug
Compound modified for click chemistry reaction	COMPOUND ALKYNE / AZIDE – BIOTIN	Streptavidin coated matrix	The reaction can be performed in a variety of conditions, Long exposures to Cu^I catalyst may be cytotoxic
Immuno-chemo-proteomics probe	COMPOUND LINKER FLAG	Antiflag beads	Sulfation of FLAG polypeptide can alter antibody specificity
Kinobeads	ATP BINDING SITE	Agarose beads	For kinases only, Some kinases do not bind to ATP structural analogs and cannot be enriched by Kinobeads
Activity based probe	WARHEAD – TAG	Streptavidin coated beads, fluorescent or radiolabell scanning	For enzymes only, warheads aren't available for all enzyme types

Fig. (3). Examples of compound immobilization strategies.

the tyrosine kinase inhibitors imatinib, nilotinib and dasatinib. The inhibitors are first chemically treated to introduce amino and acetyl groups on their surface and are then immobilized on N-hydroxysuccinimide activated Sepharose via the same groups [7]. Commonly used matrices are polysaccharide-derived (agarose, Affi-Gel®, Sepharose), methacrylate-derived (Toyopearl®) or magnetic beads (Dynabeads®, SG beads) [24]. Affinity matrices are constantly being developed and improved, to enhance binding of the specific target and to minimize non-specific interactions. Their applications, strength and limitations are reviewed in detail by Sakamoto *et al.* [25].

A competitive-binding experiment, where the free probe competes with immobilized probe for the target, is another approach for determining spurious interactions [26, 27]. The Stable Isotope Labeling of amino Acids in Cell-culture, or SILAC, is an isotope labeling technique that is used for quantifying proteins in a sample by mass-spectrometry (described in section 3.1 below) labeled (heavy, H) and unlabeled (light, L) cell-lysates are incubated with the immobilized small-molecule probe, and the unlabeled lysate simultaneously incubated with non-immobilized probe. Following incubation, the probe-bearing beads are washed, mixed and the probe-protein complexes eluted. These are separated by SDS-PAGE and analyzed by LC-MS/MS. Specifically bound target proteins have a H/L ratio greater than 1, while the non-specific ones have an H/L ratio of 1 (Fig. 4) [28]. The principle of competitive binding has been applied to the investigation of cellular kinases too. Kinases and phosphatases are frequently involved in regulation of different cellular processes because they phosphorylate and dephosphorylate proteins. Because blocking a single kinase can perturb one or more cellular pathways kinases are considered to be potentially valuable drug-targets [29, 30]. The ATP binding domain of a kinase binds to ATP to hydrolyze it to the corresponding mono-phosphate form. Multiple ATP structural analogs fused to synthetic beads (KinobeadsTM) exploit this property to isolate specific tyrosine kinases involved in CML that are targets of BCR/ABL inhibitors [31, 32]. Cell-lysate is incubated with Kinobeads in the presence and absence of inhibitors. Tyrosine kinase binding to Kinobeads is competitively inhibited by the inhibitors. The difference in the levels of bound kinases in the two samples, as measured by quantitative mass-spectrometry, distinguishes the target kinases from the false-positives. The method must be used with caution though, as some kinases do not bind to Kinobeads, even though they bear an ATP binding domain. A similar approach has identified novel targets of the multi-kinase inhibitor E-3810 [33]. As with other proteins, protein kinases may also be isolated using their respective inhibitors as probes, for example, bisindolylmaleimide X, AX14596, PP58 and purvalanol [34].

There is another less evident problem that results in false positives. It is encountered in samples where the dynamic range of protein concentrations is high [14]. A protein that is not a true target may still bind to the probe by virtue of its high concentration, even though it has a low affinity (for the probe). As a result the probe captures some non-specific high-abundance proteins (HAPs) in addition to the true (low-abundance) target. One of the strategies for overcoming this problem is called Proteominer™ (BioRad) [35-37]. The technique is based on an exhaustive combinatorial library of
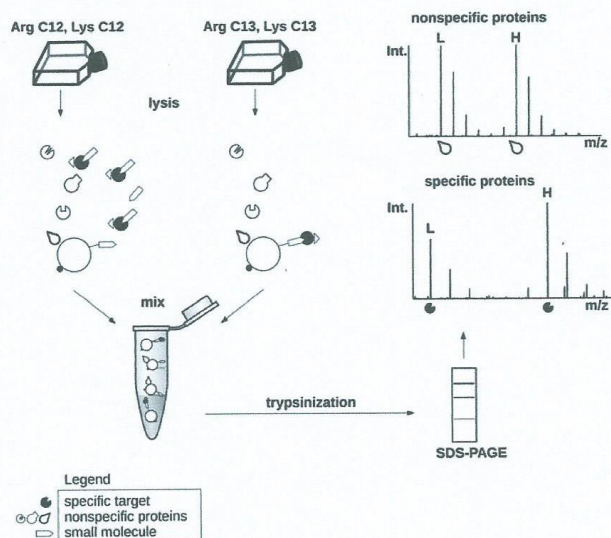
Fig. (4). Identification of protein targets by quantitative proteomics: Cells of interest are incubated with labeled (heavy, H) and non-labeled (light, L) aminoacids (SILAC). Non-labeled cell extract is simultaneously incubated with immobilized and free small-molecule. Heavy cell lysate is incubated with immobilized small-molecule alone. Afterwards, both bead-types are washed and mixed in equimolar quantities. Captured proteins are eluted, separated by SDS PAGE, analyzed by MS and quantified. Target protein has heavy to light ratio (H/L) above one and nonspecific protein has H/L ratio approximately one.

hexapeptides that can theoretically bind every possible protein in a sample. When sample is incubated with the ProteominerTM matrix, HAPs quickly saturate their binding sites and the surplus flows off, while the low-abundance proteins (LAPs) bind almost completely. This results in the depletion of HAPs and in the enrichment of LAPs, thereby effectively decreasing the dynamic range of protein concentrations in the sample by a few orders of magnitude.

Other, more conventional strategies for reducing the dynamic range of protein concentrations in serum utilize antibodies that target the most abundant proteins [38-40]. The relative rate of trypsin digestion of high- and low-abundance proteins is also a basis for improving the dynamic range of detection of proteins [41]. This technique, christened DigDeAPr, has been used with cell-lysates but can be extended to complex mixtures that have a wide range of protein concentrations [41].

2.2. Affinity Reagents that Bind Non-Covalently

2.2.1. Biotin and Streptavidin

The strong non-covalent interaction between biotin and streptavidin (or avidin) is the basis for a common type of affinity purification [42]. These interactions are the strongest known, non-covalent interactions occurring in nature ($K_D = 1*10^{-14}$). The probe is tagged with biotin and used to "fish" for interaction partners in the sample. The probe and the captured proteins can then be isolated on a streptavidin coated matrix via the biotin tag. In drug-target identification studies,

it is common practice to biotinylate the drug or inhibitor, as for instance, biotinylated 2-hydroxycinnamic acid (HCA). This drug binds to proteasome subunits (target) in lysates of SW620 colon cancer cell-line and inhibits the L3-like activity of the proteasome [43]. Biotinylated diazonamid can likewise isolate the mitochondrial enzyme ornithine delta-amino transferase from HeLa cell-lysate [44]. The primary downside to this purification strategy is that the strong strep-tavidin-biotin interaction requires stringent elution conditions that may negatively affect protein structure or function.

Key to the synthesis of the biotin label is the design of the spacer that connects the target molecule to the biotin moiety [18, 45-47]. Spacer design and its impact on the affinity purification has been intensively studied and some rules formulated [48-51]. The design must conform to these principles to perform optimally: (i) it must be sufficiently long to prevent steric repulsion between avidin and the target biomolecule; ii. it should not interact with the target biomolecule to cause a false-positive result ; iii. it must also not alter the solubility of the biotin probe in water.

Aliphatic spacers such as caproic acid derivatives have been used frequently in the past although the newer ethylene glycol (EG) spacers are now preferred, as they satisfy the above criteria better [52]. The compound of interest is typically attached to the biotin-EG system via a stable amide bond. It can be done either by acylation of the biotin-EGs-NH2 system by carboxy group-containing compounds or acylation of an amino group-containing compound with the biotin-EGs-COOH system. Derivatization has tradition-

154

ally been done using solution-phase synthesis and more recently using solid-phase synthesis. The substrate for biotinylation (or conversely the biotin-EG-NH$_2$ system) is pre-immobilized or directly synthesized on an insoluble polymer backbone, and the resulting preloaded resin then used for reaction with an appropriate compound for e.g. the Biotin-PEG-NovaTag™ (Novabiochem) [53-56]. Conversely, the biotin-EG-NH2 system may be immobilized in place of the biotinylated substrate. Preparation of a similar system for immobilization of carboxy-group containing analytes via spacers of different length has also been described [57] (Fig. **2**).

2.2.2. The Recombinant Tag

Several commercially available tags can be cloned into the protein of interest, expressed in eukaryotic of prokaryotic cells and isolated by affinity-methods. The FLAG tag is a small hydrophilic octapeptide (DYKDDDDK) that works in this manner [58]. Recombinant proteins containing this tag may be over-expressed and isolated using anti-FLAG antibodies immobilized on a suitable support resin. Isomeric forms of protein kinase C have been identified using FLAG-tagged bisindolylmaleimide III (Bis III), an inhibitor of protein kinase C [59]. The FLAG tag was considered generally applicable till a few years ago, when it was shown that a sulfation event (a post-translational modification) eliminates the interaction of the FLAG tag and anti-FLAG antibodies [60]. Such a modification lowers the yield of the purification without ever becoming evident. The sulfation was observed in insect cells and is not known to occur in the CHO and HEK293T human cell-lines. The His-tag exhibits this problem to a degree and it is likely that other tag-systems suffer from it too. A systematic, comparative investigation of the various clonal tag-systems has not been reported so far, but potential savings in time and resources may make such a study worth investing in [61].

The His-tag is a sequence of 6-histidine residues that is also cloned into the protein of interest. Histidine residues bind with high affinity to divalent metal ions on a solid matrix (Ni^{2+}, or Co^{2+}) [62-64]. Bound proteins may be eluted by a high concentration of free histidine. The GST-tag works similarly [65]. GST is a 26-amino acid enzyme called Glutathione-S-Transferase and its binding ligand is its substrate, glutathione. Glutathione is a three-residue moiety (Glu-Cys-Gly) that is immobilized on a solid matrix via the reduced cysteine. Concentrated, reduced glutathione constitutes the elution reagent. Yet another clonal tag-system is the eight-amino acid Strep-tag system [66]. It is based on the streptavidin-biotin principle and binds to streptavidin or an engineered streptavidin matrix. However, it requires much milder elution conditions than the streptavidin-biotin interaction.

The tag-systems mentioned above are archetypal of the class of clonal affinity-based tags. Each system has its strengths, and because no single tag is appropriate for all purposes a protocol may utilize two or more in a purification process. The tag may sometimes not be specific enough or its affinity of interaction may require stringent elution conditions that are harmful to proteins. Larger tags impose a larger metabolic burden on the culture organism than the smaller ones and may not be ideal for use in eukaryotic cells. Additionally, an expensive resin that cannot be recycled is also not likely to be widely used [61].

2.2.3. Click Chemistry Based Probes

The structure of the drug/inhibitor in question may sometimes be amenable to modification by click-chemistry [67]. "Click" reactions are near-ideal chemical reactions that are typically easy to perform in different conditions, have high yields that are pure, and are not affected by the reactant groups. The Huisgen's cyclo-addition reaction is the classical example of this type of chemical reactions [68]. It is the 1,3- dipolar cycloaddition reaction between an azide and a terminal or internal alkyne that yields a 1,2,3-triazole. For instance, after incubation with the sample, alkyne derivatized Orlistat is made to react with rhodamine-azide and visualized on an electrophoretic gel by fluorimetry [69]. Alternatively, if the protein-drug complex is to be recovered, Orlistat-alkyne is coupled to an affinity-tag-azide. Click-chemistry may be used in exploring drug-binding sites in proteins as well and to investigate the off-target effects of drugs [69]. Because click-reaction conditions are flexible, they are easily performed under "native" conditions to avoid harming the biological sample. An alkyne group engineered into an ABPP or photoaffinity label can expand their downstream analytical and purification options [69].

2.2.4. Identification of Drug-Targets without Isolation

Target protein identification may sometimes be performed without isolating the drug-target complex [70-73]. One technique is based on the relative conformational stabilities of free- and small molecule-bound protein and is called Drug Affinity Responsive Target Stability (DARTS). Small molecule binding may stabilize the conformational stability of the protein, with the result that it becomes more resistant to denaturation and less susceptible to proteolysis [72]. Small molecule binding may also sterically protect a protease cleavage site. This property has been made use of in the identification of the FK506-binding protein 12 (FKBP12) and the mammalian target of rapamycin (mTOR) as targets of kinase inhibitor E4 and rapamycin respectively [74]. Cellular targets of grape-seed extracts have also been successfully screened by this technique [75]. Cell-lysate is incubated with the desired small molecule or an inactive structural analog. The mixtures are subject to protease digestion and the proteins/peptides subsequently resolved by electrophoresis and identified by LC-MS/MS. A difference in the intensity of a band on an electrophoretic gel is indicative of a drug-target interaction (Fig. **6**). There are other variants of this technique and these have been discussed at length in Lomenick *et al.* [70]. DARTS is conceptually simple and the technique does not involve derivatization of the drug or molecule-of-interest. However, as with other techniques, it is not without issues. The probability of non-specific interactions increases with the complexity of the protein mixture and cell-lysates are very complex mixtures. Moreover, the cell solubilization conditions are artificial. Protease cleavage sites are occasionally missed by the proteolytic enzyme because proteolytic digestion doesn't always go to completion and because some proteins are inherently resistant to digestion [72]. The proteolytic enzyme may also act on proteins complexed with the target-protein to further complicate results [31].
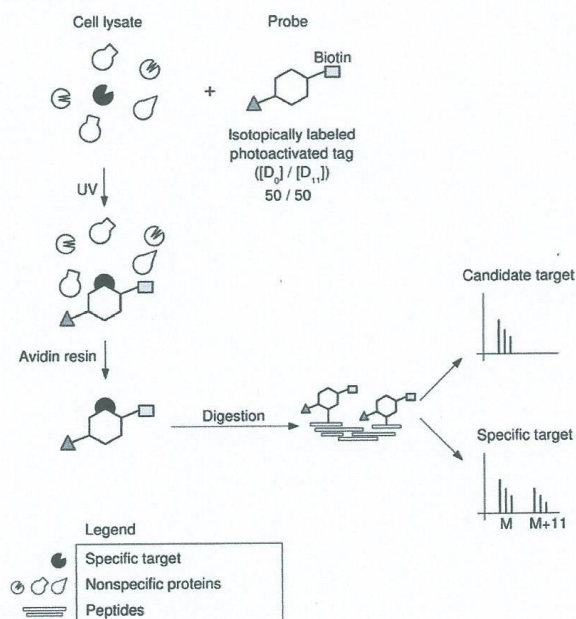
Fig. (5). Photoaffinity labeling with two isotopes: PAL probes consisting of an affinity tag (biotin) and an isotopically labeled photoreactive tag (non-deuterized, D_0 and deuterized benzophenone isotope label, D_{11}) are mixed in 1:1 ratio. Probes are incubated with cell lysate and subsequently irradiated by UV-light. Proteins are then purified via avidin resin and identified by MS. Identification of the unique isotopic pattern (M, mass of peptide with non-deuterized tag; M+11, mass of peptide with deuterized tag) of some peptides helps to distinguish valid protein targets from frequent contaminants.

2.2.5. Decreasing Sample Complexity: Capturing the Sub-Proteome

The affinity purification procedure may be designed to capture not just one protein but an entire class of proteins. The N-glycoproteome, phosphoproteome or the SUMOylated group of proteins are important druggable PTMs in cancer and have suitable purification procedures [76-79]. The probe, in this case, binds non-specifically to all proteins bearing a particular post-translational modification (PTM).

Antibodies against phosphate group epitopes are commonly used reagents for isolation of phosphorylated proteins [80]. However, because they are specific to an epitope, they allow enrichment of only one kind of phosphorylated peptide at a time. This problem is circumvented when the purification is based on phosphotyrosine, phosphoserine or phosphothreonine antibodies or a non-specific electrostatic affinity between the negatively charged phosphate groups and positively charged metal cations (Immobilized Metal Affinity Chromatography IMAC and by Metal Oxide Affinity Chromatography, MOAC) [80-82]. The negative charge on the free carboxyl groups and acidic amino acids must be neutralized for the isolation of peptides with phosphate groups by appropriate affinity resin or by conventional ion-exchange chromatography (hydroxyapatite column enrichment or Hydrophobic Interaction Liquid Chromatography, or HILIC) [83]. Conversely, the phosphate group itself may be derivatized to improve its binding to the affinity resin. The derivatization step is not always desirable because it introduces an additional step in the sample preparation workflow, and because the reaction does not always go to completion. Furthermore, phophorylated proteins or peptides can be visualized on a polyacrylamide gel using a fluorescent stain, Pro-Q Diamond. Fluorescent bands are then cut out and prepared for identification by mass-spectrometry [84].

In some cases, it is possible to reverse the affinity purification technique such that the purified target-protein is given the role of a probe to screen for active compounds. Desorption/Ionization on Silicon, or DIOS, is one such method. DIOS is now known by its commercial name NALDI^{TM} (Nano-Assisted Laser Desorption and Ionization) [85-87]. It is a matrix-free method and uses laser desorption and ionization of compounds from a porous silicon surface to directly analyze probe-target interactions by mass-spectrometry. This is illustrated in the investigation of Bovine Serum Albumin (BSA) binding partners by Zou *et al.* [88]. BSA was immobilized on a silicon surface (wafer) and incubated with a mixture of two molecules, ketoprofen and sulpiride. The silicon surface was then washed to remove unbound compound and subject to direct NALDI

analysis. The analysis yielded a signal for ketoprofen but none for sulpiride, confirming that ketoprofen binds to BSA and that sulpiride does not.

Fig. (6). DARTS. Protein lysate is incubated with a small-molecule compound and then subjected to protease digestion. Target proteins interacting with the small-molecule compound are enriched and protected against protease digestion while nonspecific proteins are digested.
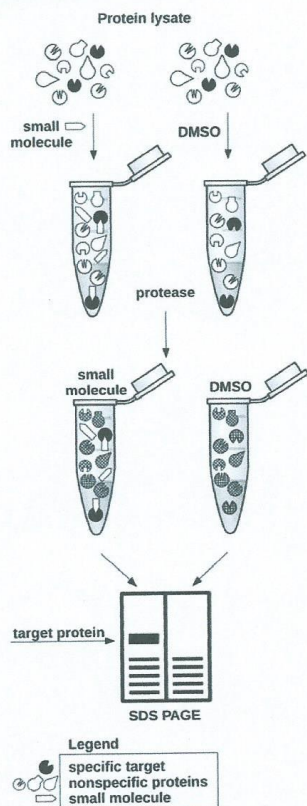
2.3. Affinity Reagents that Bind Covalently

The affinity purification techniques described so far depend on a physical interaction between the probe and its target-protein. However probes may also be engineered to form chemical bond(s) with their targets to increase their specificity and sensitivity.

2.3.1. Photo-Affinity Labeling (PAL)

The photoaffinity probe (PAP) typically consists of three components: a drug/ligand that interacts specifically with the target, a photoreactive group that forms the chemical bond with the target, and at least one reporter group (Fig. **5**) [89, 90]. The probe is incubated with the target and then irradiated with light of appropriate wavelength. The probe binds to its target and upon irradiation, the photoreactive group forms a chemical bond with the same. Photoaffinity probes are classified into roughly three types on the basis of their photoreactive group, although there are probes that fall outside this classification: benzophenones, aryl azides and diazirine. All three kinds of PAPs are used in the (high-throughput) identification of drug-leads and for the investigation of the drug-target interaction [91]. Ovalicin and fumagilin tagged with a bifunctional-PAP have been used in cellular target screens [92-94]. Labeling ideally requires that (i) the PAPs be inert in the absence of actinic light, (ii) the activating light not be of a harmful wavelength, lest the protein-target be damaged, (iii) the lifetime of the activated photoreactive moiety be smaller than the lifetime of the drug-target interaction (iv) the photoreactive and the reporter groups not get in the way of the drug-target binding and (v) that the adduct formed during the reaction be stable enough to withstand the rigors of the downstream purification or analytical process. The caveat with this technique is that the binding profile of a PAP is different in live cells and in cell-lysates.

In a variation on this principle, the photo-reactive group can be made with one (3H) or two (^1H, ^2H) different isotopes [95, 96]. When the two isotopic-PAPs are used in equimolar quantities in the same purification, they yield unique isotopic patterns in a tandem mass spectrum that can help discern valid protein targets from false-positives.

2.3.2. Activity-Based Protein Profiling (ABPP)

Activity-based protein profiling relies on chemical bond-formation for target enzyme discovery. The probe here consists of three parts, a "warhead" which can bind covalently with a functional group in the active-site of the target enzyme, a tag for the visualization or purification of target proteins, and a linker joining these two parts [97-99]. The tag is a fluorophore, a biotin group or a click-chemistry group (described in section 2.2.3). On incubation with cell-lysate the probe binds to target proteins and bound enzymes can be purified using the biotin-group, visualized by electrophoresis and identified by mass spectrometry. ABPP can be scaled for profiling proteins, and by extension their source tissues, on the basis of their biological activities. This isn't possible with other proteomic techniques such as PAGE or LC-MS. Multiple ABPP probes have been used to comprehensively map the binding-surface of a known target in order to determine a greater number of specific binding sites [100]. The different variants of orlistat (tetrahydrolipstatin, THL), THL-R, THL-L and THL-T have been used to determine orlistat's possible off-target effects [69].

2.3.3. Cell-Permeable Probes

In some cases it is desirable to have a drug/probe that is cell permeable, to monitor and identify drug-target interactions in the native state [101, 102]. Orlistat and several other ABPP, photo-affinity and click-chemistry probes have this property. The HIV Trans-activating transcriptional activator (TAT) is a nine-residue peptide (RKKRRQRRR) with a preponderance of positively charged amino acids, and can transport molecular cargo into eukaryotic cells [101, 103]. The cargo could be metabolites, peptides, proteins or nucleic

acids. The TAT peptide could potentially also transport some of the above mentioned affinity tags into the cell in studies of drug-target interactions. A composite probe consisting of the drug (Bis III), a fluorescent group and the TAT peptide has been used, for instance, for this purpose [104]. Other cell-penetrating peptides are now available and may be similarly used in future for the entire class of affinity-tags [105]. A provision for tag cleavage and removal, as by incorporation of a thrombin cleavage site is another desirable feature of a tag-based system [106]. This is important when the isolated target is to be analyzed by mass-spectrometry without interference from the affinity tag.

3. PROTEIN QUANTITATION IN DRUG-TARGET DISCOVERY

It is evident from the preceding section that drug-target identification frequently requires the relative or absolute quantification of one or more proteins in multiple samples. Protein identification and quantification is performed downstream of an affinity purification. The sample preparation protocol, the mass-spectrometer and the quantitation procedure (labeled samples or label-free; Fig. 7) is dictated by the purpose of the experiment. Proteins isolated from the affinity purification stage may directly be used for preparation of MS samples, or may be further resolved by 1- or 2-dimensional electrophoretic separation before being processed for MS. Procedures for isolating proteins from Western blot transfer membranes have also been developed [107].

3.1. Quantification Using Isotopic Labels

Quantification has traditionally been done using isotope tags. Common tagging protocols include the Stable Isotope Labeling with Amino acids in Cell culture (SILAC), Isotope Coded Affinity Tags (ICAT), Tandem Mass Tags (TMT) and the Isobaric Tag for Relative and Absolute quantification (iTRAQ) [108-111]. SILAC and ICAT are isotopic labeling protocols that use isotopes of hydrogen, carbon and nitrogen (^{2}H, ^{13}C, ^{15}N). They are based on a mass-difference between the light and the heavy isotope labels. The mass difference causes a shift in the peaks of the labeled peptides relative to the unlabeled peptide. The intensities of the two peaks indicates the relative quantities of the two peptides.

SILAC involves the labeling of cells in culture in minimal media. Cells are grown in media containing normal or labeled amino acids. Labeled amino acids are incorporated into cellular proteins via natural biosynthetic pathways. Five-ten cell-doublings later, the two cell samples are harvested, mixed, processed and trypsinized before being analyzed by mass spectrometry. Because samples are labeled during cell culture the method is suitable only for samples derived from culture and not for samples from other sources. Samples that cannot be labeled in culture may be labeled after collection using the ICAT, TMT or iTRAQ labeling procedures. The extent of labeling can be more precisely controlled in these post collection labeling techniques since it is not dependent on the *in vivo* protein metabolic rate or the cell doubling-time. The SILAC mass-difference concept, in most setups, restricts the number of samples that can be simultaneously analyzed to two. For this reason, the method cannot be used in experiments with multiple samples. Different ionization states of a peptide will alter the observed mass difference between the heavy and light peptide. Additionally, the minimal medium itself may perturb the cellular physiology such that the observed biological effect is not completely true. Deuterium-labeled amino acids create another issue. The deuterium labeled peptide migrates ahead of the unlabeled peptide in the reverse-phase chromatographic column and changes the peptide's elution profile. This causes a split in the MS1 peak of the peptide and makes quantification less
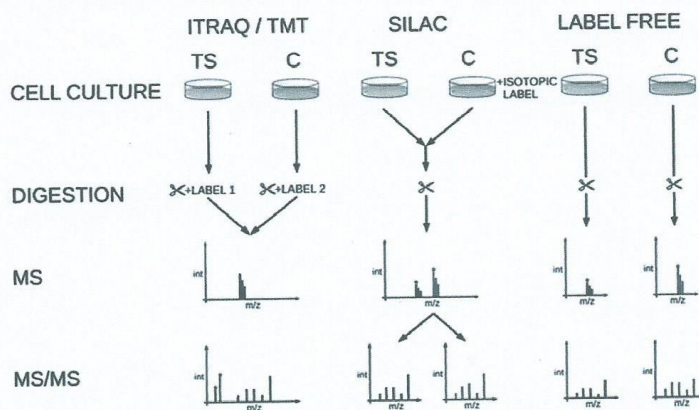
Fig. (7). A principle of mass-spectrometry peptide-labeling techniques: iTRAQ/TMT labeling is based on isobaric tag and quantification is done at the MS/MS level. SILAC labeling is based on metabolic incorporation of isotopic label into cell culture and quantification is done at the MS level. This is ideal for high resolution mass spectrometry where MS has usually higher accuracy than MS/MS. However, SILAC is more or less limited to cell cultures. Label free techniques rely on peak-intensity, spectral-count, peptide-count and/or fragment-ion intensity for quantification of protein.

accurate. Isotopes of ^{13}C and ^{15}N do not cause this problem and are therefore most commonly used. These isotopes also give rise to a larger mass-difference that can be more accurately measured.

ICAT resolves some of the issues of SILAC [109]. The ICAT tag consists of three groups- a thiol-reactive group, an isotope coded tag and a biotin moiety. A cleavable linker is sometimes included between the isotope tag and the biotin to facilitate purification [112]. The two collected samples are reduced and trypsinized and incubated with ICAT labels to allow thiol reactive groups to react with the reduced thiols on cysteine residues. Differentially labeled samples are then mixed and subject to mass-spectrometry. The property of thiol specificity is at once useful and problematic- useful because tagged peptides can be purified, and problematic because peptides lacking cysteines are lost [113]. Furthermore, the accuracy of the protocol depends on the labeling efficiency. Less than optimal labeling will bias the quantification and make the results unreliable.

3.2. Quantification Using Isobaric Labels

Labeled quantification evolved further with the introduction of isobaric tags called Tandem Mass Tags (TMTs) and isobaric tags for relative and absolute quantification (iTRAQ) [110, 111]. Isobaric tagging allows the simultaneous analysis of more than two samples and does not require the isolation of tagged peptides.

TMTs consist of at least three groups, a reporter group, a mass normalization group and a protein reactive group. These tags are amine reactive and are therefore more likely to have a higher efficiency of labeling than ICAT tags. TMTs are available in sets of two, six or ten labeling reagents (2-plex, 6-plex and 10-plex respectively) [110, 114]. Tags of a particular set have identical overall mass. For this reason, two identical peptides tagged with different TMTs will co-elute from a reverse-phase column and have the same MS^1 spectral peaks. Depending on the labeling reagent, two, six or ten samples can be simultaneously analyzed by MS. The control and treated sample sets are trypsinized, labeled, pooled and analyzed. Upon peptide fragmentation of selected MS^1 precursor-ions by collision-induced dissociation in the mass spectrometer, the MS^2 spectrum exhibits the reporter group peaks in addition to the characteristic peptide fragmentation peaks. The intensities of the different reporter group ions indicate the relative quantities of the peptide in the different sample sets. Untagged peptides will not have reporter-group peaks in the MS^2 and will therefore be disregarded in the quantification process. This makes isobaric tagging intrinsically more accurate than the ICAT labeling procedure described above. TMT has been used in the determination of targets of antidepressant drugs [115].

One assumption here is that the applied m/z window selects only a single desired precursor-ion for fragmentation. However, in reality, additional precursor-ions within a 2kDa range of the desired ion are also fragmented. Reporter groups from these additional precursors then lower the quantification accuracy [116]. Another assumption is that the different isobaric tags label proteins in the different treatment groups (samples) with equal efficiency. But it may not necessarily be so. The nature of the peptides in the samples and possibly

their concentration, influences the derivatization reaction and affects quantification [117]. The above description of tandem mass tags is also true of the iTRAQ tags, except that iTRAQ is also meant for absolute quantification. iTRAQ tags come in 4-plex and 8-plex reagent kits and enable the use of up to 8 samples [111, 118].

3.3. Quantification by Selected Reaction Monitoring (SRM)

Absolute quantification is now also possible with AQUA peptides (acronym for Absolute Quantification and with SRM (Selected Reaction Monitoring) [119-122]. SRM is the detection and quantification of specific proteins in a sample. It is based on the prior knowledge of one or more proteotypic peptides from the protein of interest. A proteotypic peptide is one which is always formed upon protein digestion and has complete or near complete ionization. The mass-to-charge ratio of a peptide's precursor- and fragment-ions and its chromatographic retention time are characteristic of the peptide and together constitute a "transition" or "assay". There may be more than one transition per peptide. The mass-spectrometer is directed to follow pre-specified transitions for a specified duration and to measure their intensities. The quantity of the peptide may be calculated from a standard curve of an identical labeled peptide (intensity versus concentration). Reliable SRM assays for most of the human, yeast and bacterial proteins are now publicly available in the SRMAtlas, an online repository [123].

SRM can precisely measure multiple proteins in a mixture of proteins on the basis of pre-supplied transition information. Transitions, of the order of 10^3, can be reliably measured in a single SRM run, boosting throughput incrementally and solving a long-standing problem in proteomics [124]. Statistical design of experiments employing SRM may be guided by a statistical software devoted to this purpose called SRMstats [125].

3.4. Label-Free Quantification

The label-free approach is a more recent quantification approach that dispenses with the labeled standard. This approach has evolved sufficiently for routine use in different studies [126-131]. It is generally agreed that the theoretical basis for such quantification is a "work-in-progress" but the convenience of the label-free approach outweighs any small loss in accuracy. The technique also does away with the labor and cost of the labeling step and can be applied to multiple datasets and to datasets retrospectively.

Bottom-up proteomics consists of piecing together protein sequence information from constituent peptides. Protein samples are processed and digested into peptides. The peptide mixture is resolved by reverse-phase liquid chromatography, ionized and injected into the mass-spectrometer. These peptide-ions, also called precursor-ions, are scanned and their intensities plotted as a function of chromatographic retention-time (Fig. **S1**). The plot is called the total ion chromatogram. A peak or a specific retention time range can be selected and the intensity of the constituent peptides plotted as a function of their mass-to-charge ratio (m/z). This graph is the MS^1 spectrum and each peak in the MS^1 spectrum represents a precursor-ion. Desired precursor-ions are selected for frag-

mentation. The fragmentation process breaks up precursor-ions into smaller peptides called fragment-ions and their intensities are graphed as a function of their m/z values in the MS^2 spectrum. For a given energy applied to the fragmentation, a precursor-ion will always yield the same fragment-ion(s). The different fragment-ions in the MS^2 spectrum are compared with peptides in a database using their masses to derive their sequence and to identify the protein.

The initial plot of peptide-ion intensity versus retention time may be used to determine the quantity of peptide in a particular mixture. The Area Under Curve (AUC) and Percentage Area (PA) are two techniques that use this parameter [122, 129, 132-136]. The latter is called by different names depending on the normalization algorithm it uses: Total AUC, PA, AUC_{STD}, or R_{PA}. Chromatographic peak intensity and peak areas exhibit a good correspondence with protein abundance but the calculation is made difficult by noise and by peptides that co-elute or elute close to each other.

A tally of MS^2 spectra from all peptides of a protein is also a measure of a protein's abundance [126, 129, 131, 137, 138]. The tally is called the spectral count. The Normalized Spectral Abundance Factor (NSAF), log_2(protein ratio), and R_{SC} all use this feature. Appropriate normalization must be applied to correct for differences in ionization efficiency though, which is frequently not ideal. Neither is detection linear across an indefinite range of protein concentrations. Additionally, because identification and sequencing is done using peptide masses, an artefact can skew the measurement. The artefact is any peptide that has the same mass as the peptide of interest but not the same sequence.

Alternatively, the number of unique peptides identified from a protein, or the peptide count, also indicates its abundance [126, 138]. Peptide and spectral counts show a good correlation with protein abundance but may tend to overestimate the abundance, especially when low spectral counts are observed.

The above quantification techniques use a single mass-spectral parameter for measuring protein quantity in a sample, either the spectral count (an MS^2 feature) or the chromatographic peak area. A more recent approach for measuring quantity uses a Normalized Spectral Index (SI_N) that is derived from the peptide count, the spectral count and the fragment ion intensity (an MS^2 feature). In comparisons of the different label-free techniques, the SI_N outperforms the others indicating that multiple features yield a more consistent and reliable measure of abundance than a feature alone [139, 140]. One or more of the above methods are now integrated into computational workflows that analyze tandem mass-spectra [140].

It is important to note that inadequacies in data acquisition can bias label-free quantification such that a biological effect is observed. The effect may not be real. It is imperative that certain standards be rigorously applied to data acquisition before the data can be considered worthy of label-free analysis. Individual (shotgun-proteomics) runs on a mass-spectrometer typically have only a 30% overlap. For this reason, multiple (5-10) runs are required (regardless of the instrument) to achieve a 95% analytical completeness of the data before the data can be used [139, 141].

4. IN PERSPECTIVE

It is important to view the drug-target discovery process in the larger context of rational drug-development. This involves the identification of one or more components of the relevant dysfunctional process. Such a component is often expressed at different levels in the normal and diseased tissue, or exhibits different levels of activity and constitutes a druggable target [5, 142-144]. The target may be a protein, nucleic acid or metabolite. Of these, proteins constitute the majority and an estimate puts the number of druggable protein targets at a few hundred [5].

4.1. The Genomic Approach, or the Proteomic?

Knowledge of the aberrant component can be obtained by examining its DNA, RNA or protein. These are complementary sources of information and the aberration can be explained more completely be considering them all. For instance, protein sequence alterations may be accurately determined by mRNA sequencing [145]. However, RNA-sequencing is of little use when it comes to investigating protein modifications that occur post-translationally. These require protein identification tools.

The information from nucleic acid is sometimes at odds with information derived from protein. In other words, there isn't always a correspondence between the RNA and protein expression profiles and the relation is yet to be completely understood [146].

The speed of the transcriptional process, the nature of the mRNA transcript, the changes wrought on the transcript post-transcription, its stability and translation into protein, the modifications subsequently made to the protein, the protein's stability and its turnover are all determinants of the relative levels of RNA and protein [146]. These RNA and protein profiles are "read" by the genomic and proteomic technique respectively, and any lack of correspondence between the two species may be attributed to one or more of the above reasons. For instance, a gene whose mRNA is unstable but is copiously translated into stable protein during its lifetime, will exhibit a large discrepancy between its RNA and protein levels. Conversely, an aberrant gene that is constitutively expressed is likely to have high levels of both mRNA and protein.

Technique has a role too in the incongruity. The method of tissue collection and storage, the sample processing protocol and the instrument influence the quantification. A large cross-platform study, much like the first NCI-CPTAC conducted study for proteomics, would go a long way in standardizing experimental conditions for the measurement of RNA and protein [147].

4.2. Validating the Target

The drug-target candidates from the different discovery approaches are collated and put through a rigorous validation procedure. Target validation is meant to confirm the role of the discovered target in the disease phenotype. It must be demonstrated in this phase that the drug-candidate effects the intended change and that it has the desired therapeutic effect [148]. The drug-candidate may cause a change in the expression level of different proteins, in a modulation of enzyme

activity, in a disruption or stabilization of protein-protein or protein-DNA interaction(s) or in the incorporation of post-translational modifications in proteins [5, 143, 144, 149]. The validation process is guided by the technique of target discovery and is normally performed in the cell- or animal models [148]. Validation is followed by lead-discovery and optimization, and then by preclinical tests, before the drug-candidate can graduate to a clinical trial.

The validation and subsequent lead development and optimization process is lengthy and expensive [150]. Only a small percentage of drug-targets pass the validation stage. It has been estimated that only three out of sixty new drug-candidates identified qualify as a marketable drug [151]. The total cost of drug-development- from target identification to market can now cost anywhere between USD4 billion and USD14 billion [151-154]. It does not help that drug-targets reported in the literature are not reliable candidates for development. Upto 60% of the relevant biomedical literature may have results that are irreproducible [155-158]. The problem is acute and some pharmaceutical companies now routinely conduct preliminary checks of reported targets before committing valuable resources to their validation and to drug-development. Discovery appears to influence overall research-and-development productivity more than anything else [153]. It makes sense therefore to improve the confidence of target-discovery such that valuable time and resources are not wasted in the validation and post-validation stages.

Increasing the specificity of the affinity-purification method such that the number of false-positives is lowered would go some distance in increasing the confidence of target identification. More specific affinity-capture reagents would help here, as would a greater number of them. To this end, the Human Proteome Project is tasked with developing antibodies for each of the 20,300 proteins coded by the human genome [159]. More rigorous standards and guidelines for investigating and reporting drug-targets would stem the decline in experimental reproducibility and facilitate drug development. Such standards have already been proposed for biomarker development and have helped [160, 161].

4.3. The Target as Part of a System

As stated at the outset, a comprehensive knowledge of the in-vivo interaction behavior of the drug-candidate can guide the design of a drug that has a more defined target or targets. There is a growing realization that biological systems, networks and modules within the cell must be considered in their entirety and that it is not enough to examine components in isolation. The observed effect of a drug is the sum total of interaction of multiple cellular and physiological systems. Systems biology has contributed to this realization. This is a relatively new discipline but has become indispensable in the drug-development enterprise in recent years. It deals with the relationships between the different components of a system to determine how they interact and how they function as a whole [162, 163]. It enables the integration of genomic and proteomic data with environmental data to better describe the organism's phenotype and to predict its response to a stimulus.

Systems biology has spawned computational tools for viewing a potential target in the larger cellular or physiologi-

cal context and to increase the confidence of target-identification. They include MetaCore™ (Thomson Reuters), Pathway Studio (Elsevier), IPA (Ingenuity Systems), the Software Tool for Researching Annotations of Proteins (STRAP), Gene Map Annotator and Pathway Profiler (GeneMAPP), Pathway Tools and the Database for Annotation, Visualization and Integrated Discovery (DAVID) [87, 164-166]. Various companies also offer in-house software for drug-target discovery, lead discovery, drug-repositioning etc. on a contractual basis.

4.4. The "Promiscuous" Drug

A review of all FDA approved therapeutics/imaging agents from the period 1998-2009 shows that most of the first-in-class drugs were those discovered by conventional phenotypic screening, and not by target-based drug-discovery [3]. Clearly, there is scope for improvement in the target-discovery approach.

Drugs frequently interact with unintended cellular components and have unpredicted and unexpected effects [167]. The polypharmacological effects of drugs were discussed in an earlier section as a rationale for a "more complete knowledge of drug-targets". Adverse side-effects are usually detected in late-stage clinical trials when the drug is administered to the patient. As the pharmacokinetics and dosage of the drug has already been tested prior to this, it makes sense to find a new use for the drug and salvage some of the developmental effort, than start all over again [168]. Ever-increasing drug-development costs can be partly offset by such "repurposing" of failed drugs [169]. Repurposing would also supplement the dwindling supply of drugs to the market [169].

Even if the drug has beneficial, if off-target effects, it is worthwhile to define and characterize the target-set. Living systems have redundant signaling pathways for any given task and this is especially true of cancer cells. The "plasticity" in the signaling network enables cancer cells to switch to alternative signaling routes when a particular component or pathway is blocked, and is the cause of their resistance to therapy [170]. Overcoming signaling "plasticity" requires that the redundant pathways be simultaneously blocked and is the reason polytherapy is preferred to monotherapy in cancer treatment. Likewise, a drug that binds to multiple cellular targets, with low affinity, may have a greater potential for safely curing a disease than one that binds "tightly" to a single target [171].

4.5. Advancing the Science

A road-map for development of proteomic tools and reagents has been laid out in an NIH-conducted workshop and seeks to partially address this question [172]. The workshop put forward feasible goals in proteomics that include (i) increasing the sensitivity of mass-spectrometry by 100- or a 1000-fold (ii) development of novel affinity-capture reagents that are more specific (in their interaction with bait) and easy and inexpensive to prepare (i.e, a general improvement in affinity-resins) and (iii) software that is better able to separate signal from noise in mass-spectral data, and that is less susceptible to over-fitting. Recommendations for advancing the cutting edge in systems-

biology-enabled medicine have also been made in work-shops and seminars in related areas [173].

4.6. Big Data

With the coming of next-generation sequencing tools and precision mass-spectrometry has come an information deluge and the need for computational tools for storage, mining and analysis of this data. The need has been recognized but the development of software is still not commensurate with the advancements in instrumentation. The ideal software would analyze mass-spectrometric data, collate related information from scientific literature and databases and prepare a report that is of value to the scientist and the medic. This is not feasible yet, although a vision of information-enabled medical science that is tailored to an individual has been articulated [174].

It is sobering to recall that the rational drug-discovery process yielded only a minority of the FDA approved drugs in the decade gone by [175]. The biomedical community must step up to the challenge of improving that score, that the promise of rational drug-design may be realized.

ABBREVIATIONS

FDA	=	Food and drug administration
PML	=	Promyelocytic leukemia
HDAC6	=	Histone deacetylase 6
SPT	=	Serine Palmitoyl transferase
SG	=	Styrene and glycidyl methacrylate
SILAC	=	Stable Isotope labelling of amino acids in cell-culture
H	=	Heavy isotopic label
L	=	Light isotopic label
SDS-PAGE	=	Sodium dodecylsulphate polyacrylamide gel electrophoresis
LC	=	Liquid chromatography
MS	=	Mass spectrometry
ATP	=	Adenosine triphosphate
CML	=	Chronic myeloid leukemia
HAPs	=	High-abundance proteins
LAPs	=	Low-abundance proteins
HCA	=	2'-hydroxycinnamaldehyde
EGs	=	Ethyleneglycols
PEG	=	Polyethyleneglycol
BIS III	=	Bisindolylmaleimide III
GST	=	Glutathione S tranfrease
DARTS	=	Drug affinity responsive target stability
FKBP12	=	FK506 binding protein 12
mTOR	=	Mammalian target of rapamycin
PTM	=	Posttranslational modification

SUMO	=	Small ubiquitin-like modifier
IMAC	=	Immobilized metal affinity chromatography
MOAC	=	Metal oxide affinity chromatography
HILIC	=	Hydrophobic interaction liquid chromatography
DIOS	=	Desorption/ionization on silicon
NALDI	=	Nano-assisted laser desorption/ionization
BSA	=	Bovine serum albumin
PAP	=	Photoaffinity probe
PAL	=	Photoaffinity label
ABPP	=	Activity based protein profiling
THL	=	Tetrahydrolipostatin
HIV	=	Human immunodeficiency virus
TAT	=	Trans-activator of transcription
ICAT	=	Isotope-coded affinity tags
TMT	=	Tandem Mass Tag
iTRAQ	=	Isobaric tag for relative and absolute quantitation
SRM	=	Selected reaction monitoring
AQUA	=	Absolute quantification
AUC	=	Area under curve
PA	=	Percentage area
NSAF	=	Normalized spectral abundance factor
Rsc	=	Ratio of spectral counts
SI_N	=	Normalized spectral index
DNA	=	Deoxyribonucleic acid
RNA	=	Ribonucleic acid
mRNA	=	Messenger RNA
NCI-CPTAC	=	National Cancer Institute - Clinical proteomics tumor analysis consortium
USD	=	United States dollars
IPA	=	Ingenuity Pathway Analysis
STRAP	=	Software tool for researching annotations of proteins
GeneMAPP	=	Gene Map Annotator and Pathway Profiller
DAVID	=	Database for Annotation, Visualization and Integrated Discovery
NIH	=	National Institutes of Health

CONFLICT OF INTEREST

The authors confirm that this article content has no conflict of interest.

ACKNOWLEDGEMENTS

AUTHOR CONTRIBUTIONS

Conception and design of the article (MH, PD), drafting (GR, TO, DH, LV, JH, MS) and/or critical revision of the content (LV, MH, PD), final approval to be published (MH).

SUPPLEMENTARY MATERIALS

Supplementary material is available on the publishers web site along with the published article.

REFERENCES

[1] Drews J. Drug discovery: a historical perspective. Science 2000; 287(5460): 1960-4.
[2] Lindsay MA. Target discovery. Nat Rev Drug Discov 2003; 2(10): 831-8.
[3] Swinney DC, Anthony J. How were new medicines discovered? Nat Rev Drug Discov 2011; 10(7): 507-19.
[4] Overington JP, Al-Lazikani B, Hopkins AL. How many drug targets are there? Nat Rev Drug Discov 2006; 5(12): 993-6.
[5] Imming P, Sinning C, Meyer A. Drugs, their targets and the nature and number of drug targets. Nat Rev Drug Discov 2006; 5(10): 821-34.
[6] Yang L, Wang K-J, Wang L-S, *et al.* Chemical-protein interactome and its application in off-target identification. Interdiscip Sci Comput Life Sci 2011; 3(1): 22-30.
[7] Rix U, Hantschel O, Dürnberger G, *et al.* Chemical proteomic profiles of the BCR-ABL inhibitors imatinib, nilotinib, and dasatinib reveal novel kinase and nonkinase targets. Blood 2007; 110(12): 4055-63.
[8] Ximenes JCM, de Oliveira Gonçalves D, Siqueira RMP, *et al.* Valproic acid: an anticonvulsant drug with potent antinociceptive and anti-inflammatory properties. Naunyn Schmiedebergs Arch Pharmacol 2013; 386(7): 575-87.
[9] Petrelli A, Giordano S. From single- to multi-target drugs in cancer therapy: when aspecificity becomes an advantage. Curr Med Chem 2008; 15(5): 422-32.
[10] Sheskin J. Thalidomide in the treatment of Lepra reactions. Clin Pharmacol Ther 1965; 6: 303-6.
[11] Kawamori T, Rao CV, Seibert K, Reddy BS. Chemopreventive activity of celecoxib, a specific cyclooxygenase-2 inhibitor, against colon carcinogenesis. Cancer Res 1998 1; 58(3): 409-12.
[12] Siow D, Wattenberg B. The histone deacetylase-6 inhibitor tubacin directly inhibits de novo sphingolipid biosynthesis as an off-target effect. Biochem Biophys Res Commun 2014 4; 449(3): 268-71.
[13] Washburn MP, Wolters D, Yates JR. Large-scale analysis of the yeast proteome by multidimensional protein identification technology. Nat Biotechnol 2001; 19(3): 242-7.
[14] Rix U, Superti-Furga G. Target profiling of small molecules by chemical proteomics. Nat Chem Biol 2009; 5(9): 616-24.
[15] Jeffery DA, Bogyo M. Chemical proteomics and its application to drug discovery. Curr Opin Biotechnol 2003; 14(1): 87-95.
[16] Campbell DH, Luescher E, Lerman LS. Immunologic Adsorbents: I. Isolation of Antibody by Means of a Cellulose-Protein Antigen. Proc Natl Acad Sci USA 1951; 37(9): 575-8.
[17] Azarkan M, Huet J, Baeyens-Volant D, Looze Y, Vandenbussche G. Affinity chromatography: a useful tool in proteomics studies. J Chromatogr B Analyt Technol Biomed Life Sci 2007; 849(1-2): 81-90.
[18] Shiyama T, Furuya M, Yamazaki A, Terada T, Tanaka A. Design and synthesis of novel hydrophilic spacers for the reduction of non-specific binding proteins on affinity resins. Bioorg Med Chem 2004; 12(11): 2831-41.
[19] Von Rechenberg M, Blake BK, Ho Y-SJ, *et al.* Ampicillin/penicillin-binding protein interactions as a model drug-target system to optimize affinity pull-down and mass spectrometric strategies for target and pathway identification. Proteomics 2005; 5(7): 1764-73.
[20] Trinkle-Mulcahy L, Boulon S, Lam YW, *et al.* Identifying specific protein interaction partners using quantitative mass spectrometry and bead proteomes. J Cell Biol 2008; 183(2): 223-39.
[21] Chen GI, Gingras A-C. Affinity-purification mass spectrometry (AP-MS) of serine/threonine phosphatases. Methods 2007; 42(3): 298-305.
[22] Gingras A-C, Caballero M, Zarske M, *et al.* A Novel, Evolutionarily Conserved Protein Phosphatase Complex Involved in Cisplatin Sensitivity. Mol Cell Proteomics 2005; 4(11): 1725-40.
[23] Yamamoto K, Yamazaki A, Takeuchi M, Tanaka A. A versatile method of identifying specific binding proteins on affinity resins. Anal Biochem 2006; 352(1): 15-23.
[24] Sakamoto S, Kabe Y, Hatakeyama M, Yamaguchi Y, Handa H. Development and application of high-performance affinity beads: toward chemical biology and drug discovery. Chem Rec N Y N 2009; 9(1): 66-85. http://onlinelibrary.wiley.com/doi/10.1002/tcr.20170/full
[25] Sakamoto S, Hatakeyama M, Ito T, Handa H. Tools and methodologies capable of isolating and identifying a target molecule for a bioactive compound. Bioorg Med Chem 2012; 20(6): 1990-2001.
[26] Zhang S, Gerhard GS. Heme mediates cytotoxicity from artemisinin and serves as a general anti-proliferation target. PloS One 2009; 4(10): e7472.
[27] Ong S-E, Schenone M, Margolin AA, *et al.* Identifying the proteins to which small-molecule probes and drugs bind in cells. Proc Natl Acad Sci USA 2009; 106(12): 4617-22.
[28] Ong S-E, Li X, Schenone M, Schreiber SL, Carr SA. Identifying cellular targets of small-molecule probes and drugs with biochemical enrichment and SILAC. Methods Mol Biol 2012; 803: 129-40.
[29] Cohen P. Protein kinases- the major drug targets of the twenty-first century? Nat Rev Drug Discov 2002; 1(4): 309-15.
[30] Zhang J, Yang PL, Gray NS. Targeting cancer with small molecule kinase inhibitors. Nat Rev Cancer 2009; 9(1): 28-39.
[31] Bantscheff M, Eberhard D, Abraham Y, *et al.* Quantitative chemical proteomics reveals mechanisms of action of clinical ABL kinase inhibitors. Nat Biotechnol 2007; 25(9): 1035-44.
[32] Kruse U, Pallasch CP, Bantscheff M, *et al.* Chemoproteomics-based kinome profiling and target deconvolution of clinical multi-kinase inhibitors in primary chronic lymphocytic leukemia cells. Leukemia 2011; 25(1): 89-100.
[33] Colzani M, Noberini R, Romanenghi M, *et al.* Quantitative chemical proteomics identifies novel targets of the anti-cancer multi-kinase inhibitor E-3810. Mol Cell Proteomics 2014; 13(6): 1495-509.
[34] Wissing J, Jänsch L, Nimtz M, *et al.* Proteomics analysis of protein kinases by target class-selective prefractionation and tandem mass spectrometry. Mol Cell Proteomics 2007; 6(3): 537-47.
[35] Thulasiraman V, Lin S, Gheorghiu L, *et al.* Reduction of the concentration difference of proteins in biological liquids using a library of combinatorial ligands. Electrophoresis 2005; 26(18): 3561-71.
[36] Righetti PG, Boschetti E. The ProteoMiner and the FortyNiners: searching for gold nuggets in the proteomic arena. Mass Spectrom Rev 2008; 27(6): 596-608.
[37] Boschetti E, Righetti PG. The ProteoMiner in the proteomic arena: a non-depleting tool for discovering low-abundance species. J Proteomics 2008; 71(3): 255-64.
[38] Yadav AK, Bhardwaj G, Basak T, *et al.* A Systematic Analysis of Eluted Fraction of Plasma Post Immunoaffinity Depletion: Implications in Biomarker Discovery. PLoS ONE 2011; 6(9): e24442. http://www.plosone.org/article/info%3Adoi%2F10.1371%2Fjournal.pone.0024442
[39] Chromy BA, Gonzales AD, Perkins J, *et al.* Proteomic analysis of human serum by two-dimensional differential gel electrophoresis

after depletion of high-abundant proteins. J Proteome Res 2004; 3(6): 1120-7.

[40] Björhall K, Miliotis T, Davidsson P. Comparison of different depletion strategies for improved resolution in proteomic analysis of human serum samples. Proteomics 2005; 5(1): 307-17.

[41] Fonslow BR, Stein BD, Webb KJ, *et al.* Digestion and depletion of abundant proteins improves proteomic coverage. Nat Methods 2013; 10(1): 54-6.

[42] Stayton PS, Freitag S, Klumb LA, *et al.* Streptavidin-biotin binding energetics. Biomol Eng 1999; 16(1-4): 39-44.

[43] Hong SH, Kim J, Kim J-M, *et al.* Apoptosis induction of 2'-hydroxycinnamaldehyde as a proteasome inhibitor is associated with ER stress and mitochondrial perturbation in cancer cells. Biochem Pharmacol 2007; 74(4): 557-65.

[44] Wang G, Shang L, Burgett AWG, Harran PG, Wang X. Diazonamide toxins reveal an unexpected function for ornithine delta-amino transferase in mitotic cell division. Proc Natl Acad Sci USA 2007; 104(7): 2068-73.

[45] O'Carra P, Barry S, Corcoran E. Affinity chromatographic differentiation of lactate dehydrogenase isoenzymes on the basis of differential abortive complex formation. FEBS Lett 1974; 43(2): 163-8.

[46] Terry MP. Affinity Chromatography. Encyclopedia of Chromatography, 3rd ed. CRC Press; 2009.

[47] Fee CJ, Van Alstine JM. Purification of pegylated proteins. Methods Biochem Anal 2011; 54: 339-62.

[48] Fasoli E, Reyes YR, Guzman OM, *et al.* Para-aminobenzamidine linked regenerated cellulose membranes for plasminogen activator purification: effect of spacer arm length and ligand density. J Chromatogr B Analyt Technol Biomed Life Sci 2013; 930: 13-21.

[49] Zamolo L, Salvalaglio M, Cavallotti C, *et al.* Experimental and theoretical investigation of effect of spacer arm and support matrix of synthetic affinity chromatographic materials for the purification of monoclonal antibodies. J Phys Chem B 2010; 114(29): 9367-80.

[50] Busini V, Moiani D, Moscatelli D, Zamolo L, Cavallotti C. Investigation of the influence of spacer arm on the structural evolution of affinity ligands supported on agarose. J Phys Chem B 2006; 110(46): 23564-77.

[51] Martin del Valle EM, Galán MA. Effect of the Spacer Arm in Affinity Chromatography: Determination of Adsorption Characteristics and Flow Rate Effect. Ind Eng Chem Res 2002; 41(9): 2296-304.

[52] Diamandis EP, Christopoulos TK. The biotin-(strept)avidin system: principles and applications in biotechnology. Clin Chem 1991; 37(5): 625-36.

[53] Gilmore BF, Quinn DJ, Duff T, Cathcart GR, Scott CJ, Walker B. Expedited solid-phase synthesis of fluorescently labeled and biotinylated aminoalkane diphenyl phosphonate affinity probes for chymotrypsin- and elastase-like serine proteases. Bioconjug Chem 2009; 20(11): 2098-105.

[54] Dang THT, de la Riva L, Fagan RP, *et al.* Chemical probes of surface layer biogenesis in Clostridium difficile. ACS Chem Biol 2010; 5(3): 279-85.

[55] Berry AFH, Heal WP, Tarafder AK, *et al.* Rapid multilabel detection of geranylgeranylated proteins by using bioorthogonal ligation chemistry. Chembiochem Eur J Chem Biol 2010; 11(6): 771-3.

[56] Baumeister B, Beythien J, Ryf J, Schneeberger P, White PD. Evaluation of Biotin-OSu and Biotin-ONp in the Solid Phase Biotinylation of Peptides. Int J Pept Res Ther 2005; 11(2): 139-41. http://link.springer.com/article/10.1007%2Fs10989-004-4707-2

[57] Cankarova N, Funk P, Hlavac J, Soural M. Novel preloaded resins for solid-phase biotinylation of carboxylic acids. Tetrahedron Lett 2011; 52(44): 5782-8.

[58] Hopp TP, Prickett KS, Price VL, *et al.* A Short Polypeptide Marker Sequence Useful for Recombinant Protein Identification and Purification. Nat Biotechnol 1988; 6(10): 1204-10.

[59] Saxena C, Zhen E, Higgs RE, Hale JE. An immuno-chemoproteomics method for drug target deconvolution. J Proteome Res 2008; 7(8): 3490-7.

[60] Schmidt PM, Sparrow LG, Attwood RM, Xiao X, Adams TE, McKimm-Breschkin JL. Taking down the FLAG! How Insect Cell Expression Challenges an Established Tag-System. PLoS ONE 2012; 7(6): e37779.

[61] Waugh DS. Making the most of affinity tags. Trends Biotechnol 2005; 23(6): 316-20.

[62] Chaga G, Hopp J, Nelson P. Immobilized metal ion affinity chromatography on Co2+-carboxymethylaspartate-agarose Superflow, as demonstrated by one-step purification of lactate dehydrogenase from chicken breast muscle. Biotechnol Appl Biochem 1999; 29 (1): 19-24.

[63] Chaga G, Bochkariov DE, Jokhadze GG, Hopp J, Nelson P. Natural poly-histidine affinity tag for purification of recombinant proteins on cobalt(II)-carboxymethylaspartate crosslinked agarose. J Chromatogr A 1999; 864(2): 247-56.

[64] Hochuli E, Döbeli H, Schacher A. New metal chelate adsorbent selective for proteins and peptides containing neighbouring histidine residues. J Chromatogr 1987; 411: 177-84.

[65] Smith DB, Johnson KS. Single-step purification of polypeptides expressed in Escherichia coli as fusions with glutathione S-transferase. Gene 1988; 67(1): 31-40.

[66] Schmidt TG, Skerra A. The Strep-tag system for one-step purification and high-affinity detection or capturing of proteins. Nat Protoc 2007; 2(6): 1528-35.

[67] Kolb HC, Finn MG, Sharpless KB. Click Chemistry: Diverse Chemical Function from a Few Good Reactions. Angew Chem Int Ed Engl 2001; 40(11): 2004-21.

[68] Rolf Huisgen. In: Centenary lecture, Proceedings of the Chemical Society. October 1961: 357-96.

[69] Yang P-Y, Liu K, Ngai MH, Lear MJ, Wenk MR, Yao SQ. Activity-Based Proteome Profiling of Potential Cellular Targets of Orlistat − An FDA-Approved Drug with Anti-Tumor Activities. J Am Chem Soc 2010; 132(2): 656-66.

[70] Lomenick B, Olsen RW, Huang J. Identification of direct protein targets of small molecules. ACS Chem Biol 2011; 6(1): 34-46.

[71] West GM, Tucker CL, Xu T, *et al.* Quantitative proteomics approach for identifying protein-drug interactions in complex mixtures using protein stability measurements. Proc Natl Acad Sci USA 2010; 107(20): 9078-82.

[72] Liu P-F, Kihara D, Park C. Energetics-based discovery of protein-ligand interactions on a proteomic scale. J Mol Biol 2011; 408(1): 147-62.

[73] Chang Y, Schlebach JP, VerHeul RA, Park C. Simplified proteomics approach to discover protein-ligand interactions. Protein Sci 2012; 21(9): 1280-7.

[74] Lomenick B, Jung G, Wohlschlegel JA, Huang J. Target identification using drug affinity responsive target stability (DARTS). Curr Protoc Chem Biol 2011; 3(4): 163-80.

[75] Derry MM, Somasagara RR, Raina K, *et al.* Target identification of grape seed extract in colorectal cancer using drug affinity responsive target stability (DARTS) technique: role of endoplasmic reticulum stress response proteins. Curr Cancer Drug Targets 2014; 14(4): 323-36.

[76] Hajduch M, Skalnikova H, Halada P, *et al.* Cyclin-Dependent Kinase Inhibitors and Cancer: Usefulness of Proteomic Approaches in Assessment of the Molecular Mechanisms and Efficacy of Novel Therapeutics. In: Clinical Proteomics: From diagnosis to therapy; Eyk JEV, Dunn MJ, eds. Wiley-VCH Verlag GmbH & Co. KGaA; 2007; p. 177-202.

[77] Huang W, He T, Chai C, *et al.* Triptolide inhibits the proliferation of prostate cancer cells and down-regulates SUMO-specific protease 1 expression. PloS One 2012; 7(5): e37693. http://www.plosone.org/article/info%3Adoi%2F10.1371%2Fjournal.pone.0037693

[78] Driscoll JJ, Dechowdhury R. Therapeutically targeting the SUMOylation, Ubiquitination and Proteasome pathways as a novel anticancer strategy. Target Oncol 2010; 5(4): 281-9.

[79] Fila J, Honys D. Enrichment techniques employed in phosphoproteomics. Amino Acids 2012; 43(3): 1025-47.

[80] Andersson L, Porath J. Isolation of phosphoproteins by immobilized metal (Fe3+) affinity chromatography. Anal Biochem 1986; 154(1): 250-4.

[81] Matsuda H, Nakamura H, Nakajima T. New ceramic titania: selective adsorbent for organic phosphates. Anal Sci 1990; 6(6): 911-2.

[82] Pan X, Whitten DA, Wu M, Chan C, Wilkerson CG, Pestka JJ. Global protein phosphorylation dynamics during deoxynivalenol-induced ribotoxic stress response in the macrophage. Toxicol Appl Pharmacol 2013; 268(2): 201-11.

[83] Alpert AJ. Hydrophilic-interaction chromatography for the separation of peptides, nucleic acids and other polar compounds. J Chromatogr 1990; 499: 177-96.

[84]   Mezhoud K, Bauchet AL, Château-Joubert S, *et al.* Proteomic and phosphoproteomic analysis of cellular responses in medaka fish (Oryzias latipes) following oral gavage with microcystin-LR. Toxicon Off J Int Soc Toxinology 2008; 51(8): 1431-9.

[85]   Shen Z, Thomas JJ, Averbuj C, *et al.* Porous silicon as a versatile platform for laser desorption/ionization mass spectrometry. Anal Chem 2001; 73(3): 612-9.

[86]   Silva JC, Gorenstein MV, Li G-Z, Vissers JPC, Geromanos SJ. Absolute quantification of proteins by LCMSE: a virtue of parallel MS acquisition. Mol Cell Proteomics 2006; 5(1): 144-56.

[87]   Bhatia VN, Perlman DH, Costello CE, McComb ME. Software tool for researching annotations of proteins: open-source protein annotation software with data visualization. Anal Chem 2009; 81(23): 9819-23.

[88]   Zou H, Zhang Q, Guo Z, Guo B, Zhang Q, Chen X. A Mass Spectrometry Based Direct-Binding Assay for Screening Binding Partners of Proteins. Angew Chem 2002; 114(4): 668-70.

[89]   Sumranjit J, Chung SJ. Recent advances in target characterization and identification by photoaffinity probes. Mol Basel Switz 2013; 18(9): 10425-51.

[90]   Vodovozova EL. Photoaffinity labeling and its application in structural biology. Biochem Mosc 2007; 72(1): 1-20.

[91]   Hatanaka Y, Sadakane Y. Photoaffinity labeling in drug discovery and developments: chemical gateway for entering proteomic frontier. Curr Top Med Chem 2002; 2(3): 271-88.

[92]   Griffith EC, Su Z, Turk BE, *et al.* Methionine aminopeptidase (type 2) is the common target for angiogenesis inhibitors AGM-1470 and ovalicin. Chem Biol 1997; 4(6): 461-71.

[93]   Dormán G, Prestwich GD. Using photolabile ligands in drug discovery and development. Trends Biotechnol 2000; 18(2): 64-77.

[94]   Han S-Y, Hwan Kim S. Introduction to chemical proteomics for drug discovery and development. Arch Pharm (Weinheim) 2007; 340(4): 169-77.

[95]   Kotake Y, Sagane K, Owa T, *et al.* Splicing factor SF3b as a target of the antitumor natural product pladienolide. Nat Chem Biol 2007; 3(9): 570-5.

[96]   Lamos SM, Krusemark CJ, McGee CJ, Scalf M, Smith LM, Belshaw PJ. Mixed isotope photoaffinity reagents for identification of small-molecule targets by mass spectrometry. Angew Chem Int Ed Engl 2006; 45(26): 4329-33.

[97]   Cravatt BF, Wright AT, Kozarich JW. Activity-based protein profiling: from enzyme chemistry to proteomic chemistry. Annu Rev Biochem 2008; 77: 383-414.

[98]   Verhelst SHL, Bogyo M. Chemical proteomics applied to target identification and drug discovery. BioTechniques 2005; 38(2): 175-7.

[99]   Sadaghiani AM, Verhelst SH, Bogyo M. Tagging and detection strategies for activity-based proteomics. Curr Opin Chem Biol 2007; 11(1): 20-8.

[100]   Adam GC, Burbaum J, Kozarich JW, Patricelli MP, Cravatt BF. Mapping enzyme active sites in complex proteomes. J Am Chem Soc 2004; 126(5): 1363-8.

[101]   Brooks H, Lebleu B, Vivès E. Tat peptide-mediated cellular delivery: back to basics. Adv Drug Deliv Rev 2005; 57(4): 559-77.

[102]   Ruben S, Perkins A, Purcell R, *et al.* Structural and functional characterization of human immunodeficiency virus tat protein. J Virol 1989; 63(1): 1-8.

[103]   Fawell S, Seery J, Daikh Y, *et al.* Tat-mediated delivery of heterologous proteins into cells. Proc Natl Acad Sci USA 1994; 91(2): 664-8.

[104]   Saxena C, Bonacci TM, Huss KL, Bloem LJ, Higgs RE, Hale JE. Capture of drug targets from live cells using a multipurpose immuno-chemo-proteomics tool. J Proteome Res 2009; 8(8): 3951-7.

[105]   Foerg C, Merkle HP. On the biomedical promise of cell penetrating peptides: limits versus prospects. J Pharm Sci 2008; 97(1): 144-62. http://onlinelibrary.wiley.com/doi/10.1002/jps.21117/full

[106]   Zheng C-F, Simcox T, Xu L, Vaillancourt P. A new expression vector for high level protein production, one step purification and direct isotopic labeling of calmodulin-binding peptide fusion proteins. Gene 1997; 186(1): 55-60.

[107]   Luque-Garcia JL, Zhou G, Spellman DS, Sun T-T, Neubert TA. Analysis of electroblotted proteins by mass spectrometry: protein identification after Western blotting. Mol Cell Proteomics 2008; 7(2): 308-14.

[108]   Ong S-E, Mann M. A practical recipe for stable isotope labeling by amino acids in cell culture (SILAC). Nat Protoc 2006; 1(6): 2650-60.

[109]   Gygi SP, Rist B, Gerber SA, Turecek F, Gelb MH, Aebersold R. Quantitative analysis of complex protein mixtures using isotope-coded affinity tags. Nat Biotechnol 1999; 17(10): 994-9.

[110]   Thompson A, Schäfer J, Kuhn K, *et al.* Tandem mass tags: a novel quantification strategy for comparative analysis of complex protein mixtures by MS/MS. Anal Chem 2003; 75(8): 1895-904.

[111]   Ross PL, Huang YN, Marchese JN, *et al.* Multiplexed protein quantitation in Saccharomyces cerevisiae using amine-reactive isobaric tagging reagents. Mol Cell Proteomics 2004; 3(12): 1154-69.

[112]   Vaughn CP, Crockett DK, Lim MS, Elenitoba-Johnson KSJ. Analytical Characteristics of Cleavable Isotope-Coded Affinity Tag-LC-Tandem Mass Spectrometry for Quantitative Proteomic Studies. J Mol Diagn 2006; 8(4): 513-20.

[113]   Shiio Y, Aebersold R. Quantitative proteome analysis using isotope-coded affinity tags and mass spectrometry. Nat Protoc 2006; 1(1): 139-45.

[114]   Werner T, Sweetman G, Savitski MF, Mathieson T, Bantscheff M, Savitski MM. Ion coalescence of neutron encoded TMT 10-plex reporter ions. Anal Chem 2014; 86(7): 3594-601.

[115]   Malki K, Campbell J, Davies M, *et al.* Pharmacoproteomic investigation into antidepressant response in two mouse inbred strains. Proteomics 2012; 12(14): 2355-65.

[116]   Sandberg A, Branca RMM, Lehtiö J, Forshed J. Quantitative accuracy in mass spectrometry based proteomics of complex samples: The impact of labeling and precursor interference. J Proteomics 2014; 96: 133-44.

[117]   Quaglia M, Pritchard C, Hall Z, O'Connor G. Amine-reactive isobaric tagging reagents: Requirements for absolute quantification of proteins and peptides. Anal Biochem 2008; 379(2): 164-9.

[118]   Christoforou A, Arias AM, Lilley KS. Determining protein subcellular localization in mammalian cell culture with biochemical fractionation and iTRAQ 8-plex quantification. Methods Mol Biol Clifton NJ 2014; 1156: 157-74.

[119]   Gerber SA, Rush J, Stemman O, Kirschner MW, Gygi SP. Absolute quantification of proteins and phosphoproteins from cell lysates by tandem MS. Proc Natl Acad Sci 2003; 100(12): 6940-5.

[120]   Kuhn E, Wu J, Karl J, Liao H, Zolg W, Guild B. Quantification of C-reactive protein in the serum of patients with rheumatoid arthritis using multiple reaction monitoring mass spectrometry and 13C-labeled peptide standards. Proteomics 2004; 4(4): 1175-86.

[121]   Picotti P, Bodenmiller B, Mueller LN, Domon B, Aebersold R. Full dynamic range proteome analysis of S. cerevisiae by targeted proteomics. Cell 2009; 138(4): 795-806.

[122]   Andersen JS, Wilkinson CJ, Mayor T, Mortensen P, Nigg EA, Mann M. Proteomic characterization of the human centrosome by protein correlation profiling. Nature 2003; 426(6966): 570-4.

[123]   Hüttenhain R, Surinova S, Ossola R, *et al.* N-glycoprotein SRMAtlas: a resource of mass spectrometric assays for N-glycosites enabling consistent and multiplexed protein quantification for clinical applications. Mol Cell Proteomics 2013; 12(4): 1005-16.

[124]   Picotti P, Aebersold R. Selected reaction monitoring-based proteomics: workflows, potential, pitfalls and future directions. Nat Methods 2012; 9(6): 555-66.

[125]   Chang C-Y, Picotti P, Hüttenhain R, *et al.* Protein significance analysis in selected reaction monitoring (SRM) measurements. Mol Cell Proteomics 2012; 11(4): M111.014662.

[126]   Gilchrist A, Au CE, Hiding J, *et al.* Quantitative proteomics analysis of the secretory pathway. Cell 2006; 127(6): 1265-81.

[127]   Takamori S, Holt M, Stenius K, *et al.* Molecular anatomy of a trafficking organelle. Cell 2006; 127(4): 831-46.

[128]   Kislinger T, Cox B, Kannan A, *et al.* Global survey of organ and organelle protein expression in mouse: combined proteomic and transcriptomic profiling. Cell 2006; 125(1): 173-86.

[129]   Old WM, Meyer-Arendt K, Aveline-Wolf L, *et al.* Comparison of label-free methods for quantifying human proteins by shotgun proteomics. Mol Cell Proteomics 2005; 4(10): 1487-502.

[130]   Zhang B, VerBerkmoes NC, Langston MA, Uberbacher E, Hettich RL, Samatova NF. Detecting differential and correlated protein expression in label-free shotgun proteomics. J Proteome Res 2006; 5(11): 2909-18.

[131]   Andersen JS, Wilkinson CJ, Mayor T, Mortensen P, Nigg EA, Mann M. Proteomic characterization of the human centrosome by protein correlation profiling. Nature 2003; 426(6966): 570-4.

[132] Cutillas PR, Vanhaesebroeck B. Quantitative profile of five murine core proteomes using label-free functional proteomics. Mol Cell Proteomics 2007; 6(9): 1560-73.

[133] Bondarenko PV, Chelius D, Shaler TA. Identification and relative quantitation of protein mixtures by enzymatic digestion followed by capillary reversed-phase liquid chromatography-tandem mass spectrometry. Anal Chem 2002; 74(18): 4741-9.

[134] Chelius D, Bondarenko PV. Quantitative profiling of proteins in complex mixtures using liquid chromatography and mass spectrometry. J Proteome Res 2002; 1(4): 317-23.

[135] Silva JC, Denny R, Dorschel C, et al. Simultaneous qualitative and quantitative analysis of the Escherichia coli proteome: a sweet tale. Mol Cell Proteomics 2006; 5(4): 589-607.

[136] Gao B-B, Stuart L, Feener EP. Label-free quantitative analysis of one-dimensional PAGE LC/MS/MS proteome: application on angiotensin II-stimulated smooth muscle cells secretome. Mol Cell Proteomics 2008; 7(12): 2399-409.

[137] Liu H, Sadygov RG, Yates JR. A model for random sampling and estimation of relative protein abundance in shotgun proteomics. Anal Chem 2004; 76(14): 4193-201.

[138] Ishihama Y, Oda Y, Tabata T, et al. Exponentially modified protein abundance index (emPAI) for estimation of absolute protein amount in proteomics by the number of sequenced peptides per protein. Mol Cell Proteomics 2005; 4(9): 1265-72.

[139] Griffin NM, Yu J, Long F, et al. Label-free, normalized quantification of complex mass spectrometry data for proteomic analysis. Nat Biotechnol 2010; 28(1): 83-9.

[140] Trudgian DC, Ridlova G, Fischer R, et al. Comparative evaluation of label-free SINQ normalized spectral index quantitation in the central proteomics facilities pipeline. Proteomics 2011; 11(14): 2790-7.

[141] Liu H, Sadygov RG, Yates JR. A Model for Random Sampling and Estimation of Relative Protein Abundance in Shotgun Proteomics. Anal Chem 2004; 76(14): 4193-201.

[142] Wells JA, McClendon CL. Reaching for high-hanging fruit in drug discovery at protein-protein interfaces. Nature 2007; 450(7172): 1001-9.

[143] Zorn JA, Wells JA. Turning enzymes ON with small molecules. Nat Chem Biol 2010; 6(3): 179-88.

[144] Mullard A. Protein-protein interaction inhibitors get into the groove. Nat Rev Drug Discov 2012; 11(3): 173-5.

[145] Wang Z, Gerstein M, Snyder M. RNA-Seq: a revolutionary tool for transcriptomics. Nat Rev Genet 2009; 10(1): 57-63.

[146] Maier T, Güell M, Serrano L. Correlation of mRNA and protein in complex biological samples. FEBS Lett 2009; 583(24): 3966-73.

[147] Ellis MJ, Gillette M, Carr SA, et al. Connecting Genomic Alterations to Cancer Biology with Proteomics: The NCI Clinical Proteomic Tumor Analysis Consortium. Cancer Discov 2013; 3(10): 1108-12.

[148] Benson JD, Chen Y-NP, Cornell-Kennon SA, et al. Validating cancer drug targets. Nature 2006; 441(7092): 451-6.

[149] Thiel P, Kaiser M, Ottmann C. Small-molecule stabilization of protein-protein interactions: an underestimated concept in drug discovery? Angew Chem Int Ed Engl 2012; 51(9): 2012-8.

[150] Petsko GA. For medicinal purposes. Nature 1996; 384(6604 Suppl):7-9.

[151] Cockett M, Dracopoli N, Sigal E. Applied genomics: integration of the technology within pharmaceutical research and development. Curr Opin Biotechnol 2000; 11(6): 602-9.

[152] Munos B. Lessons from 60 years of pharmaceutical innovation. Nat Rev Drug Discov 2009; 8(12): 959-68.

[153] Paul SM, Mytelka DS, Dunwiddie CT, et al. How to improve R&D productivity: the pharmaceutical industry's grand challenge. Nat Rev Drug Discov 2010; 9(3): 203-14.

[154] Groner B, Weber A, Mack L. Increasing the range of drug targets: Interacting peptides provide leads for the development of oncoprotein inhibitors. Bioengineered 2012; 3(6): 320-5.

[155] Mullard A. Reliability of "new drug target" claims called into question. Nat Rev Drug Discov 2011; 10(9): 643-4.

[156] Prinz F, Schlange T, Asadullah K. Believe it or not: how much can we rely on published data on potential drug targets? Nat Rev Drug Discov 2011; 10(9): 712-712.

[157] Ioannidis JPA. Why Most Published Research Findings Are False. PLoS Med 2005; 2(8): e124. http://www.plosmedicine.org/article/info%3Adoi%2F10.1371%2Fjournal.pmed.0020124

[158] Announcement: Reducing our irreproducibility. Nature 2013; 496(7446): 398-398.

[159] Legrain P, Aebersold R, Archakov A, et al. The human proteome project: current state and future direction. Mol Cell Proteomics 2011; 10(7): M111.009993.

[160] McShane LM, Altman DG, Sauerbrei W, Taube SE, Gion M, Clark GM. REporting recommendations for tumor MARKer prognostic studies (REMARK). Nat Clin Pract Oncol 2005; 2(8): 416-22.

[161] Altman DG, McShane LM, Sauerbrei W, Taube SE. Reporting Recommendations for Tumor Marker Prognostic Studies (REMARK): explanation and elaboration. PLoS Med 2012; 9(5): e1001216. http://www.plosmedicine.org/article/info%3Adoi%2F10.1371%2Fjournal.pmed.1001216

[162] Hood L, Perlmutter RM. The impact of systems approaches on biological problems in drug discovery. Nat Biotechnol 2004; 22(10): 1215-7.

[163] Hood L, Friend SH. Predictive, personalized, preventive, participatory (P4) cancer medicine. Nat Rev Clin Oncol 2011; 8(3): 184-7.

[164] Dahlquist KD, Salomonis N, Vranizan K, Lawlor SC, Conklin BR. GenMAPP, a new tool for viewing and analyzing microarray data on biological pathways. Nat Genet 2002; 31(1): 19-20.

[165] Karp PD, Paley S, Romero P. The Pathway Tools software. Bioinforma Oxf Engl 2002; 18 Suppl 1: S225-32.

[166] Huang DW, Sherman BT, Lempicki RA. Systematic and integrative analysis of large gene lists using DAVID bioinformatics resources. Nat Protoc 2009; 4(1): 44-57.

[167] Mencher SK, Wang LG. Promiscuous drugs compared to selective drugs (promiscuity can be a virtue). BMC Pharmacol Toxicol 2005; 5(1): 3. http://www.biomedcentral.com/1472-6904/5/3

[168] Ashburn TT, Thor KB. Drug repositioning: identifying and developing new uses for existing drugs. Nat Rev Drug Discov 2004; 3(8): 673-83.

[169] Rebuilding Big Pharma's Business Model. In vivo. Pharma & Medtech Business Intelligence 2003. https://www. pharmamedtechbi.com/publications/in-vivo/21/10/rebuilding-big-pharmas-business-model

[170] Hölzel M, Bovier A, Tüting T. Plasticity of tumour and immune cells: a source of heterogeneity and a cause for therapy resistance? Nat Rev Cancer 2013; 13(5): 365-76.

[171] Gujral TS, Peshkin L, Kirschner MW. Exploiting polypharmacology for drug target deconvolution. Proc Natl Acad Sci 2014; 111(13): 5048-53.

[172] Hood LE, Omenn GS, Moritz RL, et al. New and improved proteomics technologies for understanding complex biological systems: Addressing a grand challenge in the life sciences. Proteomics 2012; 12(18): 2773-83.

[173] Vidal M, Chan DW, Gerstein M, et al. The human proteome - a scientific opportunity for transforming diagnostics, therapeutics, and healthcare. Clin Proteomics 2012; 9(1): 6.

[174] Hood L, Flores M. A personal view on systems medicine and the emergence of proactive P4 medicine: predictive, preventive, personalized and participatory. New Biotechnol 2012; 29(6): 613-24.

[175] Swinney DC. Biochemical mechanisms of drug action: what does it take for success? Nat Rev Drug Discov 2004; 3(9): 801-8.

2.5 Appendix B

BURGLOVÁ K*, **RYLOVÁ G***, MARKOS A, PŘICHYSTALOVÁ H, SOURAL M, PETRÁČEK M, MEDVEDÍKOVÁ M, TEJRAL G, SOPKO B, HRADIL P, DŽUBÁK P, HAJDÚCH M, HLAVÁČ J. Identification of Eukaryotic Translation Elongation Factor 1-α 1 Gamendazole-Binding Site for Binding of 3-Hydroxy-4(1 H)-quinolinones as Novel Ligands with Anticancer Activity. *J. Med. Chem.* **61,** 3027–3036 (2018). PMID: 29498519 (*authors contributed equally)

Identification of Eukaryotic Translation Elongation Factor 1-α 1 Gamendazole-Binding Site for Binding of 3-Hydroxy-4(1H)-quinolinones as Novel Ligands with Anticancer Activity

Kristyna Burglová,[†,∇] Gabriela Rylová,[†,∇] Athanasios Markos,[†] Hana Prichystalova,[†] Miroslav Soural,[†] Marek Petracek,[†] Martina Medvedikova,[†] Gracian Tejral,[‡,∥,⊥] Bruno Sopko,[§,∥] Pavel Hradil,[†] Petr Dzubak,[†] Marian Hajduch,*,[†] and Jan Hlavac*,[#]

[†]Institute of Molecular and Translation Medicine, Faculty of Medicine and Dentistry, Palacký University, Hněvotínská 5, 779 00 Olomouc, Czech Republic

[‡]Department of Biophysics, Second Faculty of Medicine, Charles University, V Úvalu 84, 150 06 Praha 5, Czech Republic

[§]Department of Medical Chemistry and Clinical Biochemistry, Second Faculty of Medicine, Charles University and Motol University Hospital, V Úvalu 84, 150 06 Praha 5, Czech Republic

[∥]Department of Tissue Engineering, The Czech Academy of Sciences, Institute of Experimental Medicine, Vídeňská 1083, 142 20 Praha 4, Czech Republic

[⊥]University Center for Energy Efficient Buildings (UCEEB), The Czech Technical University in Prague, Třinecká 1024, 273 43 Bustehrad, Czech Republic

[#]Department of Organic Chemistry, Faculty of Science, Palacký University, Tř. 17. listopadu 12, 771 46 Olomouc, Czech Republic

S Supporting Information

Design   Synthesis   Interaction with EF1A1

ABSTRACT: Here, we have identified the interaction site of the contraceptive drug gamendazole using computational modeling. The drug was previously described as a ligand for eukaryotic translation elongation factor 1-α 1 (eEF1A1) and found to be a potential target site for derivatives of 2-phenyl-3-hydroxy-4(1H)-quinolinones (3-HQs), which exhibit anticancer activity. The interaction of this class of derivatives of 3-HQs with eEF1A1 inside cancer cells was confirmed via pull-down assay. We designed and synthesized a new family of 3-HQs and subsequently applied isothermal titration calorimetry to show that these compounds strongly bind to eEF1A1. Further, we found that some of these derivatives possess significant in vitro anticancer activity.

■ INTRODUCTION

eEF1A1, the second most abundant eukaryotic protein, is responsible for ribosomal protein synthesis. It is also involved in cytoskeletal organization and other physiological activities.[1] Given its multifunctional properties, eEF1A1 is considered as a moonlighting protein.[2] Moreover, eEF1A1 is associated with the development and progression of various cancers[3−6] and has thus been proposed as a target for anticancer therapy.[7,8] The overexpression and depletion of eEF1A1 have been shown to influence the cell apoptosis rate.[9,10] Although eEF1A1 was identified as a target a long time ago, only a few biologically active compounds have been found to interact with eEF1A1. The male contraceptive agent gamendazole (Figure 1) binds directly to eEF1A1 but does not affect protein synthesis.[11] The phosphodiesterase inhibitor cilostazol (Figure 1) influences

neurite outgrowth by binding to eEF1A1.[12] Narciclasine (Figure 1) and its analogs were reported to bind to eEF1A1 and overcome drug resistance by melanoma.[13] However, the authors were not successful in the validation of the binding site. eEF1A1 has been described as a target for two natural flavonoid derivatives (Figure 1),[14] which exhibit high efficacy against breast cancer cells through their interaction with eEF1A1. However, despite this fact, a binding site has not been elucidated. Although anticancer activity of such flavonoids caused by interaction with eEF1A1 has been shown,[13,14] systematic description of the binding site, in silico design, and synthesis of a set of compounds followed by verification of their

3027
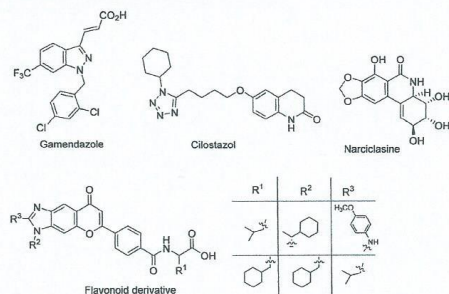
Figure 1. Structures targeting eEF1A1.[11-14]

biological activity against various types of cancer needs to be performed.

Several studies have reported that flavonoid aza-analogs, derivatives of 2-phenyl-3-hydroxy-4(1H)-quinolinone (3-HQ), exhibit significant anticancer activities.[15-18] However, until now, no study has described their molecular target. We hypothesized that 3-HQs, due to their structural similarity to other flavonoid derivatives, may serve as good ligands for interaction with eEF1A1.

In this report, we provide evidence of interaction of 3-HQ derivatives with eEF1A1 and the results of the rational design, synthesis, and *in vitro* biological evaluation of new 3-HQ derivatives.

RESULTS AND DISCUSSION

Interaction of 3-HQs with eEF1A1. The possible interaction of 3-HQs with eEF1A1 was first studied via docking experiments. Three ligands were chosen from the group of previously published active derivatives substituted by an amine at position 4′ and a nitro group at position 3′ of the 2-phenyl ring (Figure 2).[15,19]

Since the crystallographic structure of human eEF1A1 is unavailable, a homology model was built using its known sequence (UniProt database ID P68104[20]) and crystal structures of homologous eEF1A1 from yeast and rabbit. The eEF1A1 protein structure consists of three domains connected by two coiled links in sequential order. The first domain is a combination of α-helices and β-sheets. The second and third domains consist primarily of β-sheets. First, we tried to verify the chosen docking method by using the known ligand,

gamendazole, as a standard, for which the protein binding site was previously identified by MALDI-TOF.[11] The results of this docking experiment presented in Figure 3A and Table 2 show
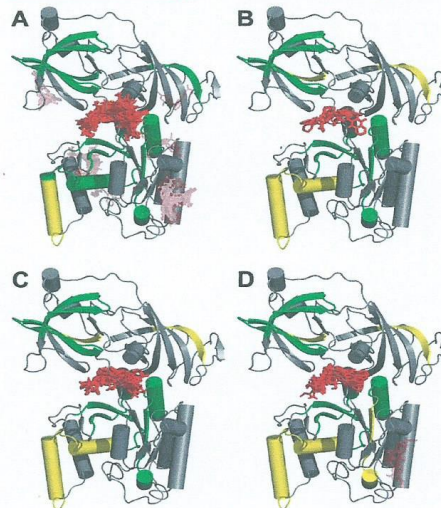
Figure 3. Results of docking of gamendazole (A) and compounds 1–3 described in Figure 2 (B, C, and D, respectively) with the homology model of human eEF1A1. Ligands in opaque red denote more favorable docking energy. The parts of the structures in green show the interaction sites identified by both MALDI-TOF[11] and our docking; those in yellow indicate sites identified by MALDI-TOF[11] only.

positive interaction of our model with gamendazole. Moreover, by comparing these results with the above-mentioned binding site, we determined the amino acid sequence of the MALDI-TOF identified domain.

To better understand the binding site, we performed the docking experiments with the previously characterized crystal structures of the homologous proteins from yeast (1F60, 1G7C, 1IJE, 1IJF, 2B7B, and 2B7C[21-25]). All these docking experiments revealed the interaction of gamendazole with
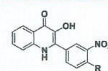
Comp. N°	R	CCRF-CEM	CEM-DNR-BULK	U2OS	K562	K562-Tax	A549	BJ
1		1.55	3.00	7.51	0.75	2.02	1.62	9.83
2		1.72	6.75	8.57	0.75	2.71	1.89	9.73
3		1.42	3.01	9.98	0.66	1.96	0.94	9.39

Figure 2. Reported IC$_{50}$ (μM) of selected 3-HQs.[19] CCRF-CEM, acute lymphoblastic leukemia; CEM-DNR-BULK, CCRF-CEM cells, daunorubicin resistant; K562, acute myeloid leukemia; K562-TAX, K562 cells, paclitaxel resistant; A549, lung adenocarcinoma; BJ, normal cycling fibroblasts cell line.

169

eEF1A1 with comparable docking energy in aa-tRNA binding site.[26,27] A verification of binding site using known crystal structures of rabbit origin (4C0S[21−25]) could not be performed because of absence of crucial amino acids together with one artificially modified residue in the identified aa-tRNA binding site.[21−25] Among all the used crystal structures, 2B7C and 2B7B exhibited interaction with eEF1A1 also in proximity to the domain identified by MALDI-TOF and not confirmed by our docking to human eEF1A1 model (see Figure 3). The docking energy is comparable to the docking in the aa-tRNA binding site (see SI, Table S1). The only-MALDI-TOF identified domain[11] is known to be highly flexible.[26,27]

We found that the overall RMS between structures 2B7C and 1F60 is 1.13 Å (0.26 pm per residue), while RMS between the only-MALDI-TOF identified domains of these structures is 2.18 Å (4.24 pm per residue). The RMS between rest of the molecules in both protein structures is 0.89 Å (0.24 pm per residue). We reasoned that because of this, no interaction of gamendazole in the only-MALDI-TOF domain was found with protein crystal structures 1G7C or 1IJF. Interaction in this domain is also less favorable in the case of 1IJE and 1F60 (see SI, Table S1). These facts led to the conclusion that our model for interaction with human eEF1A1 is valid. The 3-HQ derivatives 1−3 (Figure 2) were subjected to the docking study, and these compounds docked into the same site as gamendazole (Figure 3B,C,D). The conformation of the protein is less favorable for interaction with ligands in the highly flexible only-MALDI-TOF identified domain. This discrepancy is likely because our model does not address the loop and connecting domain flexibility.[11]

To provide evidence about the interaction of 3-HQs with eEF1A1, we performed pull-down assay with ligands A and B (Figure 4), derived from original compound 3 and immobilized
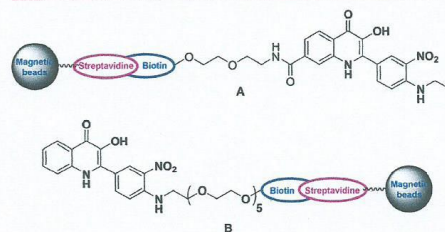
Figure 4. Ligand A and B derived from active compound 3 used for pull-down assay.

on magnetic beads via streptavidin−biotin interaction.[28] Ligand A was attached to biotin via the quinolinone benzene ring to enable interaction of proteins with the 2-phenyl moiety, whereas ligand B was biotinylated via the 2-phenyl ring to enable interaction of proteins with the opposite part of the 3-HQ scaffold. The synthesis of the biotinylated 3-HQs was performed using polystyrene resin with the combination of previously published protocols (see Experimental Section).[29]

Pull-down assay for both derivatives was performed with total protein lysate prepared from CCRF-CEM or U2OS cells. Proteins released from the ligands were analyzed using SDS-PAGE (Figure 5) and then subjected to mass spectrometry characterization. The specific ligand−protein interaction was confirmed only for derivative A, suggesting that the 2-phenyl
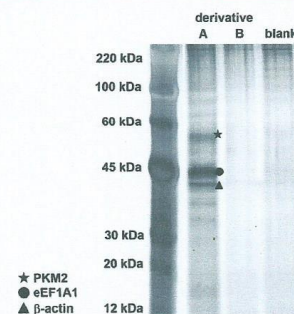
Figure 5. SDS-PAGE analysis of proteins isolated from pull-down assay of derivatives A and B incubated with CCRF-CEM protein lysate. The blank sample is represented by immobilization of biotin to streptavidin-coated magnetic beads.

moiety is the part of pharmacophore. In addition to the expected presence of eEF1A1 in the mixture of isolated proteins, we confirmed the presence of pyruvate kinase M2 (PKM2) and β-actin.

To validate identified targets, we performed Western blot to visualize isolated proteins. We identified specific bands for PKM2, eEF1A1, and β-actin only for proteins captured by derivative A, while no signal for these proteins was detected for derivative B or biotinylated beads (Figure 6).
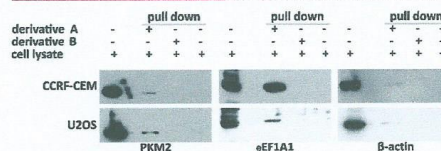
Figure 6. Characterization of proteins isolated from pull-down assay of derivatives A and B by Western blot.

Structure Design. Structural motifs of the compounds 1−3 were used to design a chemical analog set of potentially improved 3-HQ inhibitors. The toxicity of these compounds against normal cells could be diminished by replacing the nitro group with its isosteres such as carboxy or carboxamide motifs (R^1 in Figure 7). The amines substituted at position 4' of the 2-phenyl ring were selected with respect to previous studies[19] (Figure 2) and were extended to a morpholine ring (R^2 in Figure 7). Moreover, the substitution of the benzene ring of the quinolinone skeleton by hydrophobic moieties was previously reported to positively influence its cytotoxicity and selectivity.[18] According to the proven interaction of derivative A with
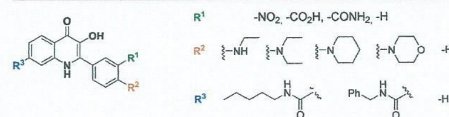
Figure 7. Analog set of 3-HQs suggested for molecular docking.

EF1A1, there is no negative effect on interaction when the moiety is bound via an amidic bond at position 7. Therefore, the pentyl and benzylamide groups in this position were selected as representatives. By combining the three diverse positions, R^1, R^2, and R^3, an analog set of 3-HQs was compiled (Figure 7) and subjected to molecular docking simulations with eEF1A1.

The analog set of 3-HQ derivatives (Figure 7) was constructed using *ab initio* methods and then subjected to virtual screening. The derivatives with the most favorable docking energy (docking energy lower than -35589.5 J·mol^{-1}) were selected. The final selection of 3-HQ derivatives was performed based on the ease of synthesis. As a result, seven 3-HQ derivatives were selected and synthesized (see Table 1).

Table 1. Synthesized 3-HQ Derivatives

Comp. N°	R^1	R^2	R^3
4	-CO$_2$H	⊦◯	-H
5	-CO$_2$H	⊦◯	-H
6	-CONH$_2$	⊦◯	-H
7	-CONH$_2$	⊦◯	-H
8	-CONH$_2$	⊦◯	-CONH-Pent
9	-CONH$_2$	⊦◯	-CONH-Bn
10	-H	-H	-H

The selected compounds included two cyclic amines (piperidine and morpholine) as R^2 substituents and substitution at position R^1 by the carboxylate and carboxamide functionalities. Further, unsubstituted derivative 10 was included as a control; it was previously described as inactive in cytotoxic assay.[16] In addition, molecular docking simulation also classified this compound as unsuitable for the target (Figure 8B). The results of the molecular docking of the selected compounds to eEF1A1 are presented in Table 2. Most of the compounds bind to the same site as gamendazole, with binding energies ranging from -38520.4 to -41032.6 J·mol^{-1} (Table 2, Figure 8A, and SI). The results of compound 10 are in accordance with the expectation because it binds at a
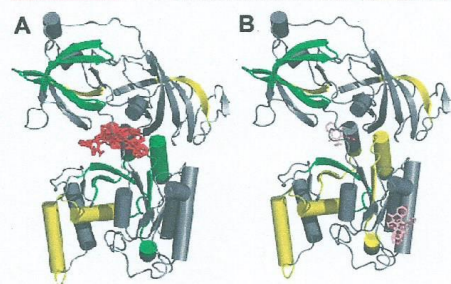
Figure 8. Docking of unsubstituted derivative 10 (B) compared with active derivative 6 (A) to an eEF1A1 model. Ligands shown in opaque red denote more favorable docking energy. The parts of the structures in green show the interactions identified by both MALDI-TOF[11] and our experiment; those in yellow indicate the interactions identified by MALDI-TOF.[11]

different location on the protein surface with the energy of -34752.1 J·mol^{-1} (Figure 8B). Some weak interactions of compound 10 with the gamendazole docking site with the energy of -31821.2 J·mol^{-1} were also revealed. We identified that all studied compounds share same binding site, which is located at the center of eEF1A1 (Table 2). The compounds interacted with the loop between the first and second domains, which was identified as part of the aa-tRNA binding site.[26,27] Moreover, this site is positioned opposite to that of the GTP, GDP, and GMP binding pockets as observed in the known PDB structures.[21,22] These results suggest that the interaction between our compounds and eEF1A1 would not reduce eEF1A1's activity by inhibiting the GTP binding site.

Synthesis. Derivatives 1−3 were synthesized according to a published protocol.[19] The synthesis of carboxylate and carboxamide analogs 4−7 is displayed in Scheme 1. Phenacyl ester 12 was prepared by the reaction of anthranilic acid with bromoketone 11. The cyclization to 3-HQ 13 was inspired by a well-established method described previously.[30,31] Hydrolysis of the methyl ester afforded carboxylate 3-HQ 14 and, following its amidation, carboxamide 3-HQ 15. These derivatives were subsequently transformed to the desired 3-HQs 4 and 5 and 6 and 7 by nucleophilic substitution with secondary amines (piperidine or morpholine) in a microwave reactor. Introduction of a carboxamide moiety into position 7 of the 3-HQs 8 and 9 was achieved in the first step of the synthesis (Scheme 2).

Starting 2-amino-4-methylterephthalate was converted to amide 16 or 17 by reaction with pentyl- or benzylamine, respectively, in pyridine. Hydrolysis of the ester group by sodium hydroxide to obtain the first building blocks 18 and 19 followed. Second building block 23 was gradually built up from ester 20 by its successive hydrolysis, chlorination, and amidation to form amide 21 followed by substitution of chlorine with piperidine and finally α-bromination (Scheme 2).

Biological Evaluation. The interaction between the prepared compounds and eEF1A1 was studied using isothermal titration calorimetry (ITC, Figure 9). ITC measures the changes in heat during interaction and provides thermodynamic information about the binding affinity of a ligand to a protein. The measured enthalpies for the interactions of the synthesized 3-HQ derivatives with the protein, and the K_a values suggest high affinities (Table 2). The only exception within the series is the unsubstituted derivative 10, used here as a negative control, which exhibited no interaction with the protein. This result is in accordance with the poor molecular docking results of compound 10. Similarly, gamendazole in the form of analytical standard[32] was subjected to the interaction studies as a positive control. As expected, binding of gamendazole with eEF1A1 was confirmed, although the interaction is much weaker than those of the 3-HQs (see the titration profile in SI).

Finally, we tested the *in vitro* activity of the prepared derivatives against cancer cell lines (Table 3). Compared to original compound 1, the replacement of the nitro group with a carboxy moiety (derivatives 4 and 5) caused loss of activity. This could be caused by the carboxy group itself, which apparently restricts the penetration of the compounds through the cell membrane. Transformation of the carboxy group to carboxamide (derivative 6) significantly improved the activity in comparison with derivatives 4 and 5 and reached similar values as that observed for derivative 1, except for CEM-DNR and U2OS cell lines. The toxicity to normal cell line BJ was improved by one order of magnitude. When the piperidine ring was replaced with morpholine (compare derivatives 6 and 7),

171

Table 2. Thermodynamic and Binding Parameters for the Interaction of the 3-HQ Compounds with eEF1A1[a]

compd no.	$\Delta_r H_m^\circ$ (kJ mol^{-1})	K_a° (M^{-1})	n	$\Delta_r S_m^\circ$ (J mol^{-1} K^{-1})	$\Delta_r G_m^\circ$ (J mol^{-1})	docking $\Delta_r G_m^\circ$ (J mol^{-1})
4	−11272	2.536×10^6	0.798	−37686	−35919	−38911
5	−1872	1.029×10^7	1.640	−6147	−39272	−38911
6	−15999	2.899×10^6	0.932	−53539	−36347	−38492
7	−7932	6.796×10^6	0.746	−26474	−38777	−38911
8	−9416	5.297×10^6	1.129	−31454	−37990	−38911
9	−9213	1.809×10^7	1.694	−30764	−40713	−43932
10[b]						
gamendazole	−1209	1.268×10^7	1.777	−3919	−40550	−36401

[a]$\Delta_r H_m^\circ$ = enthalpy change of binding; K_a = association constant; n = stoichiometry; $\Delta_r S_m^\circ$ = entropy change; $\Delta_r G_m^\circ$ = Gibbs energy change; docking $\Delta_r G_m^\circ$ = Gibbs energy change determined by molecular modeling. The value of the stoichiometric binding number (n) is approximately 1 for all the compounds. The negative changes in free energy and enthalpy confirm that the binding of the ligands to eEF1A1 is spontaneous and exothermic. An example of a calorimetric titration profile showing the ligand–protein interaction, that is, that of derivative 6 in comparison with the noninteracting derivative 10, is given in Figure 9 (for the titration profiles of other compounds, see SI). [b]No interaction.

Scheme 1. Synthesis of Selected 3-HQs
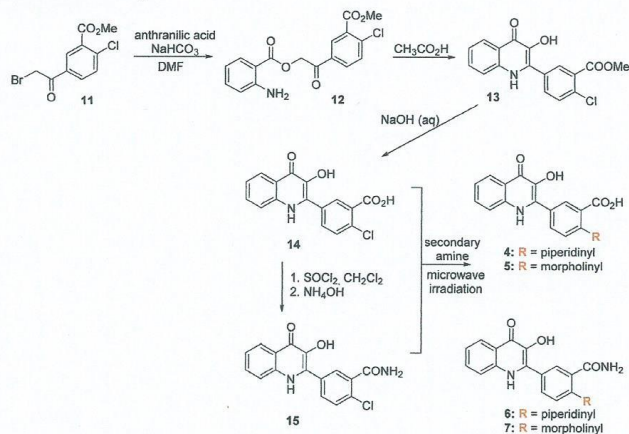
Scheme 2. Synthesis of Designed 3-HQs Substituted with 7-Carboxamide Group
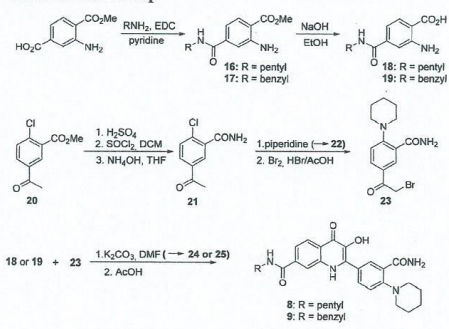
the activity was lost. As predicted, the improvement of toxicity against the majority of the cancer cell lines was achieved by insertion of the pentylamide moiety at position 7 (derivative 8).

In the case of improved toxicity, submicromolar IC$_{50}$ values were achieved for two lines. Unfortunately, the toxicity against normal BJ cells was similar to that of original compound 1. Replacement of pentylamide with the benzylamide group (derivative 9) led to IC$_{50}$ values at micromolar range for adenocarcinoma A549 line, leukemia cell lines K562, CCRF-CEM, and colorectal tumor HCT-116. Similarly, the compound displayed submicromolar IC$_{50}$ values for osteosarcoma cell lines (U2OS), whereas it did not exhibit activity against cancer cell lines (CEM-DNR and K562-TAX) resistant to chemotherapy. Most importantly, toxicity of 9 against normal cell line (BJ) was significantly higher than that of original compounds 1–3.

■ CONCLUSION

We suggested previously reported cytotoxic derivatives of 2-phenyl-3-hydroxy-4(1H)-quinolinone as ligands for eEF1A1, and via docking experiments, we provided evidence of their interaction with this target. We further described in detail the binding site of these compounds, which are similar to contraceptive agent gamendazole. The results obtained via computational study were corroborated by pull-down assay. The knowledge was used for the design of advanced derivatives

172
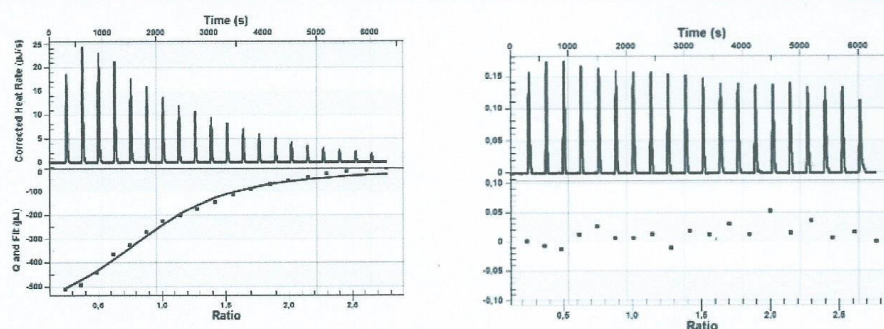
Figure 9. Calorimetric titration profile for the interaction of 3-HQ **6** (left) and **10** (right) with eEF1A1.

Table 3. Cytotoxic Activity (IC$_{50}$, μM) of Prepared Derivatives against Cancer Cell Lines

3-HQ	R^1	R^2	R^3	A549	U2OS	CCRF-CEM	CEM-DNR	HCT-116	K562	K562-TAX	BJ
4	-CO$_2$H	1-piperidinyl	H-	50	50	49.56	50	50	50	50	50
5	-CO$_2$H	4-morpholinyl	H-	50	50	49.56	50	50	50	50	50
6	-CONH$_2$	1-piperidinyl	H-	9.96	26.02	3.34	21.43	4.46	7.1	6.41	48.92
7	-CONH$_2$	4-morpholinyl	H-	44.37	50	16.24	50	30.6	50	50	50
8	-CONH$_2$	1-piperidinyl	C$_5$H$_{11}$CONH-	1.89	0.56	1.73	8.03	0.64	2.39	32.71	10.24
9	-CONH$_2$	1-piperidinyl	PhCH$_2$CONH-	3.77	0.58	1.73	>50	1.01	8.30	>50	>50
10	-H	-H	H-	>50	46.96	26.74	22.49	44.20	47.96	27.44	>50

of 3-HQs, and their interaction with eEF1A1 was confirmed using microcalorimetric measurement. Some of these derivatives possess remarkable inhibitory activity against selected cancer cell lines and low toxicity against a normal cell line, namely, fibroblasts BJ. In summary, this study is the first report describing rational design and synthesis of anticancer compounds acting as eEF1A1 ligands using in silico technique and demonstrating the molecular target for 3-HQ derivatives, which have been reported as potent anticancer agents. Detailed elucidation of the binding site can serve for future design of new eEF1A1 ligands to inhibit this relatively unexplored molecular target and set up a new strategy in anticancer treatment.

■ EXPERIMENTAL SECTION

Materials and Methods. For preparation and characterization of the compounds, LC/MS analyses were performed using UHPLC/MS with UHPLC chromatograph (Acquity) attached with a PDA detector, a single quadrupole mass spectrometer (Waters), an X-Select C18 column at 30 °C with a flow rate of 600 μL/min. The mobile phase consisted of (A) 0.01 M ammonium acetate in water and (B) acetonitrile, with a linear gradient over the course of 2.5 min; the final ratio was maintained for 1.5 min. The column was re-equilibrated with 10% B for 1 min. The APCI ionization operated at a discharge current of 5 μA, a vaporizer temperature of 350 °C, and a capillary temperature of 200 °C. Purity of the compounds was determined using the ratio of the appropriate peak area to sum of areas of all peaks of the mixture. Areas were determined by integration of the peaks from the PDA detector response. Purification was performed using semipreparative HPLC with a Waters 1500 series HPLC equipped

with a 2707 Autosampler, a 1525 binary HPLC pump, a 2998 Waters Photodiode Array Detector, and a Waters Fraction Collector III with a YMC C18 reverse phase column (20 × 100 mm, 5 μm particle size). The mobile phase consisted of acetonitrile and a 10 mM aqueous ammonium acetate gradient over 6 min. The purity of the tested compounds was determined by HPLC, which in all the cases was ≥96%.

NMR spectra were measured in DMSO-d_6 using a Jeol ECX-500 (500 MHz) spectrometer. Chemical shifts (δ) are reported in parts per million (ppm) and coupling constants (J) are reported in Hertz (Hz).

Solvents and chemicals were purchased from Sigma-Aldrich (Milwaukee, IL, www.sigmaaldrich.com).

All compounds tested on the biological activity were successfully filtered for PAINS.

Synthesis of Studied Compounds. *2-(2-(2-(4-(Ethylamino)-3-nitrophenyl)-3-hydroxy-4-oxo-1,4-dihydroquinoline-7-carboxamido)ethoxy)ethyl 2-(2-oxohexahydro-1H-thieno[3,4-d]-imidazol-4-yl)acetate(A).* Ligand A was prepared according to the following scheme:

The compound **26** was prepared on a solid support (BAL linker) according to the published procedure.[33] The resin **26** was then reacted with a solution of biotin (0.24 g, 1.0 mmol), HOBt (135 mg, 1.0 mmol), N,N-diisopropylethylamine (DIEA) (0.05 mL, 0.3 mmol), and DIC (0.15 mL, 0.3 mmol) in DMF (2 mL) for 16 h at room temperature. The obtained resin **27** was then washed three times with DMF (3 × 2 mL) and DCM (3 × 2 mL), and the compound was cleaved from the resin with 50% trifluoroacetic acid (TFA) in DCM and dried under a stream of nitrogen. Final cyclization was performed by refluxing the cleaved compound in acetic acid (AcOH) for 2 h. The obtained ligand A was purified by HPLC, which resulted in ~25% yield. MS (APCI) exact mass calculated for [M + H]$^+$ C$_{16}$H$_{11}$ClNO$_4$ 683.25; found 683.70. ^{1}H NMR (300 MHz, DMSO-d_6) δ ppm 11.70
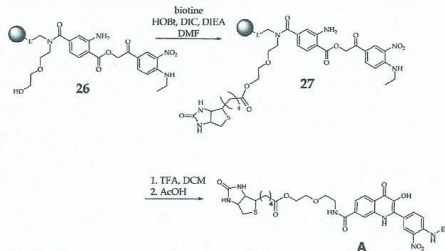
(br, 1 H), 8.60–8.76 (m, 2 H), 8.39 (t, J = 5.58 Hz, 1 H), 8.24 (br, 1 H), 8.18 (d, J = 8.42 Hz, 1 H), 8.05 (d, J = 8.42 Hz, 1 H), 7.67 (d, J = 8.60 Hz, 1 H), 7.25 (d, J = 9.15 Hz, 1 H), 6.38 (d, J = 18.66 Hz, 2 H), 4.04–4.19 (m, 3 H), 3.18–3.69 (m, 15 H), 2.79 (dd, J_1= 12.26 Hz, J_2 = 4.94 Hz, 1 H), 2.55 (d, J = 12.44 Hz, 1 H), 2.25 (t, J = 7.41 Hz, 2 H), 1.37–1.65 (m, 3 H), 1.27 (t, J = 7.14 Hz, 3 H).

2-(2-((4-(3-Hydroxy-4-oxo-1,4-dihydroquinolin-2-yl)-2-nitrophenyl)amino)ethoxy)ethyl 2-(2-Oxohexahydro-1H-thieno-[3,4-d]imidazol-4-yl)acetate (B). Ligand B was prepared according to the following scheme:
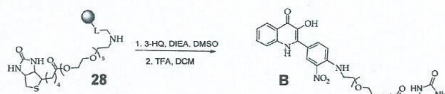
First, the polymer-supported biotinylated spacer 28 was prepared according to the previously published procedure.[34] The resin 28 (300 mg) was then shaken in a solution of 2-(4-chloro-3-nitro)phenyl-3-hydroxyquinolin-4(1H)-one (3 mmol) and DIEA (0.15 mL, 1 mmol) in DMSO (9 mL) for 16 h at room temperature. Acid-mediated cleavage (50% TFA in DCM, 30 min, room temperature) and HPLC purification were performed to obtain final ligand B.

General Procedure for Preparation of Compounds 4–7. Derivative 14 or 15 (0.28 mmol) was dissolved in the corresponding amine (3 mL), and the mixture was stirred in a microwave reactor for 6 h at 200 °C and 200 W. The precipitate formed was filtered, washed with water, and dried under vacuum.

5-(3-Hydroxy-4-oxo-1,4-dihydroquinolin-2-yl)-2-(piperidin-1-yl)-benzoic Acid (4). Yellow powder. HPLC purity: 98%. Yield: 0.14 g (40%). ^{1}H NMR (500 MHz, DMSO-d_6) δ ppm 11.64 (br, 1H), 8.43 (s, 1 H), 8.15 (d, J = 8.0 Hz, 1H), 8.06 (d, J = 7.5 Hz, 1H), 7.84 (d, J = 8.5 Hz, 1H), 7.71 (d, J = 8.5 Hz, 1H), 7.60 (t, J = 7.0 Hz, 1H), 7.28 (t, J = 7.5 Hz, 1H), 3.12 (t, J = 5.0 Hz, 4H), 1.81–1.74 (m, 4H), 1.68–1.60 (m, 2H). ^{13}C NMR (126 MHz, DMSO-d_6) δ ppm 170.1, 166.6, 151.1, 138.1, 138.0, 134.2, 131.5, 130.7, 130.3, 130.0, 124.7, 124.5, 122.6, 121.9 (2C), 118.4, 53.5, 25.6, 22.3. HRMS (ESI) calculated for [M + H]⁺ $C_{21}H_{20}N_2O_4$ 365.1496; found 365.1495.

5-(3-Hydroxy-4-oxo-1,4-dihydroquinolin-2-yl)-2-morpholinoben-zoic Acid (5). Yellow powder. HPLC purity: 98%. Yield: 0.05 g (47%). ^{1}H NMR (500 MHz, DMSO-d_6) δ ppm 11.58 (s, 1H), 8.29 (d, J = 2.0 Hz, 1H), 8.14 (d, J = 8.0 Hz, 1H), 8.00 (dd, J_1= 8.5 Hz, J_2 = 2.0 Hz, 1H), 7.71 (d, J = 8.5 Hz, 1H), 7.62–7.58 (m, 2H) 7.27 (t, J = 7.5 Hz, 1H), 3.81 (t, J = 4.5 Hz, 4 H), 3.13 (t, J = 4.5 Hz, 4H). ^{13}C NMR (126 MHz, DMSO-d_6) δ ppm 172.0, 170.0, 167.3, 151.2, 138.1, 137.9, 133.9, 131.7, 130.6, 130.2, 127.8, 124.5, 124.3, 121.9, 121.8, 120.9, 119.5, 118.4, 66.2, 52.2. HRMS (ESI) calculated for [M + H]⁺ $C_{20}H_{19}N_2O_5$ 367.1288; found 367.1288.

5-(3-Hydroxy-4-oxo-1,4-dihydroquinolin-2-yl)-2-(piperidin-1-yl)-benzamide (6). Yellow powder. HPLC purity: 98%. Yield: 0.14 g (48%). ^{1}H NMR (500 MHz, DMSO-d_6) δ ppm 8.49 (br, 1H), 8.18 (s, 1H), 8.14 (d, J = 8.0 Hz, 1H), 7.88 (br, 1H), 7.72 (br, 1H), 7.66 (s, 1H), 7.58 (t, J = 7.0 Hz, 1H), 7.32 (d, J = 8.0 Hz, 1H), 7.26 (t, J = 7.5 Hz, 1H), 2.97 (t, J = 4.5 Hz, 4H), 1.73–1.66 (m, 4H), 1.57–1.50 (m,

2H). ^{13}C NMR (126 MHz, DMSO-d_6) δ ppm 169.8, 167.9, 152.5, 138.0, 137.9, 132.3, 131.0, 130.9, 130.4, 128.1, 126.3, 124.4, 121.8, 119.3, 118.4, 53.6, 25.8, 23.3. HRMS (ESI) calcd for [M + H]⁺ $C_{21}H_{22}N_3O_3$ 364.1656; found 364.1654.

5-(3-Hydroxy-4-oxo-1,4-dihydroquinolin-2-yl)-2-morpholinoben-zamide (7). Yellow powder. HPLC purity: 99%. Yield: 0.10 g (56%). ^{1}H NMR (500 MHz, DMSO-d_6) δ ppm 11.53 (br, 1H), 8.26 (s, 1H), 8.14 (d, J = 8.0 Hz, 1H), 8.08 (d, J = 2.5 Hz, 1H), 7.88 (dd, J_1= 2.0 Hz, J_2 = 8.0 Hz, 1H), 7.72 (d, J = 8.6 Hz, 1H), 7.63 (s, 1H), 7.58 (td, J_1= 1.5 Hz, J_2 = 7.0 Hz, 1H), 7.32–7.23 (m, 2H), 3.78 (t, J = 3.5 Hz, 4H), 3.03 (t, J = 3.5 Hz, 4H). ^{13}C NMR (126 MHz, DMSO-d_6) δ ppm 169.9, 168.4, 151.0, 138.0, 137.8, 132.2, 130.9, 130.8, 130.5, 128.6, 126.1, 124.4, 121.8 (2C), 118.6, 118.4, 66.2, 52.3. HRMS (ESI) calculated for [M + H]⁺ $C_{20}H_{20}N_3O_4$ 366.1448; found 366.1447.

2-(3-Carbamoyl-4-(piperidin-1-yl)phenyl)-3-hydroxy-4-oxo-N-pentyl-1,4-dihydroquinoline-7-carboxamide (8). The phenac-yl ester 24 (0.08 g, 0.2 mmol) was dissolved in glacial acetic acid (3 mL), and the mixture was refluxed for 2 h. After cooling down to room temperature, the mixture was poured into ice-cold water. The precipitate was filtered off, washed with 10% solution of NaHCO₃, and dried under vacuum. Green powder. HPLC purity: 99%. Yield: 0.07 g (92%). ^{1}H NMR (500 MHz, DMSO-d_6) δ ppm 11.71 (s, 1H), 8.71–8.53 (m, 1H), 8.48 (s, 1H), 8.27–8.08 (m, 3H), 7.89 (d, J = 7.4 Hz, 1H), 7.72–7.52 (m, 2H), 7.33 (d, J = 8.6 Hz, 1H), 3.33–3.21 (m, 2H), 3.03–2.92 (m, 4H), 1.75–1.62 (m, 4H), 1.62–1.48 (m, 4H), 1.37–1.26 (m, 4H), 0.89 (t, J = 6.9 Hz, 3H). ^{13}C NMR (126 MHz, DMSO-d_6) δ ppm 169.5, 168.0, 165.8, 152.6, 138.4, 137.5, 136.6, 132.3, 131.6, 131.1, 128.1, 125.8, 124.6, 122.8, 119.7, 119.2, 118.4, 53.6, 40.0 (*overlay with solvent*), 28.7 (2C), 25.8, 23.3, 21.9, 13.9. HRMS (APCI) calculated for [M + H]⁺ $C_{27}H_{32}N_4O_4$ 477.2496; found 477.2503.

N-Benzyl-2-(3-carbamoyl-4-(piperidin-1-yl)phenyl)-3-hy-droxy-4-oxo-1,4-dihydroquinoline-7-carboxamide (9). The compound was prepared from phenacyl ester 25 according to the procedure described for compound 8. Green powder. HPLC purity: 99%. Yield: 0.06 g (88%). ^{1}H NMR (500 MHz, DMSO-d_6) δ ppm 9.26–9.13 (m, 1H), 8.50 (s, 1H), 8.28 (s, 1H), 8.23–8.17 (m, 2H), 7.91 (d, J = 8.0 Hz, 1H), 7.72–7.66 (m, 2H), 7.38–7.29 (m, 5H) 7.29–7.55 (m, 1H), 4.51 (d, J = 5.7 Hz, 2H), 3.01–2.94 (m, 4H), 1.76–1.63 (m, 4H), 1.60–1.51 (m, 2H). ^{13}C NMR (126 MHz, DMSO-d_6) δ ppm 172.2, 168.0, 166.0, 152.5, 139.5, 138.6, 137.7, 136.0, 132.3, 132.0, 131.1, 128.3, 128.1, 127.2, 126.8, 126.2, 124.6, 123.0, 119.6, 119.2, 119.04, 53.6, 42.7, 25.8, 23.4. HRMS (APCI) calculated for [M − H]⁻ $C_{29}H_{28}N_4O_4$ 495.2027; found 495.2022.

Methyl 5-(2-((2-Aminobenzoyl)oxy)acetyl)-2-chloroben-zoate (12). Anthranilic acid (0.97 g, 7.1 mmol) and NaHCO₃ (0.78 g, 9.3 mmol) were dissolved in DMF (50 mL) and stirred for 30 min at 100 °C. The mixture was cooled down to room temperature, and bromoacetophenone 11 (2.05 g, 7.1 mmol) was added. The reaction mixture was stirred for 16 h at room temperature. The product was extracted to EtOAc (three times); the organic layer was dried over Na₂SO₄ and evaporated to dryness. White powder. LC purity: 99%. Yield: 1.06 g (91%). ^{1}H NMR (500 MHz, DMSO-d_6) δ ppm 8.37 (d, J = 2.5 Hz, 1H), 8.18 (dd, J_1= 8.5 Hz, J_2 = 2.0 Hz, 1H), 7.81 (d, J = 8.5 Hz, 1H), 7.81 (dd, J_1= 8.0 Hz, J_2 = 1.5 Hz, 1H), 7.31–7.28 (m, 1H), 6.80 (d, J = 8.5 Hz, 1H), 6.64 (br, 2H), 6.59–6.54 (m, 1H), 5.68 (s, 2H), 3.91 (s, 3H). ^{13}C NMR (126 MHz, DMSO-d_6) δ ppm 192.1, 166.6, 164.8, 151.6, 137.1, 134.5, 132.8, 132.0, 131.6, 130.8, 130.7, 130.2, 166.6, 114.8, 108.0, 66.4, 52.9.

Methyl 2-Chloro-5-(3-hydroxy-4-oxo-1,4-dihydroquinolin-2-yl)benzoate (13). Derivative 12 (1.04 g, 3.0 mmol) was dissolved in AcOH (25 mL), and the mixture was boiled for 4 h. It was then cooled down to room temperature and poured into ice-cold water. The precipitate formed was filtered off, washed with water, and dried under vacuum. Yellow powder. LC purity: 99%. Yield: 0.86 g (87%). ^{1}H NMR (500 MHz, DMSO-d_6) δ ppm 11.64 (s, 1H), 8.67 (br, 1H) 8.23 (d, J = 1.7 Hz, 1H), 8.12 (d, J = 7.4 Hz, 1 H), 8.00 (dd, J_1= 8.3 Hz, J_2 = 2.0 Hz, 1H), 7.80 (d, J = 8.0 Hz, 1H), 7.70 (d, J = 8.6 Hz, 1H), 7.61 (t, J = 8.0 Hz, 1H), 7.28 (t, J = 7.7 Hz, 1 H), 3.91 (s, 3H). ^{13}C NMR (126 MHz, DMSO-d_6) δ ppm 170.2, 165.2, 138.1 (2C), 133.7, 132.4, 131.5,

131.4, 130.8, 130.0, 129.1, 124.5, 122.0, 121.9, 118.4, 52.8, 21.1. HRMS (ESI) calculated for $[M + H]^+$ $C_{17}H_{13}ClNO_4$ 330.0528; found 330.0527.

2-Chloro-5-(3-hydroxy-4-oxo-1,4-dihydroquinolin-2-yl)-benzoic Acid (14). Derivative 13 (0.49 g, 1.5 mmol) was treated with 10% aqueous NaOH (20 mL) for 1 h at 50 °C. The reaction mixture was then cooled down to room temperature, acidified with 1 M HCl, and extracted three times to ethyl acetate. The combined organic layers were washed with brine and dried over MgSO₄. The solvent was evaporated, and the residue was dried under vacuum. Yellow powder. LC purity: 99%. Yield: 0.25 g (90%). LC/MS analysis: MS (ESI) exact mass calculated for $[M + H]^+$ $C_{16}H_{11}ClNO_4$ 316.04; found 316.35; purity 99%. ^{1}H NMR (500 MHz, DMSO-d_6) δ ppm 13.64 (br, 1H) 11.64 (s, 1H) 8.23 (d, J = 2.5 Hz, 1H), 8.15 (d, J = 10.5 Hz, 1H), 7.97 (dd, J₁= 2.5 Hz, J₂ = 10.5 Hz, 1H), 7.76−7.70 (m, 2H), 7.61 (t, J = 10.5 Hz, 1 H), 7.28 (t, J = 9 Hz, 1H). ^{13}C NMR (101 MHz, DMSO-d_6) δ ppm 170.2, 166.4, 138.2, 138.1, 133.2, 132.4, 131.5, 131.4, 131.2, 130.8, 130.7, 129.3, 124.5, 122.0, 121.9, 118.5.

2-Chloro-5-(3-hydroxy-4-oxo-1,4-dihydroquinolin-2-yl)-benzamide (15). The compound was prepared from corresponding acid 14 (0.49 g, 1.5 mmol), which was stirred in SOCl₂ (10 mL) for 2 h at room temperature. The solvent was evaporated, and the residue was dissolved in DCM (10 mL). NH₄OH (10 mL) was added, and the mixture was stirred for 16 h at room temperature. It was then washed with 1 M HCl, water, and brine and dried over Na₂SO₄. The inorganic salt was filtered off, the solvent was evaporated, and the residue was dried under vacuum. Yellow powder. LC purity: 99%. Yield: 0.37 g (76%). LC/MS analysis: MS (ESI) exact mass calculated for $[M + H]^+$ $C_{16}H_{12}ClN_2O_3$ 315.73; found 315.34; purity 98%. ^{1}H NMR (500 MHz, DMSO-d_6) δ ppm 11.61 (br, 1H), 8.15 (d, J = 10.5 Hz, 1H), 7.99 (s, 1H), 7.92−7.89 (m, 2H), 7.74−7.67 (m, 3H), 7.60 (t, J = 9.0 Hz, 1H), 7.28 (t, J = 9.0 Hz, 1H). ^{13}C NMR (101 MHz, DMSO-d_6) δ ppm 170.2, 167.7, 138.1, 136.9, 131.4, 131.3, 131.0, 130.7, 130.5, 129.6, 129.4, 129.1, 124.5, 122.0, 121.8, 118.5.

Methyl 2-Amino-4-(pentylcarbamoyl)benzoate (16). 2-Aminomethylterephthalate (1.00 g, 5.1 mmol), 1-ethyl-3-(3-(dimethylamino)propyl)carbodiimide (EDC) (0.87 g, 7.5 mmol), and pentylamine (0.85 mL, 5.1 mmol) were stirred in pyridine (20 mL) for 16 h at room temperature. The solvents were then evaporated; the residue was dissolved in EtOAc, washed three times with 1 M HCl and saturated solution of NaHCO₃, and dried over MgSO₄. The solvent was evaporated, and the residue was dried under vacuum. Yellow powder. HPLC purity: 99%. Yield: 1.30 g (97%). ^{1}H NMR(500 MHz, CDCl₃) δ ppm 7.85 (d, J = 8.6 Hz, 1H), 7.11 (d, J = 1.1 Hz, 1H), 6.86 (dd, J = 8.0, 1.7 Hz, 1H), 6.24 (s, 1H), 5.85 (s, 2H), 3.87 (s, 3H), 3.44−3.35 (m, 2H), 1.63−1.53 (m, 2H), 1.39−1.28 (m, 4H), 0.89 (t, J = 6.9 Hz, 3H). ^{13}C NMR (126 MHz, DMSO-d_6)δ ppm 168.1, 167.0, 150.6, 140.0, 131.8, 115.9, 113.6, 112.6, 51.9, 40.3, 29.4, 29.2, 22.5, 14.1. HRMS (APCI) calculated for $[M + H]^+$ $C_{14}H_{20}N_2O_3$ 265.1547; found 265.1548.

Methyl 2-Amino-4-(benzylcarbamoyl)benzoate (17). The compound was prepared according to the procedure described for compound 16 with the use of benzylamine. Yellow oil. HPLC purity: 99%. Yield: 1.39 g (96%). ^{1}H NMR (500 MHz, CDCl₃) δ ppm 9.02−8.94 (m, 1H), 7.76 (d, J = 8.0 Hz, 1H), 7.37−7.19 (m, 6H), 6.96 (dd, J = 8.6, 1.7 Hz, 1H), 6.76 (s, 2H), 4.43 (d, J = 6.3 Hz, 2H), 3.81 (s, 3H). ^{13}C NMR (126 MHz, DMSO-d_6) δ ppm 167.4, 166.0, 151.0, 139.6, 130.8, 128.3, 127.2, 126.7, 116.0, 112.9, 110.4, 51.6, 42.6. HRMS (ESI) calculated for $[M + H]^+$ $C_{16}H_{16}N_2O_3$ 285.1234; found 285.1235.

2-Amino-4-(pentylcarbamoyl)benzoic Acid (18). Ester 16 (0.75 mg, 2.8 mmol) was dissolved in EtOH (17 mL). Aqueous solution of NaOH (0.55 mL, 1 M) was added, and the reaction mixture was stirred for 2 h at 40 °C. The solvents were then removed under vacuum, water (10 mL) was added, and the pH was adjusted to 7 by addition of AcOH. The precipitate formed was filtered off, washed with water, and dried under vacuum. Pink powder. HPLC purity: 99%. Yield: 605 mg (80%). ^{1}H NMR (500 MHz, DMSO-d_6) δ ppm 8.37−8.29 (m, 1H), 7.72 (d, J = 8.0 Hz, 1H), 7.15 (d, J = 1.7 Hz, 1H), 6.86 (dd, J = 8.6, 1.7 Hz, 1H), 3.24−3.14 (m, 2H), 1.54−1.44 (m, 2H), 1.35−1.21 (m, 4H), 0.86 (t, J = 7.2 Hz, 3H). ^{13}C NMR (126

MHz, DMSO-d_6) δ ppm 169.5, 166.1, 151.1, 139.4, 131.2, 115.5, 112.7, 112.3, 40.0 (overlay with solvent), 28.7 (2C), 21.9, 13.9. HRMS (APCI) calculated for $[M + H]^+$ $C_{13}H_{18}N_2O_3$ 251.1390; found 251.1388.

2-Amino-4-(benzylcarbamoyl)benzoic Acid (19). The compound was prepared according to the procedure described for compound 18 from derivative 17. Yellow powder. HPLC purity: 99%. Yield: 0.7 g (75%). ^{1}H NMR (500 MHz, DMSO-d_6) δ ppm 9.06−8.88 (m, 1H), 7.75 (d, J = 8.6 Hz, 1H), 7.42−7.29 (m, 4H), 7.29−7.21 (m, 2H), 6.96 (dd, J = 8.6, 1.7 Hz, 1H), 4.46 (d, J = 5.7 Hz, 2H). ^{13}C NMR (126 MHz, DMSO-d_6) δ ppm 169.2, 166.2, 151.3, 139.6, 139.3, 131.3, 128.3, 127.2, 126.7, 115.7, 112.7, 111.4, 52.6. HRMS (ESI) calculated for $[M - H]^-$ $C_{15}H_{14}N_2O_3$ 269.0921; found 269.0920.

5-Acetyl-2-chlorobenzamide (21). Starting ester 20 (0.68 g, 3.4 mmol), which had been prepared according to the published procedure,[35] was stirred in a mixture of concentrated acetic acid and concentrated sulfuric acid (8.5/1.5, w/v, 32 mL) for 2 h at 80 °C. The reaction mixture was then allowed to cool down to room temperature and was neutralized to pH 3 with saturated solution of K₂CO₃. The mixture was then extracted to DCM (3 × 50 mL); the organic layers were washed with saturated solution of NaHCO₃ and dried over Na₂SO₄. After the filtration and evaporation of the solvent, the obtained yellow powder was immediately used in the next step. The powder was dissolved in DCM (10 mL) under inert atmosphere. The suspension was stirred at 0 °C, and SOCl₂ (2 mL, 0.4 mmol) was added dropwise. The mixture was stirred for 1.5 h at 50 °C. During this time, the insoluble material was dissolved. It was then allowed to cool down to room temperature, and the solvent was removed under the stream of nitrogen. Resulting brown solid was dissolved in THF (10 mL) and cooled down to 0 °C, and NH₄OH solution (25%, 2 mL) was added. This mixture was stirred for 30 min at room temperature, followed by extraction to EtOAc (3 × 50 mL). Combined organic layers were washed with brine and dried over MgSO₄. The solvent was finally evaporated under vacuum yielding amide 21. Yellow powder. HPLC purity: 99%. Yield: 0.53 mg (78%). ^{1}H NMR(500 MHz, DMSO-d_6) δ ppm 8.04 (s, 1H), 8.02−7.93 (m, 2H), 7.72 (s, 1H), 7.64 (dd, J = 8.6, 1.1, 1H), 2.60 (s, 3H). ^{13}C NMR (126 MHz, DMSO-d_6) δ ppm 196.8, 167.4, 137.3, 135.3, 134.7, 130.2, 130.0, 128.3, 26.8. HRMS (APCI) calculated for $[M + H]^+$ $C_9H_8ClNO_2$ 198.0316; found 198.0319.

5-Acetyl-2-(piperidin-1-yl)benzamide (22). Amide 21 (0.70 g, 3.5 mmol) and piperidine (0.79 mL, 8.0 mmol) were dissolved in DMSO (3 mL). The mixture was stirred at 120 °C for 1.5 h. After cooling down to room temperature, the mixture was poured into water and extracted to EtOAc (3 × 40 mL). Combined organic layers were then washed with water (3 × 30 mL) and brine and dried over Na₂SO₄. The solvent was removed under vacuum, and the residue was filtered through silica gel with EtOAc as the eluent. White powder. HPLC purity: 99%. Yield: 0.66 g (76%). ^{1}H NMR(500 MHz, DMSO-d_6) δ ppm 8.08 (d, J = 2.3 Hz, 1H), 8.01 (s, 1H), 7.92 (dd, J = 8.6, 2.3 Hz, 1H), 7.58 (s, 1H), 7.12 (d, J = 8.6 Hz, 1H), 3.04−2.02 (m, 4H), 2.51 (s, 3H, overlay with solvent), 1.68−1.63 (m, 4H), 1.57−1.49 (m, 2H). ^{13}C NMR (126 MHz, DMSO-d_6) δ ppm 196.1, 168.9, 154.9, 131.2, 130.5, 129.2, 127.6, 118.1, 52.6, 26.4, 25.4, 23.4. HRMS (APCI) calculated for $[M - H]^-$ $C_{14}H_{18}N_2O_2$ 247.1441; found 247.1444.

5-(2-Bromoacetyl)-2-(piperidin-1-yl)benzamide (23). Acetophenone 22 (0.50 g, 2.0 mmol) was dissolved in THF (10 mL). A catalytic amount of 33% HBr in AcOH was added followed by dropwise addition of Br₂ (0.21 mL, 4.1 mmol) in THF (20 mL). The reaction was followed by TLC analysis. After the consumption of the starting material, the precipitate formed was filtered off and washed several times with diethyl ether. White powder. HPLC purity: 99%. Yield: 0.43 mg (65%). ^{1}H NMR(500 MHz, DMSO-d_6) δ ppm 8.05 (d, J = 2.3 Hz, 1H), 7.99−7.84 (m, 2H), 7.59 (s, 1H), 7.13 (d, J = 8.6 Hz, 1H), 4.77 (s, 2H), 3.15−3.05 (m, 4H), 1.70−1.61 (m, 4H), 1.58−1.50 (m, 2H). ^{13}C NMR (126 MHz, DMSO-d_6) δ ppm 190.0, 169.0, 155.0, 131.5, 130.7, 129.3, 126.7, 118.9, 52.8, 33.6, 25.2, 23.0. HRMS (APCI) calculated for $[M + H]^+$ $C_{14}H_{17}BrN_2O_2$ 325.0546; found 325.0543.

175

2-(3-Carbamoyl-4-(piperidin-1-yl)phenyl)-2-oxoethyl 2-amino-4-(pentylcarbamoyl)benzoate (24). Aminoterephthalate 18 (0.70 g, 0.3 mmol) and K_2CO_3 (0.38 g, 0.3 mmol) were suspended in DMF (20 mL). The reaction mixture was stirred for 1 h at 90 °C. It was then allowed to cool down to room temperature, and 2-bromoacetophenone 23 was added. The reaction was stirred for 1 h at room temperature and subsequently poured into the ice-cold aqueous solution of $NaHCO_3$ (10%). The precipitate formed was filtered off, washed with water, and dried under vacuum. Green-yellow powder. HPLC purity: 99%. Yield: 0.11 g (80%). ^1H NMR (500 MHz, DMSO-d_6) δ ppm 8.43 (t, J = 5.7 Hz, 1H), 8.07 (d, J = 1.7 Hz, 1H), 7.99−7.94 (m, 2H), 7.84 (d, J = 8.6 Hz, 1H), 7.60 (s, 1H), 7.24 (d, J = 1.1 Hz, 1H), 7.15 (d, J = 8.6 Hz, 1H), 6.95 (dd, J = 8.4, 1.8 Hz, 1H), 6.76 (s, 1H), 5.62 (s, 2H), 3.26−3.17 (m, 2H), 3.13−3.02 (m, 4H), 1.68−1.63 (m, 4H), 1.59−1.44 (m, 4H), 1.36−1.23 (m, 4H), 0.88 (t, J = 6.9 Hz, 3H). ^{13}C NMR (126 MHz, DMSO-d_6) δ ppm 191.0, 169.0, 166.4, 165.9, 155.0, 151,2, 140.2, 130.9, 130.7, 130.0, 127.5, 125.7, 118.0, 115.9, 112.9, 109.9, 66.3, 52.3, 40.0 (*overlay with solvent*), 28.7 (2C), 25.3, 23.4, 21.9, 13.9. HRMS (APCI) calculated for $[M + H]^+$ $C_{27}H_{34}N_4O_5$ 495.2602; found 495.2604.

2-(3-Carbamoyl-4-(piperidin-1-yl)phenyl)-2-oxoethyl 2-amino-4-(benzylcarbamoyl)benzoate (25). The compound was prepared according to the same procedure as compound 24 with the use of aminoterephthalate 19. Green-yellow powder. HPLC purity: 99%. Yield: 0.79 g (70%). ^1H NMR (500 MHz, DMSO-d_6) δ ppm 9.05−9.01 (m, 1H), 8.07 (d, J = 2.3 Hz, 1H), 7.99−7.91 (m, 2H), 7.87 (d, J = 8.3 Hz, 1H), 7.59 (s, 1H), 7.37−7.27 (m, 5H), 7.27−7.19 (m, 1H), 7.14 (d, J = 8.9 Hz, 1H), 7.01 (dd, J = 8.3, 1.4 Hz, 1H), 6.78 (s, 2H), 5.62 (s, 2H), 4.46 (d, J = 6.0 Hz, 2H), 3.16−3.02 (m, 4H), 1.68−1.63 (m, 4H), 1.59−1.52 (m, 2H). ^{13}C NMR (126 MHz, DMSO-d_6) δ ppm 191.0, 169.0, 166.4, 166.1, 155.1, 151.3, 139.9, 139.6, 131.1, 130.7, 130.0, 128.3, 127.6, 127.2, 126.8, 125.6, 117.9, 116.0, 113.0, 110.0, 66.3, 52.3, 42.6, 25.4, 23.5. HRMS (APCI) calculated for $[M + H]^+$ $C_{29}H_{30}N_4O_5$ 515.2289; found 515.2293.

■ ASSOCIATED CONTENT

Ⓢ Supporting Information

The Supporting Information is available free of charge on the ACS Publications website at DOI: 10.1021/acs.jmedchem.8b00078.

> Materials and methods description, the alignment used for homology modeling, docking studies and calorimetric titration profiles of studied compounds (PDF)
>
> Molecular formula strings (CSV)

■ AUTHOR INFORMATION

Corresponding Authors

*E-mail: jan.hlavac@upol.cz (chemistry).
*E-mail: marian.hajduch@upol.cz (biology).

ORCID Ⓞ

Jan Hlavac: 0000-0002-4652-7751

Author Contributions

▽K.B. and G.R. contributed equally. All the authors contributed to the preparation of the manuscript and have given their approval to the final version of the manuscript.

Notes

The authors declare no competing financial interest.

■ ABBREVIATIONS USED

A549, lung adenocarcinoma; APCI, atmospheric pressure chemical ionization; BJ, normal cycling fibroblasts cell line; CEM-DNR-BULK, daunorubicin resistant CEM cells; CCRF-CEM, acute lymphoblastic leukemia; 4C0S, mammalian translation elongation factor eEF1A2; DCM, dichloromethane; DIC, *N,N*'-diisopropylcarbodiimide; DIEA, *N,N*-diisopropyle-thylamine; DMF, dimethylformamide; EDC, *N*-ethyl-*N*'-(3-(dimethylamino)propyl)carbodiimide hydrochloride; eEF1A1, eukaryotic translation elongation factor 1-α 1; 3-HQ, 2-phenyl-3-hydroxy-4(1*H*)-quinolinone; HOBt, 1-hydroxybenzotriazole hydrate; IC_{50}, half maximal inhibitory concentration; ITC, isothermal titration calorimetry; K562, acute myeloid leukemia; K562-Tax, paclitaxel resistant K562 cells; PDA, photodiode array; PKM2, pyruvate kinase M2; RMS, residual mean square; SDS-PAGE, sodium dodecyl sulfate−polyacrylamide gel electrophoresis; TFA, trifluoroacetic acid; THF, tetrahydrofur-an; UHPLC, ultrahigh performance liquid chromatography

■ REFERENCES

(1) Condeelis, J. Elongation factor 1 alpha, translation and the cytoskeleton. *Trends Biochem. Sci.* 1995, 20, 169−170.

(2) Jeffery, C. J. Moonlighting proteins. *Trends Biochem. Sci.* 1999, 24, 8−11.

(3) Amiri, A.; Noei, F.; Jeganathan, S.; Kulkarni, G.; Pinke, D. E.; Lee, J. M. eEF1A2 activates akt and stimulates akt-dependent actin remodeling, invasion and migration. *Oncogene* 2007, 26, 3027−3040.

(4) Anand, N.; Murthy, S.; Amann, G.; Wernick, M.; Porter, L. A.; Cukier, I. H.; Collins, C.; Gray, J. W.; Diebold, J.; Demetrick, D. J.; Lee, J. M. Protein elongation factor EEF1A2 is a putative oncogene in ovarian cancer. *Nat. Genet.* 2002, 31, 301−305.

(5) Tomlinson, V. A.; Newbery, H. J.; Wray, N. R.; Jackson, J.; Larionov, A.; Miller, W. R.; Dixon, J. M.; Abbott, C. M. Translation elongation factor eEF1A2 is a potential oncoprotein that is overexpressed in two-thirds of breast tumours. *BMC Cancer* 2005, 5, 113.

(6) Lee, J. M. The role of protein elongation factor eEF1A2 in ovarian cancer. *Reprod. Biol. Endocrinol.* 2003, 1, 69.

(7) Neckers, L.; Neckers, K. Heat-shock protein 90 inhibitors as novel cancer chemotherapeutics - an update. *Expert Opin. Emerging Drugs* 2005, 10, 137−149.

(8) Lamberti, A.; Caraglia, M.; Longo, O.; Marra, M.; Abbruzzese, A.; Arcari, P. The translation elongation factor 1A in tumorigenesis, signal transduction and apoptosis: Review article. *Amino Acids* 2004, 26, 443−448.

(9) Duttaroy, A.; Bourbeau, D.; Wang, X. L.; Wang, E. Apoptosis rate can be accelerated or decelerated by overexpression or reduction of the level of elongation factor-1a. *Exp. Cell Res.* 1998, 238, 168−176.

176

(10) Talapatra, S.; Wagner, J. D. O.; Thompson, C. B. Elongation factor-1 alpha is a selective regulator of growth factor withdrawal and ER stress-induced apoptosis. *Cell Death Differ.* **2002**, *9*, 856–861.

(11) Tash, J. S.; Chakrasali, R.; Jakkaraj, S. R.; Hughes, J.; Smith, S. K.; Hornbaker, K.; Heckert, L. L.; Ozturk, S. B.; Hadden, M. K.; Kinzy, T. G.; Blagg, B. S. J.; Georg, G. I. Gamendazole, an orally active indazole carboxylic acid male contraceptive agent, targets HSP90AB1 (HSP90BETA) and EEF1A1 (eEF1A), and stimulates Il1a transcription in rat sertoli cells. *Biol. Reprod.* **2008**, *78*, 1139–1152.

(12) Hashimoto, K.; Ishima, T. Neurite outgrowth mediated by translation elongation factor eEF1A1: a target for antiplatelet agent cilostazol. *PLoS One* **2011**, *6*, e17431.

(13) Van Goietsenoven, G.; Hutton, J.; Becker, J. P.; Lallemand, B.; Robert, F.; Lefranc, F.; Pirker, C.; Vandenbussche, G.; Van Antwerpen, P.; Evidente, A.; Berger, W.; Prevost, M.; Pelletier, J.; Kiss, R.; Goss Kinzy, T.; Kornienko, A.; Mathieu, V. Targeting of eEF1A with Amaryllidaceae isocarbostyrils as a strategy to combat melanomas. *FASEB J.* **2010**, *24*, 4575–4584.

(14) Yao, N.; Chen, C. Y.; Wu, C. Y.; Motonishi, K.; Kung, H. J.; Lam, K. S. Novel flavonoids with antiproliferative activities against breast cancer cells. *J. Med. Chem.* **2011**, *54*, 4339–4349.

(15) Funk, P.; Motyka, K.; Dzubak, P.; Znojek, P.; Gurska, S.; Kusz, J.; McMaster, C.; Hajduch, M.; Soural, M. Preparation of 2-phenyl-3-hydroxyquinoline-4(1H)-one-5-carboxamides as potential anticancer and fluorescence agents. *RSC Adv.* **2015**, *5*, 48861–48867.

(16) Hradil, P.; Hlavac, J.; Soural, M.; Hajduch, M.; Kolar, M.; Vecerova, R. 3-Hydroxy-2-phenyl-4(1H)-quinolinones as promising biologically active compounds. *Mini-Rev. Med. Chem.* **2009**, *9*, 696–702.

(17) Soural, M.; Hlavac, J.; Hradil, P.; Hajduch, M. Efficient Synthesis and cytotoxic activity of some symmetrical disulfides derived from the quinolin-4(1H)-one skeleton. *Eur. J. Org. Chem.* **2009**, *2009*, 3867–3870.

(18) Soural, M.; Hlavac, J.; Hradil, P.; Frysova, I.; Hajduch, M.; Bertolasi, V.; Malon, M. Synthesis and cytotoxic activity of substituted 2-phenyl-3-hydroxy-4(1H)-quinolinones-7-carboxylic acids and their phenacyl esters. *Eur. J. Med. Chem.* **2006**, *41*, 467–474.

(19) Krejci, P.; Hradil, P.; Hlavac, J.; Hajduch, M. Preparation of 2-Phenyl-3-Hydroxyquinolin-4(1H)-ones for Treatment of Immune System and Proliferative Disorders. WO2008028427A1, 2008.

(20) Brands, J. H. G. M.; Maassen, J. A.; Hemert, F. J.; Amons, R.; Moeller, W. The primary structure of the alpha subunit of human elongation factor 1. Structural aspects of guanine nucleotide-binding sites. *Eur. J. Biochem.* **1986**, *155*, 167–171.

(21) Andersen, G. R.; Valente, L.; Pedersen, L.; Kinzy, T. G.; Nyborg, J. Crystal structures of nucleotide exchange intermediates in the eEF1a-eEF1Balpha complex. *Nat. Struct. Biol.* **2001**, *8*, 531–534.

(22) Andersen, G. R.; Pedersen, L.; Valente, L.; Chatterjee, I.; Kinzy, T. G.; Kjeldgaard, M.; Nyborg, J. Structural basis for nucleotide exchange and competition with tRNA in the yeast elongation factor complex eEF1A:eEF1Balpha. *Mol. Cell* **2000**, *6*, 1261–1266.

(23) Pittman, Y. R.; Valente, L.; Jeppesen, M. G.; Andersen, G. R.; Patel, S.; Kinzy, T. G. Mg^{2+} and a key lysine modulate exchange activity of eukaryotic translation elongation factor 1B alpha. *J. Biol. Chem.* **2006**, *281*, 19457–19468.

(24) Dai, S.; Crawford, F.; Marrack, P.; Kappler, J. W. The structure of HLA-DR52c: comparison to other HLA-DRB3 alleles. *Proc. Natl. Acad. Sci. U. S. A.* **2008**, *105*, 11893–11897.

(25) Crepin, T.; Shalak, V. F.; Yaremchuk, A. D.; Vlasenko, D. O.; McCarthy, A.; Negrutskii, B. S.; Tukalo, M. A.; El'skaya, A. V. Mammalian translation elongation factor eEF1A2: X-ray structure and new features of GDP/GTP exchange mechanism in higher eukaryotes. *Nucleic Acids Res.* **2014**, *42*, 12939–12948.

(26) Nissen, P.; Kjeldgaard, M.; Thirup, S.; Clark, B. F. C.; Nyborg, J. The ternary complex of aminoacylated tRNA and EF-Tu-GTP. Recognition of a bond and a fold. *Biochimie* **1996**, *78*, 921–933.

(27) Nissen, P.; Kjeldgaard, M.; Thirup, S.; Polekhina, G.; Reshetnikova, L.; Clark, B. F. C.; Nyborg, J. Crystal structure of the ternary complex of Phe-tRNAPhe, EF-Tu, and a GTP analog. *Science* **1995**, *270*, 1464–1472.

(28) Bayer, E. A.; Wilchek, M. The Use of the Avidin-Biotin Complex as a Tool in Molecular Biology. In *Methods of Biochemical Analysis*; Glick, D., Ed.; John Wiley & Sons, Inc.: New York, 1980; pp 1–45.

(29) Krupkova, S.; Soural, M.; Hlavac, J.; Hradil, P. Solid-phase synthesis of 3-hydroxy-6-nitroquinolin-4(1H)-ones with two diversity positions. *J. Comb. Chem.* **2009**, *11*, 951–955.

(30) Hradil, P.; Jirman, J. Synthesis of 2-aryl-3-hydroxyquinolin-4(1H)-ones. *Collect. Czech. Chem. Commun.* **1995**, *60*, 1357–1366.

(31) Hradil, P.; Kvapil, L.; Hlavac, J.; Weidlich, T.; Lycka, A.; Lemr, K. Preparation of 2-phenyl-2-hydroxymethyl-4-oxo-1,2,3,4-tetrahydroquinazoline and 2-methyl-4-oxo-3,4-dihydroquinazoline derivatives. *J. Heterocycl. Chem.* **2000**, *37*, 831–837.

(32) Dasari, P.; Reddy, A. V.; Bhoomireddy, R.; ChVSL, K.; Bethi, M. Development and validation of stability indicating RP-HPLC method for the determination of impurity profile in gamendazole: experimental male oral contraceptive. *J. Liq. Chromatogr. Relat. Technol.* **2015**, *38*, 1303–1314.

(33) Soural, M.; Krchnak, V. Efficient solid-phase synthesis of 2-substituted-3-hydroxy-4(1H)-quinolinone-7-carboxamides with two diversity positions. *J. Comb. Chem.* **2007**, *9*, 793–796.

(34) Soural, M.; Hlavac, J.; Hradil, P. Efficient Process for Biotinylation of Polymer Supports through Oligoethylene Glycol Linkers for Affinity Chromatography and Solid-Phase Synthesis of Biotin-Substituted Carboxamides. CZ302510B6, 2011.

(35) Subramanyam, C.; Duplantier, A. J.; Dombroski, M. A.; Chang, S. P.; Gabel, C. A.; Whitney-Pickett, C.; Perregaux, D. G.; Labasi, J. M.; Yoon, K.; Shepard, R. M.; Fisher, M. Discovery, synthesis and SAR of azinyl- and azolylbenzamides antagonists of the P2 × 7 receptor. *Bioorg. Med. Chem. Lett.* **2011**, *21*, 5475–5479.

2.6 Appendix C

PERLÍKOVÁ P, **RYLOVÁ G**, NAUŠ P, ELBERT T, TLOUŠŤOVÁ E, BOURDERIOUX A, SLAVĚTÍNSKÁ LP, MOTYKA K, DOLEŽAL D, ZNOJEK P, NOVÁ A, HARVANOVÁ M, DŽUBÁK P, ŠILLER M, HLAVÁČ J, HAJDÚCH M, HOCEK M. 7-(2-Thienyl) 7-Deazaadenosine (AB61), a New Potent Nucleoside Cytostatic with a Complex Mode of Action. *Mol. Cancer Ther.* **15,** 922–937 (2016). PMID: 26819331

Molecular
Cancer
Therapeutics

Small Molecule Therapeutics

7-(2-Thienyl)-7-Deazaadenosine (AB61), a New Potent Nucleoside Cytostatic with a Complex Mode of Action

Pavla Perlíková[1], Gabriela Rylová[2], Petr Nauš[1], Tomáš Elbert[1], Eva Tloušťová[1], Aurelie Bourderioux[1], Lenka Poštová Slavětínská[1], Kamil Motyka[3], Dalibor Doležal[2], Pawel Znojek[2], Alice Nová[2], Monika Harvanová[2], Petr Džubák[2], Michal Šiller[2], Jan Hlaváč[2,3], Marián Hajdúch[2], and Michal Hocek[1,4]

Abstract

7-(2-Thienyl)-7-deazaadenosine (AB61) showed nanomolar cytotoxic activities against various cancer cell lines but only mild (micromolar) activities against normal fibroblasts. The selectivity of AB61 was found to be due to inefficient phosphorylation of AB61 in normal fibroblasts. The phosphorylation of AB61 in the leukemic CCRF-CEM cell line proceeds well and it was shown that AB61 is incorporated into both DNA and RNA, preferentially as a ribonucleotide. It was further confirmed that a triphosphate of AB61 is a substrate for both RNA and DNA polymerases in enzymatic assays. Gene expression analysis suggests that AB61 affects DNA damage pathways and

protein translation/folding machinery. Indeed, formation of large 53BP1 foci was observed in nuclei of AB61-treated U2OS-GFP-53BP1 cells indicating DNA damage. Random incorporation of AB61 into RNA blocked its translation in an in vitro assay and reduction of reporter protein expression was also observed in mice after 4-hour treatment with AB61. AB61 also significantly reduced tumor volume in mice bearing SK-OV-3, BT-549, and HT-29 xenografts. The results indicate that AB61 is a promising compound with unique mechanism of action and deserves further development as an anticancer agent.
Mol Cancer Ther; 15(5); 922–37. ©2016 AACR.

Introduction

7-Deazapurine (IUPAC name: pyrrolo[2,3-d]pyrimidine) nucleosides have become a subject of research interest because of their powerful antibacterial, antifungal, and cytotoxic activities (1). Mechanisms of action of naturally occurring 7-deazapurine nucleosides tubercidin, toyocamycin, and sangivamycin (Fig. 1) have been extensively studied. Despite structural similarities, their biochemical and biologic properties show different features for each nucleoside. Tubercidin, toyocamycin, and sangivamycin are

all phosphorylated in cells to their $5'$-O-mono-, di-, and triphosphates which are subsequently incorporated into nucleic acids (2–4). In addition, tubercidin also inhibits nucleic acid and protein synthesis, interferes with mitochondrial respiration, rRNA processing, de novo purine synthesis (2), and it is a potent inhibitor of S-adenosylhomocysteine hydrolase (5). Toyocamycin showed inhibition of phosphatidylinositol kinase (6) and an inhibitory effect on rRNA synthesis and maturation (7, 8). On the other hand, sangivamycin acts mainly through potent and selective inhibition of protein kinase C (9).

In our previous research, nanomolar cytotoxic activities of hetaryl-7-deazapurine ribonucleosides were discovered. 6-Hetaryl-7-deazapurine ribonucleosides 1 showed strong cytotoxicity against a panel of cancer cell lines similar to that of conventional nucleoside cytostatics (gemcitabine, clofarabine; ref. 10). Similarly profound cytotoxic effects were also found in 7-hetaryl-7-deazaadenosines, that is, 7-hetaryltubercidins 2 (11). Structure–activity relationship studies revealed that modifications in the $2'$ position of the ribose moiety lead to a decrease of cytotoxicity in 7-hetaryl-7-deazapurine ribonucleosides 2 (12, 13) and completely inactive compounds in 6-hetaryl-7-deazapurine ribonucleosides 1 (14, 15). In contrast, base-modified 7-hetaryl derivatives bearing modifications in positions 2 and 6 of 7-deazapurine showed submicromolar cytotoxic activities (16). The most promising derivative among the 7-hetaryl-7-adenosines is a 2-thienyl derivative AB61 (Fig. 1), which is not only highly cytotoxic against leukemic and solid tumor–derived cell lines but also noncytotoxic to normal human fibroblasts (11). In vivo antitumor activity of AB61 was demonstrated in a mouse leukemia survival model. The preliminary studies of its mechanism of

[1]Institute of Organic Chemistry and Biochemistry, Academy of Sciences of the Czech Republic, Gilead Sciences & IOCB Research Center, Prague, Czech Republic. [2]Institute of Molecular and Translational Medicine, Faculty of Medicine and Dentistry, Palacky University and University Hospital in Olomouc, Olomouc, Czech Republic. [3]Department of Organic Chemistry, Faculty of Natural Sciences, Palacky University, Olomouc, Czech Republic. [4]Department of Organic Chemistry, Faculty of Science, Charles University in Prague, Prague, Czech Republic.

AACR

Figure 1.
Structures of 7-deazapurine nucleosides.

Tubercidin, R = H
Toyocamycin, R = CN
Sangivamycin, R = CONH$_2$
2, R = hetaryl

1

AB61, R = 2-thienyl
PNH404, R = ethynyl
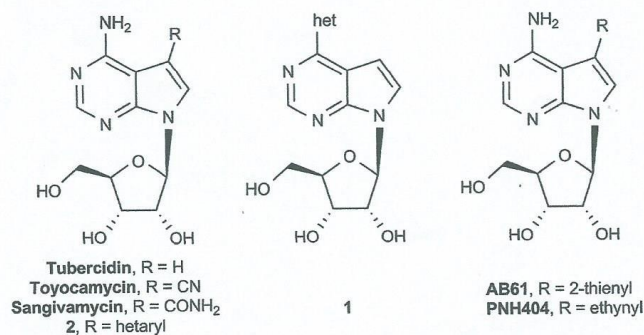
action in CCRF-CEM lymphoblasts showed fast onset of the RNA synthesis inhibition and also inhibition of DNA synthesis at higher concentrations. AB61 is efficiently phosphorylated to its 5'-O-triphosphate (AB61-TP) but only very mild inhibition of RNA polymerase II by AB61-TP was observed (11). More recently, AB61 and its related derivatives were found (17) to be weak inhibitors of human adenosine kinase and AB61 itself was found to be a weak substrate for this enzyme (2%) as compared with adenosine.

The aims of this study were to elucidate the detailed mechanism of action of AB61 and understand why its cytotoxicity is selective for cancer cell lines. We hypothesized that AB61-TP may get incorporated into nucleic acids that have impaired biologic functions. Therefore, the first goal was to investigate phosphorylation of AB61 in normal and cancer-derived cell lines, incorporation of AB61 into nucleic acids both on enzymatic and cellular levels, and the effect of AB61 on gene transcription, translation, and DNA integrity. Furthermore, we have studied the *in vivo* antitumor activity of AB61 against xenotransplanted human solid tumors to translate promising *in vitro* data into preclinical efficacy.

Materials and Methods

Analytical standards

Synthesis and characterization data of analytical standards AB61-DP, dAB61-MP, [^{3}H]AB61 and tubercidin triphosphate (Tub-TP) are given in the Supplementary Data. Synthesis of AB61, AB61-MP and AB61-TP was published previously (11).

Cell lines

The CCRF-CEM (ATCC CCL-119), HCT116 (ATCC CCL-247), K-562 (ATCC CCL-243), BJ (ATCC CRL-2522), MRC-5 (ATCC CC-171), HT-29 (ATCC HTB-38), SK-OV-3 (ATCC HTB-77), U2OS (ATCC HTB-96), and BT-549 (ATCC HTB-122) cell lines were purchased from the American Tissue Culture Collection (ATCC) in 2010–2014. HCT116p53$^{-/-}$ cell line was purchased from Horizon Discovery in 2011. The daunorubicin-resistant subline of CCRF-CEM cells (CEM-DNR-bulk) and paclitaxel-resistant subline K-562-tax overexpressing major drug resistance transporters were selected in our laboratory (18, 19). Mouse breast cancer 4T1-luc2 cell line stably transfected with firefly luciferase under cytomegalovirus promoter was a kind gift from Prof. Danuta Radzioch (McGill University, Montreal, Canada) in

2009. Cell line derived from human osteosarcoma U2OS stably transfected with 53BP1-GFP fusion gene (U2OS-53BP1-GFP) was prepared by Lipofectamine transfection of 53BP1 plasmid (ref. 20; a kind gift from Prof. Jiri Bartek, Danish Cancer Society Research Center, Copenhagen, Denmark) into parental cells and successful transfectants were selected by neomycin. Cell line authentication was performed using the Promega CELL ID TM System (8 STR markers + amelogenin) to verify that the genetic profile of the sample matches the known profile of the cell line. Mycoplasma contamination was tested using 1-My and 2-My primers by qPCR (21) for every batch of the frozen cells. The cell lines were cultured for maximum of 6 to 10 passages and tested for mycoplasma contamination on a weekly basis.

Oligonucleotides

DNA oligonucleotides were purchased from Sigma-Aldrich and Generi Biotech. ON1: 5'-GC*TAATACGACTCACTATA*GGTGAGG-TAC*TT*GTAGTGATT (T7 promoter in italics); ON2: 5'-A̲A̲TCAC-TACAAGTACCTCACCTATAGTGAGTCGTATTAGC (underlined nucleotides represent 2'-O-Me-RNA); Prim248short: 5'-CATG-GGCGGCATGGG; Prb4basII: 5'-CTAGCATGAGCTCAGTCCCAT-GCCGCCCATG; OligoA^{term}: 5'—TCCCATGCCGCCCATG; (bio)-OligoA^{term}: 5'-biotin-TCCCATGCCGCCCATG.

MTT assay

The cells were maintained in Nunc/Corning 80 cm^2 plastic tissue culture flasks and cultured in cell culture medium (DMEM/RPMI1640 with 5 g/L glucose, 2 mmol/L glutamine, 100 U/mL penicillin, 100 µg/mL streptomycin, 10% fetal calf serum, and NaHCO$_3$). Cell suspensions were prepared and diluted according to the particular cell type and the expected target cell density (25,000–30,000 cells/well based on cell growth characteristics). MTT assay was performed as described before and the IC$_{50}$ value, the drug concentration lethal to 50% of the cells, was calculated from appropriate dose–response curves (18).

Intracellular phosphorylation

HCT116 and BJ cells were seeded into 6-well plates at 60% confluence (McCoy 5A and DMEM, respectively, supplemented with 5 g/L glucose, 2 mmol/L glutamine, 100 U/mL penicillin, 100 µg/mL streptomycin, 10% fetal calf serum, and NaHCO$_3$). Next day, cells were treated with AB61 (10 µmol/L). After 3-hour

180

incubation, cultures were washed 2 times with PBS containing 0.5% FBS and 3 times with PBS. The cell pellets were extracted with 70% cold MeOH (1 mL). Supernatants were collected, dried under vacuum, and samples were resuspended in DMSO-water (1:1, 100 μL) for analysis. The samples were analyzed using ultra-performance reversed phase chromatography coupled to triple tandem mass spectrometry UPLC-MS/MS. The UPLC chromatograph used in this study was Accela Thermo Scientific system consisting of gradient quaternary pump, thermostated autosampler, degasser, column oven and triple quadrupole mass spectrometer TSQ Quantum Access (Thermo Scientific). Xcalibur data system software was used for an instrument control and data analysis. The C18 column (XBridge BEH C18, 2.5 μm, 2.1 × 50 mm) and ammonium acetate (pH 5.04)/acetonitrile gradient elution were applied for chromatographic separation. The electrospray ionization and negative selected reaction mode MS/MS were used for analyte quantification. Standard curves and quality control samples were generated for all analytes using extracts from untreated cells.

Incorporation of modified nucleoside triphosphates into RNA in vitro

A solution of template oligonucleotides ON1 and ON2 (50 μmol/L each) in annealing buffer [Tris (10 mmol/L), NaCl (50 mmol/L), EDTA (1 mmol/L), pH 7.8] was heated to 95°C for 5 minutes and then slowly cooled to 25 °C over a period of 45 minutes. The resulting dsDNA (50 μmol/L) was used as a template for transcription reactions. In vitro transcription reactions (10 μL; ApliScribe T7-Flash Transcription Kit, Epicentre) were performed in the presence of AB61-TP or Tub-TP (0.45 mmol/L, for synthesis see supporting information), CTP, GTP, UTP (4.5 mmol/L each), DTT (10 mmol/L), ApliScribe T7-Flash 10× Reaction Buffer (2 μL), template (2.5 μmol/L), [α-^{32}P]GTP (111 TBq/mmol, 370 MBq/mL, 0.4 μL), and ApliScribe T7-Flash enzyme solution (2 μL). In the negative control experiment, water was used instead of the solution of the tested compound, and in the positive control experiment, ATP (0.45 mmol/L) was used instead of the tested compound. The transcription reactions were performed at 37°C for 2 hours. RNA was purified on NucAway Spin Columns (Ambion, elution in DEPC-water). Samples (2 μL) were mixed with RNA loading dye (Fermentas; 2 μL), denatured at 90 °C for 10 minutes and cooled on ice. The samples were analyzed by gel electrophoresis on 12.5% denaturing polyacrylamide gel containing 1× TBE buffer (pH 8) and urea (7 mol/L) at 45 mA for 45 minutes. The gels were dried (85°C, 75 minutes), audioradiographed, and visualized by phosphorimager (Typhoon 9410, Amersham Biosciences).

Incorporation of modified nucleoside triphosphates into DNA by DNA polymerases

The primer extension experiments were performed under following conditions: Klenow fragment: the reaction mixture (20 μL) contained DNA polymerase I, large (Klenow) fragment (New England BioLabs, 5 U/μL, 0.04 μL), natural dNTPs (10 mmol/L, 0.4 μL), AB61-TP or Tub-TP (10 mmol/L, 1 μL), primer Prim248short (3 μmol/L, 1 μL), 31-mer template Prb4ba-sII (3 μmol/L, 1 μL), and NEBuffer 2 (2 μL) supplied by the manufacturer. Prim248short was labeled by the use of [γ-^{32}P]ATP according to standard techniques. In the positive and negative control experiments, dATP (10 mmol/L, 1 μL) and water, respectively, were used instead of the tested compound. The reaction mixtures were incubated for 15 minutes at 25°C. Human DNA polymerase β: Primer Prim248short was labeled by the use of [γ-^{32}P]ATP and annealed with template Oligo^{Aterm} (primer:template ratio 1:1.5) according to the standard techniques. The reaction mixture (10 μL) contained human DNA polymerase β (CHIMERx, 5 U/μL, 0.01 μL), AB61-TP (1 mmol/L, 1 μL), primer:template mixture (1 μmol/L primer, 1.5 μmol/L template; 1 μL), BSA (acetylated, 24 mg/mL, 0.167 μL), and glycerol (1.5 μL) and 10× buffer for DNA polymerase β (1 μL) supplied by the manufacturer. In the positive and negative control experiments, dATP and water, respectively, were used instead of AB61-TP. The reaction mixtures were incubated for 3 hours at 37°C. Human DNA polymerase γ: Primer Prim248short was labeled by the use of [γ-^{32}P]ATP and annealed with template Oligo^{Aterm} (primer:template ratio 1:1.5) according to the standard techniques. The reaction mixture (10 μL) contained human DNA polymerase γ (CHIMERx, 10 U/μL, 0.05 μL), AB61-TP (1 mmol/L, 1 μL), primer:template mixture (1 μmol/L primer, 1.5 μmol/L template; 1 μL), BSA (acetylated, 24 mg/mL, 0.25 μL), and 10× MnCl₂ solution (1 μL) supplied by the manufacturer and 10× buffer for DNA polymerase γ (1 μL) supplied by the manufacturer. In the positive and negative control experiments, dATP and water, respectively, were used instead of AB61-TP. The reaction mixtures were incubated for 3 hours at 37°C. The reactions were stopped by addition of the same volume of PAGE stop solution [80% (v/v) formamide, 20 mmol/L EDTA, 0.025% (w/v) bromophenol blue, 0.025% (w/v) xylene cyanol] and heated to 95°C for 5 minutes. Aliquots (2 μL) were analyzed by gel electrophoresis on 12.5% denaturing polyacrylamide gel containing 1× TBE buffer (pH 8) and urea (7 M) at 45 mA for 50 minutes. The gels were dried (85°C, 75 minutes), audioradiographed, and visualized by phosphorimager (Typhoon 9410, Amersham Biosciences). The incorporation of AB61-TP into DNA oligonucleotide was confirmed by MALDI-TOF analysis (see Supplementary information Fig. S1).

Incorporation of [^{3}H]AB61 into RNA or DNA in cells

CCRF-CEM cells (ATCC: CCL-119) were grown in RPMI1640 medium (Sigma) supplemented with 10% fetal calf serum, GlutaMAX (Gibco, 10 mL/L), penicillin (100 U/L), and streptomycin (100 mg/L). All experiments were done with exponentially growing cells. CCRF-CEM cells (7 × 10⁵ cells/mL, 10 mL) were incubated overnight in a humidified CO₂ incubator at 37°C. Solution of [^{3}H]AB61 (for synthesis, see Supplementary Information "Synthesis of nucleosides and nucleotides") in water (29 μL, 1 mCi/mL, 11.6 Ci/mmol) was added. The final concentration of [^{3}H]AB61 was 250 nmol/L. Samples of the cell suspension (1.5 mL) were harvested immediately after the addition of [^{3}H]AB61 or after incubation at 37°C (2.5 hours). Cells were washed twice with PBS and then either RNA was isolated using miRNeasy Mini Kit (Qiagen) according to manufacturer's protocol or DNA was isolated using using Dneasy Blood & Tissue Kit (Qiagen) according to manufacturer's protocol including RNA digestion with RNase A. Concentrations of RNA and DNA samples were measured by NanoDrop 1000 Spectrophotometer. Activity of the RNA (40 μL) or DNA (180 μL) was measured in AquaSafe 500 Plus LSC cocktail (4 mL) on a Liquid Scintillation Analyzer Tri-Carb 2900TR (Perkin Elmer).

RNA digestion and HPLC-LSC analysis. RNA was isolated from the CCRF-CEM cells treated by [^{3}H]AB61 (250 nmol/L) for 2.5 hours as described above. RNA (150 μL, 240 ng/μL) was digested by Nuclease P1 from *Penicillium citrinum* (Sigma, 1 mg/mL, 1 μL) in a

181

digestion buffer (80 mmol/L Tris-HCl; 10 mmol/L NaCl; 1 mmol/L MgCl$_2$; 0.2 mmol/L ZnCl$_2$, pH 5.3). Final volume was 167.7 µL. Digestion was performed at 50°C for 1 hour. Then, ice-cold aqueous solution TCA (10% v/v, 167.7 µL) was added and samples were cooled on ice for 10 minutes. After centrifugation (14,000 × g, 5 minutes, 4°C) supernatant was transferred into a clear microtube. The supernatant was extracted with 1,1,2-tri-chlorotrifluoroethane-trioctylamine mixture (4:1, 335.4 µL) at 4°C. The aqueous phase was evaporated using a vacuum concentrator and dissolved in water (90 µL). The sample (50 µL) was analyzed on Waters high-performance liquid chromatography (HPLC) system (2996 PDA detector, 616 HPLC pump, 600S controller, PDA software Empower) with a Supelcosil LC-18-T 3 µm column (15 cm × 3 mm) with a flow rate of 0.75 mL/min. Solution A (50 mmol/L KH$_2$PO$_4$, 3 mmol/L tetrabutylammonium hydrogensulfate, pH 3.1) and solution B [50 mmol/L KH$_2$PO$_4$, 3 mmol/L tetrabutylammonium hydrogensulfate, pH 3.1, acetonitrile (50% v/v)] were used as a mobile phase. Elution gradient: 0–5 minutes: solution A; 5–6 minutes: linear gradient 0%–5% of solution B in solution A; 6–30 minutes: linear gradient 5%–100% of solution B in solution A. Fractions were collected for 15 seconds each. Activity of the fractions was measured in AquaSafe 500 Plus LSC cocktail on a Liquid Scintillation Analyzer Tri-Carb 2900TR (Perkin Elmer). Nucleotides eluted at the following retention times: t = 3.3 minutes (CMP), 8.6 minutes (AMP), 10.8 minutes (UMP), 11.3 minutes (GMP), 13.4 minutes (AB61), and 13.6 minutes (AB61-MP).

DNA digestion and HPLC-LSC analysis. DNA was isolated from the CCRF-CEM cells treated by [^{3}H]AB61 (250 nmol/L) for 2.5 hours as described above. DNA (80 µL, 500 ng/µL) was denatured at 100°C for 10 minutes and cooled on ice. DNA was digested by Nuclease P1 from *Penicillium citrinum* (Sigma, 1 mg/mL, 10 µL) in 10× digestion buffer (15 µL; 800 mmol/L Tris-HCl, pH 5.3; 100 mmol/L NaCl; 10 mmol/L MgCl$_2$; 2 mmol/L ZnCl$_2$). Final volume was 150 µL. Digestion was performed at 50°C for 16 hours. Then, ice-cold aqueous TCA solution (10% v/v, 150 µL) was added. Samples were cooled on ice for 10 minutes. After centrifugation (14,000 × g, 5 minutes, 4°C), supernatant was transferred into a clear microtube. The solution was extracted with 1,1,2-trichlorotrifluoroethane-trioctylamine mixture (4:1, 300 µL) at 4 °C. The aqueous phase was evaporated under reduced pressure and dissolved in water (150 µL). The sample (50 µL) was analyzed on Waters HPLC system as described for HPLC analysis after RNA digestion. Nucleotides eluted at the following retention times: t = 4.2 minutes (dCMP), 11.2 minutes (dAMP), 12.3 minutes (dGMP), 13.1 minutes (dTMP), 13.8 minutes (AB61-MP), and 14.8 minutes (dAB61-MP). (For synthesis of dAB61-MP, see Supplementary Information "Synthesis of nucleosides and nucleotides").

Authentication of AB61 metabolites incorporated into RNA and DNA. RNA and DNA were isolated from the CCRF-CEM cells treated by AB61 (250 nmol/L) for 2.5 hours and digested by Nuclease P1 as described above. To detect individual AB61 metabolites in digested samples of DNA or RNA, respectively, individual samples were subjected to liquid chromatography/mass spectrometry (LC/MS) analysis using chromatograph Ultimate 3000 (Dionex) connected to mass spectrometer QTrap 5500 (AB Sciex). LC conditions were defined as: C18 column (Kinetex 2.6 µ, 100 × 3, Phenomenex), flow rate 400 µL/minute,

column oven temperature: 30°C; separation was performed in a gradient mode of mobile phase A (10 mmol/L ammonium acetate, pH = 5.02) and B phase (100% acetonitrile): 0 minutes B 10%, 4 minutes 50% B, 4.4 minutes 50% B, 4.6 minutes 10% B, 6 minutes 10% B. Mass spectrometric analysis was performed in positive ESI mode with following conditions: G1 gas 60 psi, G2 gas 60 psi, ion source temperature 600°C, curtain gas 20 psi, ionization voltage 5.5 kV. MRM mode was used for detection and quantification of AB61 metabolites. For AB61-MP MRM transition 451-330.9 and for dAB61-MP 435-81 were applied. Estimated concentrations of individual compounds were expressed in fmoles per 1 µg of DNA and RNA, respectively.

Metabolic labeling of nucleic acids by AB61 analogue PNH404 (incorporation, click-staining, and effect of inhibition of replicative polymerases)

U2OS cells were incubated on coverslips overnight in McCoy medium (with 10% FCSI, 1.5% of L-glutamine, 100 µg/mL streptomycin, and 100 U/mL of penicillin) at 37°C and 5% CO$_2$. The next day, cells were pretreated with medium or inhibitor of replicative DNA polymerases aphidicolin (ref. 22; 10 µmol/L) for 1 hour. Afterwards, cells were pulsed with 10 µmol/L of PNH404 (11) or medium for 3 hours. Coverslips with cells were washed in PBS, fixed in 4% formaldehyde, and permeabilized in 0.25% Triton X-100 in PBS for 15 minutes. Incorporated PNH404 was visualized via click chemistry using Click-iT Cell Reaction Buffer Kit (Thermo Fischer Scientific, cat.: C10269) and Azide-Fluor 568 fluorescent dye (Jena Bioscience, cat.: CLK-AZ106-5) as recommended by manufacturer. Nuclear DNA was counterstained with Hoechst 33342. Red fluorescence of incorporated PNH404 coupled to Azide-Fluor 568 and blue counterstained DNA were analyzed using confocal microscopy (Cell Observer SD, Zeiss).

In vitro transcription of EGFP-luciferase DNA template

To evaluate functionality of RNA with incorporated AB61-TP or Tub-TP, we first PCR-amplified template DNA coding EGFP-luciferase under T7 promoter. (See Supplementary Information "PCR amplification of EGFP-luciferase template for T7 polymerase transcription"). MEGAscript T7 kit (Ambion) was used for *in vitro* transcription of EGFP-luciferase template in the presence of hetaryl-7-deazapurine ribonucleoside triphosphates. *In vitro* transcription reactions were performed according to manufacturer's protocol. Each transcription reaction (20 µL) contained of EGFP-luciferase DNA template (2751 bp, 100 ng), ATP, GTP, CTP, and UTP (7.5 mmol/L each), enzyme mix (2 µL), and AB61-TP or Tub-TP (final concentration: 1 mmol/L). In the control experiment, water was used instead of the solution of the tested compound. The transcription reactions were performed at 37°C for 2 hours. Then, DNase I (2 U/µL, 1 µL) was added and the mixtures were incubated at 37°C for 15 minutes. RNA transcripts were purified on NucAway Spin Columns (Ambion). The quantity and purity of RNA transcripts was determined on Agilent 2100 Bioanalyzer (RNA 600 Nano Total RNA kit, Agilent) and by NanoDrop 1000 Spectrophotometer.

In vitro translation efficacy of EGFP-luciferase RNA transcripts with incorporated AB61-TP or Tub-TP

The EGFP-luciferase RNA transcripts with or without incorporated AB61-TP or Tub-TP were used as templates for *in vitro* translation using reticulocyte lysate system (Retic Lysate IVT Kit, Ambion) according to the manufacturer's protocol. The *in vitro*

182

Perlíková et al.

translation mixture (25 μL) contained EGFP-luciferase RNA transcript (500 ng), low salt mix-met (1 μL), high salt mix-met (0.25 μL), methionine (0.83 mmol/L, 1.5 μL), and the reticulocyte lysate (17 μL). In the positive control experiment, unmodified EGFP-luciferase RNA transcript was used, in the negative control experiment no RNA template was added. The translation reactions were incubated in water bath at 30°C for 1.5 hours. Efficacy of *in vitro* translation was evaluated via measurement of luciferase enzymatic activity (Luciferase Assay System, Promega) on EnVision Multilabel Reader (PerkinElmer) and by Western blot analysis using primary goat anti-Luciferase antibody (1:1,000, Promega) and secondary peroxidase-conjugated rabbit anti-goat IgG (1:10,000, Sigma-Aldrich). Blot was visualized by chemiluminescence (ECL Western Blotting Detection Reagent, Amersham).

Gene expression analysis

CCRF-CEM cells (1×10^6 cells/mL, 3 mL) were incubated for 3 hours in a humidified CO_2 incubator at 37°C with or without one of the following compounds at equitoxic concentrations: AB61 (250 nmol/L), Tub (550 nmol/L), or actinomycin D (1 nmol/L). Total RNA was purified from treated cell lines using TRI Reagent (Molecular Research Centre) according to the manufacturer's instructions. The concentration and purity of RNA was assessed by Nanodrop ND 1000 (ThermoScientific). RNA quality was measured using Agilent RNA 6000 Nano Kit (Agilent Technologies). Microarray analysis using the GeneChip Human Exon 1.0 ST Array and GeneChip Scanner 3000 7G (Affymetrix) was performed. The data were analyzed using R/Bioconductor freeware and additional Bioconductor packages. All arrays were preprocessed by RMA method (robust multi-array average) on the gene level using the oligo package. The processed gene expression levels were analyzed for their differential expression between the AB61-treated and control cells. Initially, the raw P values of moderated t test were calculated by the limma package, and the data were cut at $P = 0.01$ significance level which passed 732 genes. Genetic pathways and processes were evaluated using the MetaCore Analytical Suite v. 6.18 (GeneGo, Thomson Reuters). Enrichment analysis consisted of mapping gene IDs of the dataset onto IDs in entities of built-in functional ontologies represented in MetaCore by pathway maps and networks prioritized according to their statistical significance. The data discussed in this publication have been deposited in NCBI's Gene Expression Omnibus (23) and are accessible through GEO Series accession number GSE62593 (http://www.ncbi.nlm.nih.gov/geo/query/acc.cgi?acc=GSE62593).

DNA damage

A sensoric cell line derived from human osteosarcoma U2OS stable transfected with 53BP1-GFP fusion gene (U2OS-53BP1-GFP) was used to visualize DNA damage foci in the nucleus of treated/control cells. U2OS-53BP1 cells were grown in McCoy medium supplemented with 10% FBS and 100 U/mL penicillin/streptomycin at 37°C and 5% CO_2. Cells were plated in density 10^5 cells per well into a 96-well microplate in final volume of 150 μL. Following 24-hour incubation, etoposide, irinotecan, and AB61 were added to wells in final concentration of 1 μmol/L. After drug was added, cultivation of cells was continued in Operetta automated microscope (PerkinElmer) equipped with an incubation chamber. Using Operetta imaging system, 21 fields were acquired from each well with conditions of 475 nm excitation and 525 nm emission main wavelength, 40× objectives, and 200 ms

exposure time. Images of cells were taken with the time-lapse fluorescence at 1-hour intervals for 12 hours. Number of 53BP1 foci was quantified using Columbus 2.4 imaging analysis system (PerkinElmer).

The validation of the DNA damage effects demonstrated using 53BP1-GFP sensoric cell line was performed on U2OS cells grown and treated under identical conditions, but fixed after 12 hours with 4% paraformaldehyde and stained for reference DNA damage marker, the phospho-γH2AX (24), antibody: Anti-phospho–Histone H2A.X (Ser139), clone JBW301, Millipore (cat. no. 05-638), and evaluated for nuclear foci formation.

Inhibition of protein synthesis *in vivo*

4T1-luc2 cells were expanded *in vitro* in DMEM supplemented with 5 g/L glucose, 2 mmol/L glutamine, 100 U/mL penicillin, 100 μg/mL streptomycin, 10% fetal calf serum, and NaHCO₃. A total of 10^5 cells were orthoptically transplanted into right inferior mouse breast pad of syngeneic Balb/c mice (Charles Rivers). Tumor bearing mice with palpable 3 to 5 mm tumors were injected intraperitoneally with single dose of D-luciferin (150 mg/kg) and baseline tumor luminescence corresponding to firefly luciferase protein expression was recorded 10 minutes later using Photon Imager (Biospacelab). Then, the animals were injected intraperitoneally with vehicle or AB61 at dose corresponding to the maximum tolerated dose (MTD, 60 mg/kg). Luciferase activity was again recorded 4 hours later after 30-minute pretreatment with D-luciferin (150 mg/kg, i.p.). Cumulative luminescence [cpm/mm²] was used as a surrogate indicator of luciferase protein expression in tumors.

In vitro pharmacology

Pharmacologic properties of AB61 and AB61-MP, for example, stability in plasma, microsomes, and penetration through artificial membrane, were tested under *in vitro* conditions.

In vitro stability in human plasma. Tested compound was added to 1.3 mL of preheated human plasma (Transfusion Department, University Hospital Olomouc, Olomouc, Czech Republic) to yield final concentration of 3.3 μmol/L; DMSO did not exceed 0.1%. Procaine was used as a positive control of the assay. The assay was performed at 37°C. Plasma aliquots (75 μL) were sampled at 0, 15, 30, 60, and 120 minutes and the reactions were terminated adding 150 μL of acetonitrile–methanol mixture (2:1), centrifuged at 4°C for 10 minutes at 4,000 rpm. Supernatant was lyophilized, then dissolved in the 200 μL of the mobile phase and analyzed by the RapidFire RF300 system mass spectrometry (RF-MS). *In vitro* plasma half-life ($t_{1/2}$) was calculated using the equation $t_{1/2} = 0.693/k$, where k is the slope of the natural logarithm of the percent compound remaining versus time curve (25).

Parallel artificial membrane permeability assay. The parallel artificial membrane permeability assay (PAMPA) was performed with the Millipore MultiScreen filter MultiScreen-IP Durapore 0.45-μm plates and receiver plates (Merck Millipore). The assay was performed according to the manufacturer's protocol (PC040EN00). Compounds were tested at the concentration of 20 μmol/L. Briefly, filters in each well were wetted with 10% lecithin (Sigma Aldrich) in dodecane mixture to create the artificial layer. The filter plate was placed on the top of the receiver plate, which was prefilled with donor solutions (tested

183

compounds dissolved in PBS at final concentration 20 μmol/L). After incubation, 120-μL aliquots of acceptor and donor solutions were removed to the 96-well plate, lyophilized, and residues were dissolved in 200 μL of the mobile phase prior the RapidFire-MS analysis. The relative permeability logPe was calculated with equation: $logPe = log\{C \times -ln(1-drug_A/drug_E)\}$; where $C = (V_A \times V_D)/\{(V_D+V_A) \times A \times T\}$. V_D and V_A are the volumes of the donor and acceptor solutions, A is the active surface area in cm^2, T is time of the incubation in seconds, $drug_A$ and $drug_E$ is the mass of the compound in the acceptor and in the solution in theoretical equilibrium (as if the donor and acceptor were combined), respectively.

Microsomal stability assay. Reaction mixtures included tested compound (5 μmol/L), human liver microsomes (ThermoFisher Scientific, 0.5 mg/mL), NADPH generating system consisting of $NADP^+$, isocitrate dehydrogenase, isocitric acid, and $MgSO_4$ in 0.1 mol/L K_3PO_4 buffer according to the protocol (26, 27). Assay was performed at 0, 15, 30, and 60 minutes. Reactions were terminated using acetonitrile–methanol (2:1) mixture. Prototype-stable versus nonstable drugs (propranolol and verapamil, respectively) were used as a reference (28).

Bioanalytics–RF-MS system setup. The RapidFire RF300 system (Agilent Technologies) was interfaced with QTRAP 5500 (AB Sciex) mass spectrometer. For detailed description, see ref. (27). Samples were aspirated directly from 96-well plates into a 10-μL sample loop and passed through a C4 cartridge (Agilent Technologies) with solvent A (95% water/5% acetonitrile/0.1% formic acid) at a flow rate of 1.5 mL/minute for 3 seconds. After the desalting step, analyte retained on the cartridge was eluted with solvent B (95% acetonitrile/5% water/0.1% formic acid) to the mass spectrometer at a flow rate of 0.4 mL/minute for 7 seconds. The intrinsic clearance was calculated using the formula: $Cl_{int} = V^*(0.693/t_{1/2})$, where V is the volume of incubation in μL related to the weight of microsomal protein in mg per reaction. Half-life values ($t_{1/2}$) were calculated using the equation $t_{1/2} = 0.693/k$, where k is the slope of the ln of the percent compound remaining versus time curve.

Anticancer activity in human xenografts

Human colorectal cancer cell line HT-29, ovarian cancer cells SK-OV-3, and breast tumors BT-549, respectively, were grown under *in vitro* conditions, harvested, and xenotransplanted (5 × 10^6 cells/mice) subcutaneously on right flank of immunodeficient NOD/SCID mice (NOD.CB17-*Prkdc*^{scid}/NcrCrl, Charles Rivers). Tumor bearing mice (200–300 mm^3) were treated with AB61 at dose corresponding to half MTD ($MTD^1/_2$, 30 mg/kg; ref. 11) for 3 or 5 consequent days per week in two to four cycles. Tumor length versus width was measured by caliperation three times per week and tumor volume was calculated. Animals were housed in specific pathogen–free conditions, 12-hour light/night regime, clinically examined on daily basis, water, and food *ad libitum.* Experiments were approved by Animal Ethics Committee of the Faculty of Medicine and Dentistry, Palacky University (Olomouc, Czech Republic).

Results

Synthesis of nucleosides and nucleotide analytical standards

To obtain analytical standards of AB61-derived metabolites, the nucleotides dAB61-MP and AB61-DP were prepared under standard conditions for Suzuki cross-coupling reaction (11, 29, 30) of the corresponding nucleotide or by phosphorylation of the nucleoside, respectively. [^{3}H]-Labeled AB61 ([^{3}H]AB61) was synthesized by Suzuki cross-coupling reaction of 5-iodotubercidin with 5-chlorothiophene-2-boronic acid followed by tritiation (Fig. 2). For detailed information on synthesis, see Supplementary Information "Synthesis of nucleosides and nucleotides."

AB61 shows differential *in vitro* cytotoxic activity against cancer cell lines and normal fibroblasts

Cytotoxic activity of AB61 was determined using MTT assay following a 3-day incubation (Table 1). AB61 showed nanomolar IC_{50} values against cancer cell lines (A549, CCRF-CEM, HCT116, and K-562). A strong cytotoxic effect of AB61 was also observed against paclitaxel- and daunorubicin-resistant cancer cell lines overexpressing multidrug resistance transporters (K-562-tax, CEM-DNR-bulk) and a colorectal cancer cell line with inactivated p53 gene (HCT116p53$^{-/-}$). IC_{50} values of AB61 against normal lung and foreskin fibroblasts (MRC-5, BJ) were 2- to 5-orders of magnitude higher (micromolar) than the IC_{50} values against the cancer cell lines. On the other hand, cytotoxic activities of AB61-5'-O-monophosphate (AB61-MP) against cancer cell lines were always at least one order of magnitude lower than those of AB61. Interestingly, AB61-MP also showed poor selectivity towards malignant versus nonmalignant cells. Its IC_{50} values against normal fibroblasts were similar to those against cancer cell lines.

Intracellular phosphorylation of AB61 is limited in normal fibroblasts

Intracellular phosphorylation is often a key step in activation of nucleoside drugs. Efficient phosphorylation of AB61 was previously shown in a Du145 prostate cancer cell line (11). Intracellular levels of AB61, its nucleoside monophosphate (AB61-MP), diphosphate (AB61-DP), and triphosphate (AB61-TP) were determined by HPLC analysis after 1- and 3-hour treatment with AB61 (1 μmol/L or 10 μmol/L) in colon cancer cell line (HCT116) and in normal foreskin BJ fibroblasts (Table 2). High levels of AB61-MP were observed in HCT116 cells after 3-hour treatment, whereas after 1-hour treatment no or only a minor amount of AB61-MP was detected after treatment with 1 or 10 μmol/L concentration of AB61, respectively. BJ fibroblasts showed good uptake of AB61 but no AB61-MP was detected, thus indicating ineffective intracellular phosphorylation of AB61 in BJ fibroblasts. AB61-DP and AB61-TP were not detected in any cell line, presumably due to short treatment time, fast incorporation into macromolecules and/or concentrations under the detection limit. Both AB61 and AB61-MP were shown to cross artificial cellular membrane in the PAMPA assay; however, the membrane permeability for AB61-MP was one order of magnitude lower than that of AB61 (Table 3). Furthermore, AB61 is stable in plasma and human microsomes, whereas AB61-MP is slowly degraded with plasma with half time around 52 minutes, presumably to the parent nucleoside AB61 due to serum phosphatase activity (Table 3).

AB61-TP is incorporated into RNA and DNA by T7 RNA polymerase and by Klenow fragment of DNA polymerase I and DNA polymerase γ, respectively

Enzymatic incorporation of AB61-TP into RNA was tested using viral T7 RNA polymerase. The 40-mer dsDNA template contained

184

Perlíková et al.
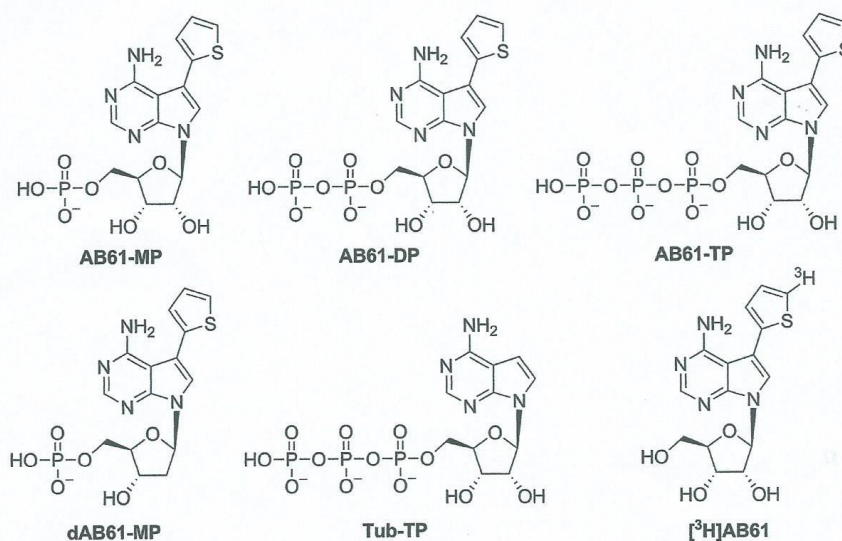
Figure 2.
Structures of nucleosides and nucleotides used in this study.

two 2'-OMe-RNA nucleotides at the 5'-end of the noncoding strand to avoid n+1 activity of the T7 RNA polymerase (31). The template is transcribed into a 21-bp RNA transcript containing four ATP insertions. The transcription reactions performed in presence of either ATP, AB61-TP or Tub-TP and three natural NTPs (GTP, UTP, and CTP) afforded a full length transcript (Fig. 3A). The results show that both AB61-TP and Tub-TP are substrates of T7 RNA polymerase and are able to substitute for ATP during transcription and to be incorporated into RNA. Furthermore, these experiments provided evidence that T7 RNA polymerase is able to further elongate the transcript after incorporation of AB61-TP. Our studies also focused on enzymatic incorporation of AB61-TP into DNA in a primer extension experiment with bacterial DNA polymerase I (Klenow fragment) and a 31-bp DNA template allowing incorporation of four dATPs. A primer

extension reaction with AB61-TP instead of dATP led to formation of a full-length product, confirming that AB61-TP was successfully incorporated into DNA without causing the polymerase to pause. In contrast, Tub-TP was not incorporated by Klenow fragment (Fig. 3B). Incorporation of AB61-TP by commercially available human DNA polymerases were also tested using a primer extension experiment. While AB61-TP is not a substrate for DNA polymerase β (Fig. 3C), AB61-TP was successfully incorporated by DNA polymerase γ (Fig. 3D). Incorporation of AB61-TP by DNA polymerase γ was also confirmed by MALDI-TOF analysis (See Supplementary Fig. S1).

AB61 is incorporated into RNA and DNA in cancer cell lines

Further studies focused on incorporation of AB61 into RNA and DNA in living cells. CCRF-CEM cells were incubated with [3H]-labeled AB61 ([3H]AB61; 250 nmol/L), cellular RNA and DNA were isolated and activities of the RNA and DNA samples were measured using liquid scintillation counting (LSC; Table 4). Significant increases in activities were observed for both RNA and DNA samples after 2.5-hour treatment. To further confirm the incorporation of AB61, RNA, and DNA samples from cells treated with AB61 or [3H]AB61 (250 nmol/L) were digested with nuclease P1 affording nucleoside monophosphates. The hydrolyzed RNA and DNA samples were analyzed by HPLC-MS (Table 5) and HLPC with UV/VIS detection and radioactivity of HPLC fractions was determined by LSC (Fig. 4). Figure 4A and D show authentic analytical standards of ribo- or deoxyribonucleos(t)ides, respectively. After digestion of RNA, peaks of all natural NMPs were

Table 1. Cytotoxic activity of AB61 and its 5'-monophosphate AB61-MP

Cell line	MTT, IC$_{50}$ (μmol/L)	
	AB61[a]	AB61-MP
A549	0.010	1.06
CCRF-CEM	0.00036	0.16
CEM-DNR-bulk	0.043	0.45
HCT116	0.0019	0.18
HCT116p53−/−	0.067	0.83
K-562	0.0095	0.21
K-562-tax	0.0083	0.99
BJ	8.00	0.24
MRC-5	11.4	7.84

[a]The data presented here are from fresh retesting.

Molecular Cancer Therapeutics

185

Table 2. Intracellular phosphorylation of AB61 at various concentrations

Cell line	Dosing (1 μmol/L, 1 hour; pmol/5 × 10⁵ cells)		Dosing (10 μmol/L, 1 hour; pmol/5 × 10⁵ cells)	
	AB61	AB61-MP	AB61	AB61-MP
HCT116	81.6 ± 3.48	0	88.1 ± 13.0	0.56 ± 0.44
BJ	76.7 ± 7.30	0	82.7 ± 7.33	0
	Dosing (1 μmol/L, 3 hours; pmol/5 × 10⁵ cells)		Dosing (10 μmol/L, 3 hours; pmol/5 × 10⁵ cells)	
HCT116	117 ± 21.6	32.0 ± 5.65	120 ± 22.8	15.6 ± 3.62
BJ	68.0 ± 1.33	0	67.6 ± 3.07	0

identified in the HPLC chromatogram (Fig. 4B). Three peaks were observed in HPLC-LSC analysis (Fig. 4C). One of the peaks corresponds with standard of AB61-MP confirming the incorporation of [³H]AB61 into RNA, while the two other peaks are presumably related to short [³H]AB61-containing oligonucleotides that were formed because of the incomplete digestion of the RNA sample. The presence of AB61-MP was also confirmed by LC-MS. Peaks of all natural dNMPs were found in the HPLC chromatogram of the digested DNA sample (Fig. 4E). A single peak was observed after digestion of DNA sample by the HPLC-LSC analysis (Fig. 4F). This peak clearly corresponds to ribonucleotide AB61-MP. In the LC-MS analysis of DNA isolated from AB61-treated cells, AB61-MP was detected as a major component, but a minor presence of the corresponding 2′-deoxyribonucleotide (dAB61-MP) was also observed. The molar ratio of AB61-MP and dAB61-MP was approximately 30:1 (Table 5). The results show that AB61 is mainly incorporated into DNA as a ribonucleotide although 2′-deoxyribonucleotide is also present in residual quantities. On the contrary, only AB61-MP was detected in the RNA of the treated cells. To localize incorporation of AB61 in cells and to further investigate the mechanisms of incorporation into the DNA, we have employed structural analogue of AB61, compound PNH404 (Fig. 1; ref. 11), which contains alkyne group available for azide-alkyne CuAAC cycloaddition of fluorescent dye Azide-Fluor 568 ("click chemistry"; ref. 32). In U2OS cells, PNH404 was incorporated predominantly into nuclei of treated cells with residual staining in the cytoplasm. Interestingly, the incorporation of the compound was not significantly inhibited by inhibitor of replicative DNA polymerases aphidicolin (ref. 22; Fig. 5).

Gene expression analysis suggests AB61 affects DNA damage pathways and protein translation/folding machinery

To evaluate the biologic activity of the AB61 more broadly, we performed transcriptional microarray profiling coupled to the pathway analysis. On the basis of the differentially expressed genes the "DNA Damage_DBS Repair" network process was identified as the most significant process network following the AB61 treatment. Furthermore, other networks indicating significantly affected protein folding and translation, cell cycle, and angiogenesis were top ranked. Upregulation of *BRIP1, RPA4, FANCF,* and *TOP1,* and downregulation of *TdT, FANCG, LIG4, LIG3, NRB54, Chk2, MGMT, RAD51B, Histone H4, Ubiquitin,* and *C1D* genes which are well known to be involved in DNA damage processes was observed. This corresponds well to the cell biology data (vide infra). Reference compounds, tubercidin (Tub) and actinomycin D (ActD), with structural or mechanistic similarity to AB61, were used. The networks involved in "development_regulation of angiogenesis" and "development and blood vessel morphogenesis" were similarly affected; however, the DNA damage, cell-cycle alteration, and protein translation and folding were not among top listed networks in cells treated with ActD and Tub (Table 6).

Induction of DNA damage in AB61-treated cells

To confirm AB61-induced DNA damage by an independent method, the U2OS human osteosarcoma cell line was stably transfected with the 53BP1-GFP (20) fusion gene. 53BP1 protein accumulates at DNA lesions, preferably at DNA double strand breaks, thus its GFP-conjugate enables visualization of DNA-damage sites in nucleus. Indeed, U2OS-53BP1-GFP cells treated with AB61 or control DNA–damaging agents like topoisomerase I or II inhibitors (irinotecan and etoposide, respectively) showed time-dependent accumulation of 53BP1 foci in the nuclei of treated cells (Fig. 6). Although the absolute number of 53BP1 foci in AB61-treated cells (Fig. 6B) was lower than in irinotecan- and etoposide-exposed cells (Fig. 6C–E), the foci were markedly larger compared with both irinotecan- and etoposide-treated versus untreated control cells (Fig. 6A). These results were independently validated using phospho-γH2AX staining in U2OS cells treated with AB61, etoposide or irinotecan, respectively (Fig. 6F–I).

Table 3. Plasma and microsomal stability and parallel artificial membrane permeability assay (PAMPA) for AB61 and its 5′-monophosphate AB61-MP

Compound	Plasma stability					PAMPA
	In vitro $t_{1/2}$ (min)	% Compound remaining				logPe[a]
		15 minutes	30 minutes	60 minutes	120 minutes	
AB61	No degradation observed	98.6 ± 11.7	102.8 ± 5.7	104.5 ± 13.6	101.7 ± 29.4	−5.29 ± 0.23
AB61-MP	51.9 ± 3.9	76.6 ± 8.4	51.4 ± 5.2	25.4 ± 1.3	20.7 ± 30.6	−6.33 ± 0.25
	Intrinsic clearance assessment from microsomal stability assay					
Compound	In vitro CL_{int} (μL/min/mg protein)	Clearance category[b]				
AB61	6.6 ± 1.7	Low				
AB61-MP	9.4 ± 7.1	Medium				

[a]According to the logPe obtained from the reference drugs, compounds with logPe > −7 were categorized as highly permeable, while those with logPe < −7 were considered as poorly permeable.
[b]Reference (28).

186

Perlíková et al.
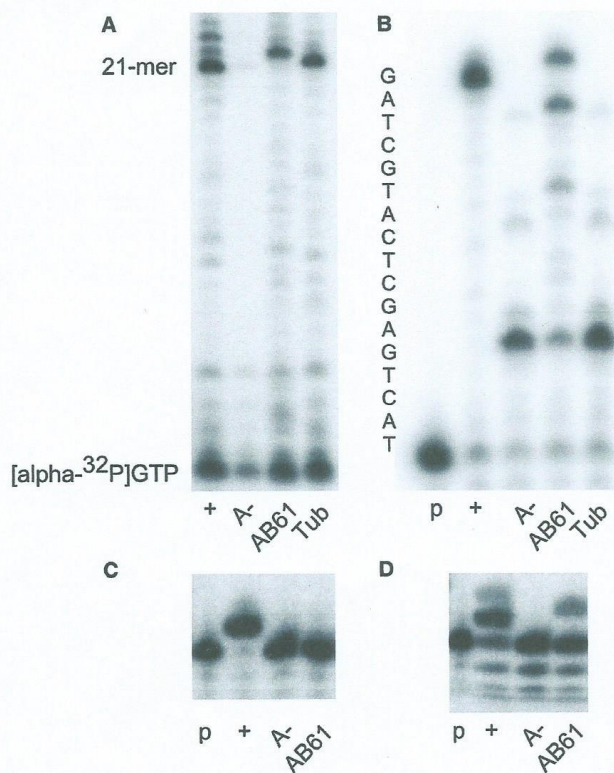
Figure 3.
Enzymatic incorporation of AB61-TP and Tub-TP into RNA and DNA. A, denaturing PAGE analysis of *in vitro* transcription reactions with T7 RNA polymerase. Key: +: all natural NTPs; A-: GTP, CTP, UTP; AB61: AB61-TP, GTP, CTP, UTP; Tub: Tub-TP, GTP, CTP, UTP. B, primer extension experiment with Klenow fragment. Key: p: ^{32}P-labeled primer; +: dATP, dCTP, dTTP, dGTP; A-: dCTP, dTTP, dGTP; AB61: AB61-TP, dCTP, dTTP, dGTP; Tub: Tub-TP, dCTP, dTTP, dGTP; C, primer extension experiment with human DNA polymerase β. Key: p: ^{32}P-labelled primer; +: dATP; A-: without dATP; AB61: AB61-TP; D, primer extension experiment with human DNA polymerase γ. Key: p: ^{32}P-labeled primer; +: dATP; A-: without dATP; AB61: AB61-TP.

Incorporation of AB61-TP into mRNA blocks its translation *in vitro*

Following the evidence of AB61-TP and Tub-TP incorporation into mRNA, we wanted to evaluate functional properties of the RNA harboring ribonucleoside analogues in terms of translational efficacy. A template with a model EGFP-luciferase fusion gene under T7 promoter was transcribed into RNA. The transcription experiments were performed in the presence of all four natural NTPs with/without AB61-TP or Tub-TP so that AB61-TP or Tub-TP could be randomly incorporated into the RNA transcripts. After the *in vitro* transcription, the template DNA was digested by DNase I and the RNA transcripts were purified. In the next step the RNA transcripts were used as templates for *in vitro* translation using a commercial reticulocyte lysate *in vitro* translation system. The resulting EGFP-luciferase protein in the translation reactions was detected on the basis of its enzymatic luciferase activity and Western blotting (Fig. 7). The results showed that the translation reactions with unmodified RNA template and RNA template

Table 4. Incorporation of [^{3}H]AB61 into RNA and DNA of living cells (data from 3 independent experiments)

Time (h)	activity (cpm/µg)	
	RNA	DNA
0	0.5 ± 0.06	3.4 ± 0.7
2.5	25.6 ± 1.6	80.9 ± 2.3

Table 5. Incorporation of AB61 into RNA and DNA samples from CCRF–CEM cells after 2.5-hour treatment and subsequent digestion with nuclease P1 (data from 3 independent experiments)

Sample	AB61-MP [fmol/µg of nucleic acid]	dAB61-MP [fmol/µg of nucleic acid]
RNA	1.68 ± 0.5	n.d.[a]
DNA	0.667 ± 0.28	0.021 ± 0.0103

[a]Not detected.

187
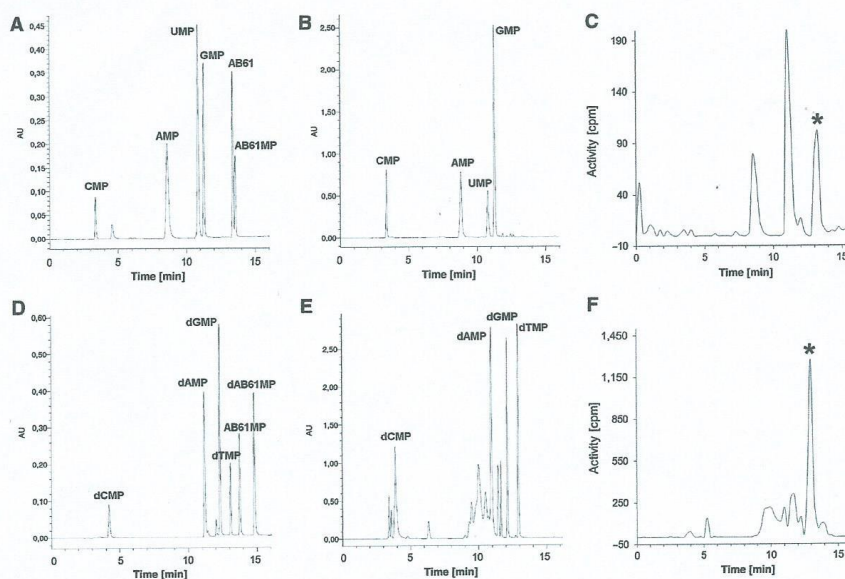
Figure 4.
Incorporation of [³H]AB61 into RNA or DNA in CCRF-CEM cells exposed to the drug for 2.5 hours. A, HPLC analysis of NMP standards. B, HPLC analysis of nuclease-P1–digested RNA. C, HPLC-LSC analysis of nuclease-P1–digested RNA sample after 2.5-hour treatment with [³H]AB61. D, HPLC analysis of dNMP standards. E, HPLC analysis of nuclease-P1–digested DNA sample. F, HPLC-LSC analysis of nuclease-P1–digested DNA sample. Asterisk indicates the peak corresponding to AB61-MP.

produced in the presence of Tub-TP afforded similar amounts of EGFP-luciferase. In contrast, synthesis of EGFP-luciferase protein from RNA template produced in the presence of AB61-TP was completely blocked, as evidenced from both the measurement of luciferase enzymatic activity and protein content (Fig. 7). This result shows that AB61-TP can be incorporated into RNA by T7 RNA polymerase in the presence of ATP. Furthermore, the presence of AB61 in the RNA hampers its function as a template for the translation. This effect was not observed for Tub-TP and to our knowledge it is the first description of such an effect in the class of cytostatic nucleosides.

AB61 inhibits protein expression and tumor growth *in vivo*

To evaluate the effect of AB61 on luciferase activity/expression *in vivo*, Balb/c mice were transplanted with the 4T1-Luc2 breast cancer cells stably transfected with luciferase under strong CMV promoter and bioluminescence imaging technique was employed to visualize and quantify the luciferase (Fig. 8). Indeed, the tumor-bearing mice treated with AB61 (MTD, 60 mg/kg) intraperitoneally demonstrated 4 hours later significant decrease of luciferase activity *in vivo* as compared with vehicle-treated mice. *In vivo* anticancer activity of AB61 was determined using human ovarian (SK-OV-3), breast (BT-549), and colorectal (HT-29) tumors xenografted to the NOD/SCID mice (Fig. 9). Animals were treated with

MTD$^{1}/_{2}$ (30 mg/kg) of AB61 in 3 (low-intensity) or 5 consequent days per week (high-intensity scheme) in two to four cycles. In all cancer models employed, highly significant reduction of tumor volume was observed in treated mice. However, significant reduction of tumor volume in ovarian cancer model SK-OV-3 was only observed with high intensity scheme suggesting dose dependent effect. AB61 also significantly prolonged survivals in BT-549 and HT-29 models, but not in the SK-OV-3 due to no efficacy in the low-intensity administration schedule and toxicity in the high-intensity regimen.

Discussion

In this study, we focused on elucidation of the mechanism of action of a novel 7-deazaadenine analogue, AB61. Despite the very strong cytotoxic effect of AB61 against cancer cell lines we found out that cytotoxic activity of AB61-MP against cancer cell lines was always lower (typically by 2 orders of magnitude) than that of AB61. The main reason is probably in lower (by one order of magnitude) permeability of the monophosphate AB61-MP through cell membrane compared with nucleoside AB61 (as confirmed by PAMPA assay) but we can also hypothesize on involvement of membrane efflux and/or complex phosphorylation/dephosphorylation dynamics. On the other hand, AB61-MP

188

Perlíková et al.

| | Azide-fluor 568 | Hoechst 33342 | Merge |
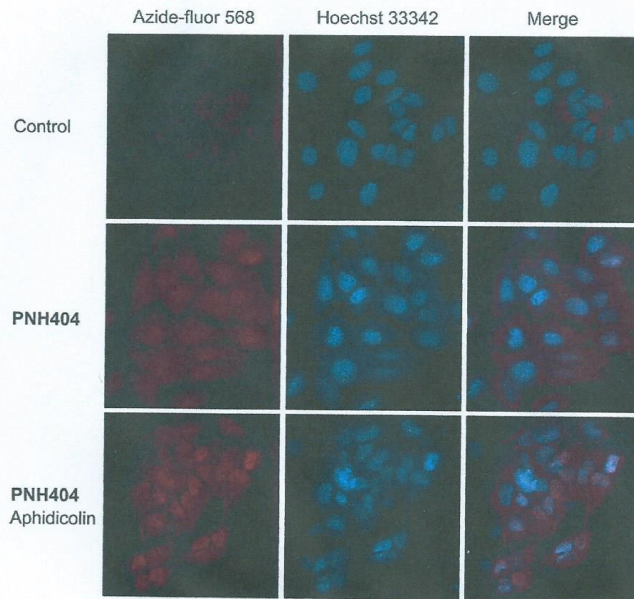
Figure 5.
Vizualization of incorporation of AB61 analogue (PNH404) *in situ* by click staining with Azide-Fluor 568 fluorescent dye (red fluorescence) in treated U2OS cells (250 nmol/L, 2.5 hours) with DNA counterstained with Hoechst 33342 (blue fluorescence) compared with untreated cells (control). Confocal microscopy demonstrates specific and preferential accumulation of PNH404 in nuclei and partially in the cytoplasm of the cells. Inhibition of replicative DNA polymerases by aphidicolin (10 μmol/L) did not decrease neither incorporation rate nor subcellular localization of the AB61 analogue.

showed higher cytotoxicity against normal fibroblasts compared with AB61, which was comparable with cytotoxicity in cancer cell lines. The PAMPA test confirmed that AB61-MP can still relatively well penetrate through membrane (though less efficiently than nucleoside AB61) causing the nonspecific cytotoxicity. Apparently, intracellular availability of AB61-MP increases the cytotoxic effect.

Table 6. Transcriptomic microarray analysis of AB61, tubercidin (Tub), and actinomycin D (Act D) cellular effects

Drug	Process networks[a]	log(P)	Networks objects
AB61	DNA damage_DBS repair	−4.81	↑ BRIP1, RPA4, FANCF, TOP1; ↓TdT, FANCG, LIG4, LIG3, NRB54, Chk2, MGMT, RAD51B, Histone H4, Ubiquitin, C1D
	Protein folding_Protein folding nucleus	−4.46	↑ PSMD4; ↓ RBBP7, SFRS4, HSP90, DJ-1, YY1, OSP94, NPM1, FKBP4, AUF1
	Cell cycle_S phase	−3.05	↑ BRIP1, TOP1, PLK1; ↓ SMC1, ORC6L, LIG4, HSP90, Chk2, UHRF2, Geminin, Histones (H1, H1.5, H4), Ubiquitin
	Development_Regulation of angiogenesis	−2.19	↑ S2P, CEACAM1; ↓ PKC, Cathepsin B, ITGB1, HB-EGF, HMDH, ID1, VEGF-A, Ephrin-B, Ephrin-B2, Calnexin, CXCR4, XCR1, CCR10, AKT
	Translation_Translation initiation	−2.07	↑ eIF4G2, RPS27A, eIF5; ↓ RPS2, RPS24, RPS10, RPS25, PAIP2, eI3S7, RPL21, RPS3A, RPS30, RPL17
Tub	Development_Blood vessel morphogenesis	−4.51	↑ PDE7A, PDE, CCR10, ANG1, Elk-3, A2aR; ↓ TERT, KLF5, HB-EGF, AKT, CXCR4, XCR1, S1PR1, S1PR3, VEGF_A, F263, AREG
	Apoptosis_Endoplasmic reticulum stress pathway	−2.89	↑ CREB-H, S2P, eIF5; ↓ Bim, XBP1, eIF3S7, HERP, NUR77
	Signal transduction_BMP and GDF signaling	−2.83	↑ CD44, CREB1, SMURF2, RUNX2; ↓ YY1, ID1, AKT, PP2A
	Proliferation_Negative regulation of cell proliferation	−2.81	↑ CCR10, Prohibitin, WARS; ↓ GAB1, Mxi1, RBBP7, IGF1R, MNT, TOB2, SHP-1, AREG, EGR1
	Development_Regulation of angiogenesis	−2.57	↑ CCR10, ANG1, S2P, CREB1; ↓ PKC, HB-EGF, ID1, AKT, CXCR4, XCR1, VEGF-A, Ephrin-B, Ephrin-B2
ActD	Proteolysis_Ubiquitin-proteasomal proteolysis	−3.41	↑ PSMA2, Rnf14, PSMB2, SENP1, SMURF2, SMURF, LNX2, PSME3; ↓ BLMH, TRC8, Ubiquitin, BAG-1, NEDD4L
	Signal Transduction_BMP and GDF signaling	−3.23	↑ RUNX2, CD44, SMURF2, SMAD1; ↓ ATF-2, PP2A, YY1, ID1, AKT
	Development_Regulation of angiogenesis	−2.26	↑ s2P; ↓ PKCA, PKC, Cathepsin B, ID1, Ephrin-B, Ephrin-B2, AKT, PLAUR, CXCR4, XCR1, CCR10, VEGF-A
	Development_Blood vessel morphogenesis	−2.18	↑ PDE, PDE7A, Elk-3; ↓ PKCA, S1PR1, S1PR3, AKT, CCR10, CXCR4, XCR1, VEGF-A, F263, AREG
	Neuro physiological process_Corticoliberin signaling	−2.06	↓ cPKC, PKCA, NUR77, EGR1, NURR1

[a]Only the most affected networks from the pathway analysis are listed; ↑, upregulated genes; ↓, downregulated genes.

189
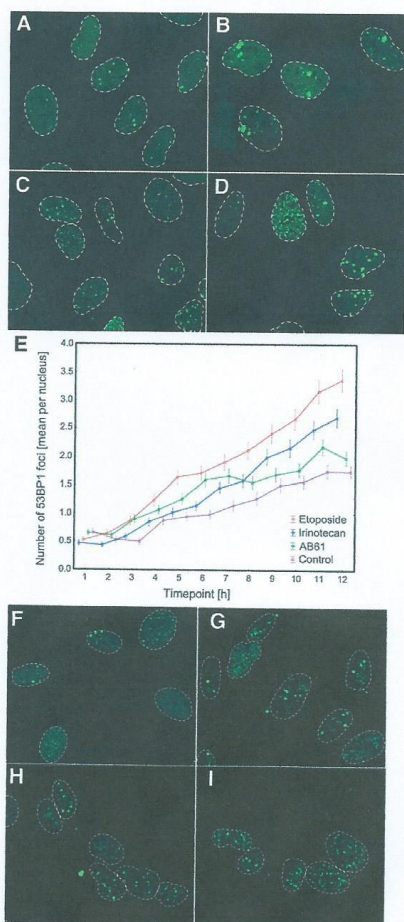
Figure 6.
53BP1 foci in U2OS-53BP1-GFP cells exposed to vehicle (A), AB61 (B), irinotecan (C), or etoposide (D) for 12 hours. E, time dependence of 53BP1 foci formation during treatment with AB61, irinotecan, and etoposide. Phospho-histone γH2AX foci in U2OS cells exposed to vehicle (F), AB61 (G), irinotecan (H), or etoposide (I) for 12 hours. All compounds were tested at 1 μmol/L concentration. Nuclei contours are highlighted by dashed line for convenience.

Our further results demonstrated that AB61 is phosphorylated in HCT116 colon cancer cell line (cytotoxicity $IC_{50} = 1.9$ nmol/L) but the phosphorylation does not proceed in normal BJ fibroblasts

(cytotoxicity $IC_{50} = 8$ μmol/L). These data are in accordance with the fact that expression of adenosine kinase, the enzyme that might be involved in the phosphorylation of AB61, is increased in colorectal tumors compared with the normal tissue (33–35). These findings reveal the importance of intracellular phosphorylation for both the efficiency and cancer selectivity of AB61 and suggests for potentially synergistic combinations with therapies increasing nucleoside phosphorylation rates in tumors, for example, radiation (36). Furthermore, we showed that AB61-TP is effectively incorporated into RNA by T7 RNA polymerase in an enzymatic assay. Although AB61-TP is not accepted as a substrate by human DNA polymerase α(13) and β, both human DNA polymerase γ and Klenow fragment successfully incorporated AB61-TP into DNA, even though it is not a 2′-deoxyribonucleotide but a ribonucleotide. However, our experimental design for AB61-TP incorporation by DNA polymerase β did not contain a single nucleotide gap substrate, which is a typical site of polymerase β action (37), nor accessory proteins involved with polymerase β activity (PARP, XRCC1; ref. 38), and therefore the incorporation of AB61-TP might not have been a suitable substrate in the cell-free system we have used. In contrary, Tub-TP is accepted neither by the human DNA polymerase α (13) nor the Klenow fragment. Both DNA polymerase γ and Klenow fragment represent A family DNA polymerases. Despite the fact that DNA polymerase γ is a mitochondrial polymerase and Klenow fragment is a bacterial enzyme, we hypothesize that AB61-TP might be also incorporated by nuclear DNA polymerases from the A family, that is, DNA polymerase θ and DNA polymerase ν which are both involved in DNA repair processes and are known for lower fidelity (39). Also treatment of CCRF-CEM cells with AB61 or [³H]AB61 resulted in its incorporation into both RNA and DNA. HPLC-MS analysis of DNA lysates revealed that AB61 is incorporated into DNA predominantly as a ribonucleotide and only rarely as a 2′-deoxyribonucleotide (30:1 ratio) which means that AB61-TP is a substrate for human DNA polymerases. Despite this finding might seem surprising, ribonucleotide incorporation into cellular DNA is quite common (40–42). In contrast, tubercidin (2) and toyocamycin (3) are incorporated into DNA only after reduction by ribonucleotide reductase as 2′-deoxyribonucleotides. Consistently with mass spectrometry data, PNH404, the ethynyl-analogue of AB61, was detected in nuclei and cytoplasm of treated U2OS cells, which is in agreement with incorporation of AB61 into DNA and RNA, respectively. Interestingly, the incorporation of AB61 analogue into nuclei was not affected by the inhibitor of replicative DNA polymerases aphidicolin, indicating (in accord with previous data) that incorporation is rather dependent on nonreplicative, for example, reparative DNA polymerases (39). To see a broader picture of the AB61-induced changes, we performed microarray gene expression profiling, which, in principle, suggested DNA damage repair networks and translational or folding machinery are primarily affected in cellular response to the AB61. Several genes involved in DNA damage and/or repair mechanisms were altered. However, the affected networks are only partially overlapping with reference compounds tubercidin and actinomycin D, suggesting a different mechanism of action. To validate DNA repair pathway at the cellular level, we used the 53BP1-GFP reporter U2OS cell line. Protein 53BP1 is known to rapidly accumulate at DNA double strand breaks leading to activation of DNA repair mechanisms (43). After treatment with AB61, formation of large 53BP1-GFP foci was observed in a time-dependent manner indicating that AB61 induces DNA damage. However, the pattern of

190
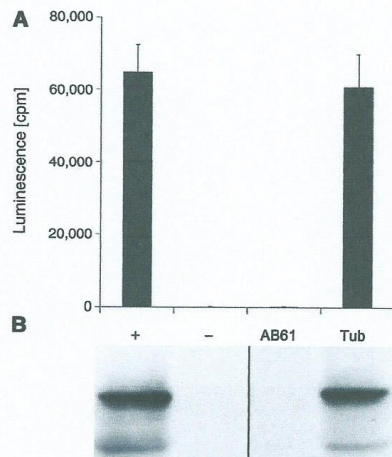
Figure 7.
In vitro translation reactions with different RNA templates for EGFP-luciferase reporter gene. A, luciferase activity; data represent averages of two independent experiments. B, Western blot analysis using anti-luciferase antibody. Key: +, unmodified RNA template; −, no template; AB61, RNA template produced in the presence of AB61-TP; Tub, RNA template produced in the presence of Tub-TP.

53BP1-GFP nuclear foci is different from the DNA damage patterns induced by topoisomerase inhibitors irinotecan, etoposide, or p53 activator 7-iodotubercidin (44), which suggests that DNA damage caused by AB61 is achieved, maintained, or (un)repaired via different mechanisms. In addition to the 53BP1-GFP accumulation in the DNA damage sites, similar staining pattern was

independently confirmed for phospho-γH2AX, one of the most robust surrogate markers of DNA double strand breaks. As (i) AB61-TP is not a substrate for human polymerase α(13) or polymerase β, (ii) incorporation of AB61 analogue into cell nuclei was not decreased upon inhibition of replicative but not reparative DNA polymerases by aphidicolin, (iii) gene expression study revealed activation of DNA damage pathway, and (iv) formation of unusually large 53BP1 and/or phospho-γH2AX DNA damage foci in treated tumor cells was observed, we hypothesize that AB61 is incorporated into DNA by polymerases involved in the repair mechanisms, thus further aggravating the local DNA damage in a positive back-loop manner and thereby inducing stronger signal for 53BP1 and/or phospho-γH2AX to accumulate.

We had previously reported poor inhibition of RNA polymerase II by AB61-TP (11). Having the evidence that AB61 is incorporated into RNA of exposed cells, the RNA polymerase II is not inhibited, but the RNA synthesis is down regulated, we focused on the possible consequences of AB61 incorporation into mRNA. We studied *in vitro* translation of RNA templates containing randomly incorporated AB61. We discovered that the incorporation of AB61 into mRNA template completely prevents formation of a protein. This result was further confirmed in mice by the observation of significant and rapid inhibition of luciferase protein expression in AB61-treated 4T1-luc tumors. In contrast, even though Tub-TP is incorporated into RNA by T7 RNA polymerase, no effect on *in vitro* translation was observed. *In vivo* studies of AB61 in human colorectal (HT-29), ovarian (SK-OV-3), and breast (BT-549) cancer xenografts revealed highly significant reduction of tumor mass in treated animals, which was reflected with increased survival preferentially in low-density regimen. Despite better tumor control of the high-intensity schedule, it was not always translated into increased survival due to cumulative therapeutic toxicity with leading symptoms of body weight lost and anorexia. Interestingly, the highest *in vivo* activity of the compound was demonstrated in slowly growing HT-29 tumors, suggesting preferential anticancer activity in slowly proliferating tumor cells. Therefore, the *in vivo* anticancer effect of AB61 is very promising and warrants further studies.
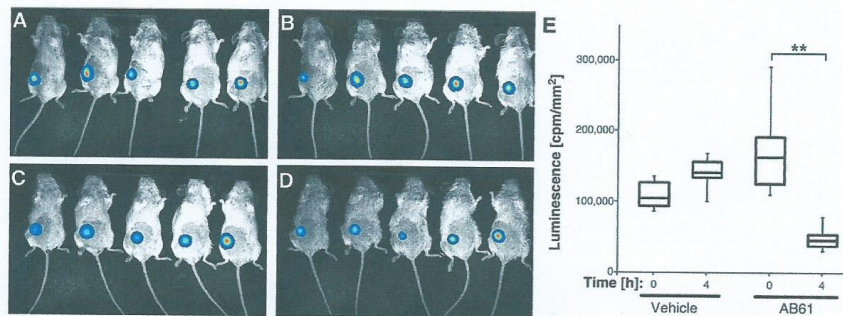
Figure 8.
Tumor luciferase activity in mice bearing 4T1-luc2 tumors 0 and 4 hours after treatment with AB61. Mice treated by vehicle at time 0 (A) and 4 hours later (B); mice treated by AB61 (60 mg/kg), time 0 (C) and 4 hours after the administration (D). E, graph representation of tumor luminescence before (0 hour) or after (4 hours) timepoints of treatment by AB61. Whiskers represent lowest and highest data within 1.5 interquartile range. Outliers are not shown. **, $P < 0.01$. Data were analyzed by paired t test.

191
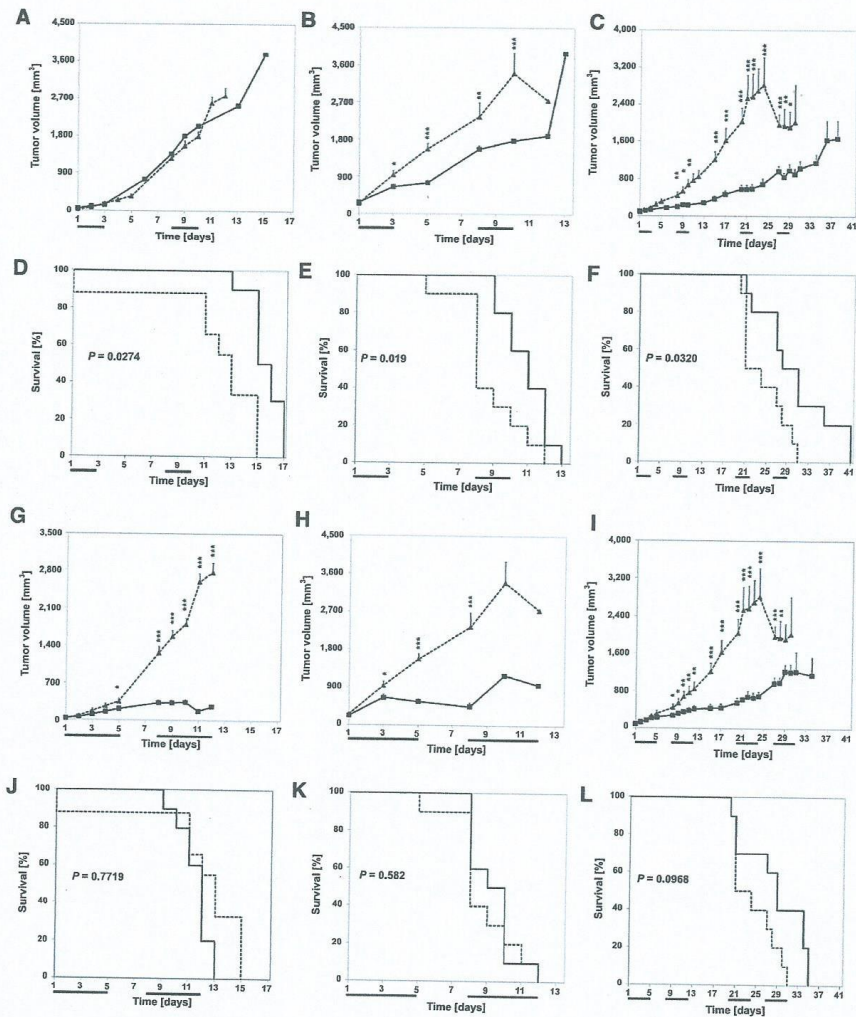
Figure 9.
In vivo antitumor activity of AB61. Mice were treated daily with AB61 (30 mg/kg). Tumor volume of human ovarian SK-OV-3 (A), breast BT-549 (B), and colorectal HT-29 (C) xenografts in SCID mice, dosing in three consecutive days. Survival of mice with SK-OV-3 (D), breast BT-549 (E), and colorectal HT-29 (F) xenografts, dosing in three consecutive days. Tumor volume of human ovarian SK-OV-3 (G), breast BT-549 (H), and colorectal HT-29 (I) xenografts in mice, treatment regimen for 5 consecutive days. Survival of mice with SK-OV-3 (J), breast BT-549 (K), and colorectal HT-29 (L) xenografts, treatment regimen for five consecutive days. Dashed line, vehicle; solid line, AB61 (30 mg/kg). Bold lines indicate therapeutic regimen and individual cycles.

192

Perlíková et al.

Most of the nucleosides used in cancer therapy are incorporated into DNA leading to termination of nascent DNA strand extension and DNA damage response activation (45). In this point of view, the mechanism of action of AB61 is more complex. The study clearly showed that the cytotoxic effect of AB61 is tightly linked with its intracellular phosphorylation and the inefficient phosphorylation in nonmalignant cells is a key factor of AB61 selectivity towards cancer cell lines. AB61 is incorporated both into DNA and RNA as a ribonucleotide (and only in trace amounts as a 2′-deoxyribonucleotide into DNA) where it leads to DNA damage and protein translation arrest, respectively. Rapid inhibition of translational machinery may also explain previously observed downregulation of RNA and DNA synthesis as a secondary effect (11). In spite of the structural similarity of AB61 with tubercidin, its mode of action seems to be unique and different from the one of gemcitabine, the only clinically used nucleoside cytostatic for treatment of solid tumors (46). The mechanism targeting at the same time DNA damage/repair and inhibition of protein translation machinery might be highly relevant for elimination of slowly proliferating, dormant, and senescent tumor cells, which are not cycling enough thus highly resistant to conventional chemotherapy and radiation. In summary, we showed that AB61 is a potent and selective cytostatic with exceptional mechanisms of action. Further pharmacologic studies of AB61 are currently under way.

Disclosure of Potential Conflicts of Interest

No potential conflicts of interest were disclosed.

Authors' Contributions

Conception and design: P. Perlíková, A. Bourderioux, M. Hajdúch, M. Hocek
Development of methodology: P. Perlíková, G. Rylová, P. Nauš, E. Tloušťová, K. Motyka, P. Znojek, A. Nová, M. Harvanová
Acquisition of data (provided animals, acquired and managed patients, provided facilities, etc.): P. Perlíková, P. Nauš, P. Znojek, A. Nová, M. Harvanová, M. Šiller

References

1. Tumkevicius S, Dodonova J. Functionalization of pyrrolo[2,3-d]-pyrimidine by palladium-catalyzed cross-coupling reactions. Chem Heterocycl Comp 2012;48:258–79.
2. Acs G, Reich E, Mori M. Biological and biochemical properties of the analogue antibiotic tubercidin. Proc Natl Acad Sci U S A 1964;52:493–501.
3. Suhadolnik RJ, Uematsu T, Uematsu H. Toyocamycin: Phosphorylation and incorporation into RNA and DNA and the biochemical properties of the triphosphate. Biochem Biophys Acta 1967;149:41–9.
4. Hardesty CT, Chaney NA, Waravdekar VS, Mead JAR. The disposition of the anitumor agent, sangivamycin, in mice. Cancer Res 1974;34:1005–9.
5. Fabianowska-Majewska K, Duley JA, Simmonds HA. Effects of novel anti-viral adenosine analogues on the activity of S-adenosylhomocysteine hydrolase from human liver. Biochem Pharmacol 1994;48:879–903.
6. Nishioka H, Sawa T, Hamada M, Shimura N, Imoto M, Umezawa K. Inhibition of phosphatidylinositol kinase by toyocamycin. J Antibiot 1990;43:1586–9.
7. Tavitian A, Uretsky SC, Acs G. Selective inhibition of ribosomal RNA synthesis in mammalian cells. Biochem Biophys Acta 1968;157:33–42.
8. Iapalucci-Espinoza S, Cereghini S, Franze-Fernández MT. Regulation of ribosomal RNA synthesis in mammalian cells: effect of toyocamycin. Biochemistry 1977;16:2885–9.
9. Loomis CR, Bell RM. Sangivamycin, a nucleoside analogue, is a potent inhibitor of protein kinase C. J Biol Chem 1988;263:1682–92.
10. Nauš P, Pohl R, Votruba I, Džubák P, Hajdúch M, Ameral R, et al. 6-(Het)aryl-7-Deazapurine ribonucleosides as novel potent cytostatic agents. J Med Chem 2010;53:460–70.
11. Bourderioux A, Nauš P, Perlíková P, Pohl R, Pichová I, Votruba I, et al. Synthesis and significant cytostatic activity of 7-Hetaryl-7-deazaadenosines. J Med Chem 2011;54:5498–507.
12. Nauš P, Perlíková P, Bourderioux A, Pohl R, Slavětínská L, Votruba I, et al. Sugar-modified derivatives of cytostatic 7-(het)aryl-7-deazaadenosines: 2′-C-methylribonucleosides, 2′-deoxy-2′-fluoroarabinonucleosides, arabinonucleosides and 2′-deoxyribonucleosides. Bioorg Med Chem 2012;20:5202–14.
13. Perlíková P, Eberlin L, Ménová P, Raindlová V, Slavětínská L, Tloušťová E, et al. Synthesis and Cytostatic and antiviral activities of 2′-Deoxy-2′,2′-difluororibo- and 2′-Deoxy-2′-fluororibonucleosides derived from 7-(Het)aryl-7-deazaadenines. ChemMedChem 2013;8:832–46.
14. Nauš P, Perlíková P, Pohl R, Hocek M. Sugar-modified derivatives of cytostatic 6-(het)aryl-7-deazapurine nucleosides: 2′-C-methylribonucleosides, arabinonucleosides and 2′-deoxy-2′-fluoroarabinonucleosides. Collect Czech Chem Commun 2011;76:957–88.
15. Perlíková P, Jornet Martínez N, Slavětínská L, Hocek M. Synthesis of 2′-deoxy-2′-fluororibo- and 2′-deoxy-2′,2′-difluororibonucleosides derived from 6-(het)aryl-7-deazapurines. Tetrahedron 2012;68:8300–10.
16. Nauš P, Caletková O, Konečný P, Džubák P, Bogdanová K, Kolář M, et al. Synthesis, cytostatic, antimicrobial, and anti-HCV activity of 6-substituted 7-(Het)aryl-7-deazapurine ribonucleosides. J Med Chem 2014;57:1097–110.
17. Snášel J, Nauš P, Dostál J, Hnízda A, Fanfrlík J, Brynda J, et al. Structural basis for inhibition of mycobacterial and human adenosine kinase by 7-substituted 7-(het)aryl-7-deazaadenine ribonucleosides. J Med Chem 2014;57:8268–79.

193

18. Gottesman MM, Fojo T, Bates SE. Multidrug resistance in cancer: role of ATP-dependent transporters. Nat Rev Cancer 2002;2:48–58.

19. Noskova V, Dzubak P, Kuzmina G, Ludkova A, Stehlik D, Trojanec R, et al. In vitro chemoresistance profile and expression/function of MDR associated proteins in resistant cell lines derived from CCRF-CEM, K562, A549 and MDA MB 231 parental cells. Neoplasma 2002;49: 418–25.

20. Bekker-Jensen S, Lukas C, Melander F, Bartek J, Lukas J. Dynamic assembly and sustained retention of 53BP1 at the sites of DNA damage are controlled by Mdc1/NFBD1. J Cell Biol 2005;170:201–11.

21. Chaudhry R, Chourasia BK, Das A. Mycoplasma. In: Dongyou L, editor. Molecular detection of human bacterial pathogens. Boca Raton: CRC Press, Taylor & Francis Group; 2011. p. 455–67.

22. Baranovskiy GA, Babayeva ND, Suwa Y, Gu J, Pavlov YI, Tahirov TH: Structural basis for inhibition of DNA replication by aphidicolin. Nucleic Acids Res 2014;42:14013–21.

23. Edgar R, Domrachev M, Lash AE. Gene Expression Omnibus: NCBI gene expression and hybridization array data repository. Nucleic Acids Res 2002;30:207–10.

24. Gagou ME, Zuazua-Villar P, Meuth M. Enhanced H2AX phosphorylation, DNA replication fork arrest, and cell death in the absence of Chk1. Mol Biol Cell 2010;21:739–52.

25. Waters NJ, Jones R, Williams G, Sohal B. Validation of a rapid equilibrium dialysis approach for the measurement of plasma protein binding. J Pharm Sci 2008;97:4586–95

26. Phillips IR, Shephard EA. Cytochrome P450 Protocols. In: Phillips IR, Shephard EA, editors. Methods in molecular biology series. Totowa, NJ: Humana Press; 2006.

27. Wu X, Wang J, Tan L, Bui J, Gjerstad E, McMillan K, et al. In vitro ADME profiling using high-throughput rapidfire mass spectrometry: cytochrome P450 inhibition and metabolic stability assays. J Biomol Screen 2012; 17:761–72.

28. Nassar AF. Drug metabolism handbook: concepts and applications. Hoboken, NJ: John Willey & Sons; 2009.

29. Čapek P, Cahová H, Pohl R, Hocek M, Gloeckner C, Marx A. An efficient method for the construction of functionalized DNA bearing amino acid groups through cross-coupling reactions of nucleoside triphosphates followed by primer extension or PCR. Chem Eur J 2007;13: 6196–203.

30. Cahová H, Havran L, Brázdilová P, Pivoňková H, Pohl R, Fojta M, et al. Aminophenyl- and nitrophenyl-labeled nucleoside triphosphates: synthe-

31. Kao C, Zheng M, Rüdisser S. A simple and efficient method to reduce nontemplated nucleotide addition at the terminus of RNAs transcribed by T7 RNA polymerase. RNA 1999;5:1268–72.

32. Neef AB, Samain F, Luedtke NW. Metabolic labeling of DNA by purine analogues in vivo. ChemBioChem 2012;13:1750–3.

33. Vannoni D, Di Pietro MC, Rosi F, Bernini A, Leoncini R, Tabucchi A, et al. Metabolism of adenosine in human colorectal cancer. Nucleos Nucleot Nucl 2004;23:1455–7.

34. Vannoni D, Bernini A, Carlucci F, Civitelli S, Di Pietro MC, Leoncini R, et al. Enzyme activities controlling adenosine levels in normal and neoplastic tissues. Mol Oncol 2004;21:187–95.

35. Giglioni S, Leoncini R, Aceto E, Chessa A, Civitelli S, Bernini A, et al. Adenosine kinase gene expression in human colorectal cancer. Nucleos Nucleot Nucl 2008;27:750–4.

36. Lee MW, Parker WB, Xu B. New insights into the synergism of nucleoside analogs with radiotherapy. Radiat Oncol 2013;8:223.

37. Ahn J, Kraynov VS, Zhong X, Tsai MD. DNA polymerase β: effects of gapped DNA substrates on dNTP specificity, fidelity and conformational changes. Biochem J 1998;331:79–87.

38. Dianova II, Sleeth KM, Allinson SL, Parsons JL, Breslin C, Caldecott KW, et al. XRCC1-DNA polymerase β interaction is required for efficient base excision repair. Nucleic Acids Res 2004;32:2550–5.

39. Loeb LA, Monnat RJ Jr. DNA polymerases and human disease. Nat Rev Genet 2008;8:594–604.

40. Dalgaard JZ. Causes and consequences of ribonucleotide incorporation into nuclear DNA. Trends Genet 2012;28:592–7.

41. Williams JS, Kunkel TA. Ribonucleotides in DNA: origins, repair and consequences. DNA Repair 2014;19:27–37.

42. Caldecott KW. Ribose-an internal threat to DNA. Science 2014;343:260–1.

43. Mochan TA, Venere M, DiTullio RA Jr, Halazonetis TD. 53BP1, an activator of ATM in response to DNA damage. DNA Repair 2004;3:945–52.

44. Zhang X, Jia D, Liu H, Zhu N, Zhang W, Feng J, et al. Identification of 5-iodotubercidin as a genotoxic drug with anti-cancer potential. PLoS One 2013;8:e62527.

45. Ewald B, Sampath D, Plunkett W. Nucleoside analogs: molecular mechanisms signaling cell death. Oncogene 2008;27:6522–37.

46. Noble S, Goa KL. Gemcitabine. A review of its pharmacology and clinical potential in non-small cell lung cancer and pancreatic cancer. Drugs 1997; 54:447–72.

194